

GENETIC CLASSIFICATION OF THE SE TURKEY CRUDE OILS
AND DELINEATION OF SOURCE ROCK TYPES WITH THE USE OF
BIOLOGICAL MARKERS

A Ph.D. Thesis
Presented by
Kadir GÜRGEY

to
the Graduate School of Natural and Applied Sciences
of Middle East Technical University
in Partial Fulfillment for the Degree of

DOCTOR OF PHILOSOPHY

in

GEOLOGICAL ENGINEERING

E. G.
Yükseköğretim Kurulu
Dokümantasyon Merkezi


MIDDLE EAST TECHNICAL UNIVERSITY

ANKARA


November, 1991

16115


Approval of the Graduate School of Natural and Applied
Science


Prof. Dr. Alpay Ankara
Director

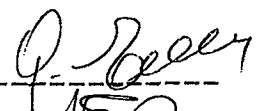
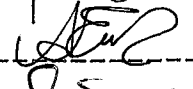
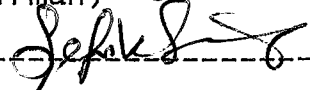
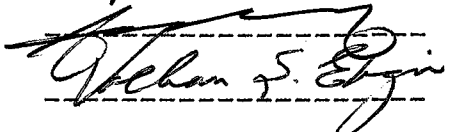
I certify that this thesis satisfies all requirements as a
thesis for the degree of Doctor of Philosophy in
Geological Engineering.


Prof. Dr. Vedat DOYURAN
Chairman of the Department

We certify that we read this thesis and that in our
opinion it fully adequate, in scope and quality, as a
thesis for the degree of Doctor of Philosophy in
Geological Engineering.


Assoc. Prof. Dr. Gökseven ESELLER
Supervisor

Examining Committee in Charge:

Assoc. Prof. Dr. Gökseven Eseller (Supervisor) 
Prof. Dr. Ayhan Erler (C.Chairman) 
Prof. Dr. Şefik Süzer 
Doç. Dr. Namık Yalçın 
Dr. Volkan Ş. Ediger

ABSTRACT

GENETIC CLASSIFICATION OF THE SE TURKEY CRUDE OILS AND DELINEATION OF SOURCE ROCK TYPES WITH THE USE OF BIOLOGICAL MARKERS

GÜRGEY, Kadir

PhD. in Geological Engineering

Supervisor: Assoc. Prof. Dr. Göksenin Eseller

November 1991, 320 pages

The purposes of this study were to classify the oils of SE Turkey genetically and to predict possible source rocks in terms of depositional environment, type of organic matter, lithology, age, and maturity using specific biomarkers. The correlation of each genetically related oils with rock units which were proven to possess adequate source potential for petroleum generation and the selection of the most distinguishing correlation parameters applicable to SE Turkey oils in general were the other objectives.

Fourty-four crude oil samples collected from SE Turkey were subjected to various organic geochemical measurements and analyses such as API gravity and sulfur content measurements; thin layer chromatographic analysis including quantifications of saturates, aromatics and

heterocompounds; gas chromatographic analysis of saturate fraction including quantifications of the n-alkanes and isoprenoids; gas chromatography- mass spectrometry (GC-MS) analysis of the branch/cyclic saturate fraction including quantification of the biomarkers such as tri-tetra-pentacyclic terpanes, pregnanes, diasteranes, and regular steranes. In order to retrieve maximum amount of information, the pertinent data were evaluated using conventional as well as sophisticated multivariate statistical analyses.

Based on the percentages of saturate hydrocarbons, Turkish oils were divided into "heavy", "aromatic", and "paraffinic" and "paraffinic-napthenic" oils. All of the gas chromatograms show similar unimodal distribution of C₁₅₊ n-alkanes maximizing around n-C₁₅, n-C₁₆, and n-C₁₇. Five different data sets obtained from terpene and sterane fragmetograms of GC-MS analyses were initially normalized and then subjected to multivariate statistical techniques. Interrelationships among the oils (oil-oil correlations) and variables were then investigated on the score and loading plots respectively. Subsequently, "twenty biomarker ratio parameters" were selected when two peaks were inversely correlated and had high loadings on the principal components.

After considering the effects of alteration processes such as thermal alteration, biological degradation and secondary migration, the Turkish oils were mainly divided into four groups with addition of those

oils of mixed origin: Batman area oils (Group I oils) showed the features of mixture composed of biologically degraded oils and normal oils. Altered molecular composition did not allow to predict source rocks of the Group I oils. Batman-Nusaybin area oils (Group II oils) were most probably derived from the evaporitic-calcareous Triassic-Jurassic aged Cudi Group. Adıyaman-Kozluk area oils (Group III) oils were most probably generated from the calcareous Karaboğaz Formation of Campanian age. Northern Diyarbakır area oils (Group IV), on the other hand, were most likely derived from the siliciclastic Upper Silurian aged Dadaş Formation. Mixed oils (Batman area oils) were most probably resulted from the mixing of the hydrocarbons derived from Karaboğaz Formation and Judi Group. This model requires secondary migration of the Karaboğaz derived hydrocarbons from Kozluk to Batman.

Key words: Crude oil, source rock, correlation, sterane, terpane, multivariate statistics, GC-MS, SE Turkey.

Science Code: 606.03.03

ÖZ

GÜNEYDOĞU ANADOLU PETROLERİNİN KÖKENSEL SINIFLAMASI
VE KAYNAK KAYA TIPLERİNİN BİYOİZLEYİCİLER
KULLANILARAK BULUNMASI

GÜRGEY, Kadir

Doktora Tezi, Jeoloji Mühendisliği Anabilim Dalı

Tez Yöneticisi: Doç. Dr. Gökseven ESELLER

Kasım 1991, 320 sayfa

Bu çalışmanın amacı, GD Türkiye petrollerini kökenlerine göre sınıflamak, olası kaynak kayaların çökelme ortamlarını, organik madde tiplerini, litolojilerini, yaşlarını, ve olgunluklarını petrollerde bulunan belirli biyoizleyicileri kullanarak tahmin etmektir. Çalışmanın diğer amaçları arasında kökensel olarak farklılıklar gösteren her bir petrol grubuyla bölgede petrol potansiyeli olan kaynak kayaları karşılaştırarak olası petrol-kaynak kaya korelasyonlarını yapmak ve GD petrollerine uygulanabilir en belirli korelasyon parametrelerini bulmaktır.

GD Türkiye'den alınan kırkdört ham petrol örneğine çeşitli organik jeokimyasal ölçümler ve analizler uygulanmıştır. Bunlar; API gravite ve kükürt miktarı ölçümleri; ince tabaka kromatografisi ile doymuş

hidrokarbon, aromatik ve heterobileşiklerin yüzde miktarları; gaz kromatografisi ile doymuş hidrokarbonların n-alkan ve izoprenoidlerin bağlı miktarları; zincirli/halkalı doymuş hidrokarbonların gaz kromatografisi-kütle spektrometresi (GC-MS) ile üç-dört-beş halkalı terpanların, pregnanların, diasteranların, ve düzenli steranların bağlı miktarlarının bulunmasıdır. Elde edilen verilerden en iyi şekilde yararlanabilmek için hem konvansiyonel ve hemde geliştirilmiş çok değişkenli istatistiksel yöntemler kullanılmıştır.

Doymuş hidrokarbonlar esas alınarak petroler "ağır", "aromatik" ve "parafinik"- "parafinik- naftenik" olmak üzere dörde ayrılmışlardır. n-C₁₅₊ alkanlar bütün gaz kromatogramlarında sadece n-C₁₅, n-C₁₆ ve n-C₁₇ bölgelerinde maksimum göstermişlerdir. GC-MS steran ve terpan fragmetogramlardan elde edilen beş farklı veri seti normalize edildikten sonra çok değişkenli istatistiksel analizlerle incelenmişlerdir. Petroller arası ilişkiler (petrol-petrol korelasyonları) skor diyagramları üzerinde ve değişkenler arasındaki ilişkilerde yükleme diyagramları üzerinde araştırılmışlardır. Ters orantılı ve temel bileşenler üzerinde yüksek yükleme gösteren piklerden yirmi biyoizleyici oran parametresi seçilmiştir.

Isısal alterasyon, biyolojik bozunma ve ikincil göç gibi alterasyon olayları gözönüne alındıktan sonra petroler karışımdan oluşan bir gruba ek olarak başlıca dört gruba ayrılmışlardır. Batman bölgesi petroleri (Grup I Petrolleri) biyolojik bozunmaya uğramış petroler ile

normal petrolerin karışımından oluşan özellikleri taşımaktadır. Bu petrolerin altere olmuş molekülleri kaynak kaya tahminine elverişli değildir. Batman-Nusaybin petroleri (Grup II Petrolleri) büyük olasılıkla evaporitik-karbonatlı Trias-Jura yaşlı Cudi Grubu'ndan türemişlerdir. Adıyaman-Kozluk bölgesi petroleri (Grup III Petrolleri) büyük olasılıkla karbonatlı Kampaniyen yaşlı Karaboğaz Formasyonu'ndan türemişlerdir. Kuzey Diyarbakır petroleri (Group IV) ise silisiklastik Üst Siluriyen yaşlı Dadaş Formasyonundan türemişlerdir. Batman bölgesi petroleri (Karışım petroleri) büyük olasılıkla Karaboğaz Formasyon'undan ve Cudi Grubu'ndan türüyen petrolerin karışımlarından oluşmuşlardır. Bu model Kozluk bölgesinde Karaboğaz Formasyonundan türeyen petrolerin Batman bölgesine doğru ikincil göçünü gerektirmektedir.

Anahtar kelimeler: Ham petrol, kaynak kaya, korelasyon, steran, terpan, çok değişkenli istatistik, GC-MS, GD Türkiye

Bilim kodu: 606.03.03

ACKNOWLEDGEMENTS

I am deeply indebted to Prof. Dr. C. Barker of University of Tulsa who introduced me to organic geochemistry and initiated this research. I also thank my wife, Ayşegül Gürgey, for her help and patience during the entire time spent for this research.

I am also grateful to my supervisor, Assoc. Prof. Dr. G. Eseller for his guidance, patience, and criticism during the completion of the manuscript.

I am deeply indebted to the Turkish Petroleum Corporation (TPAO) for supporting this research and use of laboratory facilities.

I would like to express my sincere thanks to colleagues at TPAO Research Center including H. Okay (Head), Mrs. F. Yüksel (Advisor) for supporting this research. My special thanks are also for Mrs. A. Harput and Mrs. Y. Bizim for their help for the GC-MS analyses; Mrs. S. Sayılı and Miss N. Tepecik for Iatroscan and GC analyses; Miss A. Tezcan for column chromatography; Mr. F. Dikmen for sulfur content measurements; İ. Çeçen for word processing and Mrs. K. Yılmaz for preparation of the figures.

Thanks are also due to C. Soylu and H. İztan for their permission to use their source rock data.

Thanks are extended to O. Duran, N. Bozdoğan, M. Köylüođlu, and M. Araç for discussions on the sedimentological and stratigraphic aspects of the study area. I am grateful for their comments.

I also thank Feridun Fildiş for initial adaptation of the statistical computer programs to WAX 11/780 system and Cihan Aytüre who spent many hours for running the programs to obtain statistical results from the raw data.



TABLE OF CONTENTS

	Page
ABSTRACT	iii
ÖZ.....	vi
ACKNOWLEDGEMENTS.....	ix
LIST OF TABLES.....	xv
LIST OF FIGURES	xviii
CHAPTER I: INTRODUCTION.....	1
1.1 Purpose and Scope.....	1
1.2 Geographic Setting.....	3
1.3 Geologic Setting.....	5
1.3.1 General	5
1.3.2 Stratigraphy.....	6
1.3.3 Geological Evaluation.....	17
1.4 Previous Work.....	20
1.4.1 Oil to Oil Correlations.....	20
1.4.2 Suggested Source Rocks	23
1.5 Nomenclature.....	26
CHAPTER II: METHODS OF STUDY.....	31
2.1 Sampling.....	31
2.2 Analytical Procedures.....	32
2.2.1 API Gravity.....	32
2.2.2 Sulfur Determination.....	34

2.2.3 Deasphalting.....	34
2.2.4 Thin Layer Chromatography.....	35
2.2.5 Column Chromatography.....	35
2.2.6 Gas Chromatography.....	36
2.2.7 Molecular Sieving.....	36
2.2.8 Gas Chromatography-Mass Spectrometry.....	37
2.3 Multivariate Statistical Analysis.....	37
CHAPTER III: RESULTS	40
3.1 Bulk Compositional Data.....	40
3.2 Gas Chromatography Data.....	44
3.2.1 Distribution of C ₁₅₊ n-Alkanes.....	44
3.2.2 Distribution of Acyclic Isoprenoids	46
3.3 Gas Chromatography-Mass Spectrometry Data.....	47
3.3.1 Tri-Tetra-Pentacyclic Terpanes.....	47
3.3.1.1 Tricyclic Terpanes.....	52
3.3.1.2 Tetracyclic Terpanes.....	53
3.3.1.3 Pentacyclic Terpanes.....	54
3.3.2 Steranes.....	56
3.3.2.1 Regular Steranes.....	56
3.3.2.2 Diasteranes.....	62
3.3.2.3 Pregnanes.....	64
3.3.3 Selected Biomarker Ratios and Sulfur Content.....	65
3.4 Other Data.....	74
3.4.1 Stable Carbon Isotope Data.....	74
3.4.2 Biomarker Data.....	74
CHAPTER IV: DISCUSSIONS.....	75
4.1 Oil to Oil Correlations.....	75

4.1.1	Philosophy of Oil to Oil Correlation Studies.....	75
4.1.2	Assessment of Alteration Processes.....	77
4.1.2.1	Thermal Alteration.....	77
4.1.2.2	Biological Degradation.....	88
4.1.2.3	Secondary Migration.....	92
4.1.3	Stable Carbon Isotope Ratios.....	94
4.1.4	Multivariate Data Analysis.....	97
4.1.4.1	Tri-tetracyclic Terpanes.....	97
4.1.4.2	Pentacyclic Terpanes	108
4.1.4.3	Tri-Tetra-Pentacyclic Terpanes.....	118
4.1.4.4	Steranes.....	126
4.1.4.5	Selected Biomarker Ratios.....	135
4.1.5	Predicted Source Rock Ages Using Biological Markers in the Oils.....	147
4.2	Possible Source Rocks of the Each Correlated Group of Oils.....	152
4.2.1	Batman Area Oils (Group I Oils) and Their Possible Source Rocks.....	153
4.2.2	Batman-Nusaybin Area Oils (Group II Oils) and Their Possible Source Rocks.....	157
4.2.3	Kozluk-Adıyaman Area Oils (Group III Oils) and Their Possible Source Rocks.....	167
4.2.4	Northern Diyarbakır Area Oils (Group IV Oils) and Their Possible Source Rocks.....	174
4.2.5	Batman Area Oils (Mixed Origin Oils) and their Possible Source Rocks.....	180
CHAPTER V: CONCLUSIONS and RECOMMENDATIONS.....		183

REFERENCES.....	190
APPENDICES	
APPENDIX A. TERMINOLOGY AND CHEMICAL STRUCTURE OF STERANE AND TERPANE BIOMARKERS.....	215
APPENDIX B. MULTIVARIATE DATA ANALYSIS.....	221
APPENDIX C. COMPILATION OF NORMALIZED C ₁₅₊ N-ALKANE CAPILLARY GAS CHROMATOGRAMS.....	224
APPENDIX D. COMPILATION OF M/Z 191 (TERPANE) MASS FRAGMENTOGRAMS OF BRANCH/CYCLIC SATURATE FRACTION OF THE OILS FROM SE TURKEY.....	246
APPENDIX E. COMPILATION INPUT BIOMARKER DATA MATRICES FOR STATISTICAL ANALYSES	277
APPENDIX F. COMPILATION OF M/Z 217 (STERANE) MASS FRAGMENTOGRAMS OF BRANCH/CYCLIC SATURATE FRACTION OF THE OILS FROM SE TURKEY.....	282
APPENDIX G. STABLE CARBON ISOTOPE RATIO DATA.....	314
APPENDIX H. COMPILATION OF LINEAR REGRESSION CORRELATION COEFFICIENT MATRIX DATA.....	315
CURRICULUM VITAE.....	320

LIST OF TABLES

	Page
Table 1.1 Previous Groupings of the SE Turkey Oils.....	21
Table 1.2 List of the Symbols and Abbreviations.....	27
Table 1.3 Location Area, Field/Wells, and Abbreviations for the Oil Samples Investigated in This Study.....	28
Table 3.1 Reservoir Depth, Age, Well Bottom Temperature, and Formation of Oil Samples Examined in This Study....	41
Table 3.2 Bulk Composition and Capillary Gas Chromatography Data of Oil Samples.....	42
Table 3.3 Relative Abundances of Tricyclic, Tetracyclic, and Pentacyclic Terpanes.....	48
Table 3.4. List of Identified Tri-Tetra-Pentacyclic Terpanes.....	50
Table 3.5. List of Identified Steranes.....	58
Table 3.6. Percentage Abundances of Pregnanes, Diasteranes, and Regular Steranes.....	59

Table 3.7.Explanation of the Selected Biomarker Ratios used in Table E.5.....	66
Table 4.1 The Most Distinguishing Features of the Turkish Oils.....	145
Table E.1 Molecular Distribution of Tri-Tetra-Pentacyclic Terpanes.....	277
Table E.2 Normalized Molecular Distribution of Tri-Tetracyclic Terpanes.....	278
Table E.3 Normalized Molecular Distribution of Pentacyclic Terpanes.....	279
Table E.4 Normalized Molecular Distribution of Steranes.....	280
Table E.5 Normalized Distribution of the Selected Biomarker Ratios.....	281
Table H.1 Linear Regression Correlation Coefficient Matrix of the Tri-Tetracyclic Terpanes.....	315
Table H.2 Linear Regression Correlation Coefficient Matrix of the Pentacyclic Terpanes.....	316
Table H.3 Linear Regression Correlation Coefficient Matrix of the Tri-Tetra-Pentacyclic Terpanes.....	317

Table H.4 Linear Regression Correlation Coefficient
Matrix of the Steranes.....318

Table H.5 Linear Regression Correlation Coefficient
Matrix of the Selected Biomarker Ratios.....319



LIST OF FIGURES

	Page
Figure 1.1 Location and Reservoir Formation of the Crude Oils Examined from the SE Turkey.....	4
Figure 1.2 Schematic Structural Map of SE Turkey (Rigo and Cortesini, 1964).....	7
Figure 1.3 Correlation Chart of Autochthonous Cambrian-Campanian Lithostratigraphic Units in Southeastern Turkey (Perinçek, 1991). (●) Indicate Reservoir Zones for Produced Oils and (★) Indicate the Rock Units Having Source Rock Potential.....	8
Figure 1.4 Correlation Chart of Autochthonous Aptian-Miocene Lithostratigraphic Units in Southeastern Turkey (Perinçek, 1991). (●) Indicate Reservoir Zones for Produced Oils and (★) Indicate the Rock Units Having Source Rock Potential.....	9
Figure 1.5 Chemical Structure for Isoprene (a), and Two Ways of Drawing a Monoterpene Formed From two Isoprene Units (b,c) and Numbering System of Steranes (d) and Terpanes (e) (Mackenzie, 1984).....	30

Figure 2.1 Analytical Flow Chart Employed to the Crude Oil Samples.....	33
Figure 2.2 Computer Flow Chart of Principal Component Analysis Applied to Biomarker Data.....	39
Figure 3.1 Histogram Showing Saturate (%) versus Number of Oil Samples.....	43
Figure 3.2 A representative (Cemberlitas-16;CT16) Gas Chromatogram of Saturate Fraction of Oils. Pr Pristane) Phy (Phytane).....	45
Figure 3.3 A Representative m/z 191 Mass Fragmetogram Showing Terpane Distributions in Adiyaman-3 (A3) oil. Peaks Identified in Table 3.4.....	49
Figure 3.4 A Representative m/z 217 Mass Fragmetogram Showing Sterane Distributions in Adiyaman-3 (A3) oil. Peaks identified in Table 3.5.....	57
Figure 4.1 Crossplot of Depth (m) versus Reservoir Temperature.....	79
Figure 4.2 Crossplot of Depth (m) versus API gravity..	80
Figure 4.3 Crossplot of API Gravity versus Sulfur content (wt %).	82

Figure 4.4 Ternary Diagram Showing the Bulk Composition of the Turkish Oils. □ Group I Oils, ■ Group II Oils □ Group III Oils, ⊠ Group IV Oils, and ▣ Mixed Group Oils.....	83
Figure 4.5 Crossplot of 20/20S+20R C ₂₉ Sterane versus 22S/22S+22R C ₃₂ Terpane Ratios.....	85
Figure 4.6 Petroleum Generation Phases versus Biological Marker Maturity Parameters (After Mackenzie, 1984)....	87
Figure 4.7 Ternary Diagram Showing Relative Proportions of Regular Steranes, Pregnanes, and Diasteranes of the Turkish Oils.....	91
Figure 4.8 Crossplot of Stable Carbon Isotope (δ ¹³ C) of Saturates versus Aromatics. Solid Line Drawn According to Sofer (1984).....	95
Figure 4.9 Crossplot of Tri-Tetra Cyclic Terpane Scores on PC1 versus PC2.....	99
Figure 4.10 Crossplot of Tri-Tetracyclic Terpane Loadings on PC1 versus PC2.....	101
Figure 4.11 Crossplot of Scores on PC1 versus API Gravity.....	103
Figure 4.12 Crossplot of tri-Tetracyclic Terpane Loadings on PC1 versus PC3.....	106

Figure 4.13 Crossplot of Tri-Tetracyclic Terpane Scores on PC1 versus PC3.....	107
Figure 4.14 Crossplot of Tri-Tetracyclic Terpanes(%) versus Tetracyclic Terpane (%).....	109
Figure 4.15 Crossplot of Pentacyclic Terpane Scores on PC1 versus PC2.....	111
Figure 4.16 Crossplot of Pentacyclic Terpane Loadings on PC1 versus PC2.....	113
Figure 4.17 Crosplot of C ₂₄ */C ₂₈ Ratio versus C ₂₉ Norhopane/ C ₃₀ Hopane Ratio.....	115
Figure 4.18 Crossplot of Pentacyclic Terpane Scores on PC1 versus PC3.....	116
Figure 4.19 Crossplot of Pentacyclic Terpane Loadings on PC1 versus PC3.....	117
Figure 4.20 Crossplot of Tri-Tetra-Pentacyclic Terpane Scores on PC1 versus PC2.....	121
Figure 4.21 Crossplot of Tri-Tetra-Pentacyclic Terpane Loadings on PC1 versus PC2.....	122
Figure 4.22 Crossplot of Tri-Tetra-Penta Cyclic Terpane Scores on PC1 versus PC3.....	124

Figure 4.23 Crossplot of Tri-Tetra-Pentacyclic Terpane Loadings on PC1 versus PC3.....	125
Figure 4.24 Crossplot of Sterane Scores on PC1 versus PC2.....	129
Figure 4.25 Crossplot of Sterane Loadings on PC1 versus PC2.....	129
Figure 4.26 Crossplot of Sterane Scores on PC1 versus PC3.....	133
Figure 4.27 Crossplot of Sterane Loading on PC1 versus PC2.....	134
Figure 4.28 Crossplot of C ₂₇ Diasteranes (%) versus C ₂₉ Regular Steranes.....	136
Figure 4.29 Ternary Diagram Showing Distribution of C ₂₇ :C ₂₈ :C ₂₉ Regular Steranes With a 5 α (H), 14 α (H), 17 α (H) 20R Stereochemistry. P:Plankton, OP:Open marine, E:Estuarine, HP:Higher plants, T:Terrigenous, and L:Lacustrine According to Huang and Meinschein (1976).....	137
Figure 4.30 Crossplot of Selected Biomarker Ratio Loadings on PC1 versus PC2.....	140
Figure 4.31 Crossplot of Selected Biomarker Ratio Scores on PC1 versus PC2.....	141

Figure 4.32 Crossplot of Selected Biomarker Ratio Scores on PC1 versus PC3.....	143
Figure 4.33 Crossplot of Selected Biomarker Ratio Loadings on PC1 versus PC3.....	144
Figure 4.34 Crossplot of Pristane/Phytane Ratio versus C ₂₄ */C ₂₆ ratio.....	146
Figure 4.35 Geological Distribution of Important Groups of phytoplanktons (after Tappan and Loeblich, 1970) Compared to the Mean C ₂₈ /C ₂₉ Sterane Ratio of Marine Source Rock-Derived Crude Oils (after Grantham and Wakefield, 1988).....	149
Figure 4.36 Determination of the Age of the Source Rocks of the Turkish oils in Terms of Plotting C ₂₈ /c ₂₉ Sterane Ratios on the Grantham and Wakefield's (1988) Diagram. Modified after Gürgey and Harput (1990).....	150
Figure 4.37 Batman Area Oils and Their Source Rock Distributions.....	154
Figure 4.38 Symbols of Rock used in this study.....	155
Figure 4.39 Batman-Nusaybin Area Oils and Their Source Rock Distributions.....	158

Figure 4.40 Adıyaman-Kozluk Area Oils and Their Source Rock Distributions.....	168
Figure 4.41 Northern Diyarbakır Oils and Their Source Rock Distributions.....	175
Figure 4.42 Mixed Oils (Batman) and Their Source Rock Distribution.....	182
Figure 4.43 Oil Groups and Their Distribution in SE Turkey.....	186
Figure C.1 Gas Chromatogram of the Saturate Fraction of Çelikli-18 oil.....	224
Figure C.2 Gas Chromatogram of the Saturate Fraction of Çelikli-16 oil.....	224
Figure C.3 Gas Chromatogram of the Saturate Fraction of Şelmo-5 oil.....	225
Figure C.4 Gas Chromatogram of the Saturate Fraction of Batı Şelmo-4 oil.....	225
Figure C.5 Gas Chromatogram of the Saturate Fraction of Batı Şelmo-103 oil.....	226
Figure C.6 Gas Chromatogram of the Saturate Fraction of Sinan-13 oil.....	226

Figure C.7 Gas Chromatogram of the Saturate Fraction of Silivanka-30 oil.....	227
Figure C.8 Gas Chromatogram of the Saturate Fraction of Sinan-1 oil.....	227
Figure C.9 Gas Chromatogram of the Saturate Fraction of Kastel-2 oil.....	228
Figure C.10 Gas Chromatogram of the Saturate Fraction of Kurtalan-1 oil.....	228
Figure C.11 Gas Chromatogram of the Saturate Fraction of Beyçayırı-1 oil.....	229
Figure C.12 Gas Chromatogram of the Saturate Fraction of Mağrip-53 oil.....	229
Figure C.13 Gas Chromatogram of the Saturate Fraction of Mağrip-30 oil.....	230
Figure C.14 Gas Chromatogram of the Saturate Fraction of Garzan-17 oil.....	230
Figure C.15 Gas Chromatogram of the Saturate Fraction of Garzan-90 oil.....	231
Figure C.16 Gas Chromatogram of the Saturate Fraction of Garzan-15 oil.....	231

Figure C.17 Gas Chromatogram of the Saturate Fraction of Germik-12 oil.....	232
Figure C.18 Gas Chromatogram of the Saturate Fraction of Germik-5 oil.....	232
Figure C.19 Gas Chromatogram of the Saturate Fraction of Raman-87 oil.....	233
Figure C.20 Gas Chromatogram of the Saturate Fraction of Raman-192 oil.....	233
Figure C.21 Gas Chromatogram of the Saturate Fraction of Raman-157 oil.....	234
Figure C.22 Gas Chromatogram of the Saturate Fraction of Raman-63 oil.....	234
Figure C.23 Gas Chromatogram of the Saturate Fraction of Raman-193 oil.....	235
Figure C.24 Gas Chromatogram of the Saturate Fraction of Raman-151 oil.....	235
Figure C.25 Gas Chromatogram of the Saturate Fraction of Raman-197 oil.....	236
Figure C.26 Gas Chromatogram of the Saturate Fraction of Raman-84 oil.....	236

Figure C.27 Gas Chromatogram of the Saturate Fraction of Raman-93 oil.....	237
Figure C.28 Gas Chromatogram of the Saturate Fraction of Batı Raman-47 oil.....	237
Figure C.29 Gas Chromatogram of the Saturate Fraction of Batı Raman-56 oil.....	238
Figure C.30 Gas Chromatogram of the Saturate Fraction of Batı Raman-84 oil.....	238
Figure C.31 Gas Chromatogram of the Saturate Fraction of Batı Raman-43 oil.....	239
Figure C.32 Gas Chromatogram of the Saturate Fraction of Batı Raman-211 oil.....	239
Figure C.33 Gas Chromatogram of the Saturate Fraction of Batı Raman-193 oil.....	240
Figure C.34 Gas Chromatogram of the Saturate Fraction of Batı Raman-189 oil.....	240
Figure C.35 Gas Chromatogram of the Saturate Fraction of Batı Raman-167 oil.....	241
Figure C.36 Gas Chromatogram of the Saturate Fraction of Batı Raman-176 oil.....	241

Figure C.37 Gas Chromatogram of the Saturate Fraction of Çamurlu-2 oil.....	242
Figure C.38 Gas Chromatogram of the Saturate fraction of Çamurlu-22 oil.....	242
Figure C.39 Gas Chromatogram of the Saturate Fraction of Batı Kozluca-12 oil.....	243
Figure C.40 Gas Chromatogram of the Saturate Fraction of Güney Dinçer-3 oil.....	243
Figure C.41 Gas Chromatogram of the Saturate Fraction of Güney Dinçer-15 oil.....	244
Figure C.42 Gas Chromatogram of the Saturate Fraction of Güney Sarıcak-21 oil.....	244
Figure C.43 Gas Chromatogram of the Saturate Fraction of Adıyaman-3 oil.....	245
Figure D.1 M/Z 191 Mass Fragmetogram of the Çelikli-16 oil.....	246
Figure D.2 M/Z 191 Mass Fragmetogram of the Batı Şelmo-4 oil.....	247
Figure D.3 M/Z 191 Mass Fragmetogram of the Silivanka-30 oil.....	248

Figure D.4 M/Z 191 Mass Fragmetogram of the Sinan-1 oil.....	249
Figure D.5 M/Z 191 Mass Fragmetogram of the Kaste1-2 oil.....	250
Figure D.6 M/Z 191 Mass Fragmetogram of the Kurtalan-1 oil.....	251
Figure D.7 M/Z 191 Mass Fragmetogram of the Beyçayırı-1 oil.....	252
Figure D.8 M/Z 191 Mass Fragmetogram of the Mağrip-30 oil.....	253
Figure D.9 M/Z 191 Mass Fragmetogram of the Garzan-15 oil.....	254
Figure D.10 M/Z 191 Mass Fragmetogram of the Germik-12 oil.....	255
Figure D.11 M/Z 191 Mass Fragmetogram of the Raman-87 oil.....	256
Figure D.12 M/Z 191 Mass Fragmetogram of the Raman-192 oil.....	257
Figure D.13 M/Z 191 Mass Fragmetogram of the Raman-63 oil.....	258

Figure D.14 M/Z 191 Mass Fragmetogram of the Raman-151 oil.....	259
Figure D.15 M/Z 191 Mass Fragmetogram of the Raman-197 oil.....	260
Figure D.16.M/Z 191 Mass Fragmetogram of the Raman-84 oil.....	261
Figure D.17.M/Z 191 Mass Fragmetogram of the Raman-93 oil.....	262
Figure D.18 M/Z 191 Mass Fragmetogram of the Batı Raman-47 oil.....	263
Figure D.19 M/Z 191 Mass Fragmetogram of the Batı Raman-56 oil.....	264
Figure D.20 M/Z 191 Mass Fragmetogram of the Batı Raman-84 oil.....	265
Figure D.21 M/Z 191 Mass Fragmetogram of the Batı Raman-43 oil.....	266
Figure D.22 M/Z 191 Mass Fragmetogram of the Batı Raman-211 oil.....	267
Figure D.23 M/Z 191 Mass Fragmetogram of the Batı Raman-189 oil.....	268

Figure D.24 M/Z 191 Mass Fragmetogram of the Batı Raman-167 oil.....	269
Figure D.25 M/Z 191 Mass Fragmetogram of the Batı Raman-176 oil.....	270
Figure D.26 M/Z 191 Mass Fragmetogram of the Çamurlu-22 oil.....	271
Figure D.27 M/Z 191 Mass Fragmetogram of the Batı Kozluca-12 oil.....	272
Figure D.28 M/Z 191 Mass Fragmetogram of the Güney Dinçer-3 oil.....	273
Figure D.29 M/Z 191 Mass Fragmetogram of the Güney Sarıcak-21 oil.....	274
Figure D.30 M/Z 191 Mass Fragmetogram of the Adıyaman-3 oil.....	275
Figure D.31 M/Z 191 Mass Fragmetogram of the Çemberlitaş-16 oil.....	276
Figure F.1 M/Z 217 Mass Fragmetogram of the Çelikli-16 oil.....	282
Figure F.2 M/Z 217 Mass Fragmetogram of the Şelmo-5 oil.....	283

Figure F.3 M/Z 217 Mass Fragmetogram of the Batı Şelmo-4 oil.....	284
Figure F.4 M/Z 217 Mass Fragmetogram of the Silivanka-30 oil.....	285
Figure F.5 M/Z 217 Mass Fragmetogram of the Sinan-1 oil.....	286
Figure F.6 M/Z 217 Mass Fragmetogram of the Kastel-2 oil.....	287
Figure F.7 M/Z 217 Mass Fragmetogram of the Kurtalan-1 oil.....	288
Figure F.8 M/Z 217 Mass Fragmetogram of the Beyçayırı-1 oil.....	289
Figure F.9 M/Z 217 Mass Fragmetogram of the Mağrip-53 oil.....	290
Figure F.10 M/Z 217 Mass Fragmetogram of the Garzan-15 oil.....	291
Figure F.11 M/Z 217 Mass Fragmetogram of the Germik-5 oil.....	292
Figure F.12 M/Z 217 Mass Fragmetogram of the Raman- 87 oil.....	293

Figure F.13 M/Z 217 Mass Fragmetogram of the Raman-192 oil.....	294
Figure F.14 M/Z 217 Mass Fragmetogram of the Raman-63 oil.....	295
Figure F.15 M/Z 217 Mass Fragmetogram of the Raman-151 oil.....	296
Figure F.16 M/Z 217 Mass Fragmetogram of the Raman-197 oil.....	297
Figure F.17 M/Z 217 Mass Fragmetogram of the Raman-84 oil.....	298
Figure F.18 M/Z 217 Mass Fragmetogram of the Raman-93 oil.....	299
Figure F.19 M/Z 217 Mass Fragmetogram of the Batı Raman-47 oil.....	300
Figure F.20 M/Z 217 Mass Fragmetogram of the Batı Raman-56 oil.....	301
Figure F.21 M/Z 217 Mass Fragmetogram of the Batı Raman-84 oil.....	302
Figure F.22 M/Z 217 Mass Fragmetogram of the Batı Raman-43 oil.....	303

Figure F.23 M/Z 217 Mass Fragmetogram of the Batı Raman-211 oil.....	304
Figure F.24 M/Z 217 Mass Fragmetogram of the Batı Raman-189 oil.....	305
Figure F.25 M/Z 217 Mass Fragmetogram of the Batı Raman-167 oil.....	306
Figure F.26 M/Z 217 Mass Fragmetogram of the Batı Raman-176 oil.....	307
Figure F.27 M/Z 217 Mass Fragmetogram of the Çamurlu-22 oil.....	308
Figure F.28 M/Z 217 Mass Fragmetogram of the Batı Kozluca-12 oil.....	309
Figure F.29 M/Z 217 Mass Fragmetogram of the Güney Dinçer-3 oil.....	310
Figure F.30 M/Z 217 Mass Fragmetogram of the Güney Sarıcak-21 oil.....	311
Figure F.31 M/Z 217 Mass Fragmetogram of the Adıyaman-3.....	312
Figure F.32 M/Z 217 Mass Fragmetogram of the Çemberlitaş-16.....	313

CHAPTER I

INTRODUCTION

1.1. Purpose and Scope

The oil groups of SE Turkey vary from the heavy oils (12-25 API gravity) to medium-light oils (25-36 API gravity). The latter have been distributed more widely than the first in the area. Compositionally, they range from aromatic, asphaltic, paraffinic to paraffinic-naphtenic oil groups. Source rocks of these compositionally variable oils have not been definitely proved yet although one of the most important requirements for finding oil in a basin is the identification of good source rocks. The techniques so far employed revealed the source potential of the rock units in terms of organic matter type, amount, and maturity level only. However, these source rocks have not been assigned to any particular oil group.

Recent advancement in biological marker geochemistry permits to distinguish oil groups based on the depositional environment, organic matter type, lithology, age, and maturity level of the source rocks utilizing the certain group of biological markers present in the crude oils. Further, source rock types can be

predicted by using specific biological markers present in the crude oils. This approach is particularly useful when the source rock sample is not available.

A multidisciplinary approach (geochemical, geological, and statistical) was made to determine the oil groups and to predict nature of the possible source rocks of the 44 oil samples collected from the major oil fields in the SE Turkey. Biological markers of these oil samples were statistically examined as a function of changes in the depositional environment, lithology, organic matter type, geologic age, and maturity level of their possible source rocks. This approach may allow us to achieve the following goals;

1. To select the most efficient correlation parameters in order to assist understanding genetic interrelationships among the analyzed oil samples,
2. To enhance use of biological markers that are being interpretable in terms of oil maturation, migration, biodegradation, and character of depositional environment of the source rocks,
3. To provide insight into the relationships within biological markers used in this study,
4. To predict lithology, age, depositional environment, and maturity level of source rocks for the analyzed SE Turkey oils.
5. To correlate the oils with possible source rocks.

The techniques used in achieving these goals are the API gravity and sulfur content measurements, column chromatography, thin layer chromatography, gas chromatography, and the combined gas chromatography-mass spectrometry. The principal classes of biological marker compounds used are n-alkanes, acyclic isoprenoids, tri-tetra and pentacyclic terpanes, and low molecular weight steranes (e.g pregnanes), rearranged steranes, and regular steranes. Multivariate statistical techniques were used to evaluate the data.

1.2. Geographic Setting

The SE Turkey occupies the northern part of the Middle eastern Basin. The oil samples studied from this basin were collected from the oil fields between Miocene Thrust Front in the north and Syrian border in the south (Figure 1.1). The main locations from which oil samples were taken are Adıyaman (Adıyaman-3; Çemberlitaş-16 oils), northern Diyarbakır (Güney Sarıcak-21; Kastel-2), Kozluk (Şelmo-5; Batı Şelmo-4,103; Çelikli-16, 18; Beyçayırı-1; Silivanka-30; Sinan-1, 13; Kurtalan-1; Mağrip-30, 53 oils), Batman (Germik-5, 12; Garzan-15, 17, 90; Batı Raman-211, 167, 176, 193, 189, 43, 84, 56, 47; Raman-197, 193, 84, 63, 93, 87, 192, 157, 151 oils), and Nusaybin (Çamurlu-2, 22; Batı Kozluca-12, Güney Dinçer-3, 15 oils). The study area is situated between 38 00 N and 42 00 N longitudes and 36 00 E and 39 00 E latitudes and covers approximately 90,000 square kilometers (Figure 1.1).

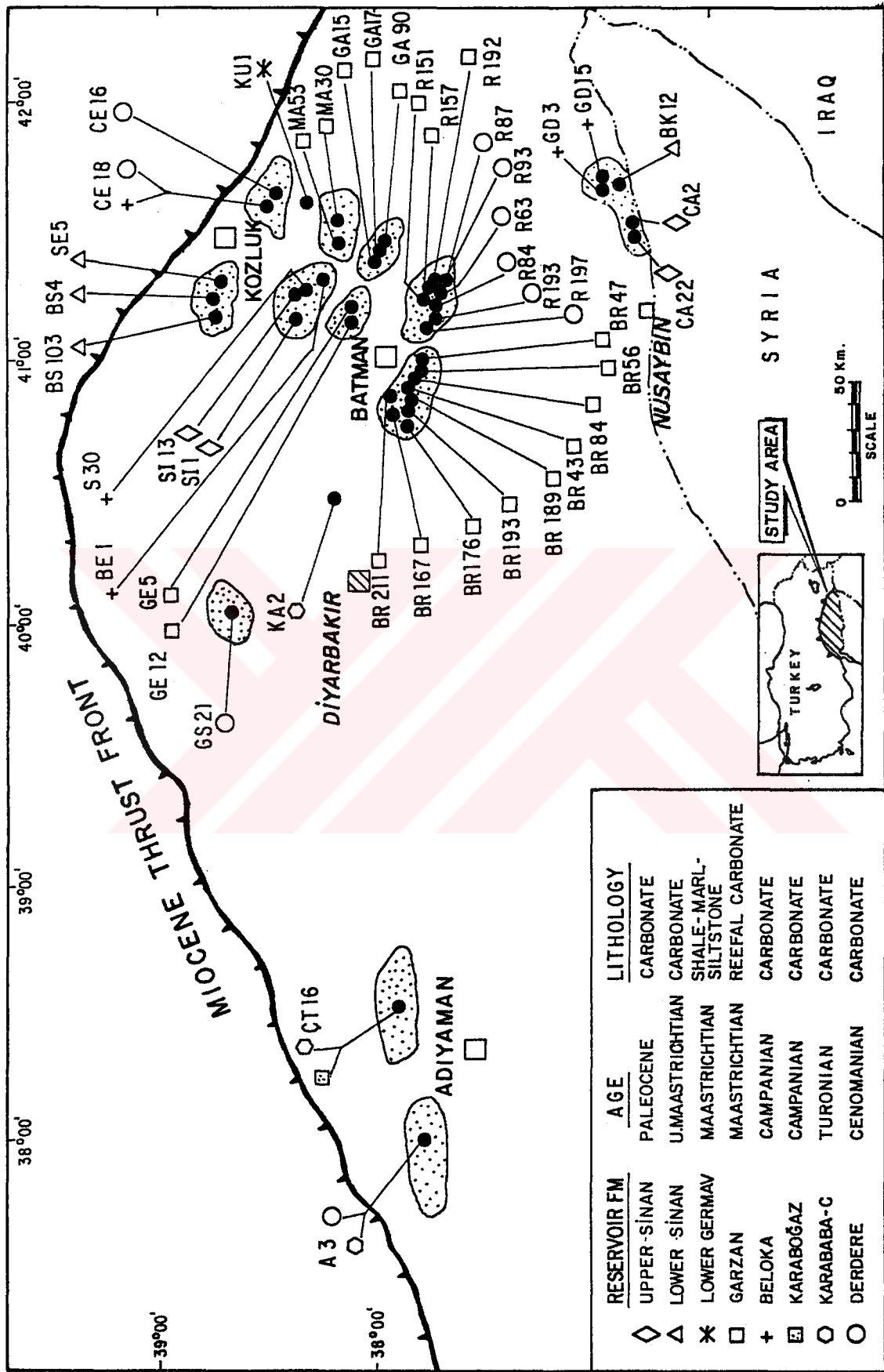


Figure .1.1 Location and reservoir formation of the crude oils examined from the SE Turkey.

1.3. Geologic Setting

1.3.1. General

Southeast Turkey embodies the northwest end of the Persian Gulf sedimentary basins which contain the prolific oil fields of the Middle East. The area of investigation is situated south of the transition zone between Arabian Plate and Alpine-Himalayan orogenic belt where, from north to south, three tectonic elements are recognized: 1. Taurus Orogenic Belt, 2. Foothill Zone, 3. Foreland Zone (folded belt) (Figure 1.2) (Righo de Righi and Cortesini, 1964; Horstink, 1980). The Taurus Orogenic Zone forms the northern boundary of the area of interest in the SE Turkey. This zone is represented by intense tectonism, igneous activity and metamorphism.

The Foothill Zone, located immediately south of the Taurus Orogenic Belt, is a highly disturbed but relatively narrow belt that was affected by at least two major phases of folding, uplift and gravity tectonics. The first phase took place in the Late Cretaceous and caused the formation of the Taurus cordillera. Development of the foothill zone occurred as a result of the second phase tectonism in the late Tertiary. Characteristics of the Foothill Zone are tight, asymmetrical folds, normal and reverse faults, and imbricated structures. Paleozoic rocks show no evidence of metamorphism in the Foothill Zone of SE Turkey. Light oils of SE Turkey with low sulfur content

and high API gravity are produced mainly in the Foothill Zone (Horstink, 1980).

The folded zone of the foreland covers large areas of SE Turkey and NE Syria and is represented by large anticlines in the east-west direction, and many normal and reverse faults (Figure 1.2). Heavy oils of SE Turkey with high sulfur content and low API gravity are produced mainly in the Foreland area (Horstink, 1980).

1.3.2. Stratigraphy

The stratigraphical sequence of the rock units of SE Turkey observed on the continental crust composed of metamorphic and granitic rocks is outlined below (Figures 1.3, 1.4) (Temple and Perry, 1962; Rigo de Righi and Cortesini, 1964; Sungurlu, 1974; Ala and Moss, 1979; Robertson Research Co., 1984; Salem, 1984; Köylüoğlu, 1986; Eseller, 1986; Duran et al., 1988; Bozdoğan and Erten, 1990; Perinçek, 1991).

Telbesmi Formation: It is composed of volcanic and sedimentary units and contains tuffaceous sediments, agglomerate and andesite-spilite lavas together with red sandstones and shales. The age of this unit is Precambrian.

Sadan Formation: The Sadan formation lies unconformably on the Telbesmi Formation and contains reddish-pink metamorphosed quartzites, siltstones,

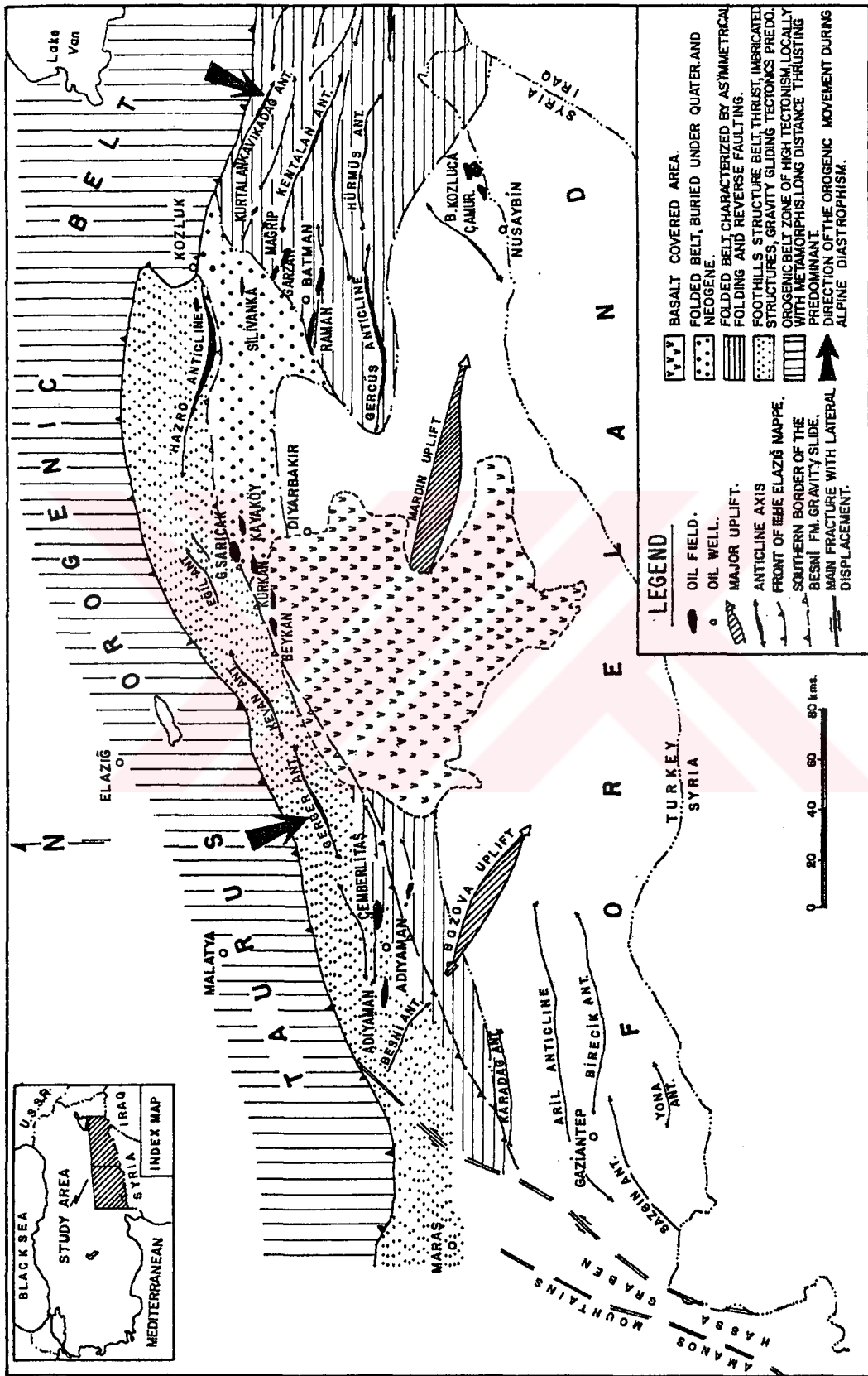


Figure 1.2 Schematic structural map of southeast Turkey. (Rigo & Cortesini, 1964).

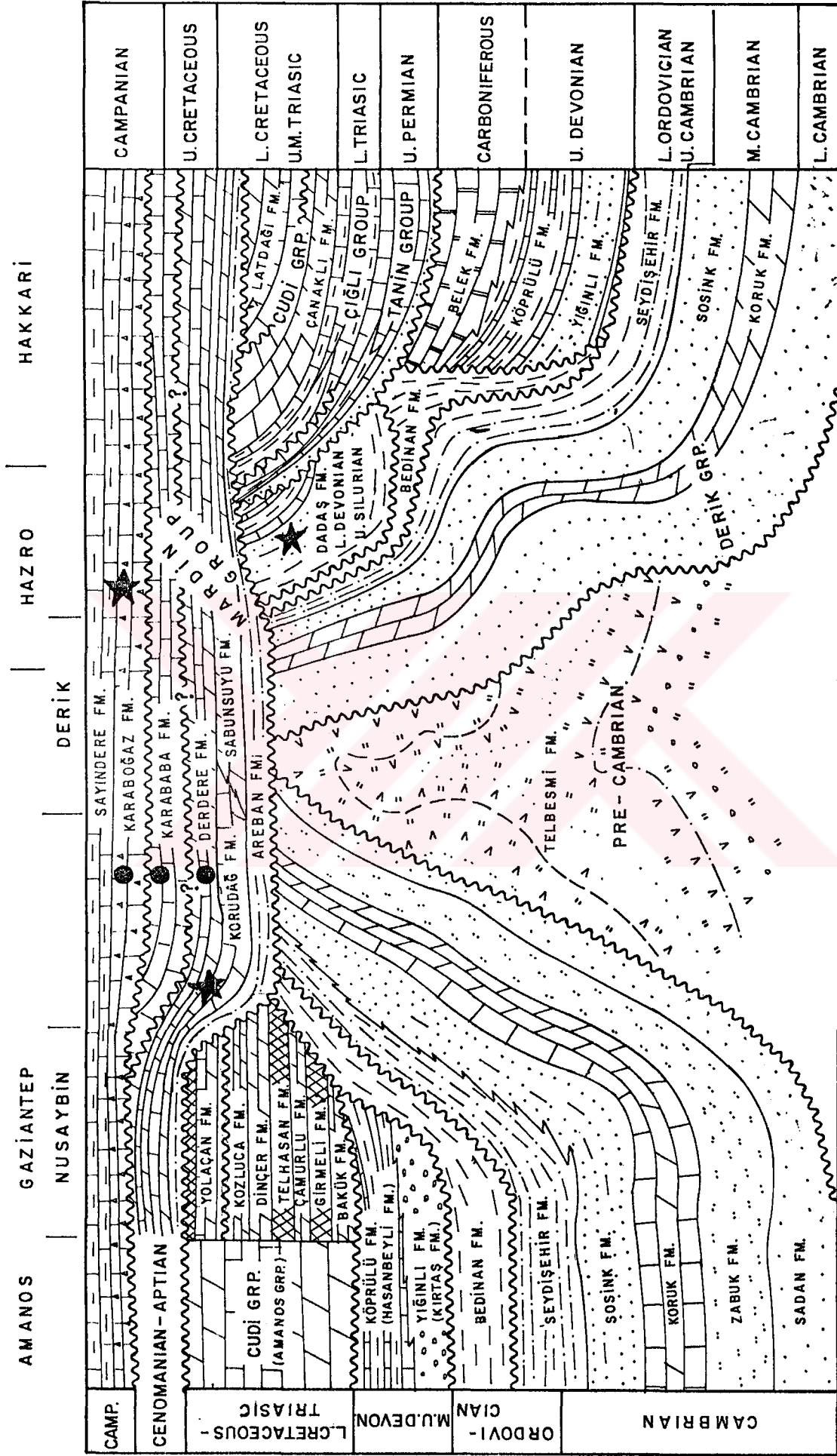


Figure 1.3 Correlation chart of autochthonous Cambrian-Campanian lithostratigraphic units in southeastern Turkey. (After Perinçek, 1991). (●) indicates reservoir zones for produced oils and (★) indicates the rock units having source rock potential.

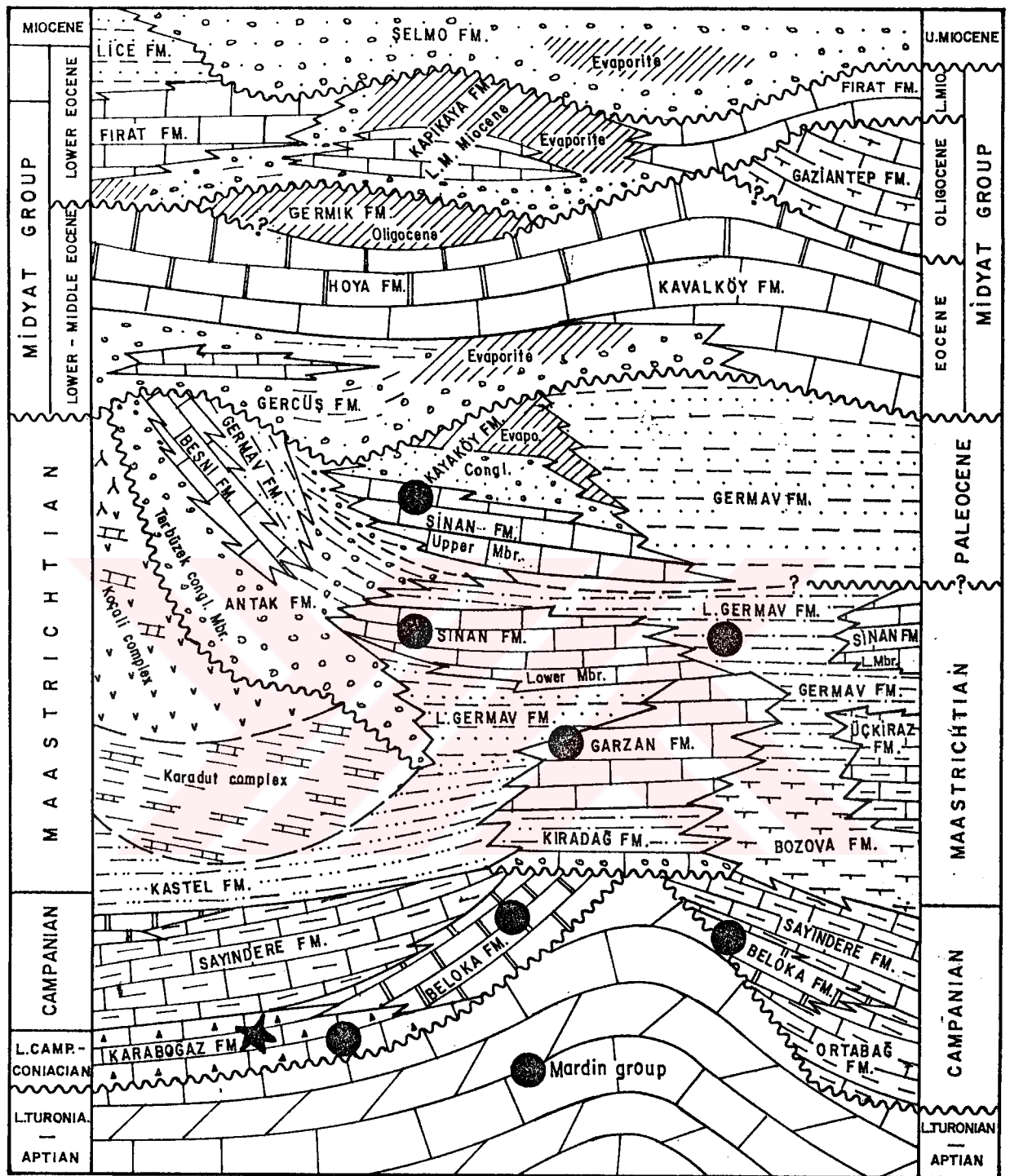


Figure 1.4 Correlation chart of autochthonous lithostratigraphic units in southeastern Turkey. (After Perinçek, 1991). (●) indicates reservoir zones for produced oils and (★) indicates the rock units having source rock potential.

conglomerates, and shales. The age of this unit is thought to be of Early Cambrian.

Koruk Formation: The Koruk formation lies conformably on the Sadan formation and is composed of dolomites and limestone intercalations. The age the Koruk formation is Middle Cambrian.

Sosink Formation: The Sosink formation is made up of quartzite, siltstone, and shale intercalations. The age of the Sosink formation is Middle to Late Cambrian.

Seydişehir Formation: The Seydişehir Formation is composed of shales, siltstones, and sandstones. The age of the Seydişehir formation is early Ordovician.

Bedinan Formation: The Bedinan Formation contains intercalated green-gray and blackish grey shales, silty shales, siltstones, and sandstones. The unit lies unconformably on the Seydişehir Formation. The age of this unit is Late Ordovician. This formation is deposited under deltaic and regressive marine environments.

Dadaş Formation: This unit lies unconformably on the Bedinan Formation and consists of three members. At the base, the Dadaş-I unit is composed of argillaceous limestones and greenish grey shale intercalations. In the middle, the Dadaş-II unit contains dark grey shales. At the uppermost, the Dadaş-III unit contains shales and sandstone intercalations. The age of the Dadaş formation

is Late Silurian to Early Devonian. This formation reflects a regressive marine environment.

Köprülü Formation: The Köprülü Formation of the Hakkari region is made up of blackish to dark grey shale with limestone intercalations. The age of the Köprülü Formation is Late Devonian to Early Carboniferous.

Hazro Formation: This unit overlies unconformably either the Bedinan, Dadaş, or at Hakkari, Köprülü Formations. The Hazro Formation consists of siltstones, sandstones, marl, shale, dolomites, limestones, and coal layers. The age of the Hazro Formation is Late Permian. Oil shows were detected in the Hazro sandstones in many wells.

Gomaniibrik Formation: This formation is made up of intercalated carbonates, shales, sandstones, and coals. The age of the unit is Late Permian.

Çığlı Group: Çığlı Group lies unconformably on the Gomaniibrik Formation. The basal unit of the Çığlı Group comprises carbonates which is overlain by red coloured shales with limestone intercalations. The uppermost part of the unit is represented by argillaceous micrites. The age of the Çığlı Group is Early Triassic.

Cudi Group: Cudi Group is divided into two formations in the Hakkari region, the Çanaklı Formation at the bottom and the Latdagi Formation at the top, whereas

in the Çamurlu region, the Cudi Group is divided into seven formations;

1. Bakük Formation (Dolomites, Limestones), 2. Girmeli Formation (Evaporite), 3. Çamurlu Formation (Dolomites), 4. Telhasan Formation (Evaporite), 5. Dinçer Formation (Dolomite), 6. Kozluca Formation (Evaporite-Dolomite), and 7. Yolaçan Formation (Dolomite) (Figure 1.3).

The Çanaklı Formation may be the lateral equivalent of the Bakük-Girmeli-Çamurlu-Telhasan-Dinçer, and/or Kozluca Formations whereas the Latdagi Formation may be synchronous with the Yolaçan Formation. The age of the Cudi Group is Early Triassic to Late Jurassic. The Cudi Group could be a significant source rock candidate since recent data on organic geochemistry of carbonate-evaporate rocks suggested that organic matter can also be preserved in evaporitive conditions (Malek-Aslani, 1980).

Mardin Group: The Mardin Group is divided into four formations; The Areban Formation, the Sabunsuyu Formation, the Derdere Formation, and the Karababa Formation. The Areban Formation contains cross-laminated sandstones and thin bedded limestone intercalations. The age of the Areban Formation is Aptian-Albian.

The Sabunsuyu Formation consists of dolomites, limestones and calcareous dolomites and is of Cenomanian age. The Derdere Formation is represented by medium to thick bedded dolomites and carbonates. It has a source rock potential in the Adıyaman region (Soylu,1991). It is of Cenomanian age. The Karababa Formation is divided into three members as a, b, and c. Much of the oil in SE Turkey is produced from the c member, particularly in the Adıyaman and northern Diyarbakır regions. The Karababa-a member has source rock potential in the Adıyaman area (Soylu, 1991).

Karaboğaz Formation: There is an angular unconformity between this formation and the Mardin Group. The Karaboğaz Formation is represented by phosphatic and cherty limestones in the Adıyaman area whereas in the Kozluk area it is represented by clayey, cherty limestones. In both, Adıyaman and Kozluk areas, it has an excellent petroleum source rock potential (İzitan, 1987; Soylu, 1991). The age of the Karaboğaz Formation is Campanian.

Sayındere formation: The unit consists of mainly argillaceous limestones. It has an important cap rock capacity for the Karababa-C reservoired oil. The age of the unit is also Campanian.

Beloka Formation: This unit is laterally transitional to the Sayındere Formation. The Beloka Formation is composed of reefal limestones which were

deposited on highs caused by tectonism. It is an oil producing formation in eastern part of the study area. The age of the this unit is of Campanian.

Şırnak Group: The age of the Şırnak Group is Late Campanian to Paleocene. This Group is divided into five formations; the Kastel Formation, the Kıradağ Formation, the Bozova Formation, the Germav Formation, and the Garzan Formation. The Kastel formation formation was deposited in an elongate, narrow, and deep trough appeared in front of the northern cordillera during the Late Campanian and Early Maastrichtian. It is composed of shales and turbiditic sandstones. Deposition of the Kastel Formation was frequently interrupted by the gravity slides of the Koçali and Karadut Complexes.

Kıradağ Formation: After the deposition of Beloka Formation the deposition of the Kıradağ Formation which consists of conglomeratic limestones, shales, and sandstones took place. While the Kıradağ Formation was deposited on the highs the Germav Formation or the Bozova Formation and the Kastel Formation were deposited in the deeper part of the study area.

Bozova Formation: This formation is made up of marls and argillaceous limestones which pass upwards into the Germav formation.

Germav Formation: The unit is made up of the intercalations of the sandstones and the shales. In the eastern part of the study area, it has significant cap

rock capacity for the oils accumulated in the Garzan Formation. The age of the Germav Formation is Upper Cretaceous to Paleocene.

Garzan Formation: The unit is composed of very fossiliferous reefal limestones. The Garzan Formation has reservoir capacity particularly in the Batman-Kozluk areas.

Sinan Formation: The Sinan Formation was deposited on the locally shallow uplifted areas of the Germav Sea. It is made up of reefal limestones. It is an oil producing reservoir rock in the Kozluk and Nusaybin areas.

Antak Formation: This formation was deposited on top of the allochthonous units, particularly, in the Diyarbakır region. It is represented by sandstones and conglomerates with shale intercalations.

Kayaköy Formation: This formation is also deposited in the Diyarbakır area. It is composed of mainly evaporites which is laterally equivalent to the Antak Formation.

Terbüzek Formation: After the deposition of the upper Kastel unit over the allochthonous units in the Diyarbakır area, the deposition of the Terbüzek Formation took place. It is made up of red coloured conglomerates and sandstones deposited in terrestrial environment.

Besni Formation: This formation was also deposited in the Diyarbakır area. It is consisted of fossiliferous limestones.

Midyat Group: The age of the Midyat Group is of Oligocene to Early Miocene. It overlies the Şırnak Group with an angular unconformity. The Midyat Formation is divided into 6 formations; 1. Gercüş Formation (red clastics), 2. Becirman Formation (limestones), 3. Hoya Formation (limestones), 4. Gaziantep Formation (limestones), 5. Fırat Formation (limestones), 6. Germik Formation (clastics, evaporites), 7. Lice Formation (clastics), 8. Kapıkaya Formation (evaporate, clastics).

Şelmo Formation: The Şelmo Formation comprises sandstones, mudstones, and conglomerates of terrestrially derived clastics. The age of the unit is Late Miocene.

Late Miocene Allochthonous Units: During the late Miocene time, the allochthonous sediments advancing from north to south covered the northern part of the Arabian-African shelf area. The Çüngüş Formation, Maden Complexes, Güleman ophiolites, and Bitlis-Pötürge metamorphics were emplaced onto the shelf sediments in succession.

Pleistocene aged Rocks: The high level of volcanic activity resulted in up to 500 meters thick Karacadağ basalts in the Diyarbakır-Karacadağ area. In other areas, the deposition of terrestrial clastics occurred.

1.3.3. Geological Evolution

By reason of its regional setting, geological evolution of SE Turkey was much affected by many tectonic pulses that consequently influenced its depositional history. Evidence of tectonic instability is provided by numerous disconformities (Figures 1.3 and 1.4).

Telbesmi formation deposited on the metamorphic-granitic continental crust in a regional scale. The deposition of the clastic sediments continued until Middle Cambrian which is the time of carbonate deposition on the gradually stabilized shelf as a consequence of decreasing material transport from the land. This was accompanied by the accumulation of micritic limestones and dolomites of the Koruk formation in the deepening sea. During the Middle to Late Cambrian times, as a result of decreasing stability of the land areas, carbonate deposition eventually gave way to deposition of the clastic sediments of the Sosink Formation. These clastics lie conformably on the limestones of the Koruk Formation. As the sea level gradually decreased, the Seydişehir Formation was deposited in a shallow marine environment. During the Late Ordovician to early Silurian times deltaic and regressive marine cycles caused the deposition of the clastic Bedinan Formation. During early Silurian times an erosional event occurred and was followed by deposition of the Dadaş Formation in a neritic to supratidal environment.

The most crucial unconformity recognized in this area is observed at the base of the Permian sediments (Figure 1.3). During the first stage of deposition, clastics of the Hazro Formation were deposited as a result of transgression. This was followed by regressive neritic carbonates, coals, clastics, and neritic carbonates of Gomanibrik formation. The Early Ordovician aged Mardin-Kahta uplift (Bozdoğan and Erten, 1990) controlled Triassic sedimentation with no deposition in that area. Çiğli Group were deposited on a stable platform in a shallow marine environment during a regressive period.

Cudi Group which has a transitional contact with the Çiğli Group was deposited under wave and tide dominated conditions during the Early Triassic to Late Jurassic times. Early Cretaceous sediments were also deposited but were removed by the erosional event which caused the important gap between the Cudi and the Mardin Groups. In the Aptian times, a new transgressive phase was initiated and deposition of the Mardin Group began to develop in the shallow sea areas. At the same time, subduction of the Arabian-African plate under the Anatolian plate led to the development of a compressive regime in which a part of the oceanic crust and some continental margin sediments were thrust over the Arabian-African continental crust in the south. This collision of the two continents during early Cretaceous time caused the central parts of the SE Turkey to be folded and uplifted.

Sedimentation continued with deposition of organic rich Karaboğaz Formation on the shelf area to the south. The Koçali and Karadut complexes were emplaced when the overthrust sheets lost their stability and started sliding into the Kastel through (Figure 1.4). With erosion of the shelf area, the other units of the Şırnak Group were deposited under the widely varying environmental conditions.

During Early Eocene times another transgression occurred and this caused the uplifted areas to be covered by the Paleocene sediments. As a result of this transgression, Gercus Formation was deposited. Continuation of this transgression to middle to late Eocene times resulted in the deposition of Hoya Formation over an extensive area.

After a non-depositional or partly erosional stage in the Oligocene, transgressional effects were once again dominant in the area. During this time, carbonates of the Fırat and the Germik formations were deposited in the northern central part of the study area. After a period of continental conditions, Şelmo formation was deposited in the shallow areas.

Miocene time reflects high tectonic activity which caused the rhythmic changes in the depth of the Miocene sea. In the course of these tectonic events the continental crust was folded and faulted with deformation becoming more intense from south to north. During the

Pleistocene, extensive volcanic activity resulted in the wide-spread exposures of the Karacadağ basalts.

1.4. Previous Work

1.4.1. Oil to Oil Correlations

There are a number of studies related to genetic oil classification of SE Turkey. Buchanan (1974) suggested geologic evidence that oils of the SE Turkey have a common origin and compositional differences in the oils are the results of the losses in various light-end hydrocarbons along the fractured zones. The preliminary study of "oil to oil correlations" in the SE Turkey was first carried out by the author (Gürgey, 1983) on the basis of bulk chemical composition, general character of n-alkanes, acyclic isoprenoids and sulfur compounds where eight oils from the northern Diyarbakır, Batman, and Nusaybin area were found to be separated into two main groups (Table 1.1).

Later work by Savcı (1983) using gas chromatography- mass spectrometry, stable isotope ratios, vanadium, and nickel contents revealed that two genetically different oil groups in the Batman Kozluk, and Nusaybin area existed (Table 1.1).

The most extensive oil to oil correlation study, however, was carried out by Robertson Research Co. (1984). Thirty oil samples were analyzed and supported by stable

Table-1.I Previous Groupings of the SE Turkey oils.

AUTHOR	OIL GROUPS				
	I	I-II	II	III	IV
Buchanan (1974)	————— ONE GRUP —————				
Gürgey (1983)	B.Raman Raman Çamurlu	Garzan Germik			G.Sarıcak Yenikoy
Savcı (1983)	B.Raman Raman Çamurlu G.Dincer	Garzan	Selno Çelikli		
Robertson Research Co. (1984)	B.Raman Raman Çamurlu G.Dincer Magrip	Garzan	Selno Celikli Oyuktas Beycayırı Sılivanka	Kahta Adıyaman Çemberlitas Bolukyayla Piyanko	Sarıcak Yeniköy Beykan Kurkan Barbes
Gurgey (1987)	B.Raman Raman G.Dincer Çamurlu	Magrip-30 Raman-178	B.Selmo Celikli Sılivanka Germik Garzan		
Chevron Oil Research Co. (1987)	Raman G.Dincer Magrip Garzan Selmo Celikli Cemberlitas B.Fırat				G.Sarıcak G.Kayakoy
Gurgey (1989)	B.Raman G.Dincer Çamurlu Kozluca		Garzan Germik Sılivanka Celikli Selmo	Adıyaman Cemberlitas	Yenikoy Sarıcak

carbon isotope data. Biomarkers such as steranes and terpanes were used in order to differentiate the oils according to their genetic relations. Subsequently, at least four groups of oil were classified (Table 1.1).

The results of author's (Gürgey, 1987) study was in agreement with the conclusions drawn by Savci (1983) that there were two groups of oil in Batman, Kozluk, Nusaybin areas but, in addition a "mixed origin oil" was also introduced. However, oils of the group II showed systematic changes in bulk and chemical parameters as well as in sterane and terpane distributions from south to north where these variations in the oil compositions of group II were attributed to the effect of thermal maturity on the oils (Table 1.1).

Chevron Oil Company (1987) reported oil grouping similar to Gürgey (1983) study that Güney Sarıcak and Güney Kayaköy oils are completely different from the eight oils from Batman, Kozluk, and Adıyaman areas. The differences in oil gravity and sulfur content in the oils of group II were interpreted to different levels of thermal maturity. In their study, the most distinguishing parameter of the oils was pristane to phytane ratio. Excluding Group I oils, all the oils of group II show very similar carbon isotope ratios. The work of Chevron Oil Co. is interesting because it is the first time that two of the oils (eg. Çemberlitaş and Fırat oils) from the Adıyaman area have been considered to have been generated from the same source rock as in the Kozluk-Batman-

Nusaybin area oils (e.g. Batı Raman, Raman oils etc.) (Table 1.1).

The most recent work related to correlation of SE Turkey oils was included in a multivariate statistical approach by the author (Gürgey, 1989). The data matrix consisted of 14 oils and 10 correlation parameters which were derived from stable carbon isotopes, column chromatography, sulfur content, and gas chromatography. As a result of this statistical approach, the author proposed four different group of oils in SE Turkey and variation in oil composition in all of the oils probably resulted from the different group of organic matter and different levels of thermal maturity (Table 1.1).

1.4.2. Suggested Source Rocks

Since very limited oil to source correlation studies present, an identification of the source rock(s) was one of the more controversial problems in the petroleum geochemistry of the SE Turkey oils. The suggested source rocks by the earlier workers included either geological considerations between the source rock candidates and reservoir oils or geochemical properties of the oils. On the basis of geologic considerations, in many cases, different source rocks for the same oils were reported.

Ala and Moss (1979) proposed the Germav Formation as a source rock for the Batman area oils. A geological

study by Horstink (1980), on the other hand, claimed that in SE Turkey, the present source rock units are grouped under three geologic ages of Paleozoic, Lower Mesozoic and Cretaceous. However, he did not name a specific rock group or formation. Horstink (1980) believed that mature Paleozoic source rocks are confined to immediately north of the present Sarıcağ and Yeniköy oil fields. He also reported that mature Lower Mesozoic source rocks are found in the eastern part of the Batman area oil fields and these rocks generated oils with low API gravity and high sulfur content similar to those in the Raman, Garzan, and Germik oil fields.

Erdoğan and Akgül (1981) proposed Ordovician aged Bedinan formation as the source rock for the oils produced from Aptian-Turonian aged Mardin Group carbonate reservoirs. Using variations in the API gravity and sulfur content of the oils, formation water salinity, reservoir temperatures and pressures, they employed a re-entrapment model of Gussow's (1954) to understand the migration pathways directions of the oils in the Mardin Group reservoirs. They claimed that changes in the oil composition are most likely resulted from processes encountered during a long history of "continuous migration". They also reported that Mardin-Kahta Uplift played a major role in the determination of migration direction in the Mardin reservoirs. They ruled out the hydrocarbon contributions of Upper Maastrichtian-Paleocene Germav shales to the Mardin oils because Germav Shale has generated oil but it has never been expelled out yet.

Geochemical considerations covered either "oil to source rock correlations" or "oil to oil correlations", however there are only a few successful oil to source rock correlation studies (Robertson Research Co., 1984). Accordingly, Upper Silurian Dadaş formation is appeared to be the source for the light oils (API>34) produced from Mardin Group reservoirs in northern Diyarbakır. Lebküchner et al., (1972) reported the similarities in infra-red spectrum between the CS₂-soluble part of the Harbol asphaltic substances and crude oil sample from the Raman oil field. Lower Mesozoic aged Cudi Group was proposed to be a source of the Raman field oils that also supports the idea of Horstink's (1980). In the following years, speculation on the genesis and group of the source rocks of SE Turkey using crude oil properties has been continued (Harput et al., 1986; Gürgey, 1987; Exxon Production Company, 1988). Harput et al., (1986) suggested the long distance migration pathways from the eastern Batman area to the Batman area similar to the model developed by Horstink (1980). They thought that decreasing API gravities in the Raman, Batı Raman, Garzan, and Germik oils are the results of the migration of these oils from east to westerly direction. Therefore, Harput et al., (1986) proposed that Cretaceous Üçkiraz-Ortaboğaz-Sayındere-Mardin-Karaboğaz formations in the area are most likely the source of oils produced in the Batman area.

The author (Gürgey, 1987) reported a short distance migration for the Batman, Kozluk and Nusaybin

oils based upon linear correlations between reservoir depths, bottom hole temperatures, and bulk and molecular level compositions of the reservoir oils. The author also reported that source rock could be calcareous in character and they should be very close to adjacent reservoir oils.

Recently, based on evolution of the phytoplanktons (Tappan and Loeblich, 1973) and sterane carbon number distribution in the oils (Grantham and Wakefield, 1988), a method has been developed to predict the age of the source rocks which is also adopted in this study. The method was applied to the Turkish oils by Exxon Production Co., (1988) but only one oil was analysed from the Şelmo oil field. It was found out that Şelmo field oils were derived from a Middle Cretaceous source rock (s).

1.5 Nomenclature

The symbols and abbreviations related to this study are listed in Table 1.2.

Location area, field/wells, and abbreviations for the oil wells (oil samples) are given in Table 1.3.

Biomarkers: Many papers cite the discovery of porphyrin pigments in geological materials by Trebs (1936) as the beginning of organic geochemistry. It was certainly the first step in that part of organic geochemistry which is now usually referred to as the study of "biological

Table-1.2 List of the symbols and abbreviations.

API.....American Petroleum Institute

API Gravity....Oil Gravity at 60°F in degrees API

ARO.....Aromatic hydrocarbons

ASPH.....Asphaltenes

$$\delta^{13}\text{C} \dots \delta^{13}\text{C} = \frac{\text{C}^{13}/\text{C}^{12} \text{ (Sample)} - \text{C}^{13}/\text{C}^{12} \text{ (Standard)}}{\text{C}^{13}/\text{C}^{12} \text{ (Standard)}} \times 1000$$

$\delta^{13}\text{C}$; Stable Carbon Isotope Ratio relative to PDB Standard

CPI.....Carbon Preference Index

GAM.....Gammacerane

GC.....Gas Chromatography

GC-MS.....Gas Chromatography-Mass Spectrometry

H.....High Total Organic Carbon Content (0.5-1.5 wt %)

L.....Low Total Organic Carbon Content (0.3-0.5 wt %)

m/z.....Mass/Charge Ratio

NSO's.....Heterocompounds

PC.....Principal Component

PCs.....Principal Components

PC1.....The First Principal Component

II-S.....Sulfur Rich, Type II Kerogen

SAT.....Saturated Hydrocarbons

TOC.....Total Organic Carbon

Tm.....18 α (H)-22,29,30 Trisnorhopane

Ts.....17 α (H)-22,29,30 Trisnorhopane

Tmax.....Temperature at which maximum kerogen degradation occurs

Pr.....Pristane

Phy.....Phytane

V.L.....Very Low TOC Content (TOC<0.3 wt %)

Table-1.3 Location area, field/wells and abbreviations used for the oil samples investigated in this study.

FIELD WELLS	ABBREVIATIONS USED IN THIS STUDY	LOCATION AREA
1 Celikli-18	CE18	Kozluk
2 Celikli-16*	CE16*	Kozluk
3 Selmo-5	SE5	Kozluk
4 Batı Selmo-4*	BS4*	Kozluk
5 Batı Selmo-103	BS103	Kozluk
6 Sinan-13	SI13	Kozluk
7 Siliyanka-30*	S30*	Kozluk
8 Sinan-1*	SI1*	Kozluk
9 Kastel-2*	KA2*	Northern Diyarbakır
10 Kurtalan-1*	KU1*	Kozluk
11 Beycayırı-1*	BE1*	Kozluk
12 Magrip-53	MA53	Batman
13 Magrip-30*	MA30*	Batman
14 Garzan-17	GA17	Batman
15 Garzan-90	GA90	Batman
16 Garzan-15*	GA15*	Batman
17 Germik-12	GE12	Batman
18 Germik-5*	GE5*	Batman
19 Raman-87*	R87*	Batman
20 Raman-192*	R192*	Batman
21 Raman-157	R157	Batman
22 Raman-63*	R63*	Batman
23 Raman-193	R193	Batman
24 Raman-151*	R151*	Batman
25 Raman197*	R197*	Batman
26 Raman-84*	R84*	Batman
27 Raman-93*	R93*	Batman
28 Batı Raman-47*	BR47*	Batman
29 Batı Raman-56*	BR56*	Batman
30 Batı Raman-84*	BR84*	Batman
31 Batı Raman-43*	BR43*	Batman
32 Batı Raman-211*	BR211*	Batman
33 Batı Raman-193	BR193	Batman
34 Batı Raman-189*	BR189*	Batman
35 Batı Raman-167*	BR167*	Batman
36 Batı Raman-176*	BR176*	Batman
37 Camurlu-2	C2	Nusaybin
38 Camurlu-22*	C22*	Nusaybin
39 Batı Kozluca-12*	BK12*	Nusaybin
40 Guney Dincer-3*	GD3*	Nusaybin
41 Guney Dincer-15	GD15	Nusaybin
42 Guney Sarıcak-21*	GS21*	Northern Diyarbakır
43 Adıyaman-3*	A3*	Adıyaman
44 Cemberlitas-16*	CT16*	Adıyaman

* samples analyzed by using Gas Chromatography-Mass Spectrometry.

marker" organic compounds. Although the terms "chemical fossil" (Englinton and Calvin, 1967) and "molecular fossil" (Calvin, 1963) have also been introduced, it is the epithet "biological marker", first coined and commonly used, and often shortened to "biomarker" by Seifert and Moldowan (1981). A biomarker is any organic compound detected in the geosphere whose basic skeleton suggests an unambiguous link between a known, contemporary natural product (Mackenzie, 1984).

The basic structural building block of the biomarkers is the isoprene unit (Figure 1.5a). Two isoprene units joined end-to-end form a monoterpene (Figures 1.5b and 1.5c). Six isoprene units can be joined either to form a "sterane" (Figure 1.5d) or a "terpane" (Figure 1.5e), depending upon how the linking is accomplished (Mackenzie, 1984).

Steranes usually contain four rings, the D-ring of which always contains five carbon atoms (Figure 1.5d). Terpanes contain three to six ring (Figure 1.5e) with five-ring (pentacyclic) species being most common. Chemical structure and naming of the sterane and terpane biomarkers is given in Appendix A.

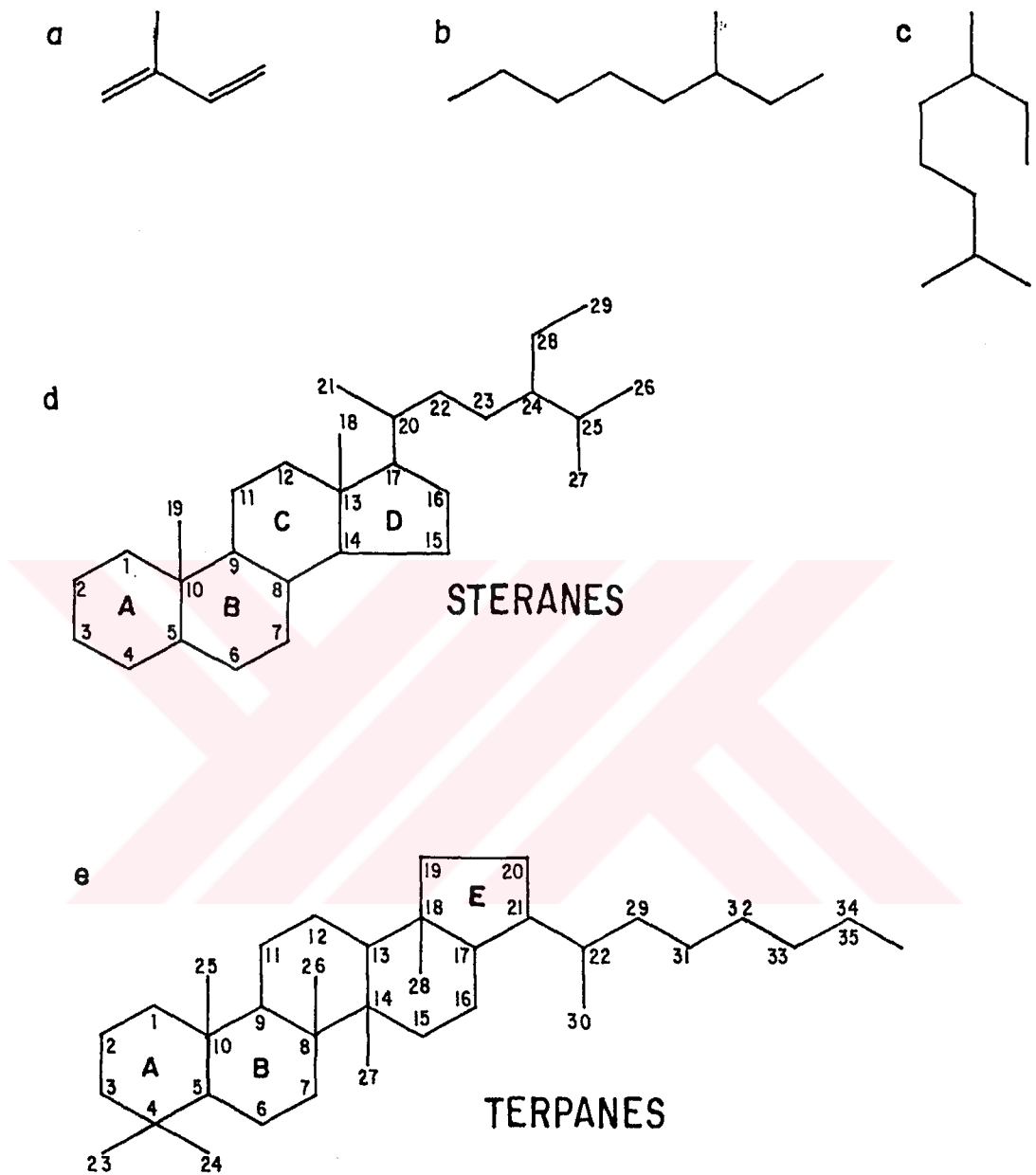


Figure 1.5 Chemical structure for isoprene (a), and two ways of drawing a monoterpene formed from two isoprene units (b,c) and numbering system of steranes (d) and terpanes (e).

CHAPTER II

METHODS OF STUDY

2.1. Sampling

Forty-four crude oil samples from seventeen oil fields in SE Turkey were collected from well-sites during the summer of 1987 and 1988. The crude oil samples taken from individual oil fields are mostly situated in the Batman, Kozluk, and Nusaybin areas (Figure 1.1) because of the problems of their wide changes in composition and unknown source rocks. There are only two samples from northern Diyarbakır area and two samples from Adıyaman area. Collected oil samples are believed to represent the general character of the oils throughout SE Turkey. Abbreviations used for the oil samples are shown in Table 1.3 which will be used in the same manner throughout this study. Location and reservoir formation of the 44 oil samples analysed in this study is shown in Figure 1.1.

Crude oil samples investigated in this study are produced from carbonate reservoir rocks that range in age from Lower Cretaceous to Upper Cretaceous- Paleocene and production depths range from 1300 to 3400 meters.

2.2 Analytical Procedure

Forty-four oil samples were analyzed for their bulk composition (e.g. API gravity, sulfur content, saturate, aromatic, NSO's, and asphaltene fractions) and their n-alkane distributions. Based on the data obtained from these analyses, similar samples, especially when oils are from the same oil field, were eliminated furthermore the number of oil samples was reduced from 44 to 32. Further analyses of 32 samples were done by introducing them into gas chromatography-mass spectrometry to obtain m/z 191 (terpane) and m/z 217 (sterane) mass fragmentograms. The oil sample S5 was not used for the terpane data set due to improper m/z 191 terpane fragmentograms. Therefore, terpane data was available only for 31 oils while the sterane data was available for 32 oils. Analytical flow chart followed in this study is shown in Figure 2.1 which was briefly described below.

2.2.1. API Gravity

In order to determine API gravity of the oils, refractive index (RI) of the oils were measured by using a Carl Zeiss-89578 model Abbe Refractometer. Measured RI were then converted to API gravities on a calibrated RI versus API gravity crossplot. Calculated API gravities were further converted to those of 16 C (60 F) since the temperature of the laboratory was 18 C (65 F) during measurements.

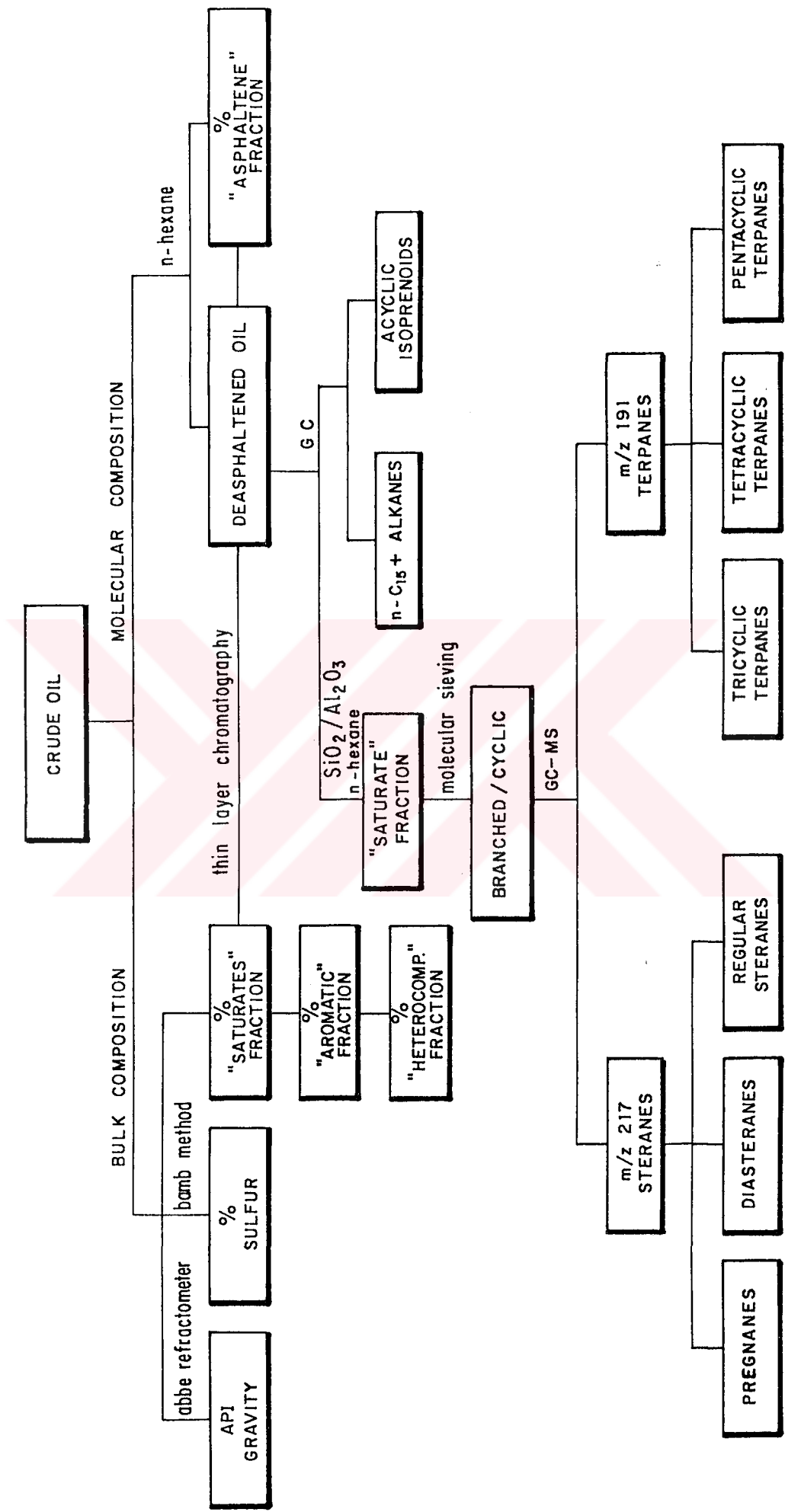


Figure - 2.1 Analytical flow chart employed to the crude oil samples.

2.2.2 Sulfur Determinations

Initially, oil samples were oxidized by combustion in a bomb containing oxygen under pressure. The sulfur, as sulfate in the bomb washing, was determined gravimetrically as barium sulfate using the following equation:

$$\text{Sulfur, (Wt \%)} = (P-B) 13.73/W$$

where;

P: grams of BaSO₄ obtained from samples,

B: grams of BaSO₄ obtained from blank, and,

W: grams of sample used.

2.2.3 Deasphalting

Forty milliliters of n-hexane (Merck, extrapure) per gram of crude oil were added and the mixture was allowed to stand for at least 24 hours. The n-hexane solution was decanted on a Millex-SR 0.5 mm filter paper. Asphaltene fraction was washed with two 10 ml aliquots of n-hexane. The n-hexane washings were further blended with the original n-hexane solution. The precipitated and washed asphaltenes were dried under nitrogen flow in the hood and then weighed. The values obtained were recorded as "weight percent asphaltenes". The rest of the sample was kept for column chromatography analysis.

2.2.4. Thin Layer Chromatography

The amount of saturated hydrocarbons, aromatic hydrocarbons, and heterocompound (NSO's) fraction of the deasphalted oils was obtained using a Iotrascan-Thio Model thin layer chromatography. The instrument has a flame ionization detector (FID) and chromarod-SII (micro powder silicagel coated) rods on which 1 ml sample is injected. Saturate, aromatic and NSO fractions were then obtained quantitatively using n-hexane (100 ml), n-hexane+toluen (25 ml+75 ml), and dichloromethane + methanol (95 ml+5 ml) respectively. The values obtained were then recorded as weight percent "saturated hydrocarbons, aromatic hydrocarbons, and heterocompounds".

2.2.5. Column Chromatography

The deasphalted oils were separated into saturated hydrocarbons and aromatic hydrocarbons using column chromatography as an initial stage of preparing samples for gas chromatography-mass spectrometry (GC-MS) analysis. The glass column used is 50 cm long with 1 cm inside diameter. Bottom 35 cm of this column was then filled with the slurry of n-hexane and activated silicagel (Merck, 70-230 mesh). The slurry of n-hexane and activated alumina (Merck, 70-230 mesh) then was added to the top of the glass column. After introducing 100 mg of deasphalted oil into the column, 100 ml of n-hexane was added. The eluate was placed in a hood with nitrogen flow

to evaporate the n-hexane. The remaining is saturated hydrocarbons.

After the whole n-hexane was drained from the column n-hexane+toluen (75 ml + 25 ml) mixture were added to elute the aromatic hydrocarbons.

2.2.6 Gas Chromatography

A gas chromatographic analysis of the saturate fractions was carried out on a "Varian 3700 FID Capillary Gas Chromatograph" using a 25 m WCOT/OV-101 (0.22 mm ID) column. Prior to analysis, oils were evaporated to constant weight at 70 C to overcome difficulties caused by the low molecular weight fractions (less than C15). The parameters which were used during the analyses are:

Initial Temperature: 30 C
Initial Hold : 2 min.
Rate : 4 C/min.
Final Temperature : 270 C
Final Hold : 60 min.
Injection Temperature: 300 C
Detector Temperature : 300 C

2.2.7. Molecular Sieving

The saturated fraction of the oils obtained from the column chromatography analysis was molecular sieved to remove n-alkanes, leaving the branched/cyclic fraction for

GC-MS. "Altech, 5A-1/16" molecular sieves were used. The sieves and cyclohexane (Merck, extrapure) solvent were added to the samples and were allowed to stand for at least 24 hours. Branch/cyclic fraction in the solvent was concentrated under nitrogen and then weighed.

2.2.8. Gas Chromatography-Mass Spectrometry

Combined GC-MS analyses were performed on 5980 model HP gas chromatograph directly connected to a Hewlett Packard 5988A mass spectrometer with electron energy of 70 eV under the control of "HP Chem-Station Series 300 Data System". The carrier gas for both GC and GC-MS was He which was 7 psi and 25 psi for 30 m and 60 m GC columns respectively. Data were collected by multiple ion detection (MID), monitoring ions at m/z 177, 191, 217, 218, 259. For the purpose of this study, only the data on m/z 191 (terpanes) and on m/z 217 (steranes) was investigated. Identification of the biomarker peaks on m/z 191 and m/z 217 mass fragmentograms was based on a comparison of relative retention times with those outlined in the literature (Palacas et al., 1984; Sofer et al., 1985; Clark and Philp, 1989). Quantitation of the peaks was done measuring the appropriate peak heights on the mass fragmentograms.

2.3. Multivariate Statistical Analysis

Principal component analysis (PCA) which is also known as a multivariate factor analysis technique was

applied to the various combination of sterane and terpane data in order to extract more information and as a tool to visualize the compositional variations within the forty-four SE Turkey oils (Q-mode). PCA also highlights which parameters are the most significant in discriminating the oil samples (R-mode). The input data set for PCA and the computer flow chart of this statistical technique is given in Figure 2.2. A more detailed information concerning the PCA technique is given in Appendix B.



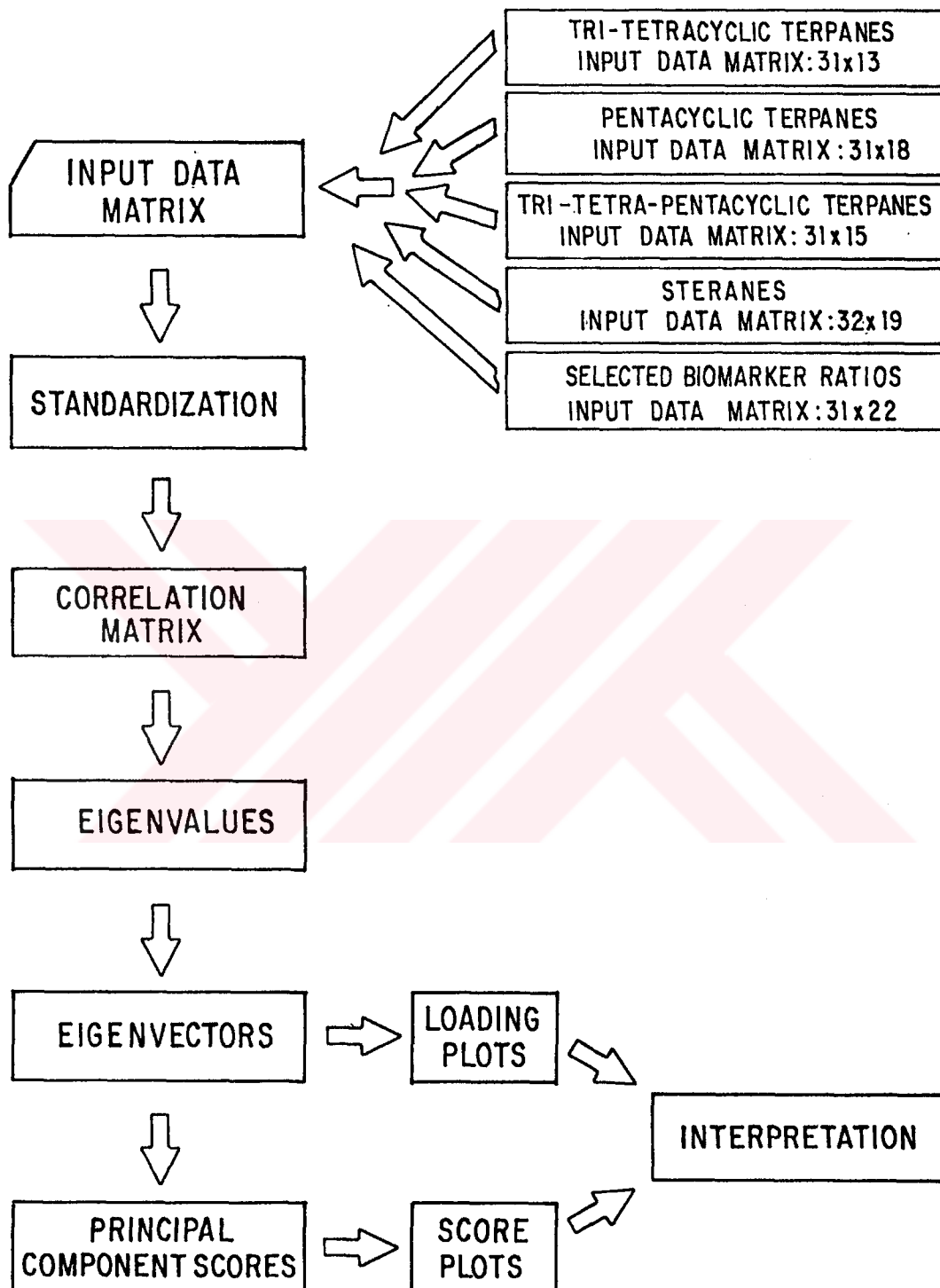


Figure_ 2.2 Computer flow chart of principal component analysis applied to the biomarker data.

CHAPTER III

RESULTS

Forty-four crude oil samples from SE Turkey were analyzed according to the procedure outlined in Figure 2.1. Depth, age, temperature, and formation of the reservoir oils are given in Table 3.1. In the following section, the data obtained from these analyses are presented.

3.1. Bulk Compositional Data

Bulk composition in terms of API gravity, sulfur content (%), saturates (sat, %), aromatics (aro, %), heterocompounds (NSO's, %), and asphaltenes (asph, %) fraction of the oils is given in Table 3.2 where API gravity (12-35), sulfur content (0.41-7.21 %), saturates (8-86 %), aromatics (9-44 %), heterocompounds (3-28 %), asphaltenes (5-55 %), and saturate/aromatic ratios (0.3-9.1) show a wide variation.

Based on the percentages of saturate hydrocarbons, the Turkish oils were divided into three groups according to the classification scheme of Tissot and Welte (1984); heavy oils, aromatic oils, and paraffinic and paraffinic-napthenic oils (Figure 3.1). The Raman, Batı

Table-3.1 Reservoir depth, age and formation of oil samples examined in this study.

ABBREVIATIONS USED IN THIS STUDY	OIL FIELD/ WELL	DEPTH (m)	TEMPERATURE (C)	AGE	FORMATION	
1	CE18	CELIKLI-18	3150	122	Cenomanian-Campanian	Derdere+Beloka
2	CE16*	CELIKLI-16	3385	133	Cenomanian	Derdere
3	S5	SELMO-5	1800	-	Upper Maastrichtian	Lower Sinan
4	BS4*	BATI SELMO-4	1810	80	Upper Maastrichtian	Lower Sinan
5	BS103	BATI SELMO-103	1808	-	Upper Maastrichtian	Lower Sinan
6	SI13	SINAN-13	1500	-	Paleocene	Upper Sinan
7	S30*	SILVANKA-30	2415	-	Campanian	Beloka
8	SI1*	SINAN-1	-	-	Paleocene	Upper Sinan
9	KA2*	KASTEL-2	2320	86	Turonian	Karababa
10	KU1*	KURTALAN-1	1870	108	Maastrichtian	Lower Germay
11	BE1*	BEYCAVIR-1	2340	-	Campanian	Beloka
12	MA53	MAGRIP-53	1710	76	Maastrichtian	Garzan
13	MA30*	MAGRIP-30	1724	-	Maastrichtian	Garzan
14	GA17	GARZAN-17	1450	-	Maastrichtian	Garzan
15	GA90	GARZAN-90	1500	72	Maastrichtian	Garzan
16	GA15*	GARZAN-15	1400	-	Maastrichtian	Garzan
17	GE12	GERMIK-12	1934	99	Maastrichtian	Garzan
18	GE5*	GERMIK-5	1950	-	Maastrichtian	Garzan
19	R87*	RAMAN-87	1310	-	Cenomanian	Derdere
20	R192*	RAMAN-192	1256	86	Maastrichtian	Garzan
21	R157*	RAMAN-157	1156	-	Maastrichtian	Garzan
22	R63*	RAMAN-63	1175	-	Cenomanian	Derdere
23	R193*	RAMAN-193	1280	69	Cenomanian	Derdere
24	R151*	RAMAN-151	1263	-	Cenomanian	Derdere
25	R197*	RAMAN-197	1280	81	Cenomanian	Derdere
26	R84*	RAMAN-84	1290	-	Cenomanian	Derdere
27	R93*	RAMAN-93	1360	-	Cenomanian	Derdere
28	BR47*	BATI RAMAN-47	1200	-	Maastrichtian	Garzan
29	BR56*	BATI RAMAN-56	1280	-	Maastrichtian	Garzan
30	BR84*	BATI RAMAN-84	1350	-	Maastrichtian	Garzan
31	BR43*	BATI RAMAN-43	1379	-	Maastrichtian	Garzan
32	BR211*	BATI RAMAN-211	1300	-	Maastrichtian	Garzan
33	BR193	BATI RAMAN-193	1340	-	Maastrichtian	Garzan
34	BR189*	BATI RAMAN-189	1300	-	Maastrichtian	Garzan
35	BR167*	BATI RAMAN-167	1300	71	Maastrichtian	Garzan
36	BR176*	BATI RAMAN-176	1300	-	Maastrichtian	Garzan
37	CA2	CAMURLU-2	1300	53	Paleocene-Maastrichtian	Upper Sinan
38	CA22*	CAMURLU-22	1400	80	Paleocene-Maastrichtian	Upper Sinan
39	BK12*	BATI KOZLUCA-12	1475	-	Paleocene-Maastrichtian	Lower Sinan
40	GD3*	GUNEY DINCER-3	-	77	Campanian	Beloka
41	GD15	GUNEY DINCER-15	-	81	Campanian	Beloka
42	GS21*	GUNEY SARICAK-21	1575	89	Cenomanian	Derdere
43	A3*	ADIYAMAN-3	1603	79	Campanian	Karabogaz
44	CT16	CEMBERLITAS-16	3200	118	Cenomanian	Derdere

Table-3.2 Bulk composition and capillary gas chromatography data of oil samples.

OIL	DEPTH (M)	BULK COMPOSITION							GAS CHROMATOGRAPHY				CPI**
		API GRAVITY	SULFUR WT%	SAT %	ARO %	NSOs %	ASPH %	SAT	PRISTANE	PRISTANE	PHYTANE		
								ARO	PHYTANE	N-C17	N-C18		
1 CE18	3150	35	0.61	81	9	3	7	9.1	1.16	0.65	0.61	1.17	
2 CE16*	3385	33	0.55	86	11	2	1	7.8	1.13	0.48	0.49	0.84	
3 S5	1800	32	1.24	71	19	5	6	3.7	1.05	0.65	0.71	0.98	
4 BS4*	1810	32	1.14	69	20	5	6	3.5	0.95	0.51	0.57	1.11	
5 BS103	1808	31	1.14	73	18	4	5	4.1	0.98	0.54	0.57	1.16	
6 SI13	1700	15	1.51	34	32	14	20	1.1	0.86	0.46	0.78	0.90	
7 S30*	2415	19	2.92	56	28	5	11	2.1	0.87	0.33	0.48	0.97	
8 SI1*	1753	15	1.55	29	27	28	16	1.1	0.74	0.45	0.73	1.08	
9 KA2*	2320	33	0.91	68	15	12	5	4.5	1.61	0.61	0.41	1.09	
10 KU1*	1670	32	1.22	76	14	3	7	5.4	0.99	0.23	0.25	0.93	
11 BE1*	2340	24	1.76	58	28	7	7	2.1	0.71	0.28	0.41	0.98	
12 MA53	1710	15	3.49	47	23	4	26	2.1	0.72	0.39	0.62	0.98	
13 MA30*	1724	15	3.51	45	26	8	21	1.7	0.77	0.28	0.45	1.04	
14 GA17	1450	23	2.95	56	27	4	13	2.1	0.81	0.43	0.63	1.23	
15 GA90	1500	22	2.88	53	30	4	13	1.8	0.75	0.49	0.66	0.97	
16 GA15*	1400	24	2.88	53	31	6	8	1.8	0.76	0.53	0.53	1.04	
17 GE12	1934	23	2.67	58	33	6	13	1.4	0.81	0.37	0.45	0.94	
18 GE5*	1950	17	2.68	44	33	7	18	1.3	0.63	0.27	0.46	0.96	
19 R87*	1310	17	1.23	29	44	11	16	0.7	0.67	0.25	0.45	0.97	
20 R192*	1256	17	2.26	28	37	16	19	0.8	0.65	0.25	0.45	1.01	
21 R157	1156	16	3.38	29	33	15	23	0.8	0.65	0.27	0.51	0.97	
22 R63*	1200	17	2.77	33	42	6	19	0.8	0.69	0.25	0.45	0.94	
23 R193	1250	17	3.73	28	33	12	26	0.8	0.63	0.26	0.51	0.98	
24 R151*	1263	17	1.65	32	44	9	16	0.7	0.69	0.33	0.48	0.98	
25 R197*	1270	18	3.18	29	37	15	19	0.8	0.79	0.31	0.45	0.95	
26 R84*	1290	17	1.82	31	44	20	15	0.7	0.65	0.31	0.46	ND	
27 R93*	1360	15	1.93	29	37	8	26	0.8	0.64	0.28	0.48	ND	
28 BR47*	1200	12	5.21	14	26	15	44	0.5	0.66	0.27	0.53	1.01	
29 BR56*	1280	13	4.59	13	29	17	49	0.4	0.51	0.23	0.49	1.01	
30 BR84*	1350	12	4.84	14	42	10	32	0.3	0.61	0.22	0.49	0.96	
31 BR43*	1379	13	5.66	17	34	12	28	0.5	0.56	0.26	0.52	0.99	
32 BR211*	1300	13	4.76	12	34	21	39	0.4	0.61	0.27	0.52	1.01	
33 BR193	1320	12	7.09	14	44	14	31	0.3	0.62	0.24	0.46	1.06	
34 BR189*	1300	12	4.31	24	29	12	28	0.8	0.62	0.24	0.53	1.04	
35 BR167*	1300	12	4.61	9	23	18	55	0.4	0.61	0.21	0.48	0.99	
36 BR176*	1300	13	4.92	11	29	12	29	0.4	0.61	0.23	0.45	1.05	
37 CA2	1300	12	7.14	18	42	11	31	0.4	0.71	0.21	0.35	1.18	
38 CA22*	1400	12	7.21	22	41	8	31	0.5	0.64	0.22	0.42	0.89	
39 BK12*	1475	14	6.67	23	41	8	29	0.6	0.67	0.21	0.37	0.92	
40 GD3*	1500	14	3.11	26	41	12	23	0.6	0.75	0.21	0.32	0.99	
41 GD15	1550	16	5.48	31	41	8	23	0.8	0.83	0.24	0.33	0.94	
42 GS21*	1575	31	0.41	71	18	7	5	3.9	1.91	0.49	0.31	1.05	
43 A3*	1603	24	1.24	58	26	7	9	2.2	0.61	0.35	0.35	0.98	
44 CT16*	3100	31	1.05	52	33	6	9	1.6	0.61	0.33	0.25	0.98	

** CPI= $1/2 (C23+C25+C27+C29)/(C24+C26+C28+C30)/(C23+C25+C27+C29)/(C22+C24+C26+C28)$
(Curiale, 1983).

* Oil analyzed by GS-MS

ND: not determined.

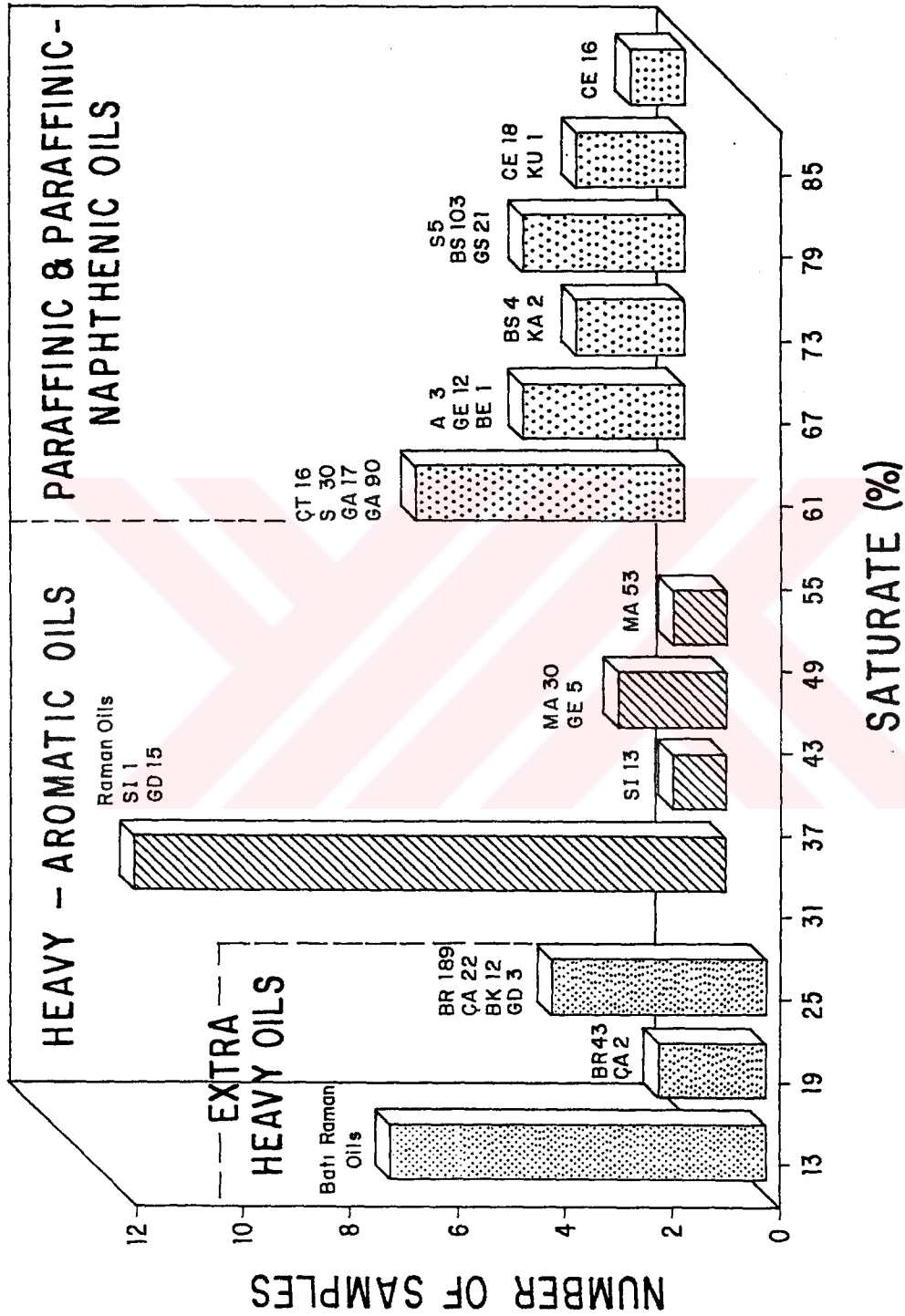


Figure_3.1 Histogram showing saturates versus number of the Turkish oils.

Raman, Çamurlu, Batı Kozluca, Güney Dinçer and Mağrip field oils (Batman-Nusaybin area) are all heavy oils.

3.2. Gas Chromatography Data

Gas chromatograms were obtained on the saturate fraction of the oils in order to assess "C₁₅₊ n-alkane" distributions and to determine n-alkane to acyclic isoprenoid ratios. A representative gas chromatogram is given in Figure 3.2 and the list of gas chromatograms are given in Appendix C.

3.2.1. Distribution of C₁₅₊n-alkanes

All the gas chromatograms show similar unimodal distributions of C₁₅₊ n-alkanes maximizing around n-C₁₅, n-C₁₆, and n-C₁₇ (Appendix C). This probably indicates phytoplankton and/or bacteria source of marine environment (Oro et al., 1967). In all samples, n-alkane distributions from n-C₂₃ to n-C₃₀ show a slight even-carbon number predominance (CPI₂₃₋₃₀ = 0.84 to 1.17) (Table 3.2). Even over odd predominance of n-alkanes (CPI < 1) is commonly associated with highly reducing evaporate-carbonate depositional environments rather than high energy shale depositional environments (Dembicki et al., 1976; Connan, et al., 1985; Palacas et al., 1984; Clark and Philp, 1989).

Some oil samples (CE18, GA17, CA2) which have CPI values greater than 1.0 contain unusually high n-C₂₅

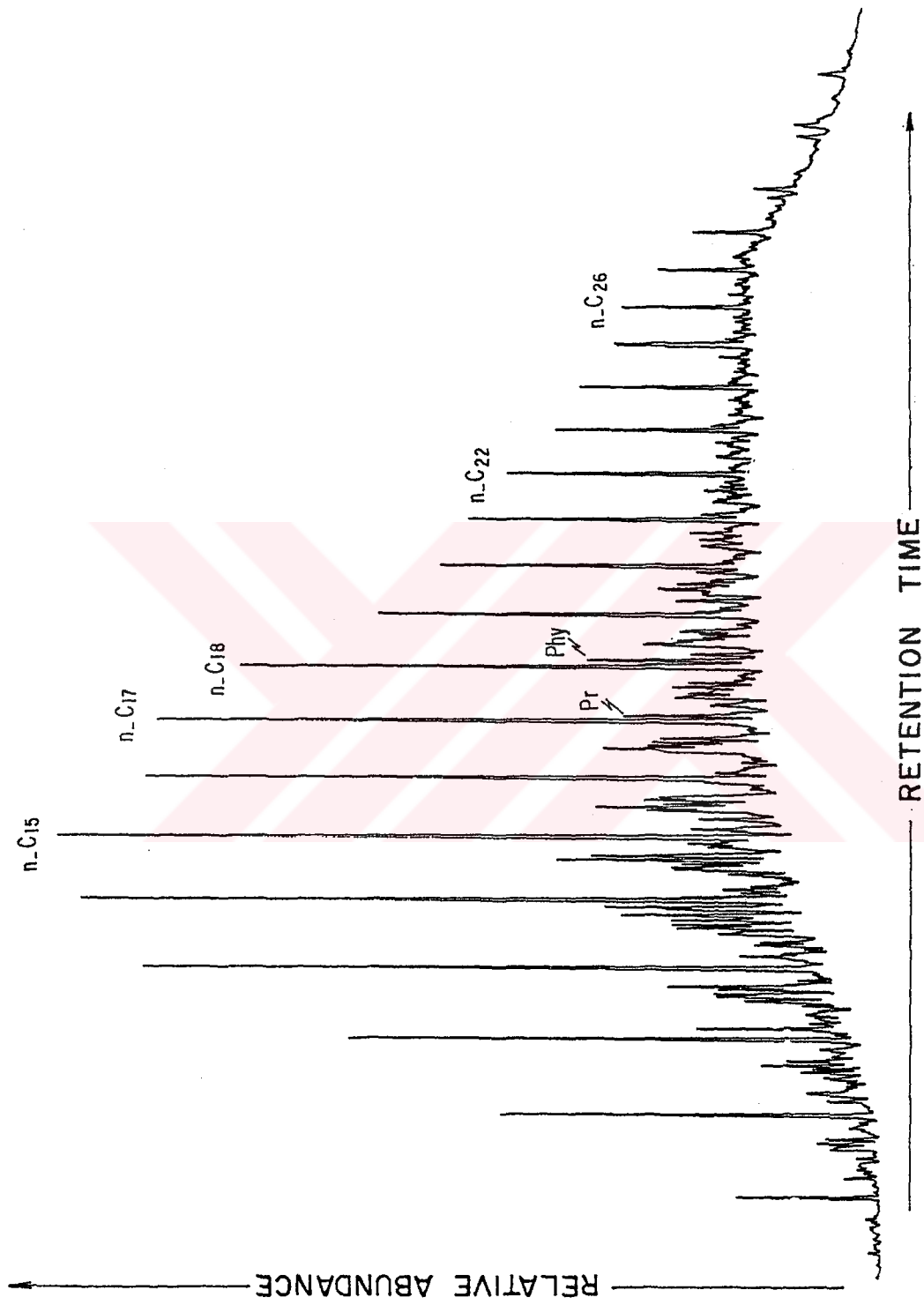


Figure _3.2 A representative (Çemberlitaş _16; CT16) gas chromatogram of saturate fraction of oils. Pr (Pristane), Phy (Phytone).

concentration on the gas chromatograms (Figures C.1, C14, and C.37). The n-C₂₅ is also observed with unexpectedly high concentrations on the gas chromatograms of rock extracts from SE Turkey. It is believed that some of the contamination were due to mud additives added during the drilling operations or from the laboratory contamination during analysis of the oil samples.

3.2.2. Distribution of Acyclic Isoprenoids

The pristane to phytane ratio (Pr/Phy) was used extensively for characterization of depositional environments as outlined by Didyk et al., (1978). The ratio indicates whether the depositional environment of the source rock is anoxic (Pr/Phy<1) or oxic (Pr/Phy>1). Iron-poor calcareous anoxic environment is the one which is favorable for incorporation of sulfur into organic matter on the other hand, in iron-rich siliclastic environments sulfur forms pyrite (FeS₂). Consequently, low Pr/Phy ratios of the oils indicate higher sulfur content and lower API gravity, whereas higher Pr/Phy ratios indicate lower sulfur content and higher API gravity (Hughes and Holba, 1988). Care should always be taken during interpretation of this ratios because it works only when the source of pristane and phytane is the phytol side chain of chlorophyll. Indeed, most recently, ten Haven et al., (1987) and Gürgey and Sayılı (1990) suggested that in hypersaline environments, prolific growth of halophilic bacteria containing the phytanyl will lead to much reduced Pr/Phy values.

Acyclic isoprenoid hydrocarbons, i.e., pristane and Phytane, are present in all the oil samples. In the forty-four oil samples analysed in this study, Pr/Phy ratios range from 0.51 to 1.91. The amount of n-C₁₇ and n-C₁₈ greatly exceed the amount pristane and phytane in all samples (Table 3.2).

3.3. Gas Chromatography-Mass Spectrometry Data

3.3.1. "Tri-Tetra-Pentacyclic" Terpanes

Since the source of "tri-tetra-pentacyclic" terpanes is believed to be triterpenoids in bacteria, a wide variety of triterpenoids is probably produced among many groups of microorganisms present in different depositional environments (Ourisson et al., 1984).

Based on the number of rings, terpanes can be divided into three groups: Tricyclic terpanes, tetracyclic terpanes and pentacyclic terpanes (see also Appendix A). These three groups of terpanes can be distinguished by monitoring their ion at m/z 191 mass fragmentograms. Comparison of normalized distributions of tricyclic terpanes, tetracyclic terpanes, and pentacyclic terpanes are given in Table 3.3. Figure 3.3 shows a representative "m/z 191 mass fragmentogram" and identification of the peaks are given in Table 3.4. Compilation of these fragmentograms is given in Appendix D. Terpanes are present in all of the oil samples. In general, tricyclic terpene region is dominated by the C₂₃ tricyclic (I) and

Table-3.3 Relative abundances of tricyclic, tetracyclic and pentacyclic terpanes.

OIL	1	2	3	4	5	6	7	GAM
1 CE16	60	5	35	12.00	1.71	0.08	3.26	a
2 BS4	38	3	59	12.67	0.64	0.08	2.95	a
3 S30	34	3	63	11.33	0.54	0.09	3.05	a
4 SI1	20	3	78	6.67	0.26	0.15	1.62	hd
5 KA2	38	1	61	38.00	0.62	0.03	15	a
6 KV1	36	6	57	6.00	0.63	0.17	1.63	-
7 BE1	36	3	61	12.00	0.59	0.08	2.45	a
8 MA30	14	5	81	2.80	0.17	0.36	0.84	-
9 GA15	19	4	77	4.75	0.25	0.21	1.19	hd
10 GE12	21	4	75	5.25	0.28	0.19	1.37	hd
11 R87	9	4	87	2.25	0.10	0.44	0.79	hd
12 R192	10	4	86	2.50	0.12	0.40	0.89	hd
13 R63	11	4	85	2.75	0.13	0.36	1	hd
14 R151	11	5	84	2.20	0.13	0.45	0.87	hd
15 R197	15	5	80	3.00	0.19	0.33	1.13	p
16 R84	10	4	86	2.50	0.12	0.40	0.87	p
17 R93	9	4	87	2.25	0.10	0.44	0.87	p
18 BR47	9	3	88	3.00	0.11	0.33	0.89	hd
19 BR56	9	3	88	3.00	0.11	0.33	0.69	hd
20 BR84	6	3	91	2.00	0.07	0.50	0.71	hd
21 BR43	11	4	85	2.75	0.13	0.36	1.2	hd
22 BR211	11	3	86	3.67	0.13	0.27	1.4	hd
23 BR189	13	9	78	1.44	0.17	0.69	0.5	-
24 BR167	8	7	85	1.14	0.09	0.88	0.39	-
25 BR176	8	4	88	2.00	0.09	0.67	0.72	hd
26 CA22	7	3	90	2.33	0.08	0.43	0.82	p
27 BK12	10	4	88	2.50	0.12	0.57	0.82	p
28 GD3	11	4	85	2.75	0.13	0.36	0.94	p
29 GS21	24	1	75	24.00	0.32	0.04	19	a
30 A3	46	5	49	9.20	0.94	0.11	3.73	hd
31 CT16	44	5	51	8.80	0.86	0.11	2.78	hd

1-Tricyclic (%), 2-Tetracyclic (%), 3-Pentacyclic (%),
4-Tricyclic/Tetracyclic Ratio, 5-Tricyclic/Pentacyclic Ratio
6-Tetracyclic/Triicyclic Ratio, 7.C23 tricyclic/C24* Tetracyclic
a absence, p presence, hd hardly detected, GAM Gammacerane

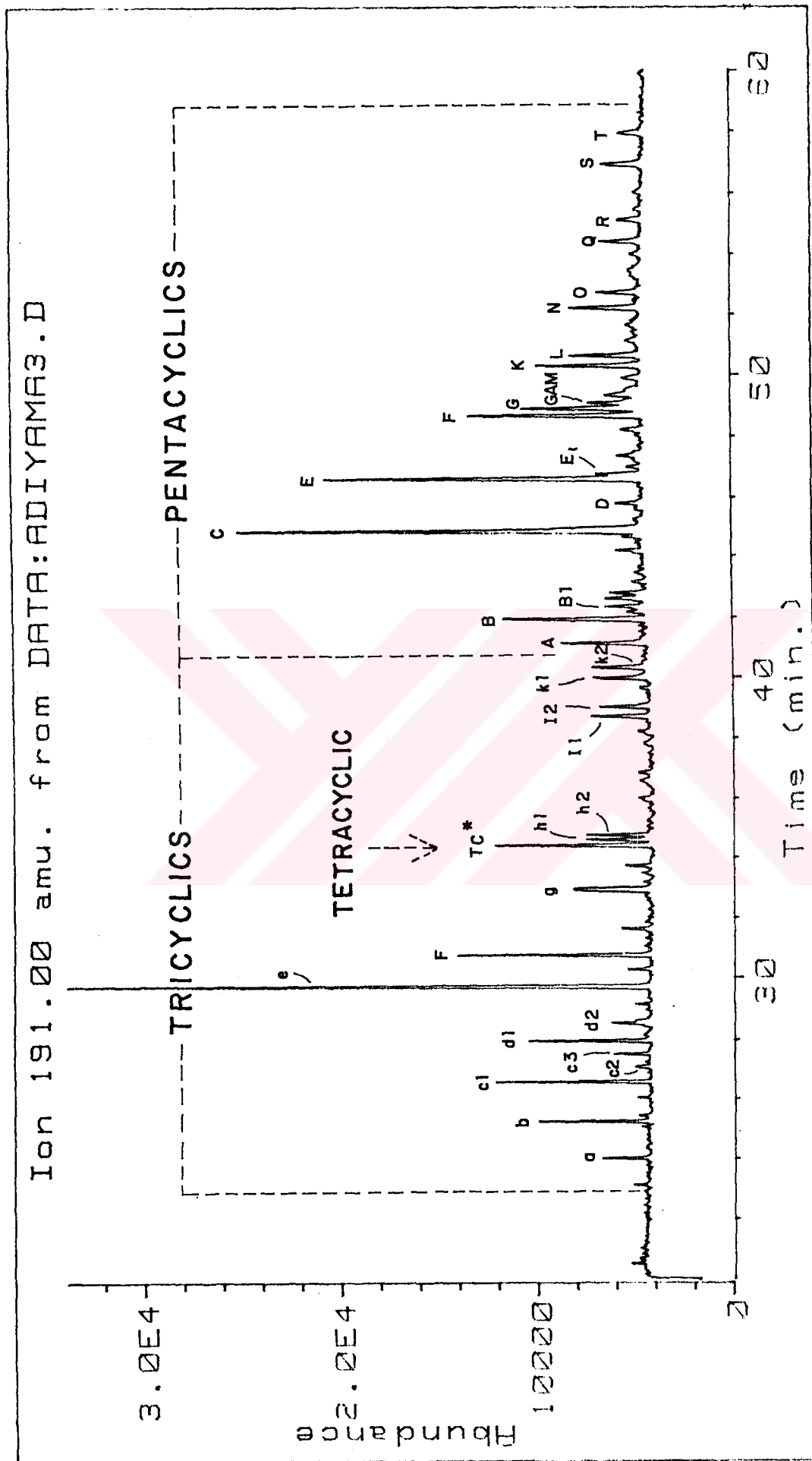


Figure - 3.3 A representative m/z 191 fragmentogram showing terpene distribution in Adiyaman-3 (A3) oil. Peaks identified in Table 3.4.

Table 3.4 List of identified tri-tetra-pentacyclic terpanes.

PEAK LABEL	COMPOUND	FORMULA
a	C19- tricyclic terpane	C19H34
b	C20- tricyclic terpane	C20H36
c1	C21- tricyclic terpane	C21H38
c2	C21- tricyclic terpane	C21H38
c3	C21- tricyclic terpane	C22H40
d1	C22- tricyclic terpane	C22H40
d2	C22- tricyclic terpane	C23H42
e	C23- tricyclic terpane	C24H44
f	C24- tricyclic terpane	C25H46
g	C25- 22S+22R- tricyclic terpane	C24H42
TC*	C24- tetracyclic terpane	C26H48
h1	C26-22S- tricyclic terpane	C26H48
h2	C26-22R- tricyclic terpane	C26H48
i1	C28-22S- tricyclic terpane	C28H52
i2	C28-22R- tricyclic terpane	C28H52
k1	C29-22S- tricyclic terpane	C29H54
k2	C29-22R- tricyclic terpane	C29H54
A	18 (H) 22,29,30- trisnorhopane (Ts)	C27H46
B	17 (H) 22,29,30- trisnorhopane (Tm)	C27H46
B1	Unidentified	
C	17 (H), 21B(H)- 30- norhopane	C29H50
D	17B(H), 21 (H)- 30- norhopane	C29H52
E	17 (H), 21B(H)- hopane	C30H52
E1	Unidentified	
F	17B(H), 21 (H)- moretane	C30H52
G	17 (H), 21B(H), 22S-30- homohopane	C31H54
H	17 (H), 21B(H), 22R-30- homohopane	C31H54
GAM	gammacerane	C30H52
K	17 (H), 21B(H), 22S-30, 31- bishomohopane	C32H56
L	17 (H), 21B(H), 22R-30- 31- bishomohopane	C32H56
N	17 (H), 21 B(H), 22S-30, 31, 32- trishomohopane	C33H58
O	17 (H), 21B(H), 22R-30, 31, 32- trishomohopane	C33H58
Q	17 (H), 21B(H), 22S- C34 extended hopane	C34H60
R	17 (H), 21B(H), 22R- C34 extended hopane	C34H60
S	17 (H), 21B(H), 22S- C35 extended hopane	C35H62
T	17 (H), 21B(H), 22R- C35 extended hopane	C34H62

tetracyclic terpane (II). In the C₂₇ pentacyclic hopane region T_m, 17 α (H),22,29,30 trisnorhopane peak (III) is always higher than T_s, 18 α (H),22,29,30 trisnorneohopane (IV). Roman numerals in the paranthesis indicate the structure group of the compound as given in Appendix A. The C₂₉-C₃₅ pentacyclic region of the m/z 191 fragmetograms of all the samples is dominated by C₂₉ 17 α (H),21 β (H)-norhopane (V) and C₃₀-hopane, however, 17 β (H),21 α (H)-moretanenes (VI) are of lesser abundance. Oil samples BR189 and BR167 are the only oils which show unusually high 17 α -Trisnorhopane (III) and unusualy low tricyclic terpanes relative to pentacyclic terpanes. In general, Raman, Batı Raman, Mağrip and in the south Nusaybin Area oils (e.g., Çamurlu, Batı Kozluca, Güney Dinçer field oils) show relatively low tricyclic terpane to pentacyclic terpane ratios. These oils also show relatively higher concentration of tetracyclic terpane (II) in the tricyclic region of the mass fragmetograms.

Measured peak heights of the individual terpane compounds on the m/z 191 mass chromatograms of the oils is given in Table E.1 where some of the peaks were combined and given as one paramemeter. For example, the column 10 consists of summation of the 10 pentacyclic terpane peaks as indicated lower part of the Table E.1. The reason behind combination of these peaks is that it will reduce the data and make interpretation relatively simpler.

3.3.1.1 Tricyclic Terpanes

Tricyclic terpanes, which may come from different species of bacteria are usually present in much lower concentrations than the pentacyclics, but they may occasionally be present in large, even dominant amounts. Distribution of tricyclic terpanes in oils has been suggested by several workers to be source-related (e.g. Zumberge, 1983; Reed, 1977; Sofer et al., 1985; Philp, 1985; Jones and Philp, 1990). They are more resistant to bacterial degradation than pentacyclic terpanes and regular steranes (Seifert and Moldowan, 1979). Therefore, their usage in oil to oil correlations is a very powerful tool to differentiate oils according to their source difference.

The carbon number of tricyclic terpanes ranges from C₁₉ to C₄₀ (Moldowan et al., 1985) but only C₁₉-C₂₉ range tricyclic terpanes were identified and used in this study due to low concentration of higher molecular weight ones. Figure 3.3 shows the identification of the C₁₉-C₂₉ range tricyclic terpanes on the m/z 191 mass fragmentograms based on a comparison of relative retention times with those detailed by Sofer et al., (1985) and Palacas et al., (1984). Table E.2 shows the normalized molecular distribution of 12 tricyclic terpanes with an additional of one tetracyclic terpane molecule. The C₂₃ (peak e in Figure 3.3) is clearly the dominant peak in all the Kozluk-Adıyaman and northern Diyarbakır oil samples and its percentage ranges from 21.6 % in oil sample GS21 to

35.4 % in oil sample A3 (Table E.2). As stated earlier, relative amount of tricyclic terpanes appears to be low in oils from the Batman-Nusaybin and higher in oils from the northern Diyarbakır areas.

3.3.1.2. Tetracyclic Terpanes

Tetracyclic terpanes (II) are another class of biomarkers that are found to be fairly widely distributed in crude oils and rock extracts. The C₂₄-C₂₇ members are commonly observed. However, the C₂₄ tetracyclic terpane, because of its higher abundance and resistance to bacterial degradation (Reed, 1977; Ourisson et al., 1979) gathered greater attention in oil to oil correlations (Clark and Philp, 1989).

There has been some debate over the origin of the C₂₄ tetracyclic terpane. Theories favored for the origin of the C₂₄ tetracyclic terpane are (a) thermocatalytic degradation of hopane precursors (Aquino Neto et al., 1981) and (b) microbial opening of the E ring of hopanoids (Philp, 1985), and (c) direct derivation from vascular plants (Philp, 1985).

The most peculiar of the m/z 191 mass fragmentograms in the tricyclic region (Figure 3.3, Table D) is the presence of various amounts of the C₂₄ tetracyclic terpane (TC* in Figure 3.3). Identification of this compound is based on a comparison of relative retention times with those reported by Philp (1985) and

Palacas (1984). Normalised molecular distribution of this compound with respect to the 12 tricyclic terpane compounds and the percentage distribution of this compound relative to tricyclic and pentacyclic terpanes are given in Table E.2 and Table 3.3 respectively. The oil samples BR189, BR167, BR56, and BR176 contain significantly high relative amounts of the C₂₄ tetracyclic terpanes. In contrast, the oil samples KA2 and GS21 have almost no C₂₄ tetracyclic terpane which is analogous to the oils derived from Midcontinent Paleozoic source rocks, USA (Clayton, 1989). Abundance of this compound relative to tricyclic and pentacyclic terpanes varies from 1 % in the GS21 oil to 9 % in the BR189 oil (Table 3.3).

3.3.1.3. Pentacyclic Terpanes

Pentacyclic terpanes based on the hopane structure (V) are known to have a bacterial origin (Aquino Neto et al., 1981). They are present virtually in all oils. They generally occur in the C₂₇-C₃₅ range. Their regular decrease (staircase form) in peak heights from the C₃₁ members to C₃₅ is usually observed in oils generated from siliciclastic source rocks. Unusually high amount of the C₃₅ member peaks is usually associated with oils derived from marine carbonate or evaporate sources (Connan et al., 1985; Philp and Gilbert, 1985; Mello et al., 1988; Clark and Philp, 1989).

Another pentacyclic terpane that does not have the hopane structure and whose presence is an indicative of an

oil derived from hypersaline environment is gammacerane (VII). The exact origin of gammacerane (GAM in Figure 3.3) is suggested to be certain protozoan favoring saline type of environments that contribute significantly to the higher yields of gammacerane in the saline oils (Mello et al., 1988).

In this study, all the oil samples contain detectable amount of C₂₇-C₃₅ pentacyclic terpanes (e.g., hopanes) on the m/z 191 mass fragmentograms (Figure 3.3, Appendix D). Identification of these compounds is based on the peak descriptions as given by Sofer et al., (1985), Palacas et al., (1984), and Philp (1985) and is given in Table 3.4. Excluding the oil samples BR189 and BR167, all the oil samples show the dominance of hopanes with 17 α (H),21 β (H) structure over the moretanes with 17 β (H),21 α (H) structure. The T_m (17 α -trisorhopane) in the BR189 and BR167 oils is 55 unusually higher than the C₂₉ and the C₃₀ hopanes. This is analogous to the oils of the Michigan Basin reported by Rullkötter et al., (1985). The T_m of the most Turkish oils, even in the mature ones, predominates the T_s (18 α -trisorhopane) (Table E.3).

The two peaks (B1 and E1 in Figure 3.3) were not identified in the literature. However, in this study, interrelationships between these two peaks and other pentacyclic terpane peaks were also investigated in terms of source, maturity migration and biodegradation. Gammacerane (peak GAM in Figure 3.3) was not included in Table E.3 since its identification presents some

uncertainty. Instead, it was evaluated as being present or absent form. The only oils which do not contain gammacerane were found to be the samples CE16, BS4, S30, KA2, BE1, and GS21 (Table 3.3).

3.3.2. Steranes

Steranes are derived from sterols which are common in most higher plants and eucaryotic organisms (having a distinct nucleus) but rare or absent in procaryotic organisms (lacking a distinct nucleus) (Ourisson et al., 1979). In this study steranes will be treated as regular steranes, diasteranes (also called rearranged steranes), and pregnanes (lower weight steranes). A representative m/z 217 mass fragmentogram of steranes is given in Figure 3.4 and Appendix F. Steranes identified in Figure 3.4 and Appendix F is given in Table 3.5. Their compound class normalized distributions in terms of pregnanes, diasteranes, and regular steranes are given in Table 3.6. Normalised molecular distribution of the steranes are given in Table E.4.

3.3.2.1. Regular Steranes

The regular steranes (XII, XIII) are the main class of biomarkers, precursor of which are the sterols containing 27, 28, 29 and 30 carbon atoms. They only differ by the addition of a sequence of -CH₂- unit at a certain place in the molecule (Appendix A). The term

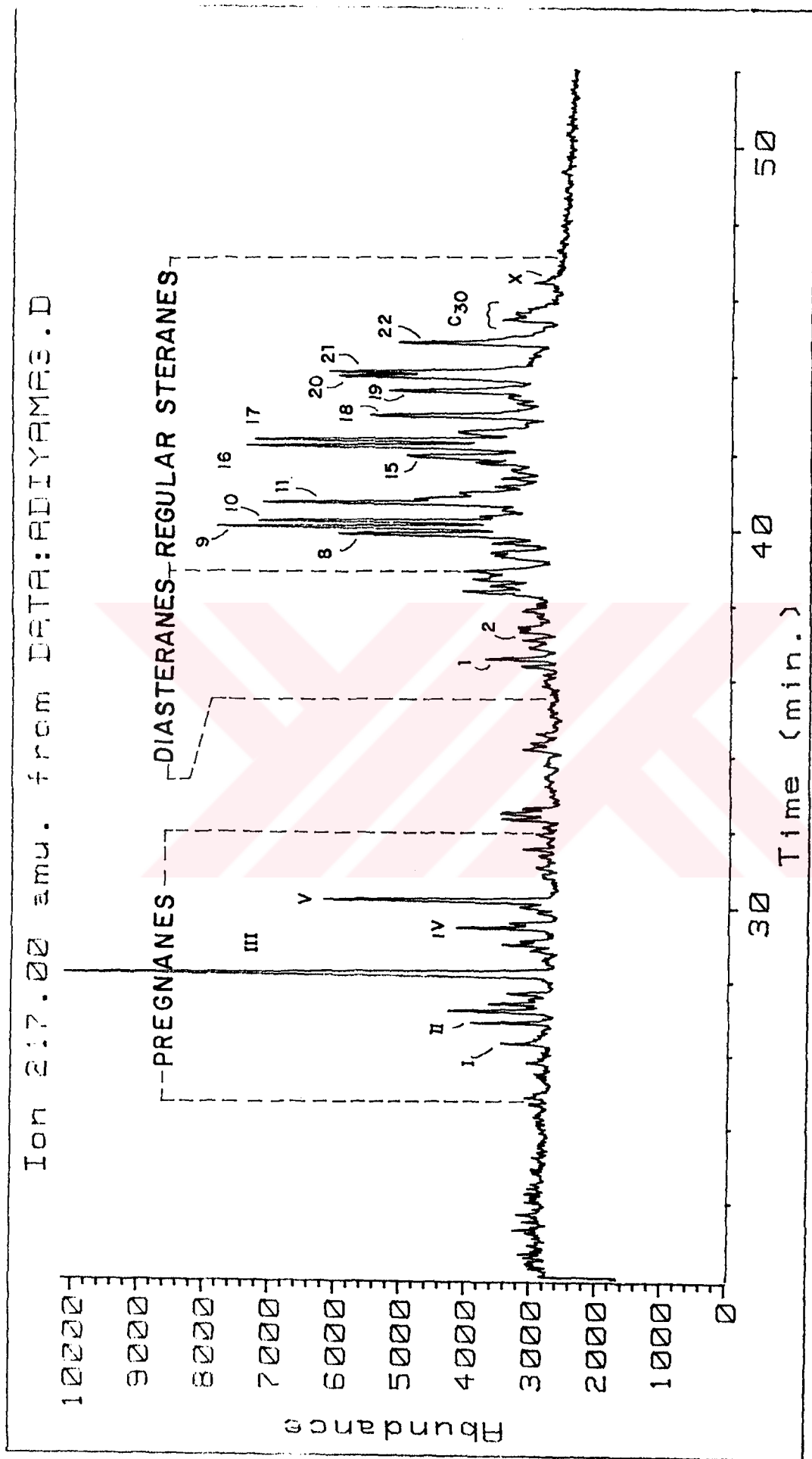


Figure - 3.4. A representative m/z 217 mass chromatogram showing sterane distribution in Adiyaman - 3 (A 3) oil. Peaks identified in Table 3.5.

Table 3.5 List of identified steranes.

PEAK LABEL	COMPOUND	FORMULA
I	13 β (H), 17 α (H) - DIAPREGNANE	C21H36
II	5 α (H), 14 β (H), 17 α (H) - PREGNANE(C21) (13 α (H), 17 β (H)- DIAPREGNANE C21?)	-
III	5 α (H), 14 β (H), 17 β (H)- PREGNANE 5 α (H), 14 α (H), 17 α (H)- PREGNANE (C21)	-
IV	4 α -METHYL- 5 α (H), 14 β (H), 17 β (H)-PREGNANE 4 α -METHYL- 5 α (H), 14 α (H), 17 α (H)-PREGNANE(C22)	-
V	5 α (H), 14 β (H), 17 β (H)- HOMOPREGNANE 13 β (H), 17 α (H)- BISHOMODIAPREGNANE (C23)	-
1	13 β (H), 17 α (H)- DIACHOLESTANE (20S)	C27H48
2	13 β (H), 17 α (H)- DIACHOLESTANE (20R)	C27H48
8	5 α (H)- CHOLESTANE (20S) + 5 β (H)- CHOLESTANE (20R)	C27H48
9	5 α (H), 14 β (H), 17 β (H)- CHOLESTANE + 13 β (H), 17 α (H)- DIASTIGMASTANE (20S)	C27H48 C29H52
10	5 α (H), 14 β (H), 17 β (H)- CHOLESTANE (20S)	C27H48
11	5 α (H), 14 β (H), 17 β (H)- CHOLESTANE (20R)	C27H48
15	5 α (H), 14 β (H), 17 α (H)- ERGOSTANE (20S)	C28H50
16	5 α (H), 14 β (H), 17 β (H)- ERGOSTANE (20R) 5 β (H)- ERGOSTANE (20R)	C28H50 C28H50
17	5 α (H), 14 β (H), 17 β (H)- ERGOSTANE (20S)	C28H50
18	5 α (H), 14 α (H), 17 α (H)- ERGOSTANE (20R)	C28H50
19	5 α (H), 14 α (H), 17 α (H)-STIGMASTANE (20S)	C29H52
20	5 α (H), 14 β (H), 17 β (H)- STIGMASTANE 5 β (H)- STIGMASTANE (20R)	C29H52 C29H52
21	5 α (H), 14 β (H), 17 β (H)- STIGMASTANE (20S)	C29H52
22	5 α (H), 14 α (H), 17 α (H)- STIGMASTANE (20R)	C29H52

Table 3.6 Percentage abundances of pregnanes, diasteranes, and regular steranes.

OIL	STERANES			aaa 20R			COMPOUND	
	PREGNANES	DIASTERANES	REGULAR	C27	C28	C29	C30	X
	%	%	%	%	%	%		
1 ÇE16	17	12	71	42	28	30	p	a
2 S5	23	7	70	36	30	34	p	-
3 BS4	22	10	68	40	30	30	p	a
4 S30	18	8	74	38	28	34	p	a
5 SI1	16	5	79	38	24	38	p	hd
6 KA2	28	11	60	43	20	37	p	a
7 KV1	36	9	55	46	17	37	p	a
8 BE1	17	7	76	42	26	32	p	a
9 MA33	24	3	73	35	18	48	p	p
10 GA15	21	5	74	38	19	43	p	hd
11 GE5	25	2	73	38	21	41	p	hd
12 R87	25	3	72	35	19	48	p	p
13 R192	27	2	71	33	19	48	p	p
14 R63	29	3	68	35	20	45	p	p
15 R151	28	3	69	39	17	45	p	p
16 R197	17	3	79	33	25	42	p	p
17 R84	16	2	82	32	22	48	p	p
18 R93	21	2	77	33	22	45	p	p
19 BR47	23	4	73	33	17	50	p	p
20 BR56	16	2	82	35	18	47	p	p
21 BR84	18	2	80	32	18	50	p	p
22 BR43	18	3	79	34	22	44	p	p
23 BR211	17	6	76	32	20	48	p	p
24 BR189	17	2	81	42	22	38	p	-
25 BR167	14	1	85	40	21	39	p	p
26 BR176	25	2	73	35	20	45	p	p
27 CA22	17	1	82	39	19	42	p	p
28 BK12	20	2	78	40	19	41	p	p
29 GD3	25	2	73	44	19	38	p	p
30 GS21	15	11	74	37	17	46	p	a
31 A3	25	3	72	45	29	26	p	a
32 ÇT16	30	4	66	47	26	27	p	a

a absence

p presence

hd hardly detected

"regular" indicates that the carbon skeleton are the same as in the biological precursors.

The steranes inherited directly from plants and algae are the 20R epimers of the 5 α (H),14 α (H),17 α (H) forms of the C₂₇, C₂₈, C₂₉, and C₃₀ steranes. However, the relative proportion of each of these regular steranes can vary greatly from sample to sample.

Triangular diagram of C₂₇:C₂₈:C₂₉ regular steranes have often been employed successfully to make facies interpretations (Huang and Meinschein, 1976). In spite of such successes, however, one must be cautious, about oversimplified facies interpretations. Most marine sediments, including those deposited in pelagic environments, show predominances of C₂₉ steranes (Volkman, 1986). Traditionally, these steranes would indicate a terrestrial high plant source. Furthermore, lower Paleozoic and Precambrian sediments often contain substantial amounts of C₂₉ sterane, even though land plants could not contribute (Grantham, 1986; Waples and Machihara, 1990). Fowler and Douglas (1987) suggested that some C₂₉ steranes may come from cyanobacteria (blue-green algae). In spite of these difficulties, use of the triangular sterane diagram is now common because it is a useful way to display sterane data.

The ratio of C₂₇/C₂₉ steranes has been also used to provide an indication of the relative amounts of marine versus terrestrial source material in an oil (Huang and

Meinschein, 1976; Jones and Philp, 1990). This has been possible since there is a predominance of C₂₇ sterols in marine organisms compared with C₂₉ sterols in higher plant source materials (Huang and Meinschein, 1976). In addition, it has been proposed that the presence of C₃₀ steranes in an oil is another indicator of a contribution of marine organic material to the sample (Moldowan et al., 1985). Latter, Mello et al., (1988) have confirmed these conclusions for the Brazilian Basin oils.

Recently, an extremely interesting and radically new interpretation of regular-sterane distribution was put forth by Grantham and Wakefield (1988). It was showed that ratio of C₂₈/C₂₉ regular steranes in marine environments was determined by geologic age rather than facies. The increase in C₂₈/C₂₉ ratio from past to present was attributed to evolutionary trends within living phytoplankton determined by Tappan and Loeblich (1973).

In this study, C₂₇:C₂₈:C₂₉ regular steranes are present in all the oils. and aa 20R percentages of them are given in Table 3.6. Peak identification is based on a comparison of retention times of Palacas et al., (1984) (Table 3.5). It appears that the C₂₉ steranes dominate over the C₂₇ and C₂₈ steranes in most of the samples except in the oils from the Kozluk-Adıyaman area.

The ββ-steranes (Peaks 9, 10,16,17,20,21 in Figure 3.4) are always in higher abundance than their aa counterparts (peaks 8, 11, 15, 18, 19, 22) in Figure

3.4). In general, a greater abundance of $\beta\beta$ -steranes over $\alpha\alpha$ -steranes have been observed in mature oils as a result of isomeric conversion of $\alpha\alpha$ -steranes to $\beta\beta$ -steranes with increasing thermal activity (Mackenzie et al., 1985). In a recent study by Zhusheng et al., (1988) also reported that $\beta\beta$ steranes dominate over $\alpha\alpha$ steranes in early generated oils and migrated oils.

3.3.2.2. Diasteranes

Diasteranes (also called rearranged steranes) are present in significant quantities in many samples that are at least moderately mature (Mackenzie, 1984; Rohrback, 1983). They are well known as C_{27} - C_{30} species. The 20R and 20S forms of the C_{27} and the C_{29} diasteranes are usually the most dominant and easily observed. The C_{27} diasteranes are well separated from other important peaks, but the C_{29} diasteranes frequently overlap with the C_{27} regular steranes. Since the relative amount of diasteranes seems to depend on both sediment lithology and maturity, diasteranes are frequently used to distinguish clastic sources from carbonate sources when the oils are immature (Mello et al., 1988; Longman and Palmer, 1987). The idea was originally proposed by Sieskind et al., (1979) that the presence of diasteranes in geological materials is the products of thermal activity on the regular steranes in the presence of acid-clay catalysis. Diasteranes seem to be more stable than regular steranes, and thus become more dominant with increasing maturity. They are also more

resistant to bacterial degradation than regular steranes (Seifert and Moldowan, 1978).

In this study, two diasterane peaks C₂₇-20S and C₂₇-20R (peaks 1, 2 in Figure 3.4) were identified based on the peak descriptions of Palacas et al., 1984 (Table 3.5). The C₂₇-20S diasterane is always in higher concentration than the C₂₇-20R diasterane. The oil samples CE16, KA2, and the GS21 which are higher in gravity contain highest percentage (4.59-6.8 %) of C₂₇-20S among the Turkish oils (Table E.4). When the amount of diasteranes are normalized to the pregnanes and the regular steranes, the CE16, KA2, and GS21 oils have significantly higher diasterane contents (10-12 %) (Table 3.6). The low gravity oils from the Batman-Nusaybin area, on the other hand, contain very low diasterane content (excluding BR211 oil) (1-4 %). Presence of diasteranes, in some cases, has also been observed in carbonate rocks, for example in carbonate La Luna Formation (Zumberge, 1987). However, consideration should be given to the possibility that some if not all the diasterane precursors might have been a product of microbial activity in a highly reducing environment. Although little evidence was available to test such a hypothesis, Simoneit et al., (1980) gave some credence to this idea observing C₂₈-C₂₉ diasteranes in a 1 cm-thick recent algal mat and in the underlying anoxic black mud of Lake Chile.

3.3.2.3. Pregnanes

Pregnanes (IX,X), the lower molecular weight steranes (< C₂₇), have received less attention in the petroleum geochemical studies. However, their importance has been discussed by several workers (ten haven et al., 1985; Wingert and Pomerantz, 1986; Mello et al., 1988; Clark and Philp, 1989). Among the other pregnane compounds, C₂₁ pregnane and C₂₂ homopregnane have been proposed to have specific natural precursors in hypersaline environments (ten Haven et al., 1985; Clark and Philp, 1989), but a thermal origin has also been proposed by Wingert and Pomerantz (1986). The 5 α (H),14 α (H),17 β (H) pregnane and homopregnane isomers have been shown to coelute with the thermodynamically less stable 5 α (H),14 α (H),17 α (H) compounds (Wingert and Pomerantz, 1986). It is reported that the 5 α (H),14 β (H),17 β (H) isomers are predominant in the highly mature samples although this remains to be confirmed. It is also stated that in heavy oils of Alberta, Canada, the C₂₁ pregnane and C₂₂ homopregnanes increase as the diasteranes decrease (Brooks et al., 1988).

In this study, five pregnane compounds were identified (Figure 3.4 and Table 3.5) by a comparison of relative retention times with m/z 217 mass fragmentograms of Wingert and Pomerantz (1986), Hughes and Holba (1986), and Mello et al., (1988). The dominant pregnane compounds are C₂₁ pregnane (peak III in Figure 3.4) and to lesser extent C₂₂ homopregnane (peak V in Figure 3.4). The C₂₁

pregnane in the KU1 oil sample is unusually high (21.25 %) but it reaches the lowest values in the GS21 (5.46%) and SI1 (6.44%) oils. The S5 and the CT16 samples also have exceptionally high other pregnane peak (peak I, in Figure 3.4). Within the normalised pregnanes, regular steranes, diasteranes, pregnane percentages ranges from 14 % in the oil sample BR167 and 36 % in the KU1 oil (Table 3.6). In general their percentages are always between the diasteranes and regular steranes.

3.3.3. Selected Biomarker Ratios and Sulfur Content

Twenty biomarker ratios which were believed to contain the most diagnostic features of the Turkish oils were selected from the 31 samples (Table 3.7). Table E.5 tabulates the values of the selected biomarker ratios. This selection was based on two criteria. The first was to select the biomarker compounds (tri-tetra-pentacyclic terpanes, steranes, n-alkanes, acyclic isoprenoids) which show high loadings on PCs. When the biomarkers are inversely correlated, the ratios obtained from them contain higher amount of information to differentiate the oils. However, maturity sensitive biomarkers are not used for the ratio calculations. For example, 20S and 20R C29-steranes are not used because of their high sensitivity to maturity (e.g., heat) (Mackenzie, 1984; Philp, 1985; Johns, 1986). The second criteria in the selection of biomarker ratios was to select the ratios which was most universally measured in GC-MS analysis (Philp, 1985; Hughes and Holba, 1988; Jones and Philp,

Table-3.7 Explanation of the selected biomarker ratios used in Table E.5.

-
- R1: PHY/N-C18 (PHYTANE/OCTADECANE) = GC-FID PEAK HEIGHT FROM SATURATE FRACTION.
R2: PR/PHY (PRISTANE/PHYTANE) = GC-FID PEAK HEIGHTS FROM SATURATE FRACTION.
R3: SAT/ARO (SATURATES/AROMATICS) = THIN LAYER CHROMATOGRAPHY FROM TABLE 3.2
R4: % S (% SULFUR) = ATOMIC BOMB METHOD FROM TABLE 3.2
R5: C24*/C26 (TETRACYCLIC/TRICYCLIC) = GC-MS (M/Z 191) HEIGHT OF PEAKS TC*/h1+h2.
R6: C24*/C21 (TETRACYCLIC/TRICYCLIC) = GC-MS (M/Z 191) HEIGHT OF PEAKS TC*/d.
R7: C23/C20 TRICYCLICS = GC-MS (M/Z 191) HEIGHT OF PEAKS e/b.
R8: C23/C24 (TRICYCLIC) = GC-MS (M/Z 191) HEIGHT OF PEAKS e/f.
R9: C19+C20/C23 TRICYCLICS = GC-MS (M/Z 191) HEIGHT OF PEAKS a+b/e.
R10: Tm+Ts/C28+C29 (PENTACYCLICS/TRICYCLICS) = GC-MS (M/Z 191) HEIGHT OF PEAKS
A+B/i1+i2+k1+k2.
R11: C35/C34 EXTENDED HOPANES = GC-MS (M/Z 191) HEIGHT OF PEAKS S/Q.
R12: C29NH/C30H (NORHOPANE/HOPANE) = GC-MS (M/Z 191) HEIGHT OF PEAKS C/E.
R13: Tm/Ts TRISNORHOPANE = GC-MS (M/Z 191) HEIGHT OF PEAKS A/B.
R14: C24*/C30H (TETRACYCLIC/HOPANE) = GC-MS (M/Z 191) HEIGHT OF PEAKS C24*/E.
R15: C23/C30H (TRICYCLIC/HOPANE) = GC-MS (M/Z 191) HEIGHT OF PEAKS e/E.
R16: C21+C21+C21+C22+C22/C29 (PREGNANES/STERANES) = GC-MS (M/Z 217)
R17: C21/C22 PREGNANES = GC-MS (M/Z 217) HEIGHT OF PEAKS III/IV.
R18: C21+C21/C21+C21+C22 PREGNANES = GC-MS (M/Z 217) HEIGHT OF PEAKS I+II/III+IV+V.
R19: C22/C27 DIA (HOMOPREGNANE/DIASTERANES) = GC-MS (M/Z 217) HEIGHT OF PEAKS V/1+2.
R20: C27/C29 STERANES = GC-MS (M/Z 217) HEIGHT OF PEAKS 11/12.
R21: C28/C29 STERANES = GC-MS (M/Z 217) HEIGHT OF PEAKS 18/12.
R22: REG C27/DIA C27 STERANES + GC-MS (M/Z 217) HEIGHT OF PEAKS 8+11/1+2.
-

R Ratios.

- * For further explanation of the m/z 191 peaks, see Figure 3.3 and Table 3.4.
** For further explanation of the m/z 217 peaks, see Figure 3.4 and Table 3.5.

1990). Again a special attention was paid to select ratios which were associated with organic matter types and the particular type of depositional environment of source rocks. The following is a brief summary of the definition, range and application of these biomarkers.

R1: Phytane to n-C18 (phy/n-C18) ratio (Appendix B). This ratio is usually greater than 1 encountered for oils generated from carbonate source rocks (Palacas et al., 1984). For the Turkish oils, it ranges from 0.25 to 0.73.

R2: Pristane to phytane (Pr/Phy) ratio (Appendix B). It reflects whether the depositional environment of the source rock was anoxic (Pr/Phy < 1) or oxic (Pr/Phy >1) (Didyk et al., 1978). Although it is generally accepted that the Pr/Phy ratio of an oil does reflect depositional environment, such interpretations must be made with caution since several studies have shown that the Pr/Phy ratio increases with increasing terrestrial input to the sediment (Powell and Mckirdy, 1973), with increasing thermal maturity (Alexander et al., 1981). And also, some of the isoprenoid alkanes could be derived from sources other than phytol degradation (Illich, 1983; ten Haven and Sinnighe, 1987). In this study, there are only four oils whose Pr/Phy ratios are greater than 1 (Appendix E.5).

R3: Saturate to aromatic (Sat/Aro) ratio is selected even though it is not a biomarker ratio. However,

it was thought that its large range (0.41–5.58) for the Turkish oils may be source rock related.

R4: Sulfur content (% S) of the oils is also adopted as a biomarker ratio because it is a depositional environment indicator although its changes with increasing maturity may be misleading in interpretation (Orr, 1974; Orr, 1978). It is becoming a common belief that oils with high sulfur contents are mainly generated from high sulfur kerogens which can most probably be formed in evaporate-carbonate depositional settings (Palacas et al., 1984; Orr, 1986). The Turkish oils are generally characterized by moderate to high sulfur contents. The oils, in particular, from the Batman-Nusaybin area are richer in sulfur which ranges from 1.23 % to 7.14 %.

R5: C₂₄ tetracyclic terpane to C₂₆ tricyclic terpane ratio (C₂₄*/C₂₆) (peak TC*/Peak h₁+h₂; in Figure 3.3). It has been reported that high values of this ratio reflects evaporate-carbonate environments (Connan et al., 1985; Connan and Dessort, 1987; Palacas et al., 1984; Jones and Philp, 1990). However, in certain terrestrial environments, high ratios of C₂₄*/C₂₆ are also observed (Philp, 1985). On the other hand, Aquino Neto et al., (1981) quoted increasing C₂₄* tetracyclic contents with increasing maturity. In this study, this ratio ranges from 0.11 to 10.65.

R6: C₂₄ tetracyclic terpane to C₂₁ tricyclic terpane ratio (C₂₄*/C₂₁) (peak TC*/peak c1; in Figure 3.3). It is selected and defined for the first time in this study because of the fact that C₂₄ tetracyclic terpane and C₂₁ tricyclic terpane both have high loadings and they are inversely correlated along the principal components generated from the tricyclic terpane data (Table E.1). This feature makes these compounds more appropriate for the ratio selection. The ratio ranges from 0.01 for the GS21 oil to 110.1 for the BR167 oil. The reason for the very low ratio for the GS21 oil is due to fact that it contain negligible amount of C₂₄ tetracyclic terpane. The high ratio for the BR167 oil, on the other hand, results from the lack of the C₂₁ tricyclic terpane in this oil.

R7: C₂₃ tricyclic terpane to C₂₀ tricyclic terpane ratio (C₂₃/C₂₀) (peak e/peak b; in Figure 3.3).

R8: C₂₃ tricyclic terpane to C₂₄ tetracyclic terpane ratio (C₂₃/C₂₄) (peak e/peak TC*; in Figure 3.3). Since peak e and peak TC* were the important compounds of tri-tetracyclic terpane region of the m/z 191 mass fragmetograms, it was decided to see their ratio changing.

R9: (C₁₉+C₂₀) tricyclic terpane to C₂₃ tricyclic terpane ratio (C₁₉+C₂₀/C₂₃) (peak a+peak b)/peak e; in Figure 3.3). This ratio has been used recently to characterize North Sea oils but it has not been assigned to a particular geochemical process yet.

R10: (Tm+Ts) pentacyclic terpane to (C₂₈+C₂₉) tricyclic ratio (Tm+Ts/C₂₈+C₂₉). This ratio is computed as: (peaks (A+B))/(i1+i2+k1+k2); Figure 3.3. This ratio has recently been introduced as a source input parameter by Jones and Philp (1990). The ratio shows a large range for the Turkish oils which is from 17.67 for the BR84 oil to the 0.67 for the CE16 oil (Table E.5).

R11: Pentacyclic terpane ratio (C₃₅/C₃₄). The ratio is computed as : (peaks S+T/peaks Q+R); Figure 3.3 . It has been shown in several studies that the ratio of C₃₅ to C₃₄ pentacyclic terpane may permit to distinguish oils from 70 carbonate sources and those from clastic sources (McKirdy et al., 1983; Palacas et al., 1984). The ratio also reflects the reducing nature of the depositional environment (Jones and Philp, 1990). This ratio ranges from 0.68 for the CE16 oil to 1.18 for The BR211 oil (Table E.5). However, within this range, the ratio is not diagnostic as previously found.

R12: C₂₉ norhopane to C₃₀ hopane ratio (C₂₉NH/C₃₀H). The ratio is computed as: (peak C/peak E); Figure 3.3. The ratio is sensitive to depositional environment and lithology (Palacas et al., 1984; Rullkötter et al., 1985). The ratio is greater than 1 for carbonate derived oils and smaller than 1 for clastic derived oils (Philp, 1985). For the Turkish oils, it ranges from 0.52 for the GS21 oil to 1.67 for the BR167 oil.

R13: 18 α (H) 22,29,30 trisnorhopane to 17 α (H) 22,29,30 trisnorhopane (T_m/T_s) ratio. The ratio is computed as: (peak A/Peak B); Figure 3.3. This ratio is commonly used as a maturity parameter for oils of similar sources and may also be used to indicate source differences for oils of similar maturity (Seifert and Moldowan, 1978). In fact, this ratio covers a large range in the Turkish oils. It ranges from 0.42 for the CE16 oil to 8.81 for the BR189 oil (Table E.5).

R14: C₂₄ tetracyclic terpane to C₃₀ pentacyclic hopane ratio (C₂₄*/C₃₀). The ratio is defined for the first time in this study and computed as: (Peak TC*/peak E); Figure 3.3. This ratio is selected because the C₂₄ tetracyclic terpane and C₃₀ pentacyclic terpane contain high information as will be discussed later. This ratio for the Turkish oils range from 0.01 for the GS21 oil to 1.15 for the BR189 oil (Table E.5).

R15: C₂₃ tricyclic terpane to C₃₀ pentacyclic terpane (C₂₃/C₃₀) ratio. The ratio is computed as: (peak e/peak E); Figure 3.3 and has been used to show the relative proportion of the tricyclic terpane/pentacyclic terpane in a simple form (Sajgo, 1984). For the most oils, this ratio is less than 1 with the exception of the GS 21 oil (1.83) and the CE16 oil (2.51) (Table E.5).

R16: (C₂₁+C₂₁+C₂₁+C₂₂+C₂₂) pregnanes to C₂₉ regular steranes (P/C₂₉) ratio. The ratio is computed as: (peaks I+II+III+IV+V/peaks 19+20+21+22); Figure 3.4. The

origin of the pregnanes is not well known. Wingert and Pomerantz (1986) reported that increasing ratio of pregnanes to C_{29} regular sterane ratio in a heating experiment on a North Sea oil. McKirdy et al., (1983) and ten Haven et al., (1985) also suggested that this ratio can be used as a source indicator. It ranges from 0.87 for the CE16 oil to 2.88 for the BR 167 oil (Table E.5).

R17: C_{21} pregnane to C_{22} homopregnane ratio. The ratio is computed as: (peak III/peak V); Figure 3.4. Among the pregnanes used in this study, the C_{21} pregnane and C_{22} homopregnane are better known compounds. The higher concentration of the two compounds are observed consistently in oils derived from evaporate-carbonate source rocks deposited in hypersaline environment (ten Haven et al., 1985; Clark and Philp, 1989). As shown in Table E.5, these two compounds are high in concentrations in the Turkish oils. The range of this ratio is from 1.86 for the GS21 oil to 2.88 for the R93 oil (Table E.5).

R18: $(C_{21}+C_{21})$ pregnane to $(C_{21}+C_{22}+C_{22})$ pregnane ratio. This ratio is computed as: (peaks I+II/peaks II+IV+V) and via is selected again for further understanding of pregnane compounds with respect to depositional environments of the Turkish source rocks. The ratio is less than 1 for the majority of The Turkish oils excluding CE16 oil which has a ratio of 1.05 (Table E.5).

R19: C₂₂ pregnane to C₂₇ diasteranes ratio The ratio is computed as: (peak IV/peak 1+2); Figure 3.4 and was selected for the first time in this study. The ratio shows a large range which is from 0.09 for the CE16 oil to 2.83 for the GD3 oil (Table E.5).

R20: C₂₇ regular sterane to C₂₉ regular sterane ratio. The ratio is computed as: (peak 11/peak 22): Figure 3.4. The C₂₇/C₂₉ ratio is widely used to provide an indication of the relative amounts of marine versus terrestrial source material in an oil (Huang and Meinschein, 1976). This has been possible since there is a predominance of the C₂₇ sterols in marine organism compared with C₂₉ sterols in higher plant source materials. However, the 73 alternative source of C₂₉ sterols is also possible. Indeed, Patterson (1971) found the C₂₉ component to dominate the sterol distribution in brown algae. The ratio for the Turkish oils ranges from 0.65 for the BR211 oil to 1.74 for the CT16 oil (Table E.5).

R21: C₂₈ regular sterane to C₂₉ regular sterane (C₂₈/C₂₉) ratio. This ratio is computed as: (peak 18/peak 22); Figure 3.4. The source of C₂₈ regular steranes has been suggested to be diatoms (Grantham and Wakefield, 1988; Volkman, 1988) which are the common organisms in recent upwelling environments as in Peru and Walvis Bay (Volkman, 1988). This ratio ranges from 0.33 for the BR47 oil to 1.11 for the A3 oil probably reflecting different source environments from these oils (Table E.5).

R22: C₂₇ regular steranes to C₂₇ diasteranes (R C₂₇/D C₂₉) ratio. The ratio is computed as: (peaks 8+11/peak 1+2); Figure 3.4. Diasteranes are frequently used to distinguish clastic source facies (high diasteranes) from carbonate source facies (low diasteranes) (Palacas et al., 1984; Mello et al., 1988). The ratio show a large changes from 0.94 for the CE16 oil to 10.01 for the CA22 oil which virtually contain no diasteranes (Table E.5).

3.4. Other Data

3.4.1. Stable Carbon Isotope Ratio Data

Stable carbon isotopic composition data of the Turkish oils pertinent to study area was made available to the author (Robertson Research, Geochem Lab., KSEPL). This data includes stable carbon isotope data of saturate hydrocarbons as well as stable isotope data of aromatic hydrocarbons (Appendix G). This data was used primarily for oil to oil correlation purposes and for completeness of the petroleum scenario.

3.4.2. Biomarker Data

The sterane and terpane mass fragmetograms of the oils taken from the Kastel-2 and the Kurtalan-1 wells were generated by Shell and Occidental oil companies and were made available to this study.

CHAPTER IV

DISCUSSIONS

4.1. Oil to Oil Correlations

4.1.1. Philosophy of Oil to Oil Correlation Studies

Oil to oil correlations based on comparisons of chemical and physical properties of two or more oil samples are used in order to establish whether there is a genetic relationship among the oils. If the oils are physically similar it is often quite easy to get a definitive answer. However, when one attempts to correlate a normal oil with a highly mature oil or condensate or with a biodegraded oil, any genetic similarities can be heavily masked by chemical transformations or fractions. In such cases, a definitive answer to a correlation problem may not be possible (Barker, 1979; Hunt, 1979; Tissot and Welte, 1984).

When correlations are made, negative evidence is stronger than positive evidence. No amount of positive evidence can ever prove conclusively that two oils are genetically related (Waples, 1981). Sterane and terpane distributions even in unrelated oils may show simple similarities. This is not conclusive enough to establish a

strong positive correlation. In carrying out oil to oil correlations, therefore, unusual steranes and terpanes should be considered. With negative correlation, the problem is often simpler. We need to find only one important difference between the samples that can not be explained by natural variation or transformation.

It should be noted that correlation parameters should be multiple and should be sensitive to genetic differences in oils. Commonly used correlation parameters are stable carbon isotopes, steranes (including pregnanes, diasteranes, regular steranes), and terpanes (including tricyclic, tetracyclic, pentacyclic terpanes). Other properties such as API gravities, CPI, and n-alkan distributions are somewhat dependent upon the origin of the oils, but may be influenced to a greater extent by such transformation processes as maturation, biodegradation, and migration (Seifert and Moldowan, 1978).

Sterane and terpane biomarkers are now accepted as the most powerful correlation tool. However, because biomarker distribution changes with maturity correlations should be based on biomarker parameters that should be independent from maturity (Mackenzie, 1984).

While steranes and terpanes are very powerful correlation tools, they only represent 1 % of the total oil sample and therefore they are very susceptible to contamination or mixing. Contamination may occur during

secondary migration in the carrier beds, and/or in the reservoirs (Philp, 1985).

The most common method of oil to oil correlation studies is direct visual inspection of chromatographic tracings. Others have employed ratios between pair of hydrocarbon compounds; e.g., pristane/phytane ratio or ternary diagrams (Bockmeulen et al., 1983). However, these methods cover only two or three correlation parameters at a time. To handle all the correlation parameters at the same time, there are advanced methods of multivariate data analysis presently available (Telnaes and Dahl, 1985; Zumberge, 1987; Ediger et al., 1990). R and Q-mode principal component analyses are particularly useful for oil to oil correlation studies when the data set is large enough to handle by eyes or hands.

4.1.2. Assessment of Alteration Processes

Prior to attempting oil to oil correlations and therefore differentiation of the depositional paleoenvironments of the source rocks of SE Turkey oils, it is important to assess effect of thermal alteration (maturation), biodegradation, and/or migration on the crude oil compositions.

4.1.2.1 Thermal Alteration

Thermal alteration is the term which is used for all processes that occur as an inevitable consequence of

increasing age and depth of burial (Barker, 1979). It should be noted that some authors use "maturation" as a synonym for "thermal alteration". The increasing depth of burial that accompanies increasing temperature leads to thermal maturation of the crude oil. As a result, bulk parameters such as API gravity and saturates increase whereas asphaltenes and sulfur content of oils decrease (Barker, 1979; Tissot and Welte, 1984). The convenient way of examining the effect of maturity on crude oil composition is to examine the present day bottom hole temperatures which are frequently shown on the sonic logs. However, the temperatures on the sonic logs do not reflect the actual bottom hole temperatures because of cooling by circulation of drilling fluids, temperatures obtained from the sonic logs of the selected wells were corrected according to the procedure outlined by Nwachukwu (1976). These corrected temperatures were tabulated in Table 3.1. Consequently, the effect of maturity on the Turkish oils was examined on a reservoir temperature versus reservoir depth diagram (Figure 4.1). As can be seen, the deepest reservoir depth and the highest reservoir temperatures belong to the CE16, CE18, and CT16 oils. If the reservoir depth and temperatures control the maturity level of these three oils then the highest API gravity should be belong to the these oils. In fact, as can be seen on the API gravity versus reservoir depth diagram (Figure 4.2), these oils have the highest API gravities and produced from the deepest wells. In general, heavier Turkish oils ($API < 20$) are produced from the shallow depths. The data on Figure 4.2, however, are highly scattered. Some of

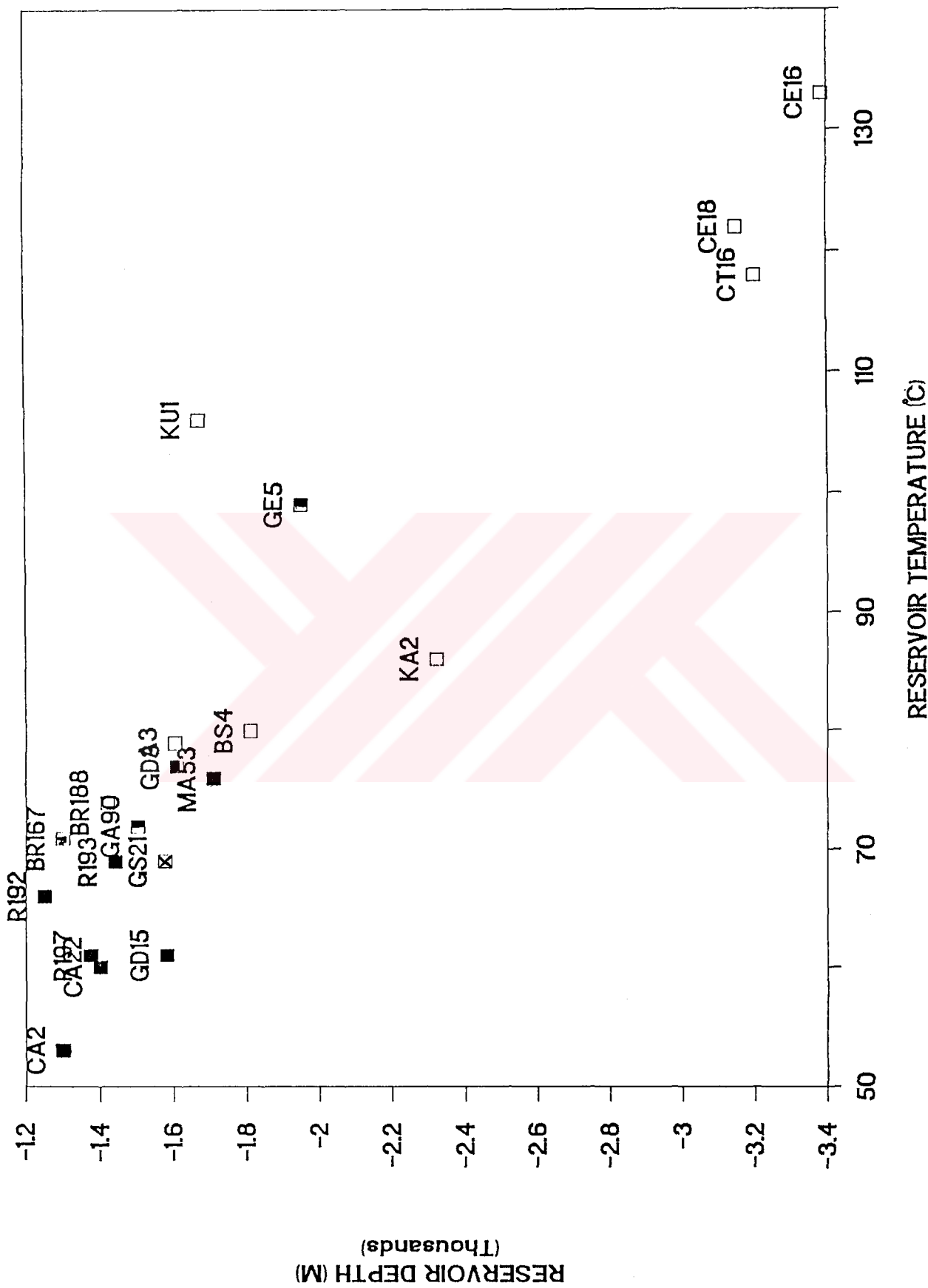


Figure_4.1 Crossplot of depth (m) versus reservoir temperature.

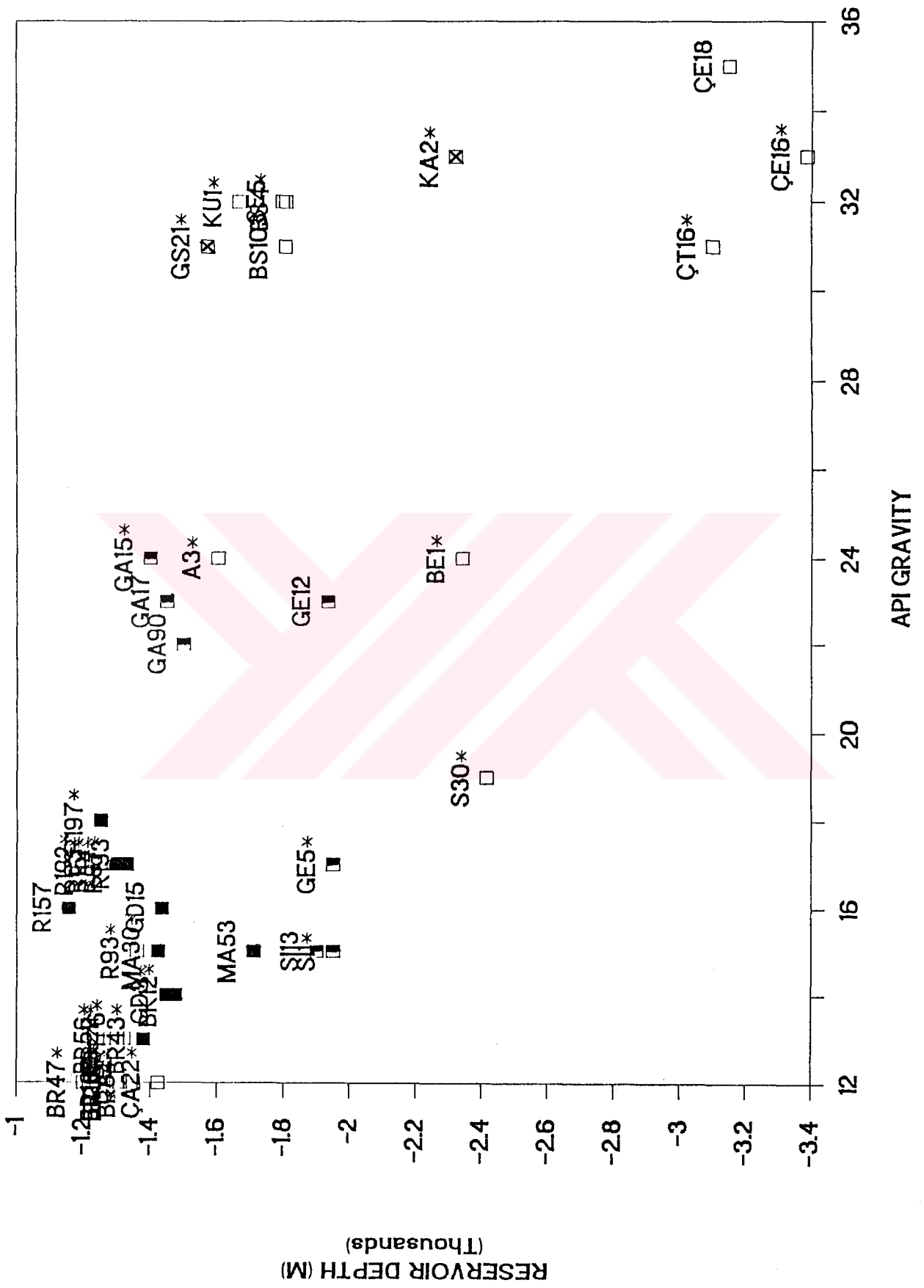


Figure_4.2 Crossplot of depth (m) versus API gravity.

the scattering can probably be explained by the maturity effects. API gravity versus sulfur content plot also shows the same trend (Figure 4.3). Distribution of different API gravities in a large range (17 to 35) at the same depth (2000 m) is probably resulted from migration of the oils from the depocenter of the basin or differences in source character (e.g. GS21 oil). When the relative positions of the oils in Figures 4.1, 4.2, and 4.3 were considered altogether in terms of maturity levels, oils can be divided into three groups; immature oils, mature oils, and moderately mature oils. The normalised percentage compositions of the saturate, aromatic and NSO+Asphaltene fractions of the each oil sample plotted on a ternary diagram depicts essentially the same maturity trend as the previous ones (Figure 4.4).

In addition to bulk parameters, maturity level of the Turkish oils was also dealt with using sterane and terpane biomarkers which have been extensively used to determine maturity level of the oils (Seifert and Moldowan, 1981; Mackenzie, 1984). This is possible since many biomarkers undergo predictable configurational changes as a function of subsurface temperatures and the length of time (Mackenzie, 1984; Philp, 1985).

The most important and reliable biomarker maturity parameter is the proportion of two epimer forms (20R and 20S) of the 5 α (H), 14 α (H), 17 α (H)-C₂₉ regular steranes (Mackenzie, 1984; Rullkötter and Marzi, 1988). This proportion is usually expressed as 20S/(20S+20R). With

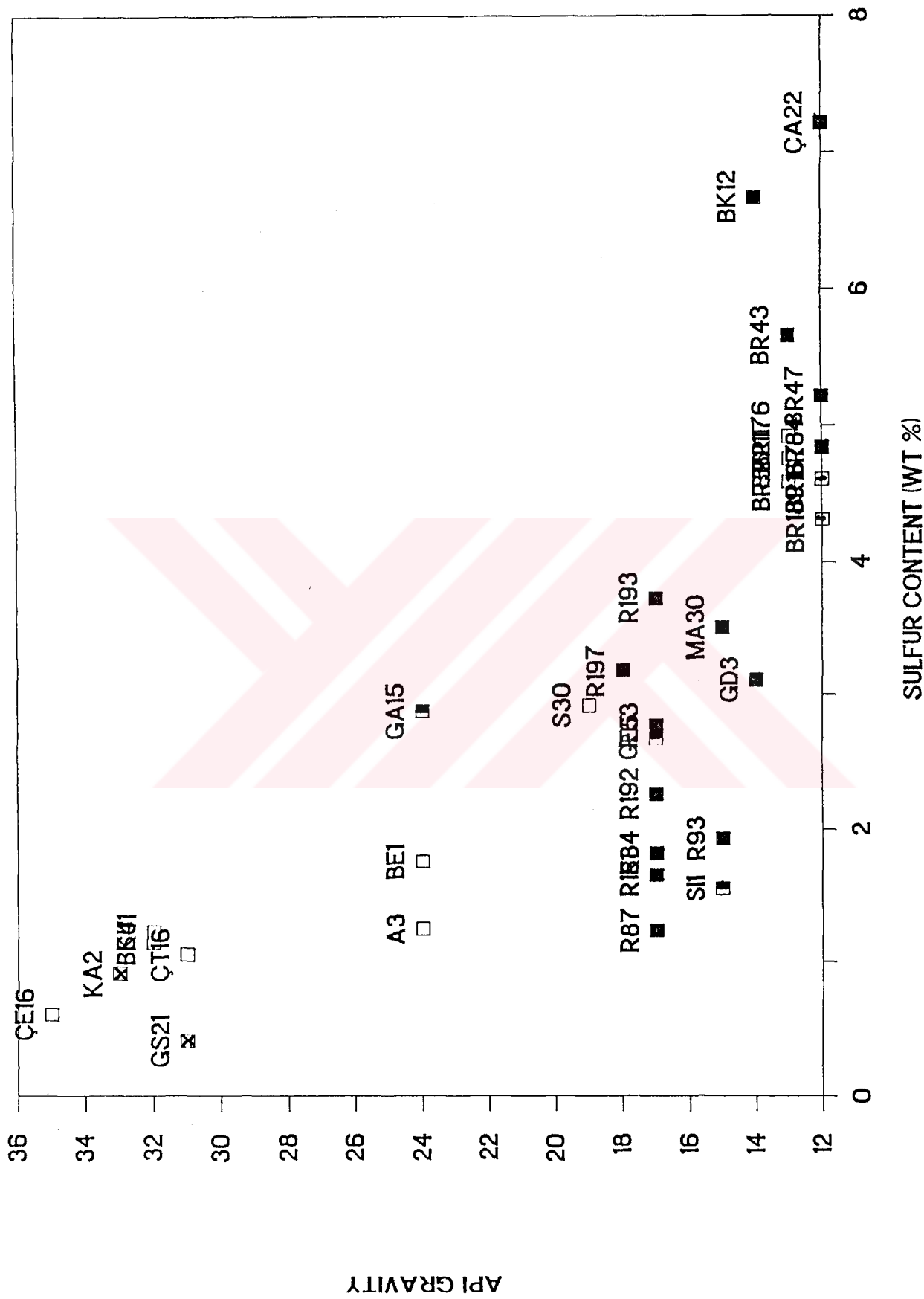


Figure_4.3 Crossplot of depth (m) versus sulfur content (WT %).

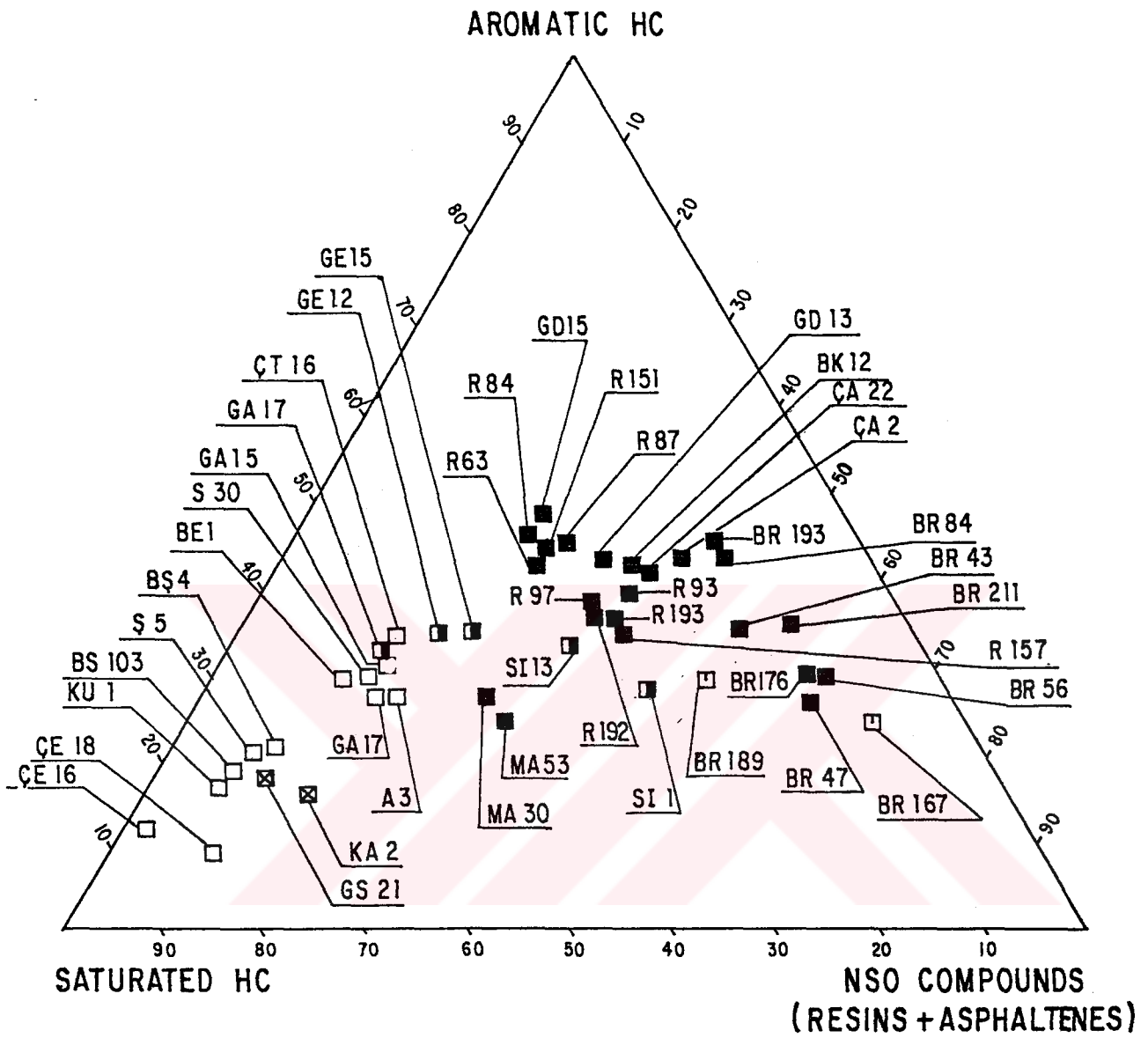
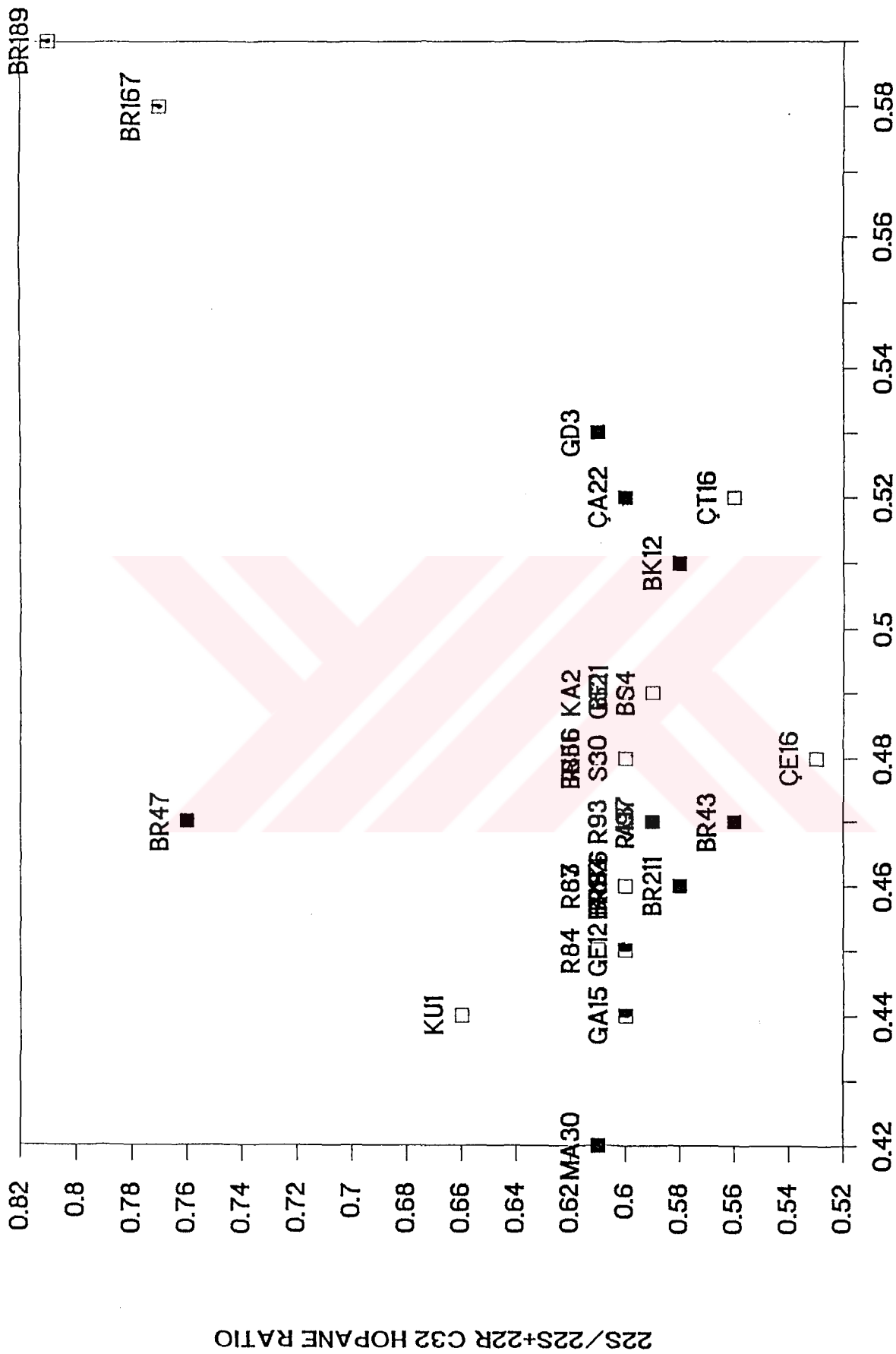


Figure 4.4 Ternary diagram showing the bulk composition of Turkish oils.
 (□ Group I oils, ■ Group II oils, □ Group III oils, ⊠ Group IV oils,
 ■ mixed group oils).

increasing maturity the proportion of 20S increases with respect to 20R. Eventually an equilibrium between two forms is reached, comprising approximately 55 % 20S. Transformation of the biologically produced 22R form of the C₃₂ extended 17 α (H)-hopane to the 22S epimer occurs in the same manner as the 20R-20S conversion for the steranes but a faster rate. The 22/(22S+22R) ratio, at equilibrium, is 60 % 22S.

A plot of the 20S/(20S+20R) sterane (peaks 19/(19+22) in Figure 3.4) ratio against the 22S/(22S+22R) hopane (peaks F/F+G in Figure 3.3) is shown Figure 4.5. As can be seen from this diagram, that the 20S/(20S+20R) sterane ratio of the majority of the oils has not reached equilibrium value of 0.55 whereas the 22S/(22S+22R) ratio of the majority of the oils has approached the equilibrium value of 0.60. It is interesting to note that the oil samples CT16 and CE16, appears to be immature although bulk maturity parameters suggested otherwise. The oil samples BR167, and BR189, on the other hand, seem as mature oils although they have very low API gravities, low Sat/Aro ratios and very high sulfur contents (Table 3.2).

Unexpectedly high 20S/(20S+20R) sterane ratios have been usually observed in oils generated from sulfur rich kerogens compared to sulfur poor kerogens with equivalent thermal history (Zumberge et al., 1984). Orr (1986) defined such a kerogen as type II-S kerogen where "S" stands for sulfur. Higher 22S/(22S+22R) ratios, on the



20S/20S+20R C29 STERANE RATIO

Figure_4.5 Crossplot of 20S/20S+20R C29 sterane ratio versus 22S/22S+22R C32 hopane ratio.

other hand, have been observed in usually bacterially degraded oils (Seifert and Moldowan, 1979).

Biomarkers in the oils are also valuable for estimating the approximate maturity and depth of their possible source rocks provided that the oils have been in the reservoir at temperatures low enough to minimize maturation. A general correlation chart between the biological marker maturity parameters and vitrinite reflectance (Figure 4.6) suggested by Mackenzie (1984) was used for the purpose of predicting maturity level of the possible source rocks. It is evident from this diagram that completeness of 22R conversion to 22S ($22S/(22S+22R) = 0.60$) corresponds a vitrinite reflectance value of at least 0.60 which suggests that the oils were generated from a source rock at least at or after the "onset of oil generation phase" (Figure 4.6). However, incompleteness of 20R conversion to 20S ($20S/(20S+20R) < 0.55$) of the majority of the oils suggests that source rocks have never reached the "maximum oil generation phase" (e.g., 0.9-1.0 R %). This may imply that the Turkish oils analyzed in this study were generated from the marginally mature source rocks whose vitrinite reflectance values were approximately between 0.6 and 0.8. However, one should be in caution that application of epimerization reactions of steranes and hopanes to estimate either kerogen maturation or oil generation phases is only approximate. Because, these reactions do not occur at the same rate as kerogen maturation (e.g. vitrinite reflectance), and are not precisely parallel to oil generation (Waples and

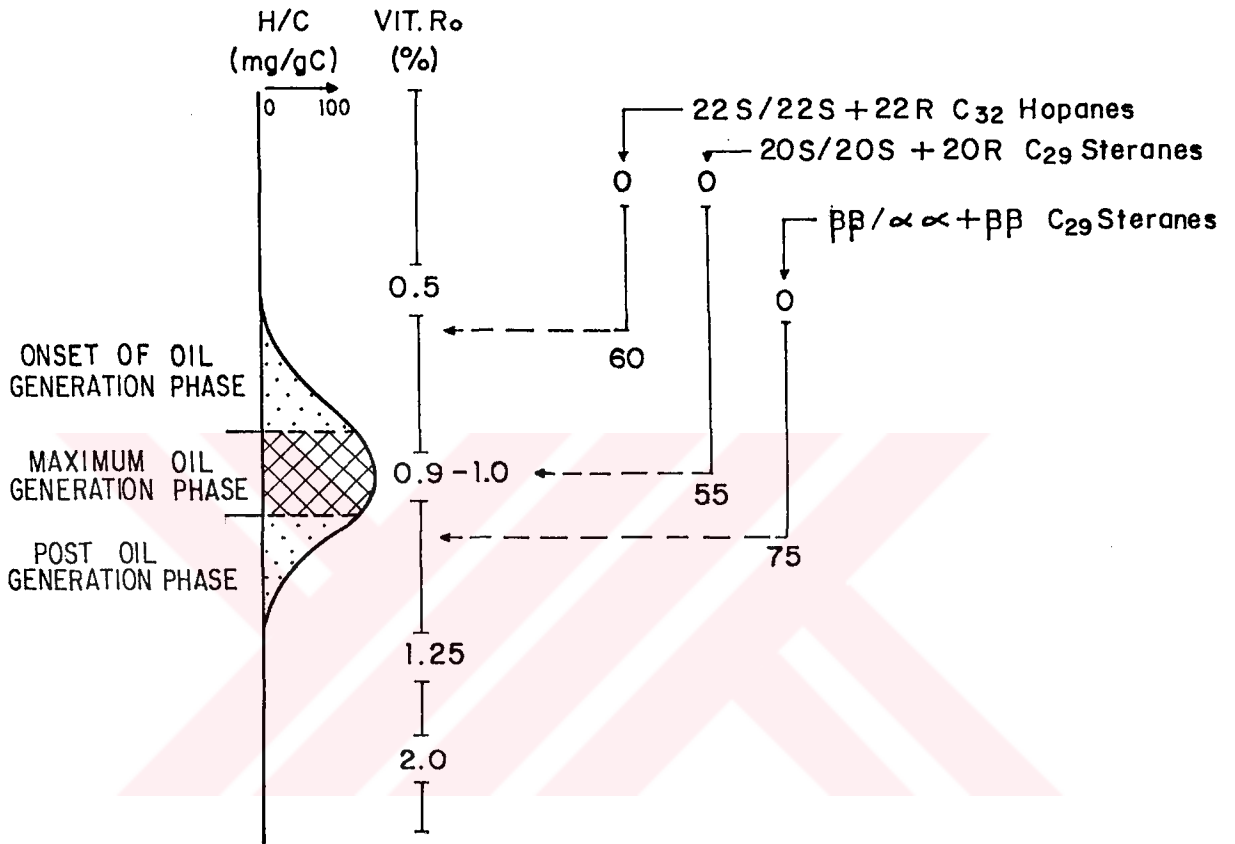


Figure 4.6 Petroleum generation phases versus biological workers maturity parameters (modified after Mackenzie, 1984).

Machihara, 1990; Zumberge, 1987). Nevertheless, such an approach is useful.

4.1.2.2. Biological degradation

In addition to thermal alteration, biological degradation (biodegradation) can also alter the crude oil composition. The most important elements necessary for a biodegradation process include nutrients and oxygen rich freshwater in which bacteria can survive. Subsurface water must contain dissolved oxygen on the order of maximum 8 ppm and reservoir temperatures should not exceed 80 C (176 F) (Williams and Winters, 1969; Phillipi, 1977; Barker, 1979; Connan, 1984). Since the bacteria can not live in the crude oil itself bacterial degradation of crude oils is concentrated at the oil-water contact. When the conditions mentioned above are satisfied then bacteria preferentially degrades lower molecular weight n-alkanes first then it is followed by isoalkanes, cycloalkanes, and aromatics (Williams and Winters, 1969; Evans et al., 1971). After the depletion of n-alkanes, the degradation of the isoprenoids (pristane and phytane) takes place. As a result, oils become heavier (lowering API gravity and n-alkane contents increasing asphaltene and sulfur contents etc.).

In this study, reservoir temperature requirement for the occurrence of biodegradation process was satisfied particularly by the heavy oil reservoirs (Table 3.1). In fact, in the Batman-Nusaybin area, the Raman, Batı Raman,

Çamurlu, Güney Dinçer, Batı Kozluca, and Mağrip field oils with their low API gravities, high asphaltene, and sulfur contents were suspected to be degraded by bacteria. Several lines of evidence, however, indicate that none of the heavy oils was biodegraded. Gas chromatograms of the oils show that the low molecular weight n-alkanes are apparently present and unaltered (Appendix C). The low Pr/n-C₁₇ and the low Ph/n-C₁₈ ratios (Table 3.2) of the heavy oils also suggest that biodegradation has not occurred. Therefore, lower API gravity, higher sulfur content, and higher asphaltene content of the Turkish heavy oils can not be explained by biodegradation processes in terms of gas chromatogram of the oils. Similar results were also found by the author (Gürgey, 1987).

Among the biological markers used in this study, diasteranes, pregnanes, and tricyclic terpanes may hardly be removed during severe biodegradation than regular steranes and pentacyclic terpanes (Curiale, 1983; Reed, 1977; Brooks et al., 1988). The C₂₁ and C₂₂ pregnane contents increase in abundance relative to the diasteranes in oil sand and heavy oils of Western Canada Basin as the biodegradation progress (Brooks et al., 1988). Tetracyclic terpanes may also better survive after severe biodegradation than regular steranes and pentacyclic terpanes and may occur in very severely degraded heavy oils, solid bitumens, and asphalts (Sofer et al., 1985; Rullkötter and Wendish, 1982).

As shown in the m/z 217 sterane mass fragmentograms (Appendix F) and ternary diagram of percentages of diasteranes, pregnanes, and regular steranes (Figure 4.7), the Turkish heavy oils contain very low concentrations of diasteranes, low concentrations of pregnanes and relatively higher concentrations of regular steranes than the light oils. These heavy oils also contain extremely low concentration of the tricyclic terpanes relative to pentacyclic terpanes. As a result, the tricyclic to pentacyclic terpane ratio is very low ranging from 0.12 to 0.19 (Table 3.3).

It is also important to know how biomarker isomer distributions are altered by biodegradation if they are to have used for making maturity determinations. In the first instance of biodegradation, 20R configuration of steranes and the 22R configuration of hopanes are removed more rapidly than their 20S and 22S counterparts (Seifert and Moldowan, 1979; Rullkötter and Wendish, 1982). Two oils from the Batı Raman oil field (BR167 and BR189) having unusually high 20S/20S+20R and 22S/22S+22R ratios (Figure 4.5) bring the fact that both oils are biologically degraded. But as explained previously, these oils show complete series of the n -alkanes on the gas chromatograms and have very low pristane/ n -C₁₇ and phytane/ n -C₁₈ ratios (Table 3.2) suggesting that both are normal crude oils. Thus, the BR167 and BR189 oils carry signs of degraded as well as signs of normal crude oils. The mixing hypothesis for these conflicting evidence is the most plausible explanation.

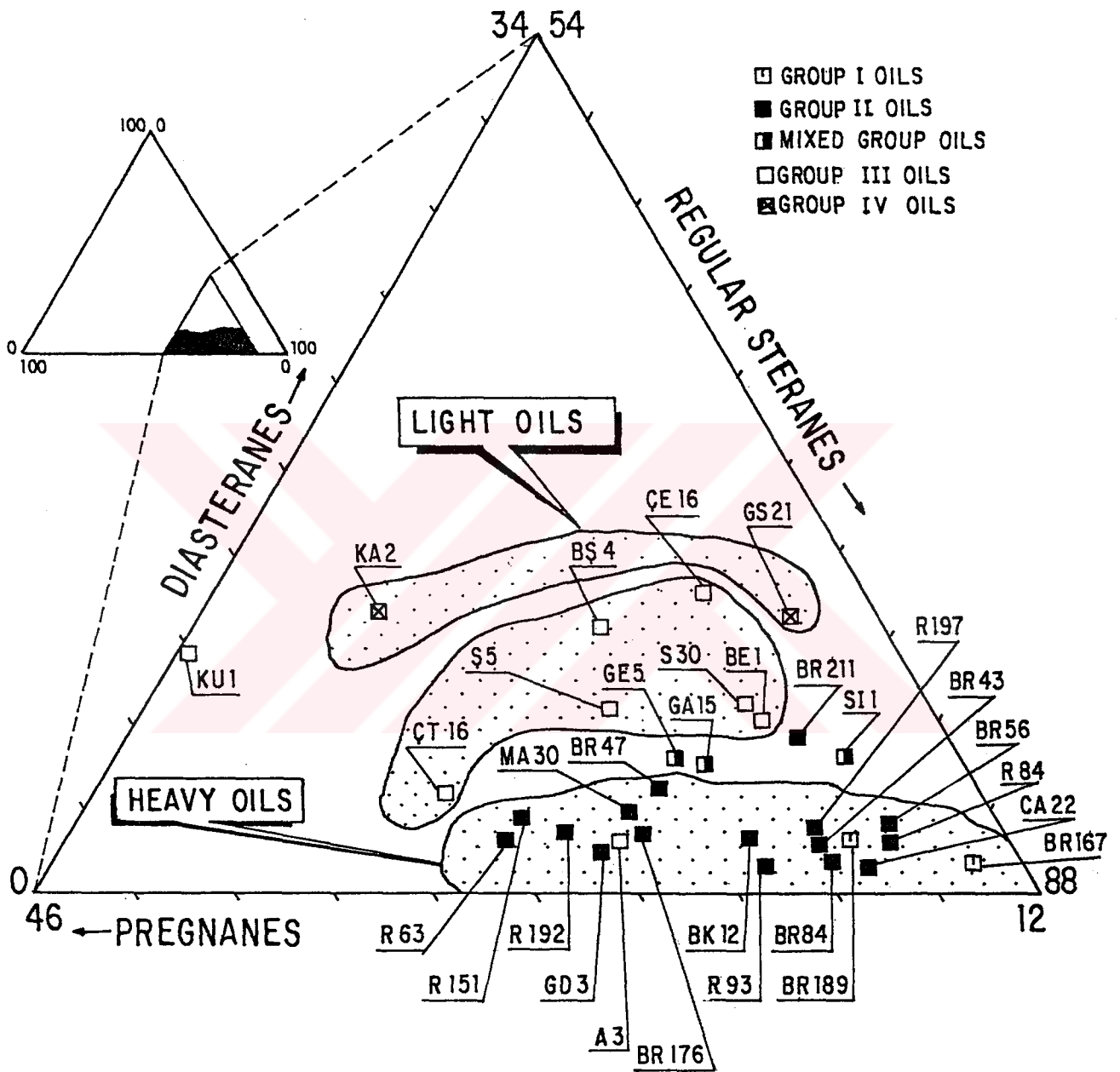


Figure_4.7 Ternary diagram showing relative proportions of regular steranes, pregnanes, and diasteranes of the Turkish oils.

4.1.2.3. Secondary Migration

Secondary migration is the remobilization of oils from the generation side (source rock) to the accumulation side (reservoir) (Waples, 1981; Hunt, 1979; Tissot and Welte, 1984). Mechanism and changes in oil composition during secondary migration are two research areas of geochemistry that have been currently receiving a great deal of attention. Among the several migration models, (i.e., Gussow's (1954) differential entrapment model, and Silverman's (1965) phase separation models) Seifert and Moldowan's (1981) geochromatographic-fractionation model was demonstrated to be more useful in explaining changes in crude oil composition and obtaining information on relative secondary migration distances. Accordingly, the low molecular weight n-alkanes will migrate faster than the higher molecular weight n-alkanes (Illich et al., 1981; Leythausen et al., 1983). Among the biomarkers certain sterane isomers, namely $\beta\beta$ steranes migrate faster than their corresponding aa steranes and rearranged steranes faster than regular steranes (Seifert and Moldowan, 1981; Carlson and Chamberlain, 1986). In the terpanes, the tricyclic terpanes migrate faster than the pentacyclic terpanes (Seifert and Moldowan, 1981; Leythausen et al., 1983). Hence, oils with relatively long migration pathways will possess higher concentration of low molecular weight n-alkanes, $\beta\beta$ -steranes, diasteranes, and tricyclic terpanes if all effects, such as source, biodegradation, and maturity on the crude oils, are equal.

As explained in the previous section, immaturity, not biodegradation was found to be the main cause of the low API gravities of the heavy, sulfur rich oils in the Batman-Nusaybin area excluding BR189 and BR167 oils. If the geochromatographic-fractionation model is applied to the heavy oils, the lower concentration of tricyclic terpanes (Table 3.3), lower concentration of diasteranes (Table 3.6) and higher concentration of heavy molecular weight asphaltenes (Table 3.2) suggest that the heavy oils have not migrated long distances. This implies that source rock of the heavy oils is very close to their present day reservoir rocks. Similar conclusions were also drawn by the author (Gürgey, 1987). However, presence of high concentration of $\beta\beta$ -steranes in the heavy Turkish oils is not fitting the geochromatographic fractionation model of migration. Recent study by Zhusheng et al., (1988) showed that $\beta\beta$ steranes are frequently present in the early generated and subsequently expelled oils. As the maturity of oils increases it becomes difficult to differentiate migration effects from maturation effects (Seifert and Moldowan, 1981; Mackenzie, 1984). It was indicated in this study that maturity is obviously affected the light oils of the Adıyaman-Kozluk and Northern Diyarbakır regions in terms of present day reservoir depth, temperature, and several bulk, and molecular level maturity parameters. However, at this point of the research, it is very difficult to distinguish migration effects from the maturity effects. Therefore, prediction of migration distances of the Adıyaman-Kozluk and the northern Diyarbakır oils between their source rock site and

reservoir site was difficult to determine. This may be possible only when the successful oil to source rock correlations are carried out.

4.1.3. Stable Carbon isotope Ratios

Stable carbon isotopes have been widely used for oil to oil correlation studies (Stahl, 1978; Mackenzie et al., 1985; Peters et al., 1989). A positive correlation is usually established when the isotopic differences in a group of oils do not exceed 1.0 per mil. It has been observed that biodegradation of oils can result in an isotopic shift of the aromatic fraction toward more negative values while the isotopic composition of saturate fractions remains essentially unchanged (Sofer, 1984). It has been also observed that isotopic changes caused by maturity makes oils richer in C13 and these differences in a single family of oils probably do not exceed 2 per mil (Sofer, 1984).

Carbon isotope values of SE Turkey oils show distinct differences that help organize the oils into genetic groups (Appendix G). For example, when the stable carbon isotope values of saturate fraction of the oils were plotted against the stable carbon isotope values of aromatic fractions of the oils, presence of two genetically different oils were distinguished (Figure 4.8). The Sarıcak and Kastel-2 oils of the northern Diyarbakır area were clearly different from the remaining SE Turkey oils by having the lighter (more negative)

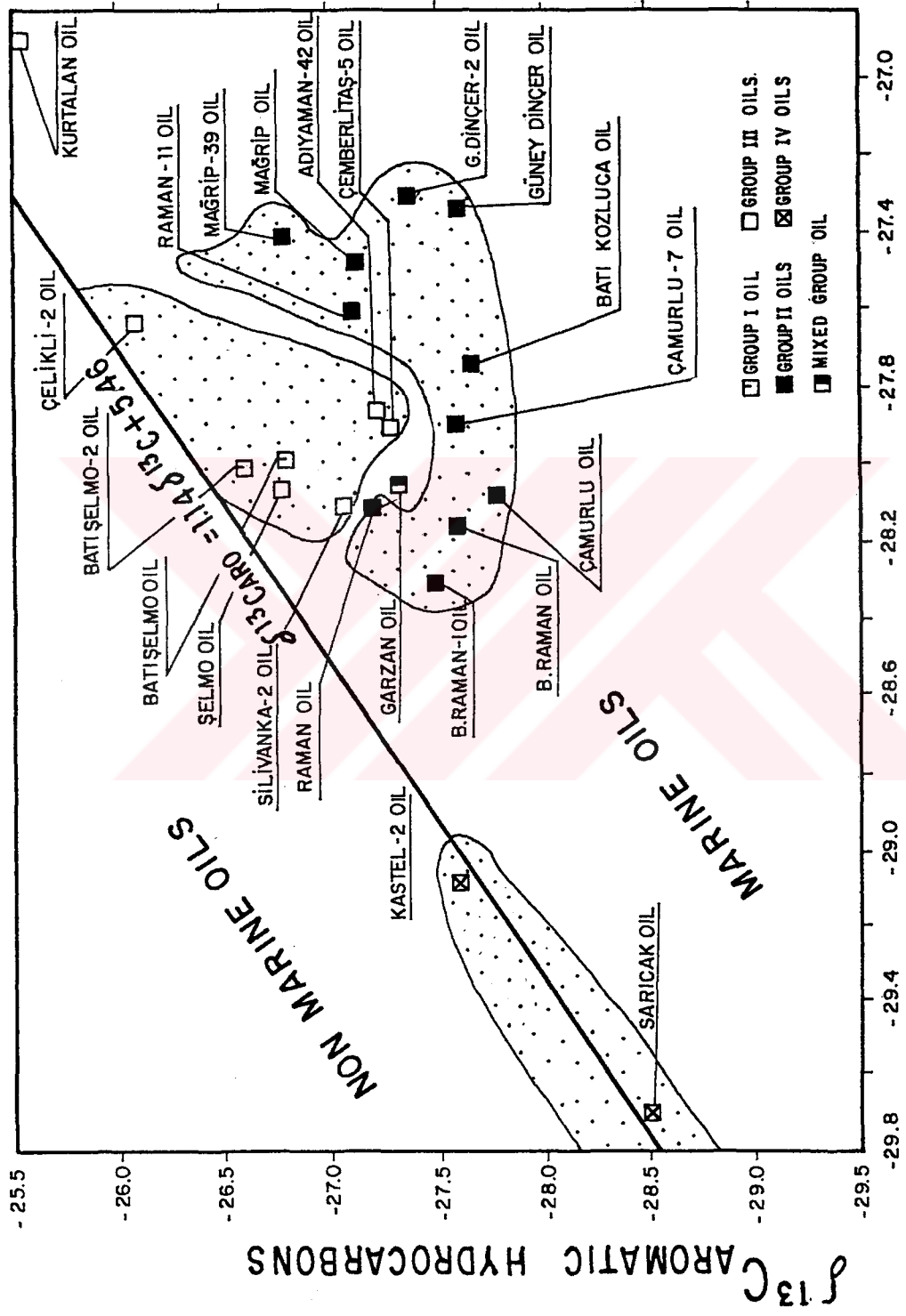


Figure_4.8 Stable carbon isotope ($\delta^{13}C$) of saturates versus aromatics. Solid line drawn according to Sofer (1984).

saturate and aromatic carbon isotope values. The solid line in Figure 4.8 separates the oils that have sources dominated by waxy (non-marine oils) and non-waxy (marine oils) organic matter (Sofer, 1984). The Sarıcağ and Kastel-2 oils being on the solid line may be attributable to some terrigenous waxy input into the depositional environment of their source rocks. Higher pristane to phytane ratios ($Pr/Phy > 1$) of these oils support this argument.

Oils from the Kozluk-Adıyaman and from the Batman-Nusaybin area were hardly distinguished from each other by their heavier carbon isotope values. The Çelikli-2 oil is the most mature oil also has the heaviest $\delta^{13}C$ value among the Kozluk area oils. Kurtalan oil has a completely different $\delta^{13}C$ value. The reason could be an extremely strong maturity effect on this oil and/or its different organic matter origin from the rest of oils. The Batman-Nusaybin oils were slightly different from the Kozluk-Adıyaman oils by having slightly heavy $\delta^{13}C$ value of aromatic hydrocarbons.

The separation into two different oil families with different isotope values is due to their origin from at least two different source beds in SE Turkey. However the separation of the Kozluk-Adıyaman and Batman-Nusaybin oils as seen in Figure 4.8 is not conclusive.

4.1.4. Multivariate Data Analysis

There are advanced methods of multivariate data analysis. The methodology and applicability of the analysis to geology is well documented in general text books (Davis, 1973; Joreskog, et al., 1976; Govett, 1983). Principal component analysis (PCA) which is one of R- and Q-Mode factor analysis techniques is particularly useful for classifying oil samples (Q-Mode) and clarifying relationships among the variables (R-Mode) where the data set is large (Christie et al., 1984; Telnaes and Dahl, 1985; Zumberge, 1987). In the following sections, PCA will be applied to five different data sets; (1) Tri-Tetracyclic terpane data set, (2) Pentacyclic terpane data set, (3) Tri-tetra-pentacyclic terpane data set, (4) Sterane data set, and (5) Selected biomarker ratio data set. Results of these statistical data analyses will be interpreted in order to establish genetically different oil groups (Q-mode). In order to determine the most distinguishing parameters for SE Turkey oils, interrelationships among the biomarker variables will be also examined.

4.1.4.1. Tri-tetracyclic Terpanes

An application of R- and Q-mode PCA to the tri-tetracyclic terpane data set (Table E.2) was initially resulted in linear regression correlation coefficients for each combination of thirteen tri-tetracyclic terpane compounds (Table H.1). Not surprisingly, there are high

positive and negative correlation coefficients. The negative ones may in part be attributed to closure effect which occurs when the data is defined to a constant sum (Kvalheim, 1985). The C₁₉, C₂₀, and C₂₁ tricyclic terpanes have relatively high positive correlation coefficients with each other ($r=+0.85$, $+0.71$, $+0.51$). However, only the C₂₁ triyyclic terpane shows relatively high correlation coefficients with the C₂₂ through the C₂₈ tricyclic terpanes. The C₂₄* tetracyclic terpane (TC* in Figure 3.3), on the other hand, shows negatively high correlations with the C₂₀, C₂₁, C₂₄, C₂₅, and with the two C₂₈ tricyclic terpanes suggesting that it may have a different origin than the tricyclic terpanes.

PCA applied to the tri-tetracyclic terpane data (Table H.1) further gave three significant principal components (PCs) which accounted for 40.15, 22.28, and 14.04 % of the total variance of the data respectively. The scores of the 31 oils onto the first two PC axes were given in Figure 4.9 which displays the relationship between the oils. Samples falling close to each other are considered to be similar with respect to the distributions of 12 tricyclic terpanes and 1 tetracyclic terpane. It can be seen that the oils were separated into four groups based on the 62.43 % of information content carried by the data in Table H.1.

Geochemically meaningful grouping of the oils on the score plot of PC1 vs PC2 (Figure 4.9) requires a geochemical characterization of each PC in terms of

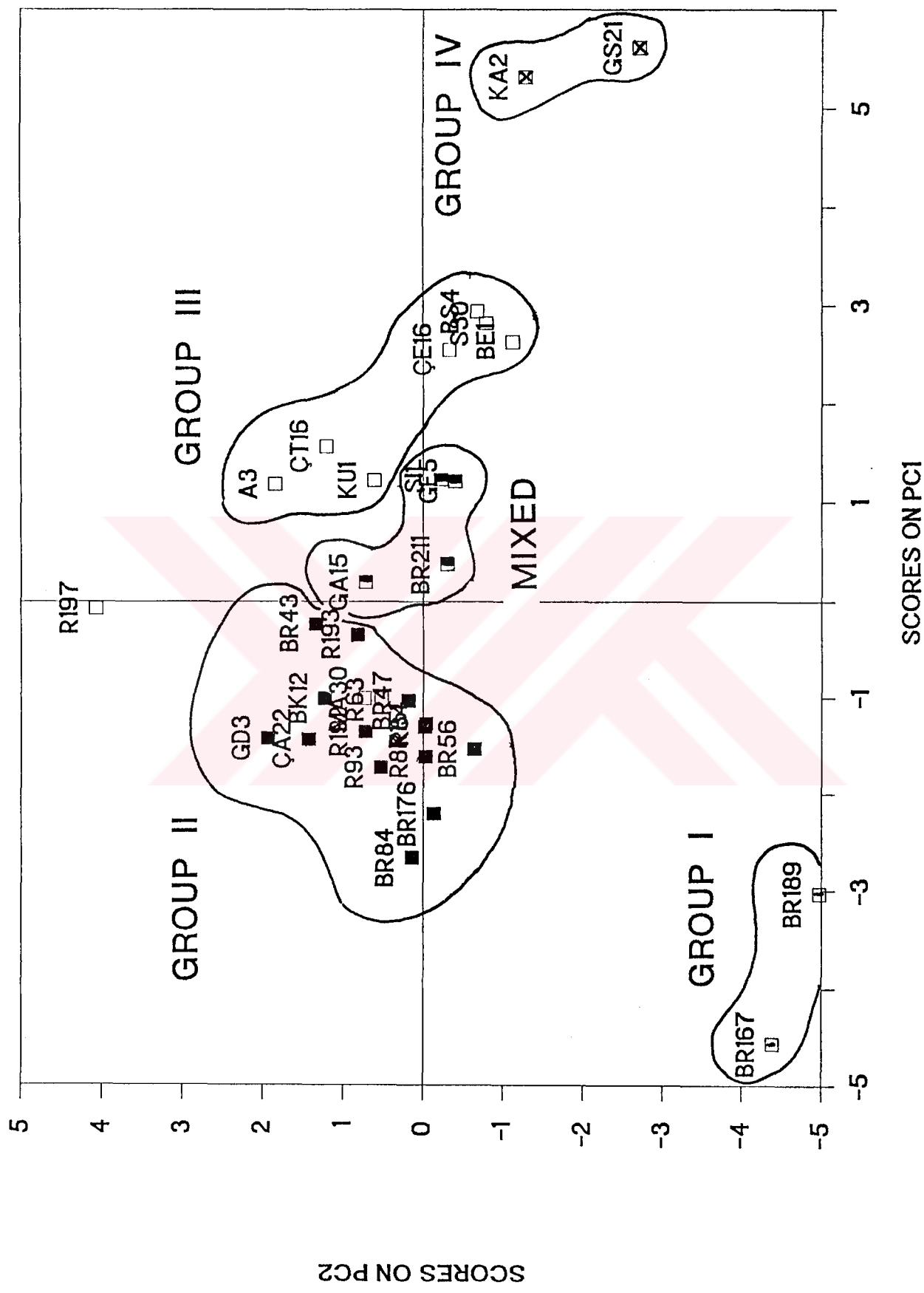


Figure_4.9 Crossplot of tri-tetracyclic terpene scores on PC1 versus PC2.

maturity, migration, depositional environment, and source input. This characterization was possible since the input data matrices of the statistical data were initially scaled (e.g., the mean is subtracted from each corresponding value and divided by the standard deviation) so that the score plots and the loading plots become compatible. The loading plot displayed the relationships between the original variables and helped to characterize the PC axes (Figure 4.10). Here, PC1 was dominated by the relative amount of the C₂₄ tetracyclic terpane (TC*) and the C₂₁(c1), C₂₄(f), C₂₅(g), and C₂₈ (h1 and h2) tricyclic terpanes. Since the C₂₄* tetracyclic terpane had negative value and the tricyclic terpanes had positive values for the loadings these classes of compounds were negatively correlated along PC1.

The C₂₄* tetracyclic terpane has been originally proposed as a degradation product of the pentacyclic hopanes (Aquino Neto et al., 1981). It has been also reported that the C₂₄* tetracyclic terpane is the dominant peak in terrestrially derived Australian crude oils with almost no tricyclic terpane (Philp, 1985). Extensive geochemical studies on C₂₄* tetracyclic terpane showed that within evaporate-carbonate basins, organisms are particularly rich in C₂₄* tetracyclic terpane. It has been observed as a major peak in a sabkha environment, Guatemala (Connan et al., 1985), in an evaporate sequence from the Camogué Basin, South France (Connan and Dessort, 1987), in evaporate-carbonate rocks and oils from the Lower Cretaceous Sunniland Formation in South Florida

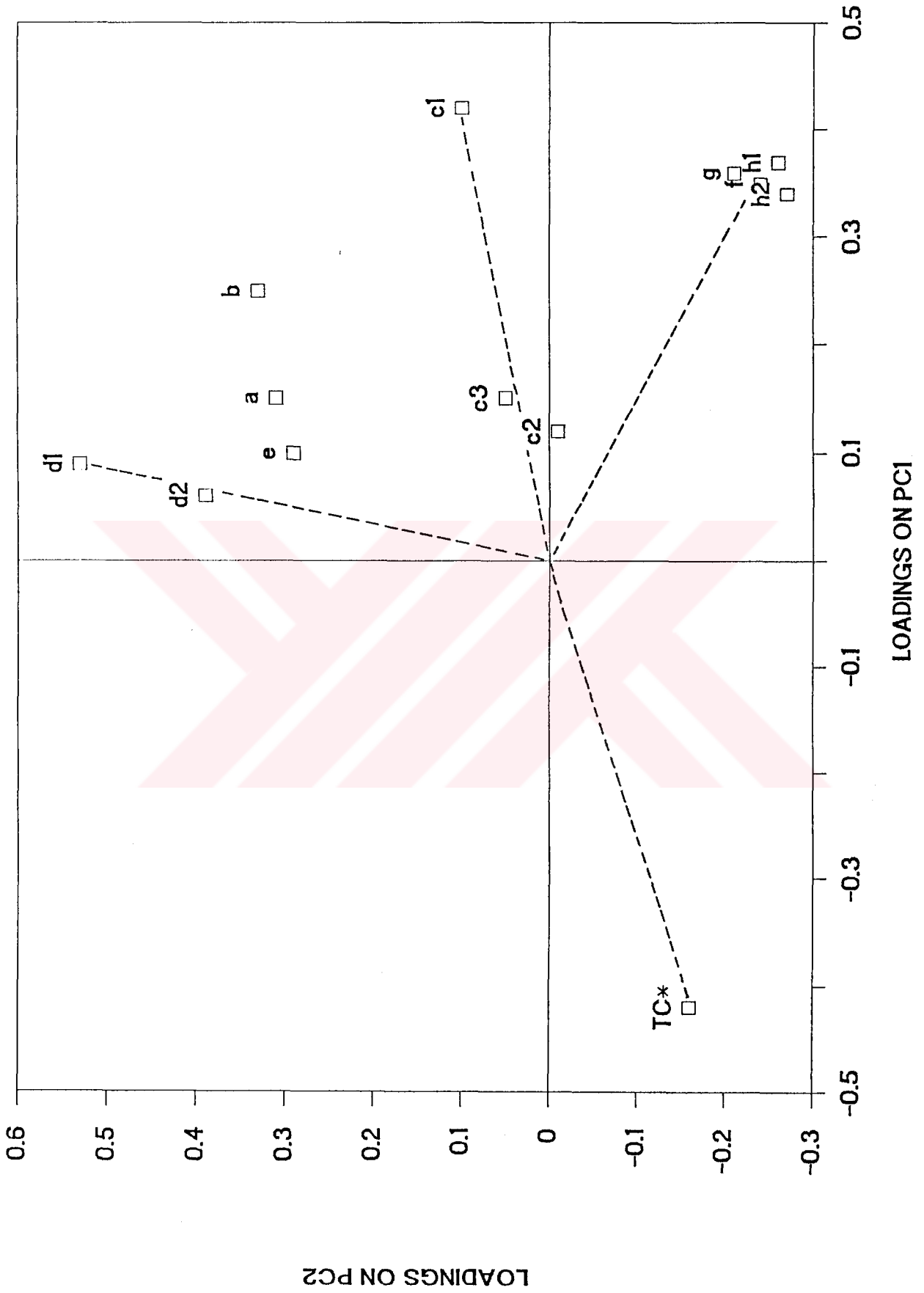


Figure_4.10 Crossplot of tri - tetracyclic terpene loadings on PC1 versus PC2.

(Palacas et al., 1984). A recent study by Clark and Philp (1989) also demonstrated that evaporate-carbonate Black Creek Basin rocks and oils in Canada contain an abundance of C₂₄* tetracyclic terpane. This further supports its use as a biomarker for hypersaline environments within the evaporate-carbonate systems. On the basis of geochemical study on worldwide selection of 216 crude oil samples by Zumberge (1987), the C₂₁ and the C₂₄, C₂₅ tricyclic terpanes have been shown to be in great abundance in lacustrine oils and in deeper marine facies oils respectively. It has been believed that tricyclic terpanes including the C₂₁ terpanes have microbial or algal origin (Aquino Neto et al., 1981). It is clear that PC1 is characterized by depositional environment (evaporate-carbonate), and organic matter type (microbial and/or algal).

PC1 was also influenced by maturity. This is well explained on the API gravity versus PC1 crossplot (Figure 4.11) which shows fairly good linear correlation between the API gravity and the PC1. This implies that in addition to the depositional environment and organic matter type, maturity is also an important factor on PC1.

PC2, on the other hand, seems to be dominated by the high loadings by the C₂₂ and the lesser extent by the C₂₃, C₁₉ and C₂₀ tricyclic terpanes (Figure 4.10). Therefore, it is difficult to characterize and to group of the oils along the PC2 axis.

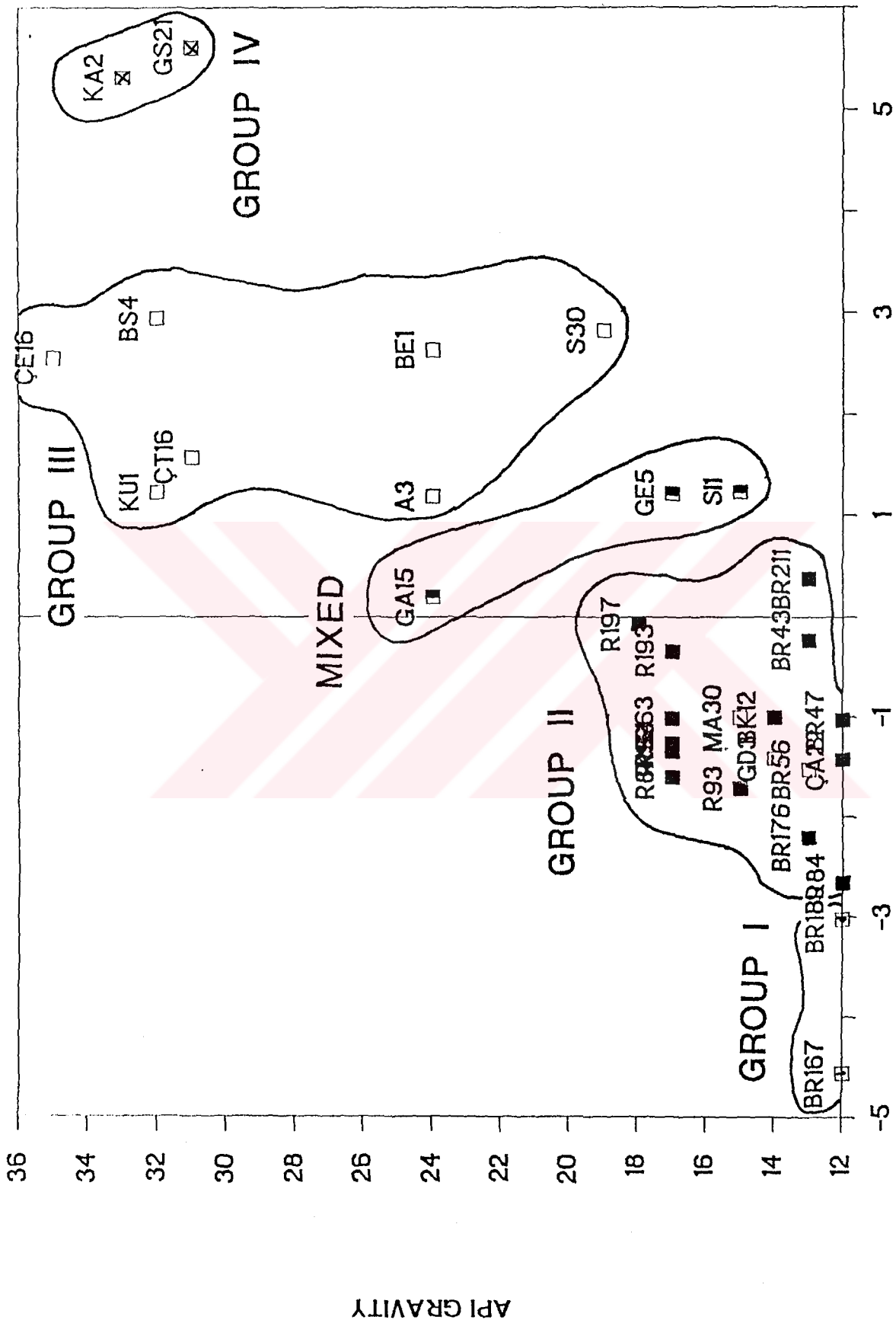


Figure_4.11 Crossplot of scores on PC1 versus API gravity.

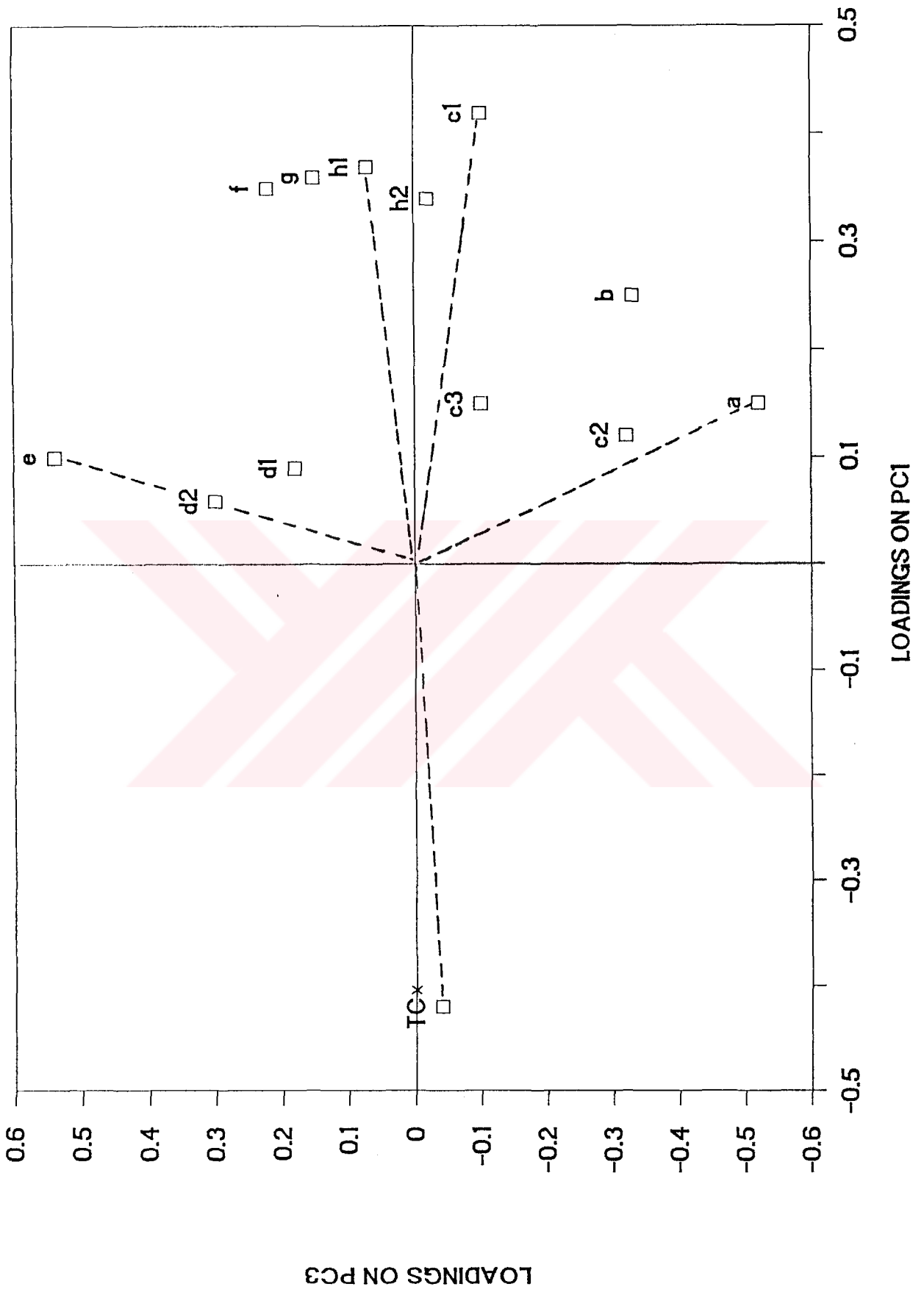
On the basis of discussion above, SE Turkey oils can be separated into four groups. Along the PC1 axis, there are two end members (Figure 4.9) which are separated from each other based upon a strong contribution of the C₂₄ tetracyclic terpane and C₂₁, C₂₄, C₂₅, and C₂₆ tricyclic terpane peaks (Figure 4.10). The first end member oils, the Group I and Group II oils, contain high concentration of the C₂₄* tetracyclic terpane which probably implies that the possible source for the Group I and Group II oils is an evaporate-carbonate rock deposited in a hypersaline environment. The second end member oil (Figure 4.9), the Group IV oils, in contrast to the Group I and Group II oils contain no C₂₄* tetracyclic terpane but higher abundances of the tricyclic terpanes maximizing at the C₂₃ tricyclic terpane. Between the two end member oils namely the Group I-II and Group IV oils, there are also other oils considered as the Group III oils and mixed origin oils. The most distinguishing features of the Group III oils is that they contain relatively higher concentrations of the C₂₃ peak (e) and higher tricyclic terpane percentages relative to the other oil groups. Tricyclic terpane to pentacyclic terpane ratio of these oils range from 0.59 in the BE1 oil to 1.71 in the CE16 oil. It was reported that the C₂₃ triyclic terpane concentration appears to be the most dominant peak in the oils derived from phosphate rich carbonate source rocks (Powell et al., 1975; Zumberge, 1987). This may help to assign phosphate rich carbonate source rocks to the Group III oils which are distributed in the Adıyaman-Kozluk areas. Thus geochemical correlation within the Group III oils becomes

interesting. Such a correlation between the Adiyaman and Kozluk oils has not been observed by the previous workers. This correlation obviously requires an organic rich carbonate source rock present both in the Adiyaman and Kozluk areas.

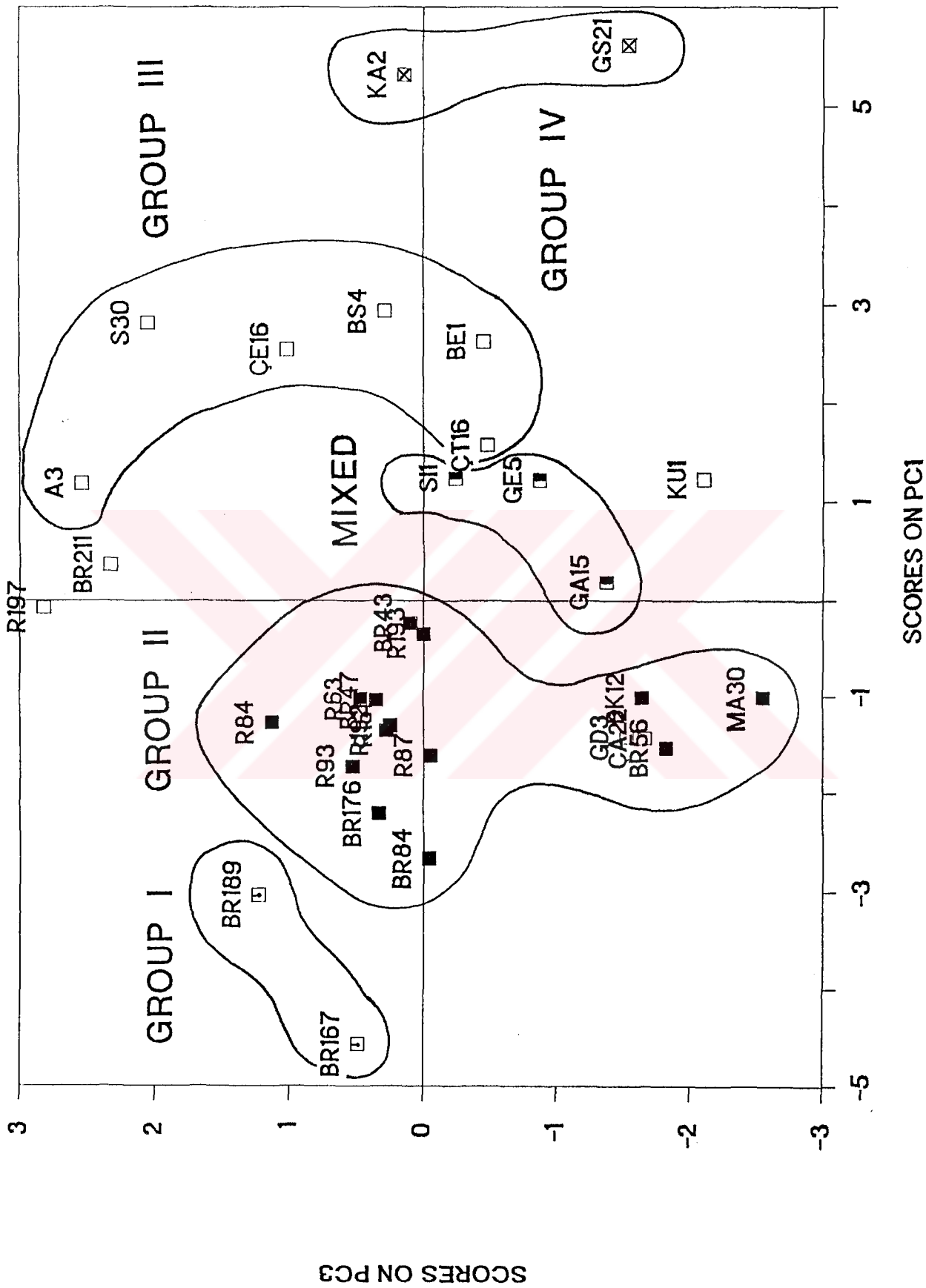
The oils (the GA15, GE5, SI1, and BR211 oils) showed tri-tetracyclic terpane distributions between Group II and Group III oils (Figure 4.9), are also located between the Group III oils of the Kozluk area and the Group II oils of the Batman area. This strongly suggests that these oils are mixture of the Group II and Group III oils.

Figure 4.12 shows the score crossplot of PC1 versus PC3 and Figure 4.13 shows the loading crossplot of PC1 versus PC3. The same grouping of the oils is again repeated. PC3 is dominated by strong negative correlation of the C₂₃(e) and the C₁₉(a) tricyclic terpanes. However, based on these terpanes, interpretation of the PC1 axis is very difficult. Carbonate effect on this PC is also reflected by overlapping of the C₂₃ peak on the Adiyaman oil when Figure 4.12 and Figure 4.13 are compared.

One of the advantageous of R-mode PCA in oil to oil correlation studies is to select the most distinguishing parameters which can cause grouping of the oils. For example, application of PCA to tri-tetracyclic terpanes revealed that the C₂₄* tetracyclic terpane and the relative concentration of the tricyclic terpanes best



Figure_4.12 Crossplot of tri-tetracyclic terpene loadings on PC1 versus PC3.



Figure_4.13 Crossplot of tri-tetracyclic terpane scores on PC1 versus PC3.

separate the Turkish oils into the genetic groups. In order to use this characteristic of the PCA, the plot of the C₂₄ tetracyclic terpane percentage versus the tricyclic terpane percentage was prepared (Figure 4.14). As can be seen from the figure, this plot also provides the same grouping but separation among the oil groups are now very obvious.

4.1.4.2. Pentacyclic Terpanes

As mentioned before, the first step of PCA is the conversion of the original input data matrix (Table E.3) into a correlation matrix which essentially provided the quantitative measure of linear regression correlation coefficients among the 18 pentacyclic molecules (Table H.2). The highest positive correlation ($r=+ 0.97$) and the highest negative correlation ($r=- 0.82$) were observed between the C₃₅ 22S:C₃₄ 22S, and Tm:C₃₁ 22R pairs respectively. The Tm also shows negatively high correlations with the C₃₁-C₃₅ extended hopanes. However, this negative correlation is in conflict with the literature which suggest that both parameters contain similar information in terms of organic matter type, maturity, and anoxicity of the environment of deposition. The Tm and C₃₁-C₃₅ extended pentacyclic terpanes are known to decrease with maturity (Seifert and Moldowan, 1981) and the precursor of the Tm and the extended terpanes is known to have the same bacterial origin (Aquino Neto et al., 1981). Therefore, it may be concluded that the Tm in the Turkish oils is probably source related rather than

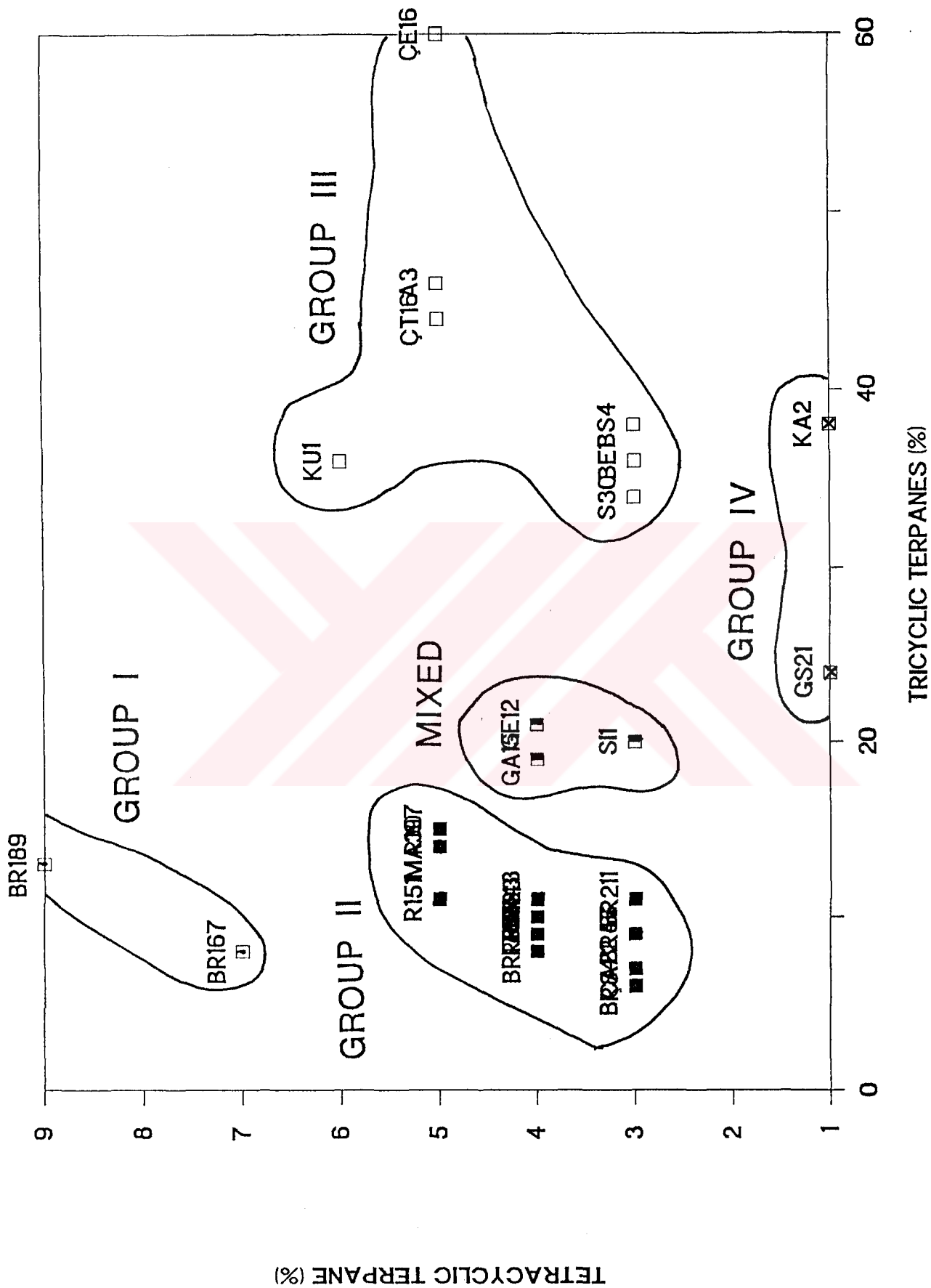


Figure_4.14 Crossplot of tricyclic terpanes (%) versus tetracyclic terpane (%).

maturity. Very low negative correlation coefficients between the T_m and T_s ($r=-0.55$) also confirms that T_m in the Turkish oils is not strictly maturity dependent although, well known a negative correlation between T_m and T_s has frequently been demonstrated in several basins around the world (Seifert and Moldowan, 1978; Philp, 1985; Rullkötter et al., 1985).

Relation between two unidentified peaks B1 (peak B1 in Figure 3.3) and the E1 (peak E1 in Figure 3.3) was also examined to see the behavior of these compounds with respect to geochemically better known compounds. The peak E1 has been recently identified as 30-Norhopane (Prof. Dr. R.P Philp, University of Oklahoma, personal communication, 1991). The compounds B1 shows positively high correlations with the C_{29} norhopane ($r= 0.69$), with the E1 ($r=0.75$) and negatively high correlations with the $C_{31}22S$ ($r=-0.75$) and $C_{33}22R$ ($r=-0.65$) extended hopane. The compound E1, on the other hand, shows negatively high correlation coefficients with the T_s ($r=-0.61$) and the $C_{31} 22S$ ($r=-0.61$). These correlations may reveal that both the B1 and E1 somehow carry the same information, however, their information with respect to other pentacyclic terpane is presently unclear.

Application of PCA to the pentacyclic terpane data set (Table E.3) further gave three significant components accounting for 38.14, 28.61, and 15.54 % respectively of the total variance. Figure 4.15 shows the scores of the 31 oils onto the first two principal component axes. This

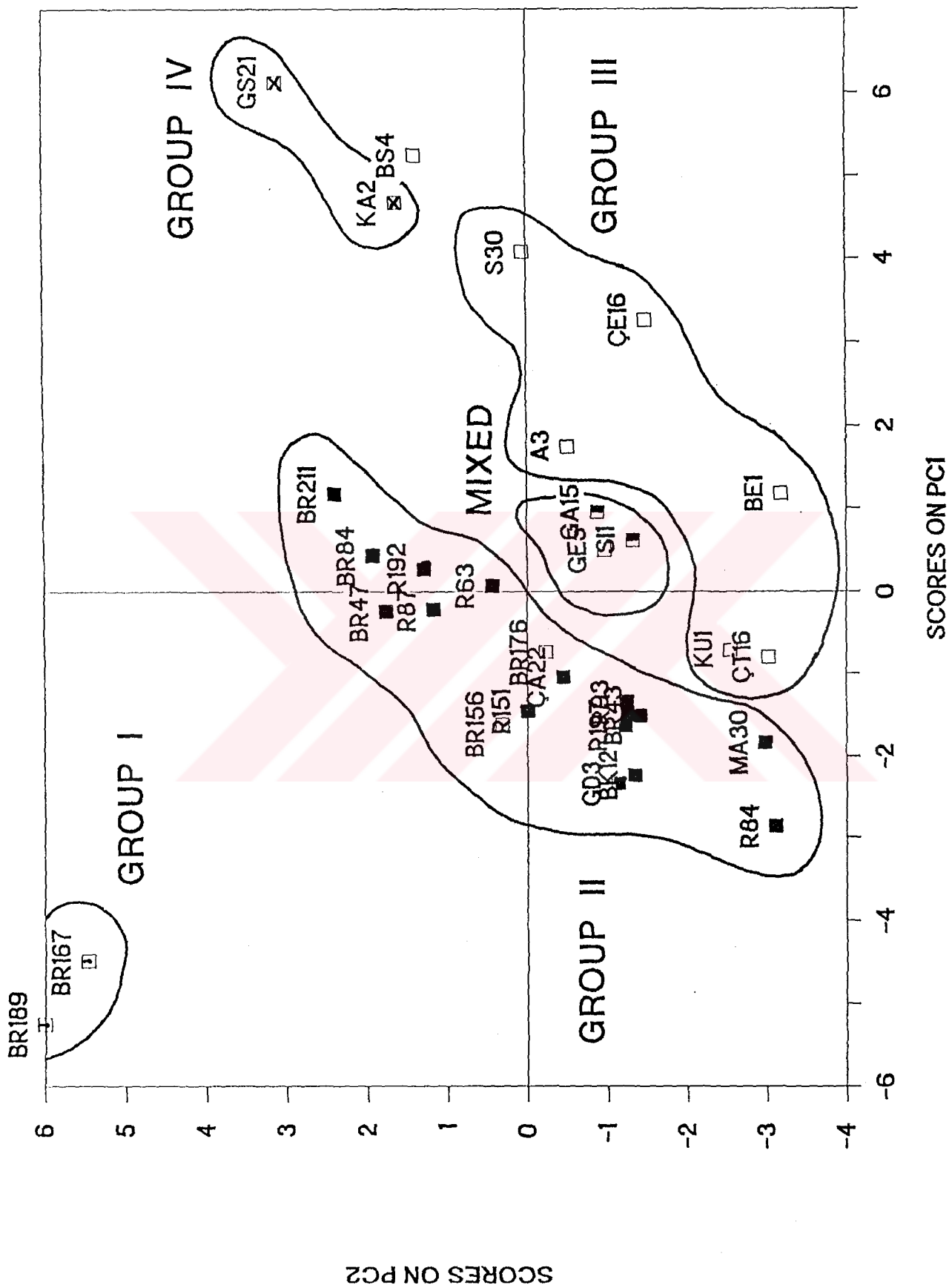
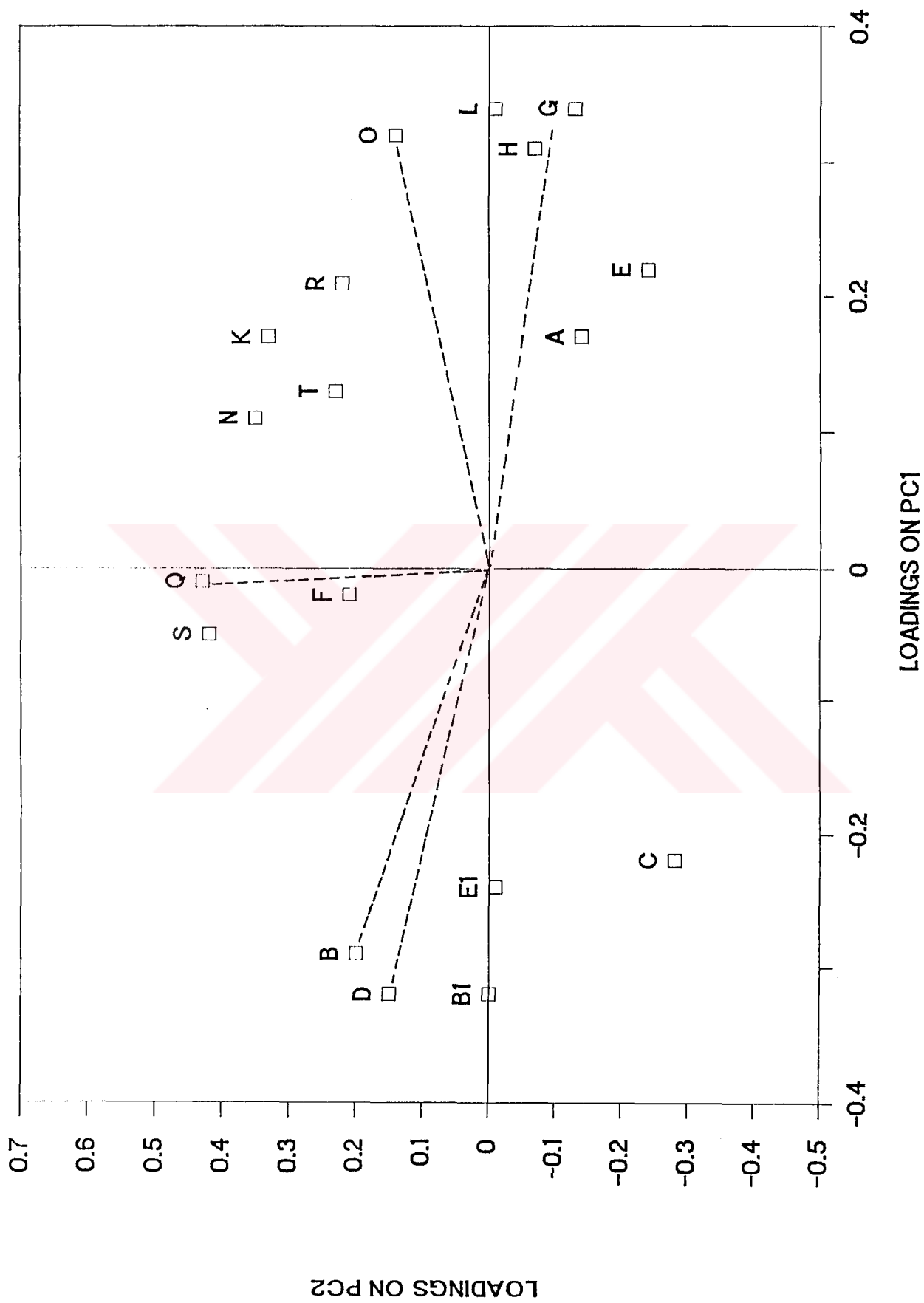


Figure 4.15 Crossplot of pentacyclic terpene scores on PC1 versus PC2.

score plot displays the relationships between 31 oils in terms of 18 pentacyclic terpane compounds and revealed that there are four distinct oil groups. This is consistent with those of the previous tri-tetracyclic terpane grouping. The Group I and Group IV oils again are the two end members. The mixed group oils (e.g., GA15, GE5, SI1) again take their place between the Group II and Group III oils.

In order to find out which pentacyclic terpane compounds caused the separation of the oils in Figure 4.15, geochemical characterization of PC1 and PC2 was carried out utilizing the loading plot of PC1 versus PC2 (Figure 4.16). As shown by the loading plot, PC1 is most strongly effected by the Tm (B), C₂₉-normoretane (D), B1 and E1 (C₃₀-norhopane) on the one side and the C₃₁-22R (H), C₃₁-22S (G), C₃₂-22R (L), and C₃₃-22R (O) extended hopanes, on the other side. As stated earlier, bacteria are the main source of the extended hopanes (Ourisson et al., 1984). It is also interesting to note that positions of the Tm and Ts in Figure 4.16 exactly reflects their abundance in the oils. For example, the Group I oils contain highest amount Tm and Group IV oils contain lowest amount of Tm. Therefore, it may be concluded that the Tm to Ts ratios for the Turkish oils can be one of the most useful distinguishing feature for the Turkish oils. With a similar approach, beside the Tm to Ts ratio, the C₂₉-norhopane to C₃₀-hopane ratio of the Turkish oils seems also a significant correlation parameter. For example, when the C₂₉-norhopane to C₃₀-hopane ratio is

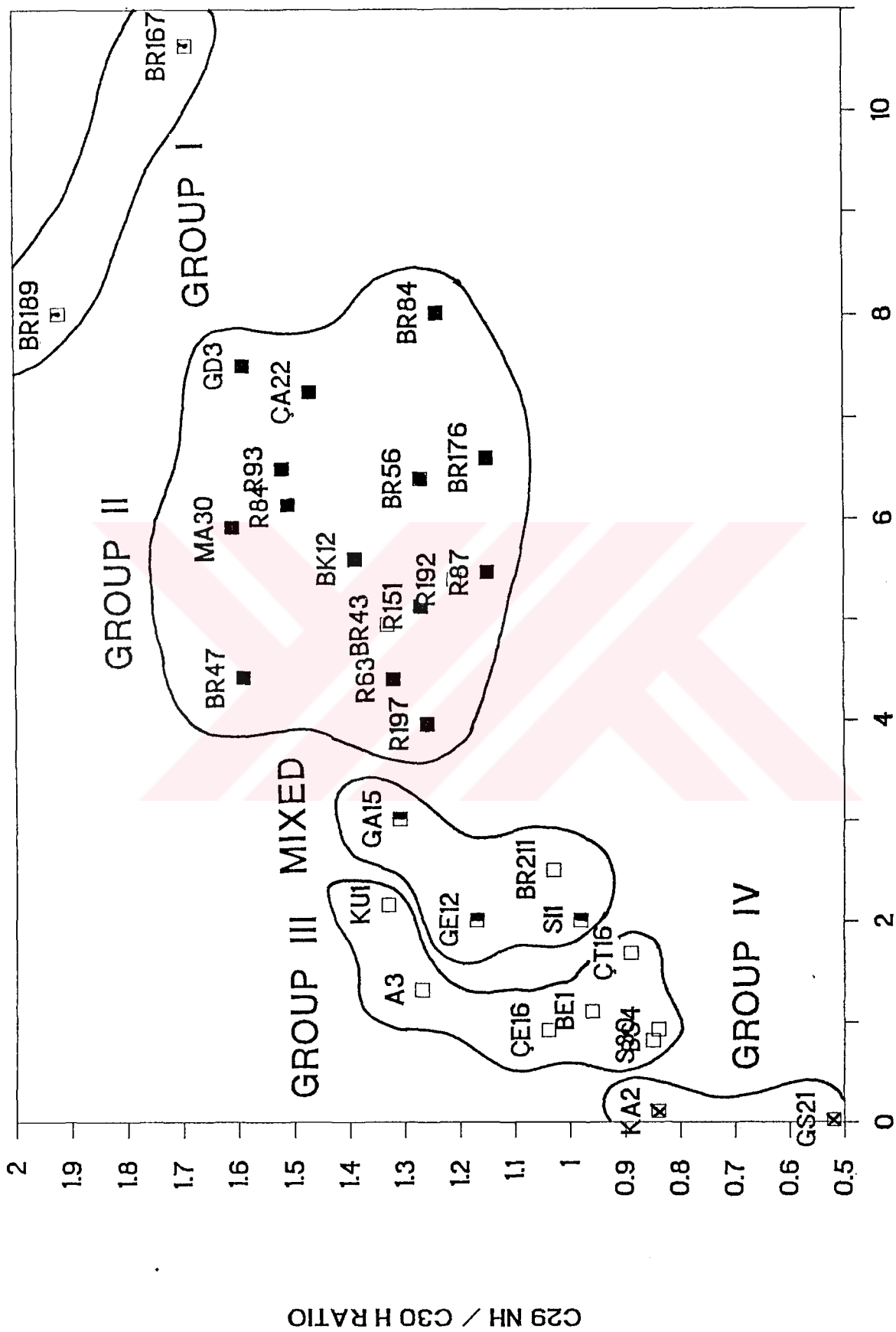


Figure_4.16 Crossplot of pentacyclic terpene loadings on PC1 versus PC2.

plotted against the C_{24^*}/C_{26} ratio (see tri-tetracyclic terpane section) similar oil groupings were obtained (Figure 4.17) but separation among the oil groups was sharper. As mentioned earlier, since high C_{29} -Norhopane to C_{30} -Hopane (>1) ratios are frequently found in carbonate sourced oils and high C_{24} tetracyclic to C_{26} tricyclic terpane ratios (>2) in evaporate-carbonate sourced oils. Grouping of the oils in this plot is based on the depositional environment of the possible source rocks. This also implies that along the PC1 axis, oils are also grouped according to their source depositional environment.

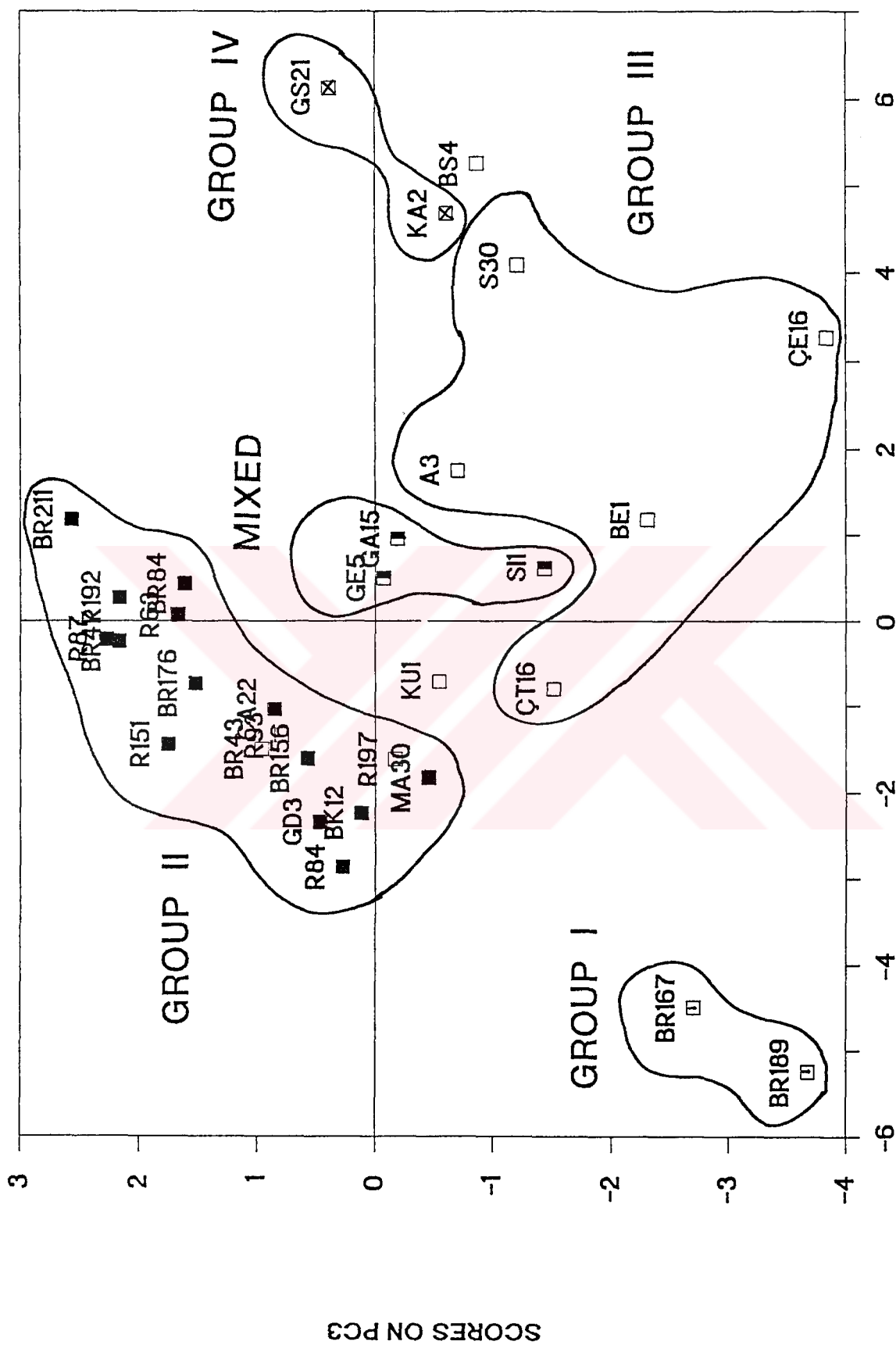
PC2 is dominated by the relative amount of C_{34} -22S (Q) and C_{35} -22S (S) extended hopanes which are not enough to interpret PC2 axis geochemically. However, the C_{35} -22S peak is usually greater than the C_{34} -22S peak in oils derived from evaporate-carbonate source rocks (ten Haven et al., 1988; McKirdy et al., 1983; Clark and Philp, 1989). The range of the ratio for the Turkish oils changes from 0.68 to 1.18. Some of the Group II oil which are believed to generate from evaporate-carbonate sources based on tri-tetracyclic terpane data have this ratio smaller than one (Table E.5).

The score plot of PC1 versus PC3 and corresponding loading plot are shown in Figures 4.18 and 4.19 respectively. Here again, the score plot resulted in essentially the same oil grouping. The mixed oil samples GA15, GE5, SI1 again take place very close to the



C24* / C26 RATIO

Figure_4.17 Crossplot of C24*/C26 ratio versus C29 norhopane / C30 hopane ratio.



SCORES ON PC1

Figure_4.18 Crossplot of pentacyclic terpene scores on PC1 versus PC3.

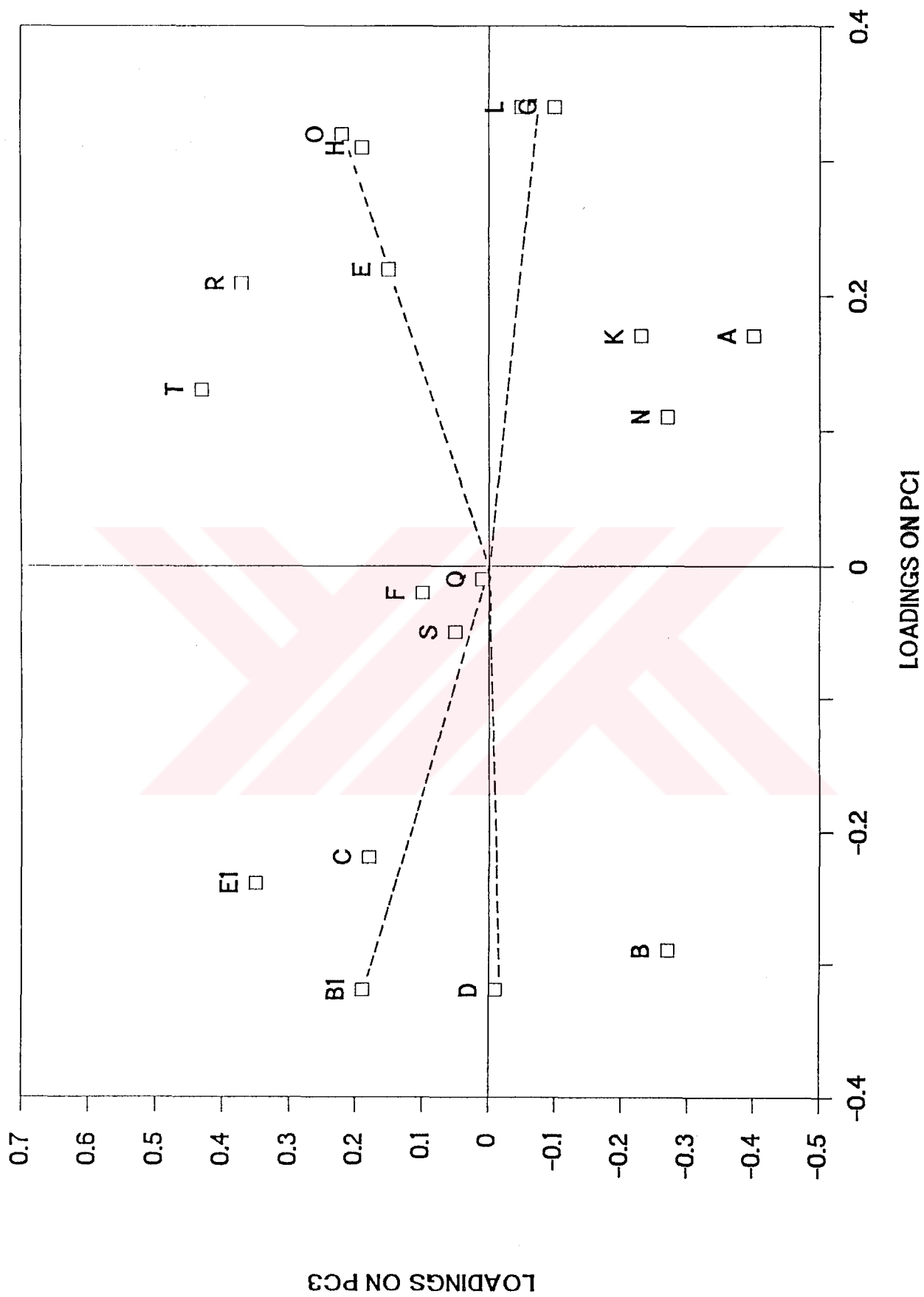


Figure_4.19 Crossplot of pentacyclic terpene loadings on PC1 versus PC3.

separation line of the Group II and Group III oils on the graph. The oil sample KA2 of the Group IV oils appears as a member of the Group III oils and the oil sample BS4 of the Group III oils seems to be a member of the Group IV oils. The reason may be the similarity of the KA2 and BS4 oils in terms of the C₃₃-22R, C₃₄-22R, and C₃₂-22R compounds. This may happen as a result of mixing of the oils. However, high maturity level of these oils should also be considered because while the maturity level increases, oils become increasingly similar (Barker, 1979).

Another unusual aspect of the pentacyclic terpane distribution is the presence of the gammacerane (VII) which was not used in the statistical treatment of the data input. This compound appears to be associated with organism that thrive in hypersaline environments (Moldowan et al., 1985). In particular, all the Group I and Group II oils contain notable gammacerane concentrations (Table 3.3). Hence, presence of gammacerane is also evidence that the source rocks of the Group I and Group II oils were deposited in hypersaline environment.

4.1.4.3. Tri-Tetra-Pentacyclic Terpanes

In the previous sections, applications of PCA to tri-tetracyclic terpanes and pentacyclic terpanes were discussed separately. In this section, PCA will be applied to the data matrix (Table E.1) which is a combination of

the tri-tetracyclic terpanes and pentacyclic terpanes data together.

Linear regression correlation coefficient matrix data resulted from this application is given in Table H.3. All the tricyclic terpane compounds show relatively high positive correlations with each other with correlation coefficients ranging from 0.69 to 0.97. This implies that tricyclic terpanes contain similar type of information but contain different information than the tetracyclic terpane and pentacyclic terpanes. This is probably because of the reflection of their obvious common marine origin (Ourisson et al., 1984) but does not agree with the terrestrial origin of the C₁₉ and C₂₀ tricyclic terpanes as Reed (1977) reported. It is also interesting to note that the C₂₄* tetracyclic terpane show no correlations either with the tricyclic terpanes or with the pentacyclic terpanes. This unusual character of the C₂₄* tetracyclic terpane suggests that it carries different type of information than the tricyclic and pentacyclic terpanes. Bacterial reworking which is a common process in hypersaline evaporate-carbonate depositional environments is probably the source of C₂₄* tetracyclic terpanes in the Turkish oils. Within the pentacyclic terpanes, high correlation between the C₃₀ hopane and C₃₁-C₃₅ extended hopanes implies that they may have a common bacterial origin (Ourisson et al., 1984). The Ts is the only pentacyclic terpane which shows positive correlations with the tricyclic terpanes.

PCA applied to the tri-tetra-pentacyclic terpene data set further gave three significant principal components accounting for 64.10, 13.25, and 9.06 of the total variance respectively. Figure 4.20 shows the scores for 31 oils on the first two principal components. Again, four different oil groups in addition to a one mixed origin group are distinguishable. It is also interesting to note that position of mixed origin oils between the Group II and Group III oils, further supports the possibility of hydrocarbon contributions from the Group II and Group III oils.

PC1 versus PC2 loading plot of the 15 terpene variables showed that the Ts (A) forms a cluster with the C₁₉ (a) through C₂₉ (k) tricyclic terpanes to the right, the C₃₀-hopane (H) and the C₃₁-C₃₅ extended hopanes cluster at the bottom, the C₂₉-norhopane (NH) to the left and Tm (B) and C₂₄* (TC*) at the top (Figure 4.21). PC1 is dominated by the inverse correlation of the tricyclic terpanes and one pentacyclic terpene Ts, and pentacyclic C₂₉-norhopane (NH). As the linear correlation coefficient data suggested, these two group of compounds are negatively correlated along PC1 which probably resulted in a distinct separation of oil groups along the PC1 axis (Figure 4.20). Therefore, it is suggested here that percentage of the C₂₉-norhopane and the percentage sum of the individual tricyclic terpanes could be an excellent correlation parameter for SE Turkey oils.

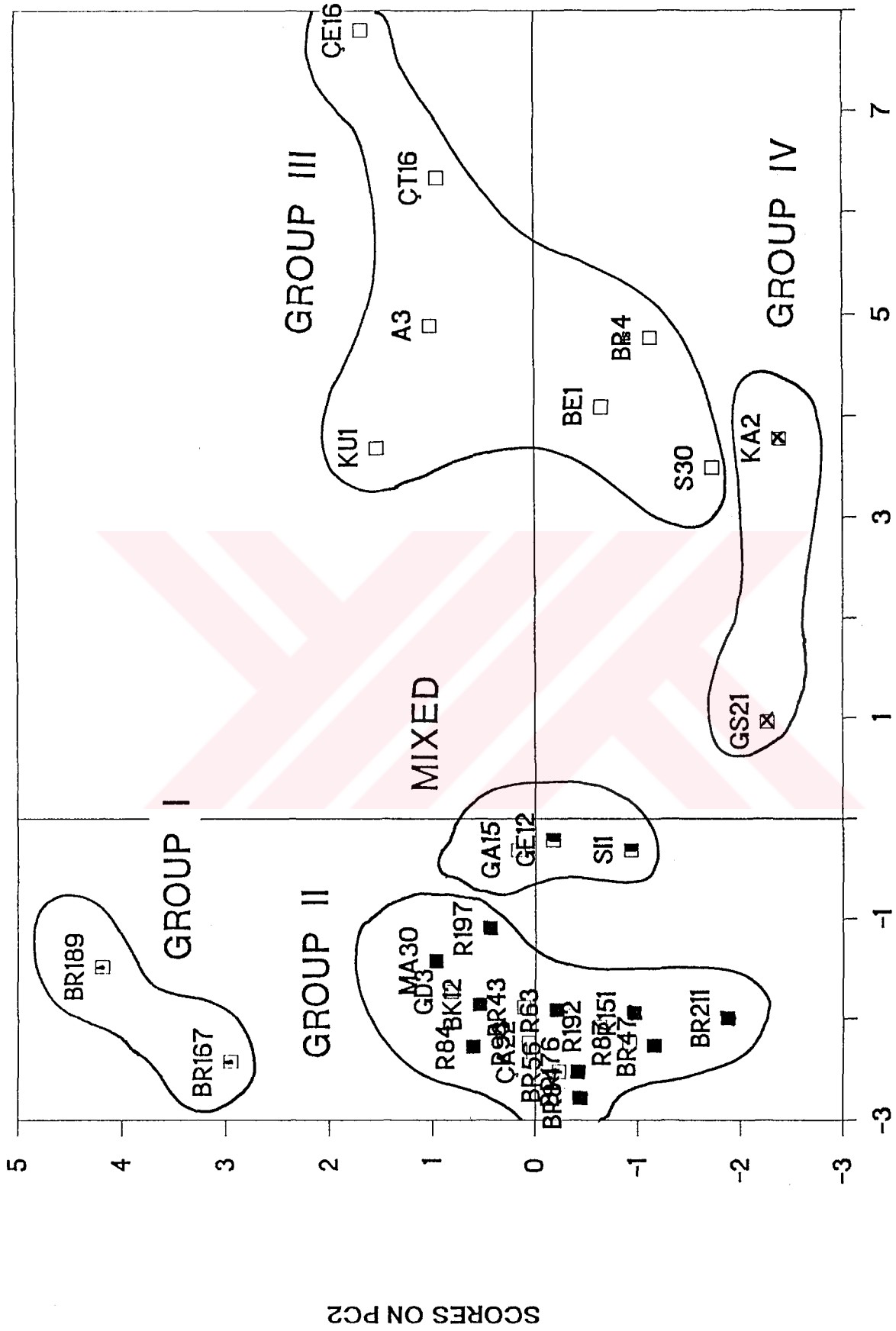


Figure_4.20 Crossplot of tri-tetra-pentacyclic terpene scores on PC1 versus PC2.

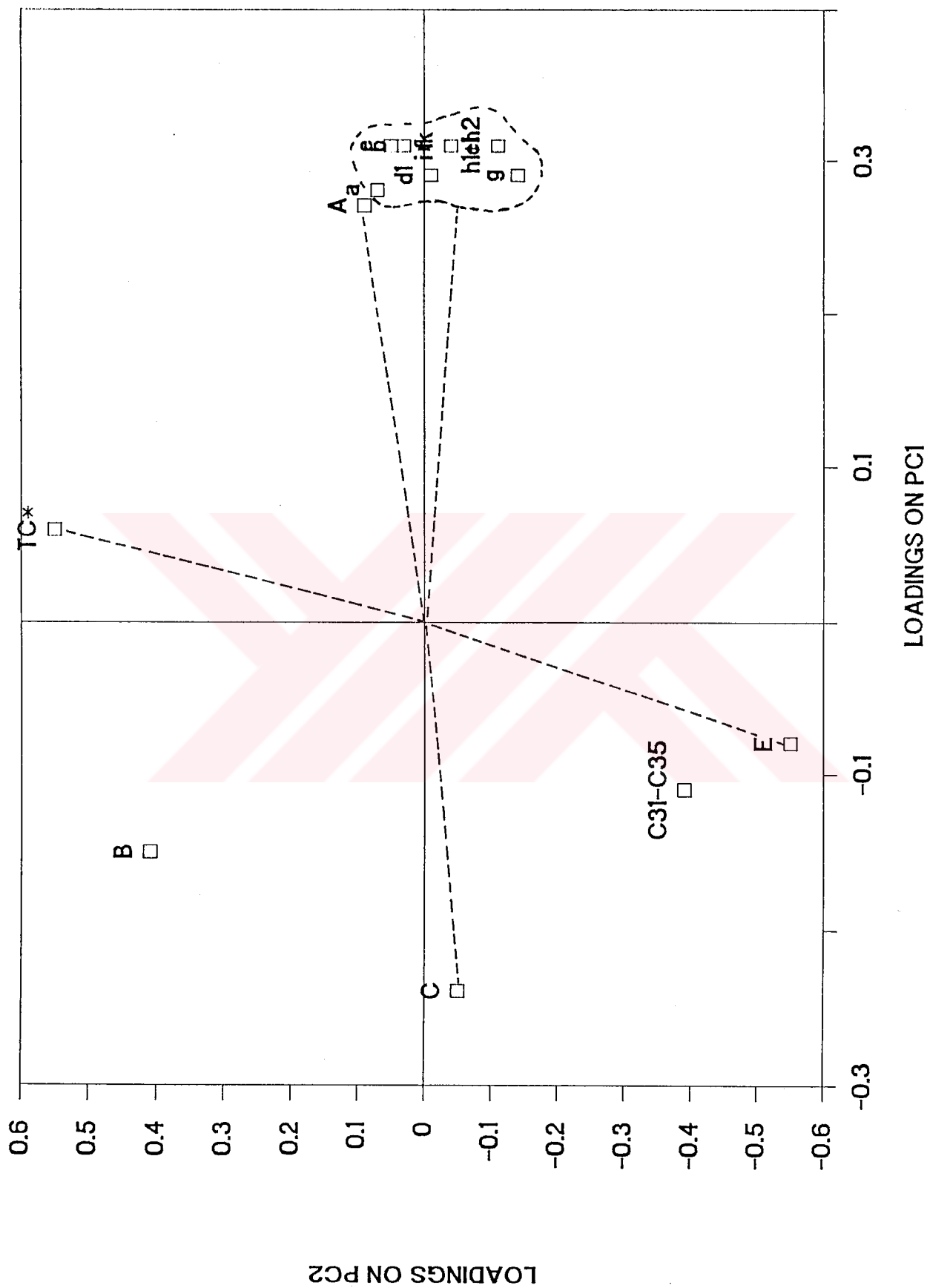


Figure_4.21 Crossplot of tri-tetra-pentacyclic terpene loadings on PC1 versus PC2.

PC2, on the other hand, is dominated by negative correlations between the C₂₄* tetracyclic terpane and the C₃₁-C₃₅ extended hopanes and the C₃₀-hopane (H) (Figure 4.21). Since the source of the C₃₀-hopane and the C₃₁-C₃₅ extended hopanes is well known to be bacteria (Ourisson et al., 1984), negative correlation of the C₂₄* tetracyclic terpane with the C₃₁-C₃₅ and C₃₀ hopane implies that the source of the C₂₄* tetracyclic terpane in the Turkish oils can not be bacteria. In this case, microbial opening of the E ring of hopanoids in hypersaline evaporate-carbonate environment is the most reasonable source of the C₂₄* tetracyclic terpane in the Turkish oils (Philp, 1985; Hughes and Holba, 1988). Therefore, along the PC2 axis oils are separated according to their source depositional environment characters (Figure 4.20).

Figure 4.22 displays the scores on PC1 and PC3 axes which essentially gave rise to similar grouping of the oils. Figure 4.23 shows the corresponding loading plot where PC3 is dominated by the C₃₀-hopane (H), Tm (B), C₃₁-C₃₅ extended hopanes, and the C₂₄* tetracyclic terpanes (TC*). Clustering of these terpanes together suggests that they contain similar group of information along the PC3 axis. As mentioned earlier, elevated concentration of C₃₁-C₃₅ extended hopanes has been reported to indicate anoxic conditions during source rock deposition (Moldowan et al., 1986; Philp and Zhaoan, 1987). Correlation of the C₂₄* tetracyclic terpane with the extended hopanes helps to assign an anoxic-hypersaline character to the PC3 axis. Therefore, the Group I and II

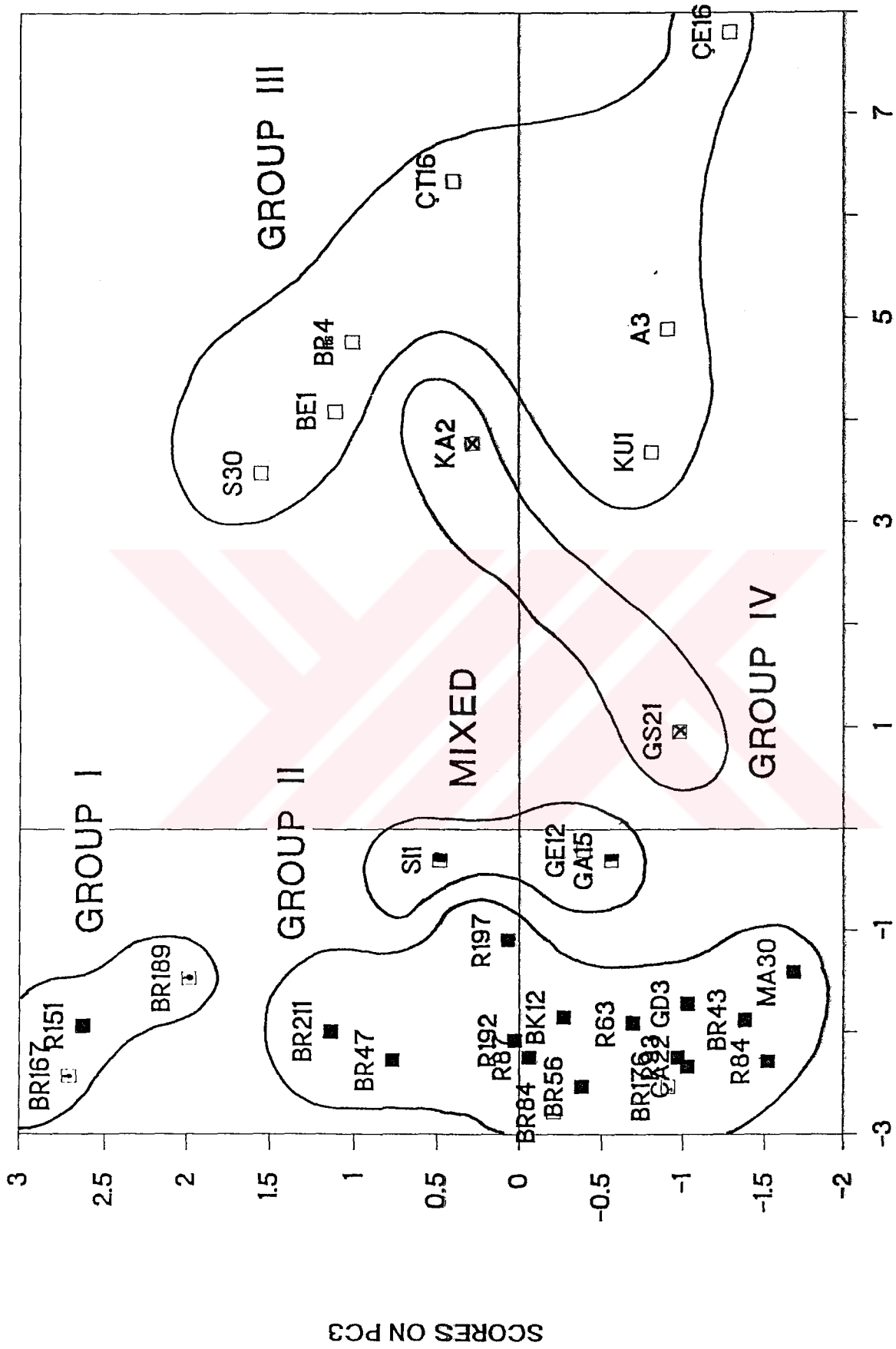


Figure_4.22 Crossplot of tri-tetra-pentacyclic terpene scores on PC1 versus PC3.

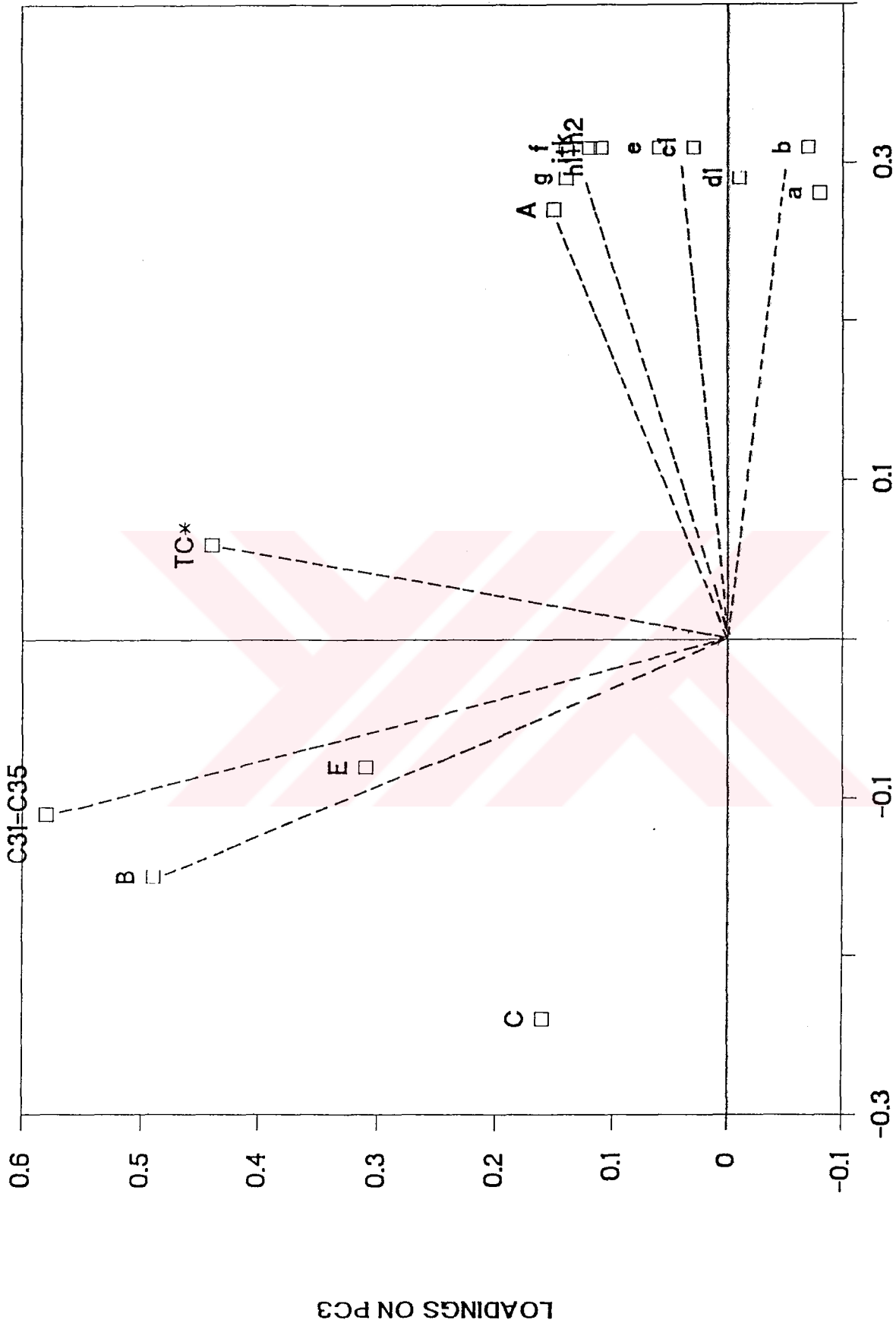


Figure_4.23 Crossplot of tri - tetra - pentacyclic terpene loadings on PC1 versus PC3.

oils (Figure 4.22) could perhaps reflect bacterial source from the anoxic-hypersaline conditions whereas the Group III oils presents high bacterial/algal source with anoxic and less saline conditions. Connan et al., (1985) also reports low abundances of tricyclic terpanes in rock samples from Guatemalan hypersaline environments.

Statistical analysis of tri-tetra- and pentacyclic terpane compounds so far revealed that the C₂₄* tetracyclic terpane(%), T_m, T_s, C₃₁-C₃₅ extended hopanes, C₂₉-norhopane, C₃₀-hopane, Tricyclic terpanes (%) are useful parameters to differentiate the oils for the correlation purposes. Thus, this compound and compound classes will be used particularly to generate selected biomarker ratio data.

In summary, an application of PCA to three groups of terpanes (i.e., tri-tetra-pentacyclic terpane) regarding 31 oils from SE Turkey revealed four genetically different oils in addition to one mixed origin group.

4.1.4.4. Steranes

In this section, PCA was applied to the molecular distributions of the 19 steranes including 5 pregnanes, 2 diasteranes and the 12 regular steranes to investigate correlations among the 32 Turkish oils (Table E.4). Application of PCA to steranes initially resulted in linear regression correlation coefficient data matrix among the 19 sterane compounds (Table H.4). The most

salient features of this data matrix are that the C₂₂ (peak V in Table H.4) pregnane do not correlate with any of the diasteranes and with the regular steranes. However, the C₂₁ pregnane (peak II in Table H.4) shows higher positive correlations with the two diasteranes (peak 1 and 2) ($r = +0.89, +0.88$) which may indicate that the C₂₁ pregnane could be lithology dependent. It also shows negatively high correlations with the four regular C₂₉ steranes (peaks 16, 17, 18, 19, in Table H.4) ($r = -0.83, -0.64, -0.79, -0.73$). This implies that the C₂₁ pregnane could be originated from the C₂₉ regular steranes. Diasteranes are better known compounds and they are frequently used to learn more about the effect of lithology on the crude oil the crude oil compositions (Sieskind et al., 1979). Based on a laboratory heating experiment of the North Sea oils, a recent study by Wingert and Pomerantz (1986) showed that the abundance of the C₂₁ pregnane (peak III in Table H.4) and C₂₂ homopregnanes (peak V in Table H.4) increased with thermal maturity while C₂₇-C₂₉ regular steranes decreased. The C₂₁ pregnane shows inverse correlations only with the C₂₈ regular steranes. The C₂₂ homopregnane, however, does not show any kind of correlation with the C₂₈ or C₂₉ regular steranes. Another C₂₂ pregnane, P4, (peak IV in Table H.4) correlates inversely with the C₂₇ regular steranes.

Application of PCA to the correlation coefficient matrix given in Table H.4 further gave three significant PCs which accounted for 41.11, 25.06, and 10.25 %

respectively, of the total variance. Figure 4.24 shows the scores of the 32 oils on to the PC1 and PC2 axes. It can be seen clearly that oils are separated mainly along the PC1 axis which is exactly the same as in the previous ones. However, the Group I oils appear to be grouped together with the Group II oils and the GS21 oil of the Group IV oils plots together with the mixed origin oils. The KU1 oil also plots out of the Group III region unexpectedly. These observations reflect the average character of PCA and the fact that steranes and terpanes do not carry quite the same information.

Geochemically meaningful separation of the oils along the PC1 requires characterization of the PC1 and PC2 axes of the score plot (Figure 4.24). PC1 which accounts for 41.11 % information of the original variables is contributed by inverse correlations between the C₂₉ regular steranes (peaks 19, 20, 21, 22) and the C₂₇ diasteranes (peaks 1, 2) and C₂₇ ββ steranes (peaks 9, 10, 16) (Figure 4.25). The presence of C₂₉ steranes in a crude oil or source rock has frequently been cited as evidence for the presence of land-plant derived organic matter in the source (Huang and Meinschein, 1976). However, as previously discussed, none of the Turkish oils shows land plant input into their source rocks. Volkman (1986) reported that unicellular algae such as some particular green algae, and cyanobacteria can be sources of C₂₉ sterols.

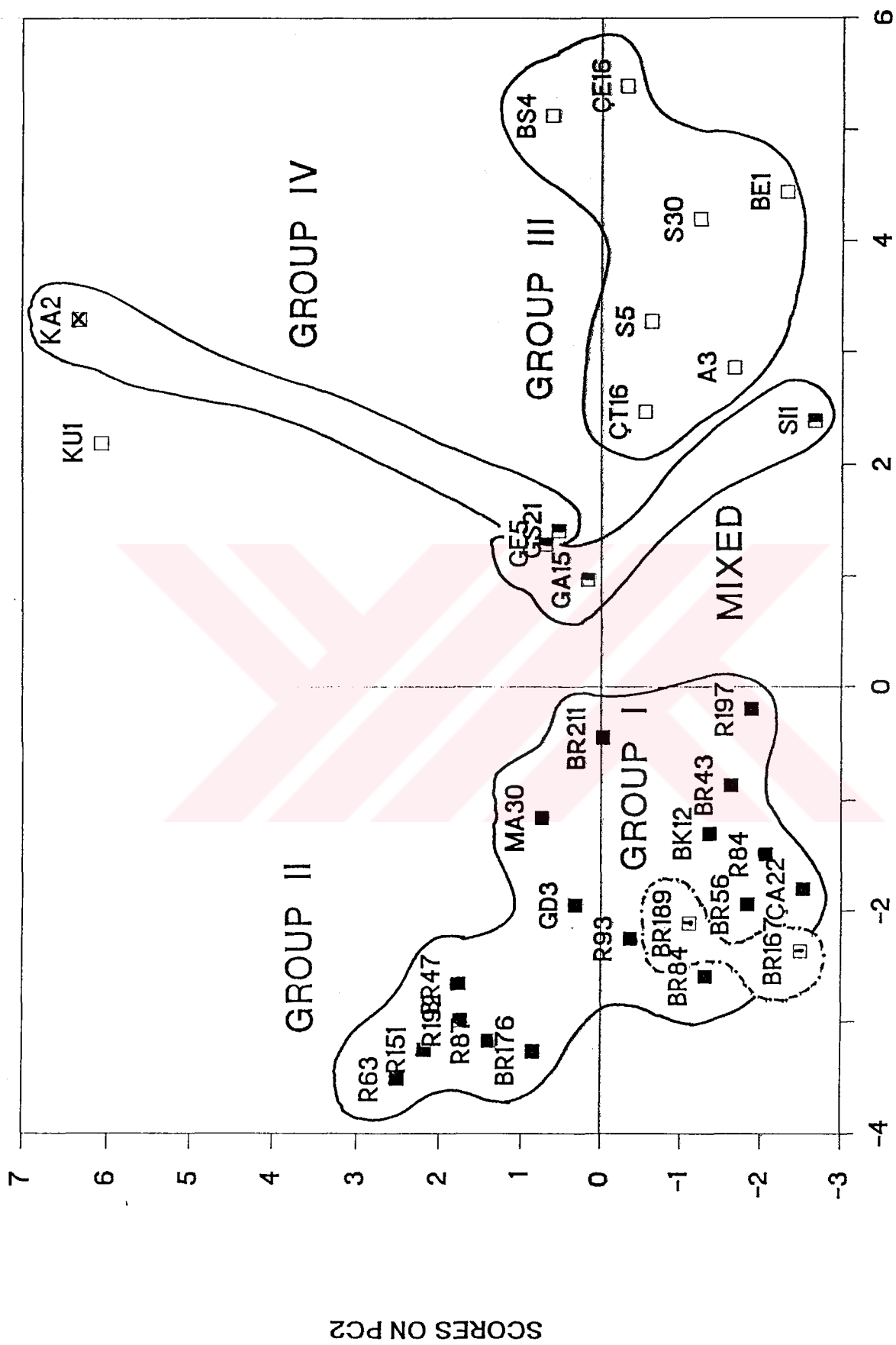


Figure_4.24 Crossplot of sterane scores on PC1 versus PC2.

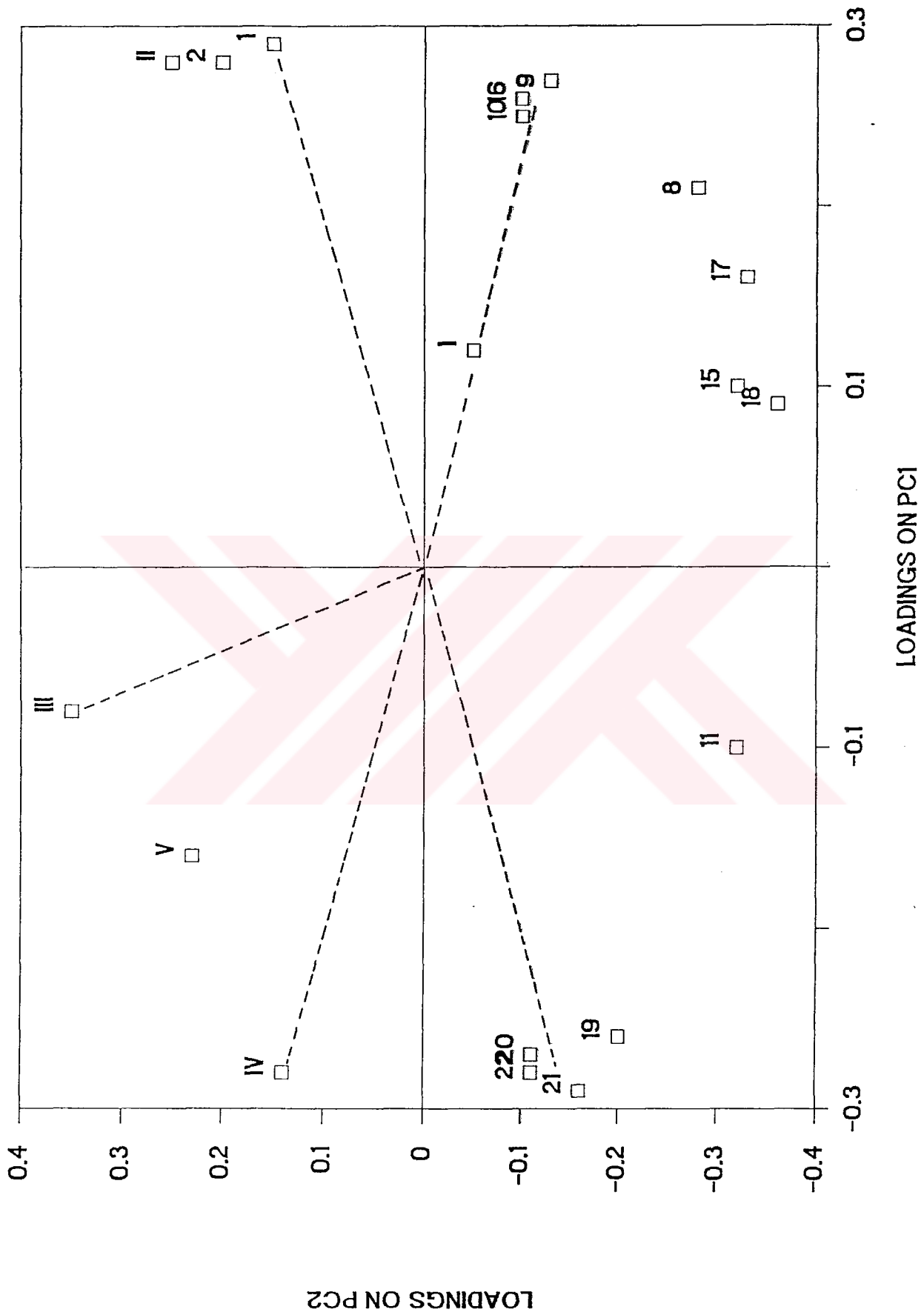


Figure_4.25 Crossplot of sterane loadings on PC1 versus PC2.

The presence of diasteranes in crude oil implies the generation of that crude from a siliciclastic source rock e.g., shale. The presence of relatively low concentration of diasteranes in a crude oil, on the other hand, could imply its generation from a carbonate-rich source rock (Palacas, 1984). Thus, the PC1 axis may be assigned as an indicator of depositional environment of the source rocks where two groups of oil were recognized (Figure 4.24). The Group I and Group II oils contain higher amount of the C₂₉ steranes but very low amount of the C₂₇ diasteranes. The Group III oils, on the other hand, contain higher relative amount diasteranes but very low concentrations of the C₂₉ regular steranes. The diasterane content in the Group III oils, however, do not exceed the regular sterane contents implying that excess diasterane contents are resulted from maturity effect rather than lithology on these oils. Indeed, as discussed earlier, maturity influence on the CE16, BS4 and on the S5 oils were recognized explicitly.

In Figure 4.25, PC2 is characterized by the dominance of C₂₈ regular steranes (peaks 15, 16, 17, 18 in Figure 3.4) which may be sourced from both marine and/or terrestrial organic matter (King and Claypool, 1983). However, they are also abundant in diatoms of upwelling environments (Volkman, 1988; Waples and Machihara, 1990). Thus, one would expect an abundance of C₂₈ regular steranes in crude oils derived from diatomaceous organic matter. In fact, diatom-derived sterols were readily recognized in contemporary sediments from the Peru

upwelling (Gagosian, 1983). Hence, the Group III oils represented by C₂₈ regular steranes (Figures 4.24 and 4.25) carry the evidence of their source rock being deposited in an upwelling environment. PC2 is also affected by the C₂₁ pregnane (peak III in Figure 3.4) which probably resulted in separation of the KU1 and the KA2 oils from the rest of the oils. Indeed, both oils contain relatively higher amount of the C₂₁ pregnane (Table E.4). Higher concentration of the C₂₁ pregnane together with the C₂₂ homopregnane has been detected usually in crude oils derived from source rocks which are deposited in hypersaline environments (Fu Jiamo et al., 1986; ten Haven et al., 1988; Clark and Philp, 1989; Jones and Philp, 1990).

When the scores on PC1 are plotted against PC3, again the mixed origin oils are clearly separated from the Group II and the Group III oils (Figure 4.26). The separation is consistent with the previous genetic separations of the Turkish oils. However, the Group I oils, BR167 and BR189, are plotted in the Group II oil region indicating that there may be a genetic relation between the Group I and Group II oils. The loading plot of PC1 versus PC3 also reveals some of distinguishing sterane compounds of the oils (Figure 4.27). These compounds are relative amount of the C₂₉ regular steranes, C₂₇, and C₂₈ regular steranes, and diasteranes. For example, when the C₂₉ regular steranes percentage is plotted against the C₂₇ diasterane percentage, individual oil groups are clustered tightly and the separation is improved dramatically.

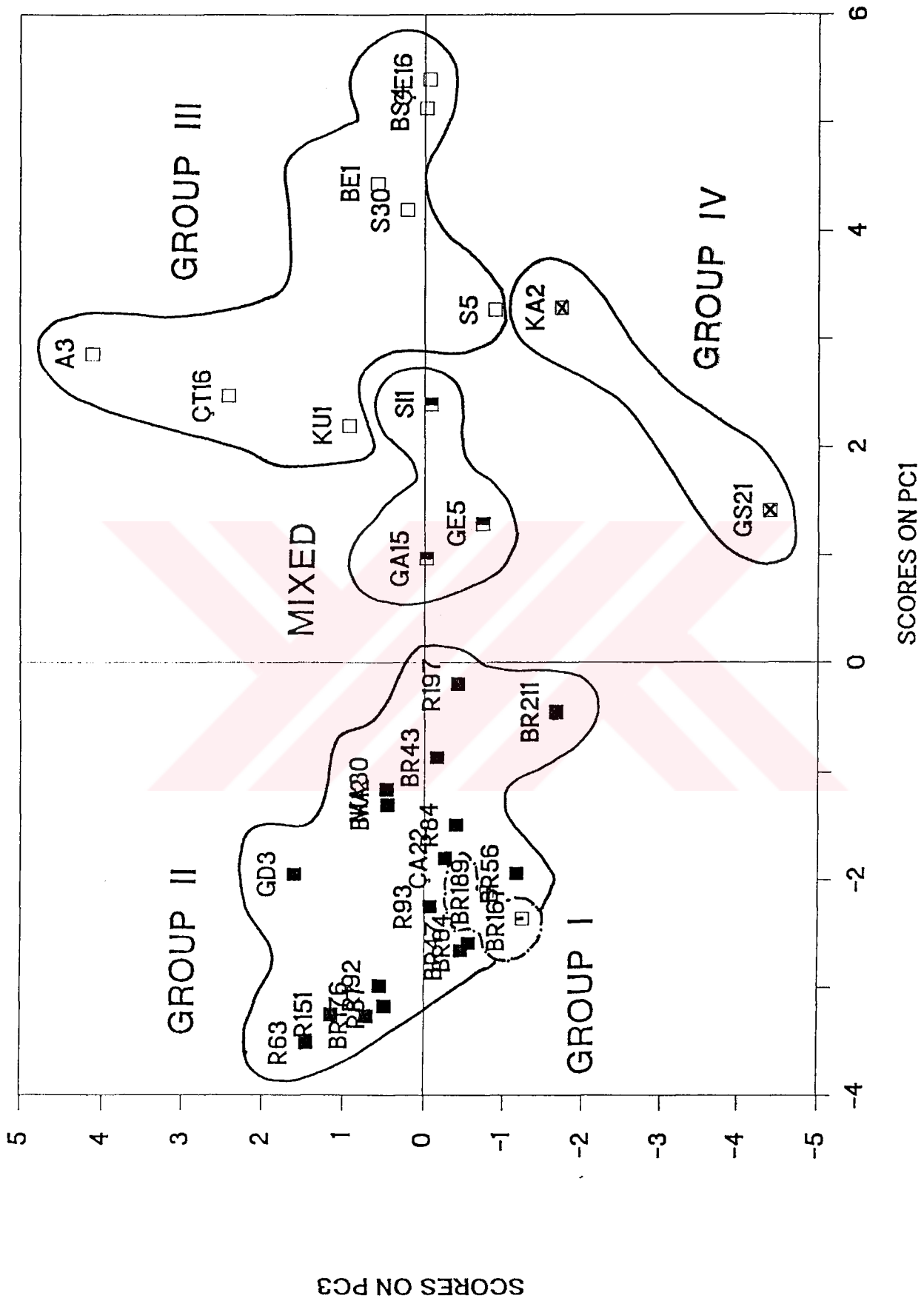


Figure_4.26 Crossplot of sterane scores on PC1 versus PC3.

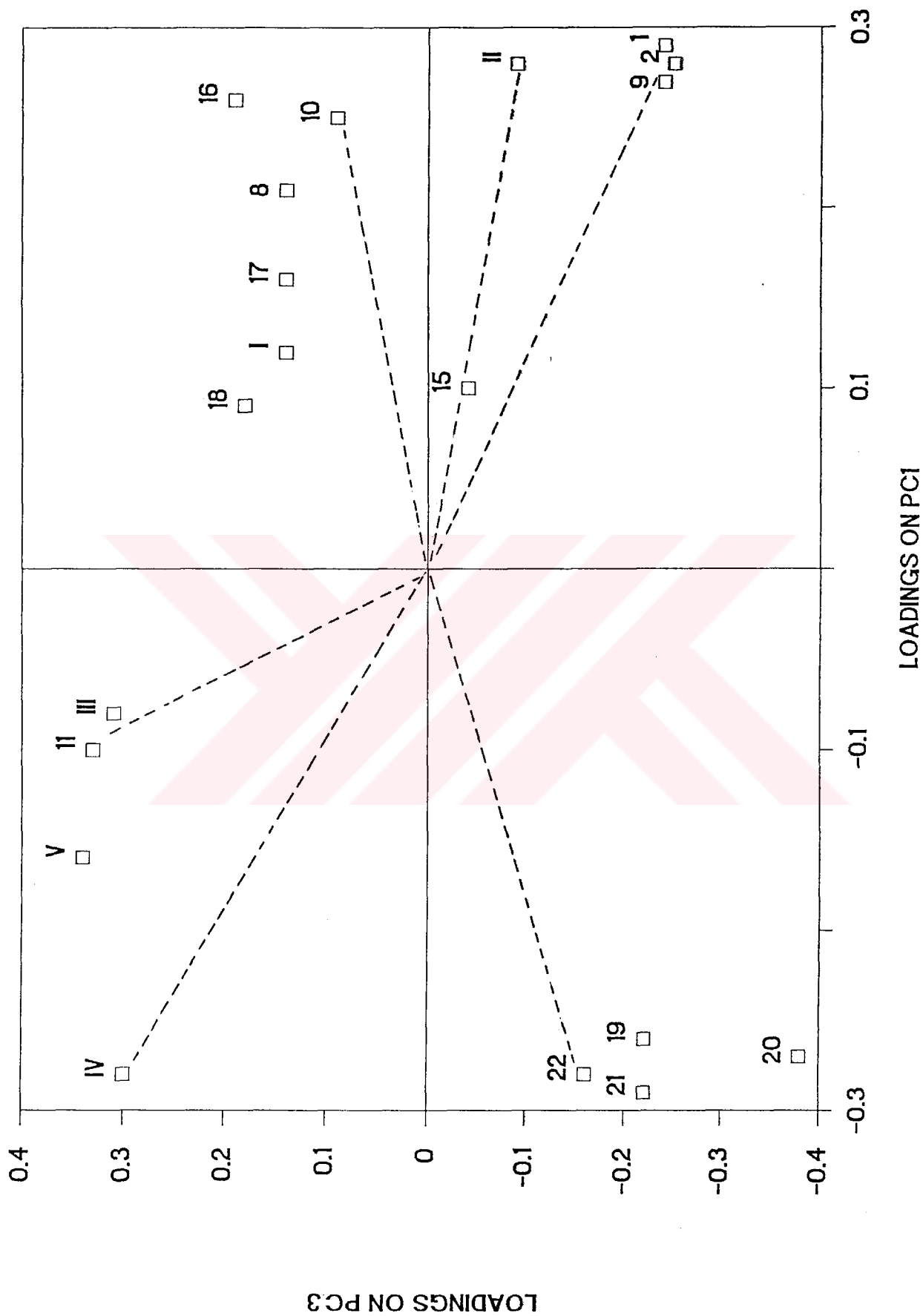


Figure_4.27 Crossplot of sterane loadings on PC1 versus PC3.

Interestingly, the Group I oils again plots together with the Group II oils (Figure 4.28).

In addition to statistical correlations, an attempt was also made to investigate correlations among the Turkish oils using a conventional $20R\ C_{27}:C_{28}:C_{29}$ ternary diagram. This approach proved to be extremely useful for correlating one oil with another and is also useful for determining the organic facies of source rocks as suggested by Huang and Meinschein (1976). Such data for the 32 Turkish oils are given in Table 3.6 and a ternary diagram using these data is constructed in Figure 4.29. As can be noticed, in the upper left diagram, all the oil samples fall into a tight cluster, suggesting a highly similar source rock depositional environment for the Turkish oils. However, when the scale of the upper left diagram is enlarged, it is seen that the Group I, Group II, and Group III oils are clearly separated but the Group IV oils do not show distinct differences from the other oil groups. In spite of the differences in the oils, all the Turkish oils are generated from the source rocks deposited in an open marine to estuary type of environment (Figure 4.29).

4.1.4.5. Selected Biomarker Ratios

Twenty-two biomarker ratios (including S % and Sat/Aro ratio) were selected according to the procedure outlined in Section 4.4.1.5 to extract maximum amount of information pertinent to correlations among the 31 oils.

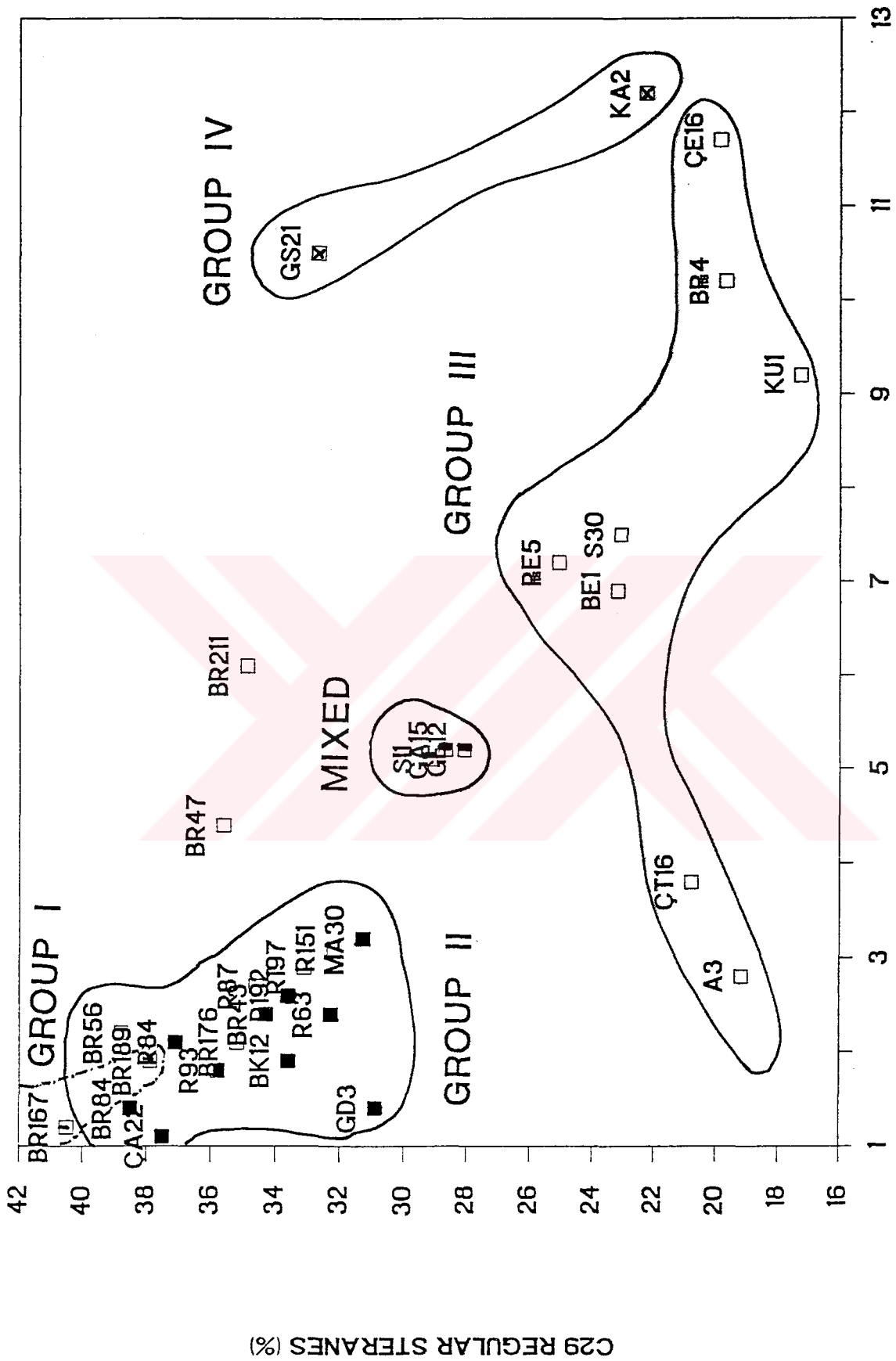


Figure_4.28 Crossplot of C27 diasteranes (%) versus C29 regular steranes (%).

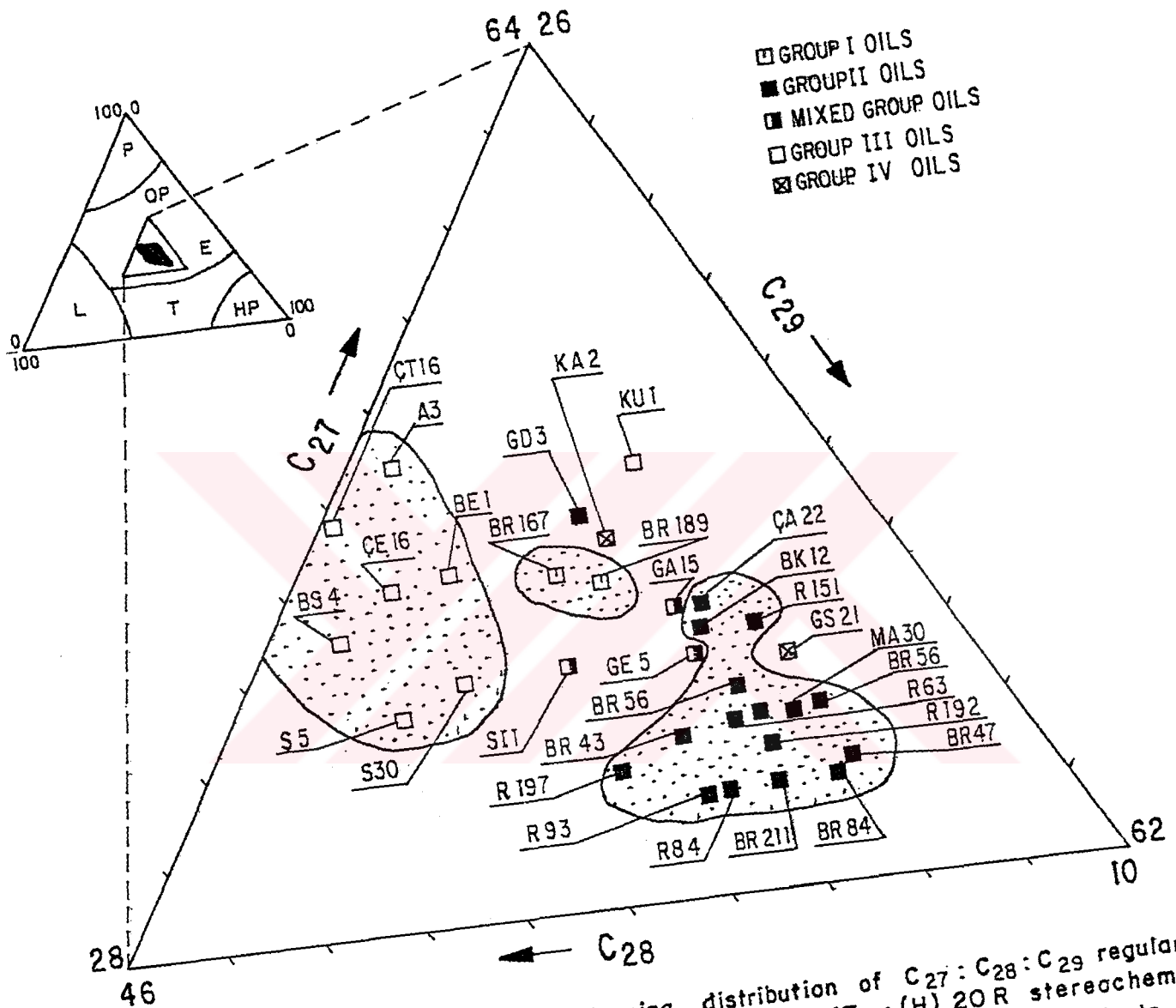


Figure 4.29 Ternary diagram showing distribution of C₂₇:C₂₈:C₂₉ regular steranes with a 5 α (H), 14 α (H), 17 α (H) 20R stereochemistry. P: Plankton, OP: Open marine, E: Estuarine, HP: Higher plants, T: Terrigenous and L: Lacustrine according to Huang and Meinschein (1979).

These ratios were briefly explained in Table 3.7. PCA applied to the selected biomarker ratio data shown in Table E.5 initially gave linear regression correlation coefficients among the 22 variables (Table H.5).

Among twenty-two selected biomarker ratios, Phy/n-C₁₈ ratio does not show correlation with any of the ratios if the correlation coefficient values are smaller than 0.50 is considered to be insignificant. The C_{24*} tetracyclic/C₂₆ tricyclic terpane ratio appears to show positively high correlations with the C₂₃/C_{24*} (r=0.65), Tm+Ts/C₂₈+C₂₉ (r=0.88), C₂₉ NH/C₃₀ H (r=0.79), and C₂₇ REG/C₂₇ DIA (r=0.76) ratios. These high correlations are expected because, as mentioned earlier, all of these ratios are indicators of carbonate derived oils. Moderate correlation (r=0.55) between the C_{24*}/C₂₆ ratios and sulfur contents further support the C_{24*}/C₂₆ ratio the usage for evaporate-carbonate depositional environments. High sulfur content in oils designate usually evaporite-carbonate source rocks (Prof. Dr. R.P. Philp, University of Oklahoma, personal communication, 1991).

Application of PCA to the selected biomarker ratio data further gave three significant PCs which were accounted for 54 % of information carried by the original data. PC1 accounted for 37.58 % variance and heavily weights the inverse contributions of the S %, C_{24*}/C₂₆, Tm+Ts/C₂₈+C₂₉, Tm/Ts, and Sat/Aro, and I+II/III+IV+V pregnane ratios. PC2 accounted for 16.22 % variance and

dominated by the C_{23}/C_{20} , C_{24^*}/C_{21} , and C_{24^*}/C_{30} ratios (Figure 4.30).

In the score plot of PC1 versus PC2 (Figure 4.31), five groups of oils are readily distinguished along to the PC1 axis. This grouping is consistent with the previous grouping of this study. As seen, mixed oils still keep their place between the Group II and Group III oils. When Figure 4.30 and Figure 4.31 are compared, it is recognized that the heavy Group I and II oils are presented by high S %, high C_{24^*}/C_{26} , high $Tm+Ts/C_{28}+C_{29}$, and high Tm/Ts ratios but low sat/aro and $I+II/III+IV+V$ ratios. The light oils, on the other hand, is presented by high Pr/Phy ratios which clearly indicate that PC1 is associated anoxicity, lithology, and type of organic matter of the source of the Turkish oils. Further examination of Figure 4.31 reveals that heavy gravity oils are placed for to the left whereas light oils are plotted on the right. Therefore, it is inferred that PC1 separates the oils based on both physical appearance and molecular composition. That means, in this special case, in addition to molecular composition physical properties are also useful to separate the oils genetically. One may further speculate that composition of the Turkish oils has not been changed significantly after they were expelled from their source rocks.

PC2 is contributed mostly by the C_{24^*}/C_{30} , C_{23}/C_{20} , and C_{24^*}/C_{21} ratios which are positively correlated with each other (Figure 4.30). This indicates

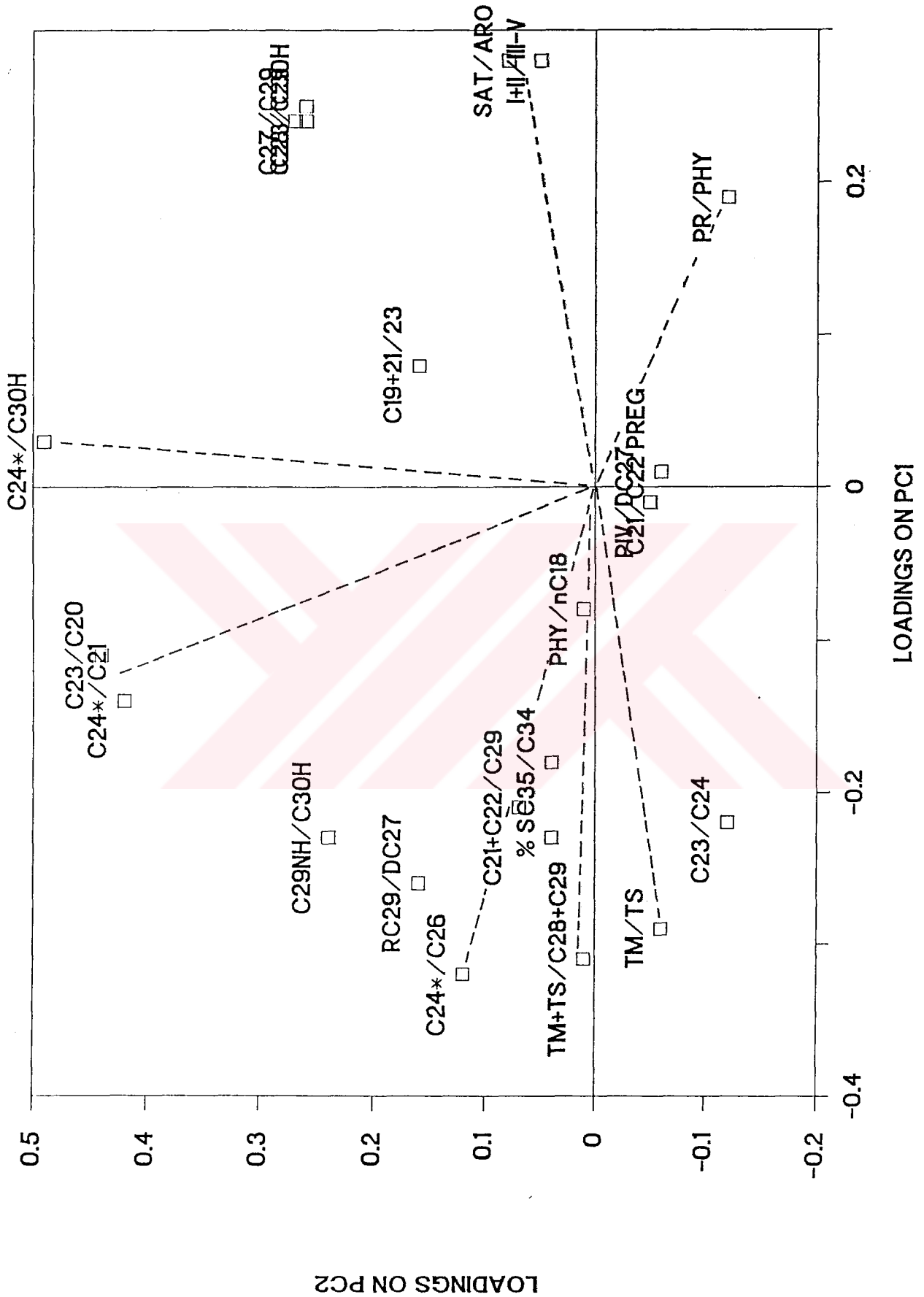


Figure_4.30 Crossplot of selected biomarker ratio loadings on PC1 versus PC2.

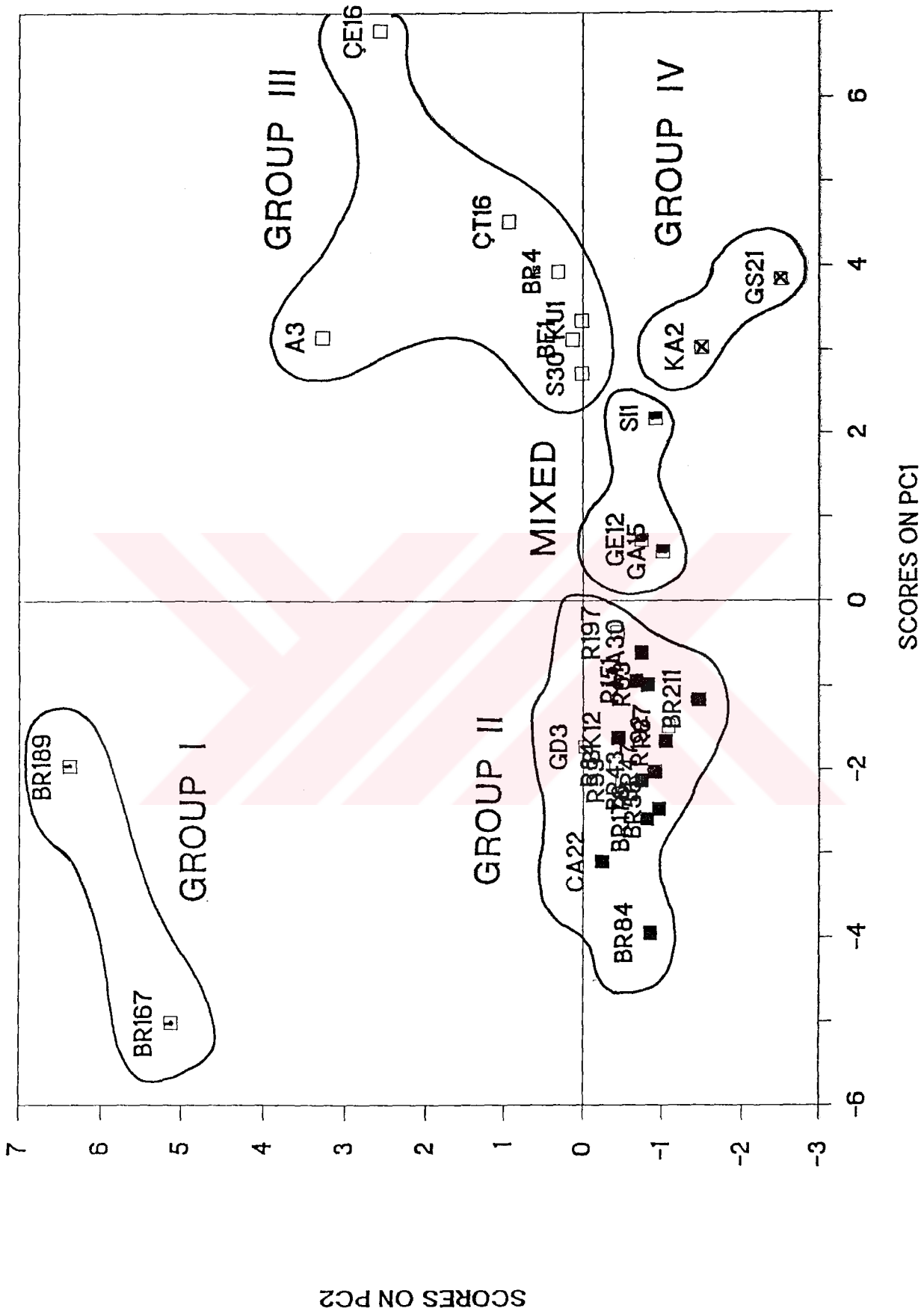
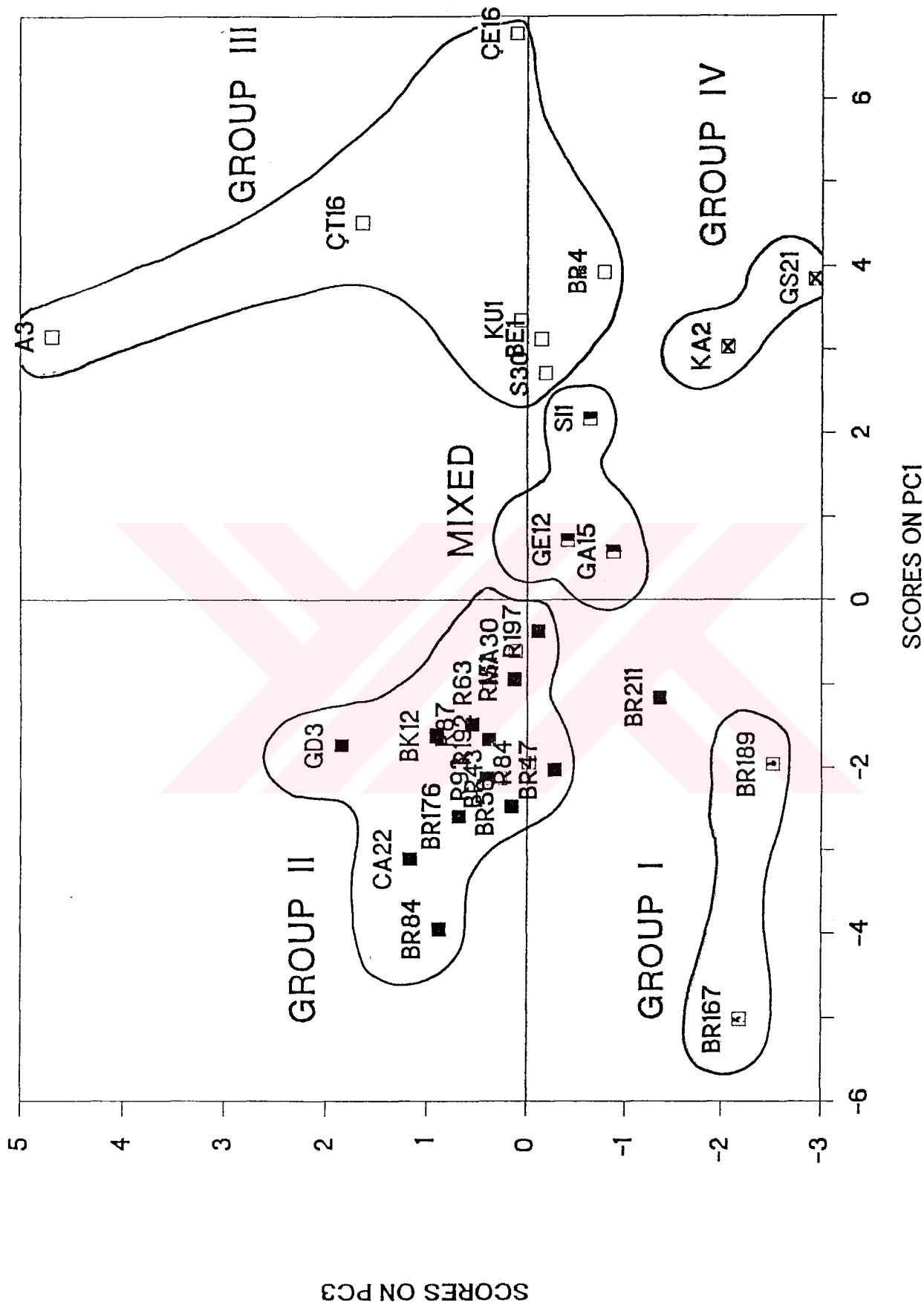
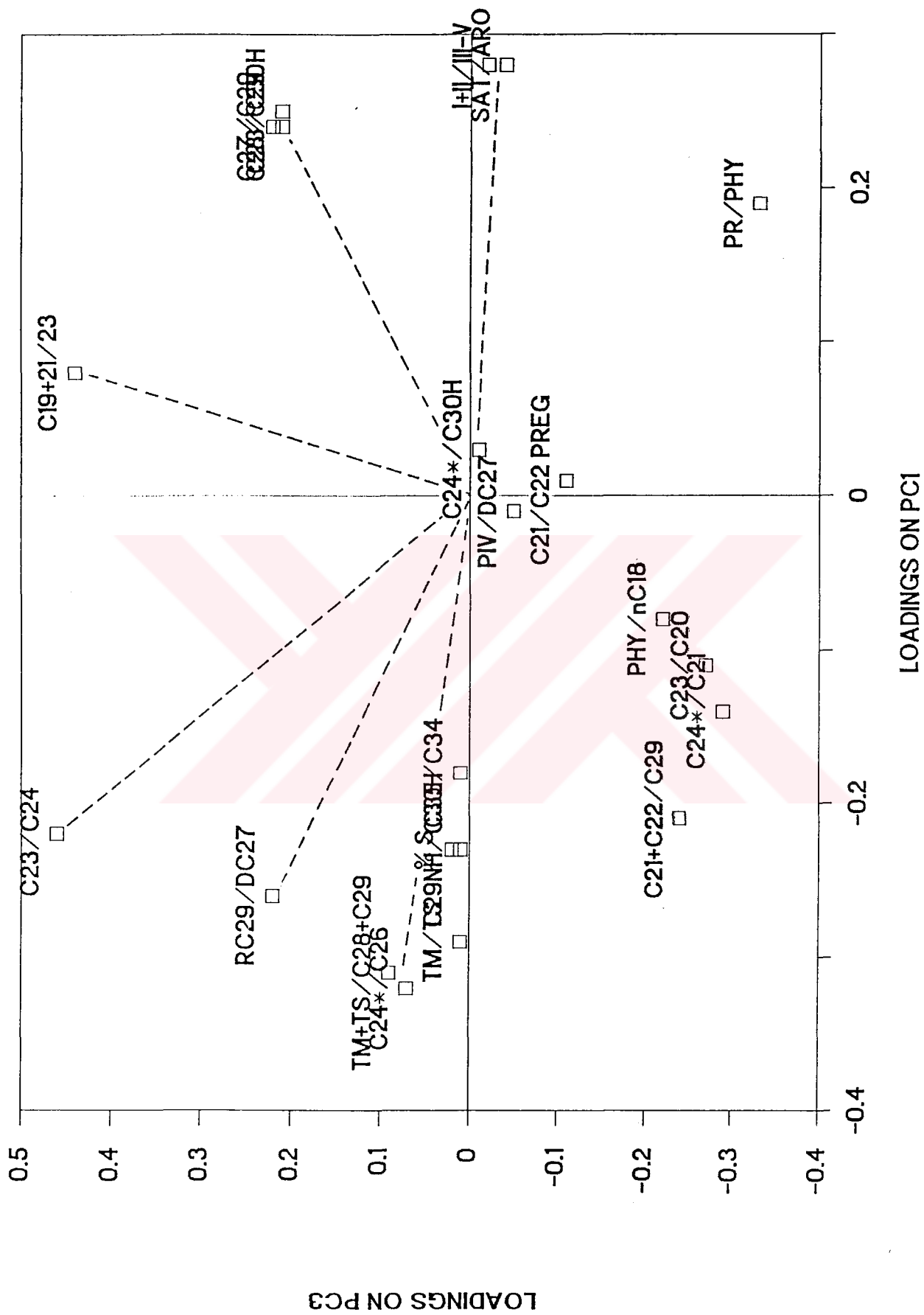


Figure - 4.31 Crossplot of selected biomarker ratio scores on PC1 versus PC2.

that these ratios contain the same type of information and caused the separation of the Group I oils from the Group II oils along the PC2 axis. Another words, The Group I oils are characterized with the high C_{24^*}/C_{30} , C_{23}/C_{20} , and C_{24^*}/C_{21} ratios. Scores of 32 oils on PC3 and PC1 revealed again the same four group of oils in addition to a mixed type (Figure 4.32). PC3 is strongly contributed by the $C_{19}+C_{21}/C_{23}$ ratio and lesser extent by the C_{23}/C_{24} tricyclic ratio (Figure 4.33). From an initial set of twenty-two ratios taken from; n-alkanes, isoprenoids, pregnanes, diasteranes, regular steranes, and tri-tetra- and pentacyclic terpane families biomarkers, eleven ratios were selected to be significant for correlation purposes of the Turkish oils. The eleven ratios are Pr/Phy (R2), sat/aro (R3), C_{24^*}/C_{26} (R5), C_{24^*}/C_{21} (R6), C_{23}/C_{20} (R7), $Tm+Ts/C_{28}+C_{29}$ (R10), $C_{29} \text{ NH}/C_{30} \text{ H}$ (R12), Tm/Ts (R13), C_{24^*}/C_{30} (R14), I+II/III+IV+V (R18), and C_{27}/C_{29} (R20). Table 4.1 tabulates these ratios and their ranges in the Turkish oil groups. The sulfur (% S;R4), asphaltene (% asph), diasterane (% Dia), and tricyclic contents (% Tri) were also found to be significant and added to Table 4.1. Among the significant ratios, R6, R7, and R14 have been used for the first time in this study. These ratios probably reflect depositional environment and organic input factors which control the composition of the kerogen and ultimately of the derived crude oil. For example, two biomarker ratios mentioned above, namely, Pr/Phy and C_{24^*}/C_{26} ratios were plotted against each other and gave similar oil groups as previously found ones of this study (Figure 4.34). What is interesting on this Figure 4.34 is



Figure_4.32 Crossplot of selected biomarker ratio scores on PC1 versus PC3.



Figure_4.33 Crossplot of selected biomarker ratio loadings on PC1 versus PC2.

Table-4.1 The most distinguishing features of the Turkish oils.

Ratios	Type I Oils	Type II Oils	Mixed Oils	Type III Oils	Type IV Oils
R2 PR/PHY	0.81	0.51-0.81	0.8-0.8	0.8-1.2	1.6-1.9
R3 SAT/ARO	0.4	0.3-1.7	1.1-1.8	1.6-7.8	1.2-3.9
R4 X S	4.3-4.6	1.2-7.1	1.5-2.9	0.6-3.0	0.4-0.9
- X ASPH	28-55	15-49	8-20	1-11	5
TERPANES					
R5 C24*/C26	7.0-11.0	2.5-8.0	2.0-3.0	0.8-1.7	0.02-0.1
R6 C24*/C21	>20.0	2.0-8.0	2.0-2.4	0.8-1.7	0.02-0.1
R7 C23/C20	>20.0	4.3-9.0	4.8-5.8	4.0-12.0	4.0-6.3
R10 Im/Ts/C28+C29	8.4-12.0	5.2-17.7	1.9-2.3	0.7-1.5	1.1-1.3
R12 C29 NH/C30 H	1.7-2.0	1.0-1.6	1.0-1.3	0.8-1.3	0.5-0.8
R13 Im/Ts	8.2-8.8	1.7-10.1	2.0-2.5	0.9-4.5	0.8-1.0
R14 C24*/C30 H	1.2-0.7	0.2-0.3	0.3	0.2-0.8	0.01-0.1
- C23/C24*					
STERANES					
R18 I+II/III+IV+V	0.05-0.10	0.1-1.0	0.2-0.7	0.1-1.0	0.2-0.4
R20 C27/C29	1.0	0.7-1.2	0.9-1.0	1.2-1.7	0.8-1.2
- X DIA	1-2	1-8	2-5	3-12	11
- X IC	8-13	8-15	19-21	34-60	24-38

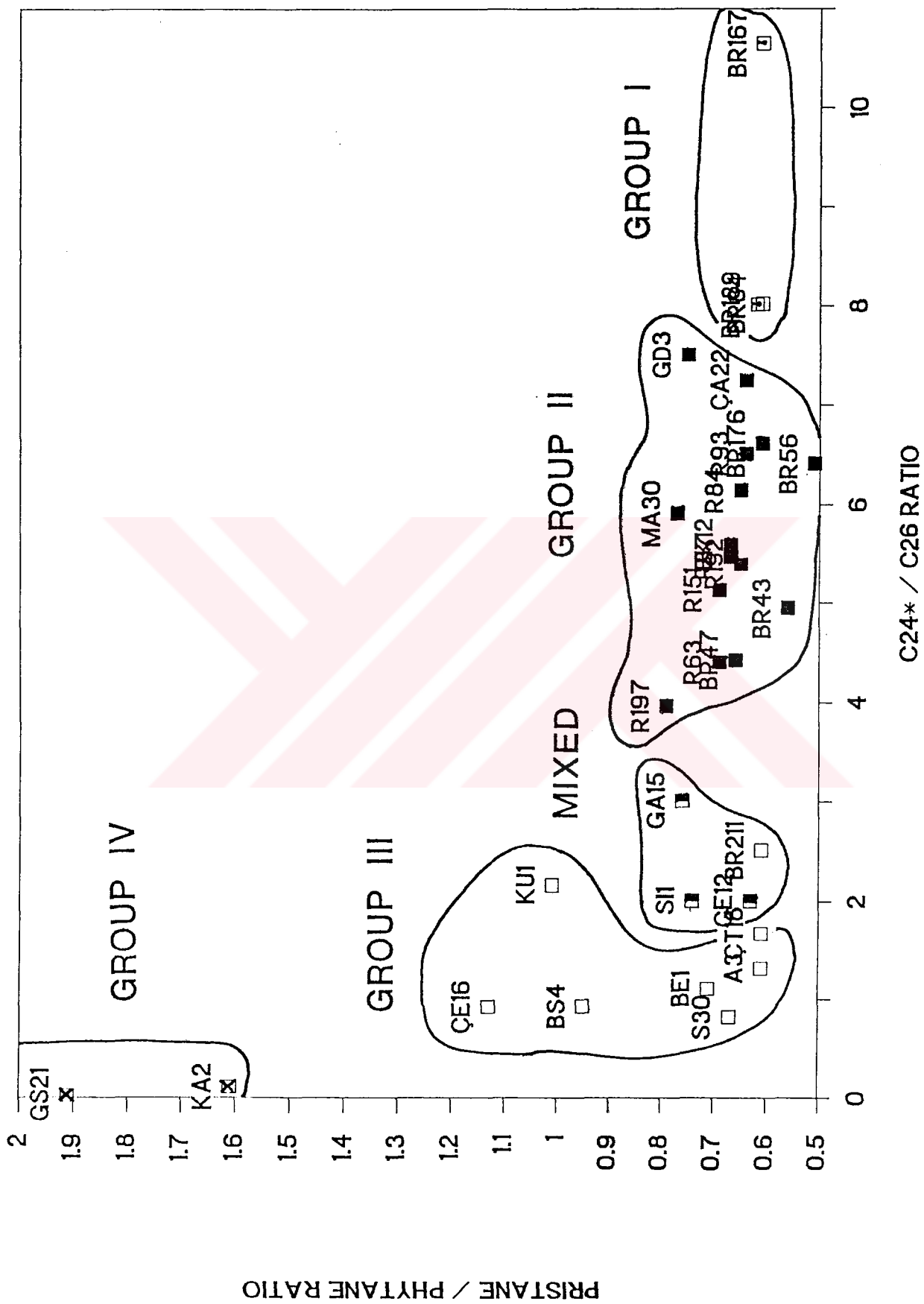


Figure_4.34 Crossplot of Pristane/Phytane ratio versus C24*/C26 ratio.

that Pr/Phy ratio can separate the clastic sourced Group IV oils from the rest of the oil groups but can not be able to separate the Group, I, II, and III oils. In this case, C_{24^*}/C_{26} ratio becomes effective to separate the oils (Figure 4.34). It appears that where the C_{24^*}/C_{26} ratio is nearly zero, source rock consists of nearly 100 percent siliciclastic material, where the ratio reaches values of 1-2, source rock loses its siliciclastic character and turns to a calcareous and then calcareous-evaporitive character.

4.1.5 Predictions of the Ages of Source Rocks from which SE Turkey Oils Were Generated

A number of parameters has suggested by geochemists to predict the ages of source rocks using biological markers in crude oils (Grantham et al., 1983; Grantham and Wakefield, 1988). The C_{29} and C_{28} sterane carbon distributions in the oils together with the concept of the evolution of the phytoplanktons were suggested to be sensitive to the age of the petroleum source rocks. Because sterane carbon number distributions can be correlated not only to depositional environments (Huang and Meinschein, 1976) but also to the time at which the marine source rocks were deposited. These hypotheses are based on the C_{28}/C_{29} ratios of 414 oils and their known source rock ages of which range from the Precambrian to the Tertiary (Grantham and Wakefield, 1988). There are increases in the relative content of C_{28} steranes and decreases in the relative content of C_{29} steranes through

geological time. Grantham and Wakefield (1988) observed that there is correspondence between the C₂₈/C₂₉ sterane ratio of marine source rocks and the emergence of a more diversified phytoplanktonic assemblage of Tappan and Loeblich (1973) through time (Figure 4.35). The ratio increases as phytoplankton diversification increases and becomes significant at the end of the Paleozoic/Early Mesozoic when major diversification took place with the appearance of the dinoflagellates and coccolithophores. Thereafter, the ratio increases more rapidly in the Late Cretaceous with the appearance of the silicoflagellates and diatoms.

The C₂₈/C₂₉ sterane ratios were calculated for the selected Turkish oils according to the procedure outlined in Gürgey and Harput (1990) and were plotted on the Grantham and Wakefield's diagram (Figure 4.36). Since the plot gives an idea about the ages of the source rocks, it can be also utilized for oil to oil correlation purposes. Consequently, Figure 4.36 suggests that the Turkish oils analyzed in this study are derived from the source rocks of three distinct age units:

- a. Cretaceous source rocks,
- b. Paleozoic source rocks, and
- c. Triassic-Jurassic source rocks.

This age related source rock prediction for the SE Turkey oils is consistent with those of Horstink (1980) as previously mentioned. It appears clearly from Figure 4.35

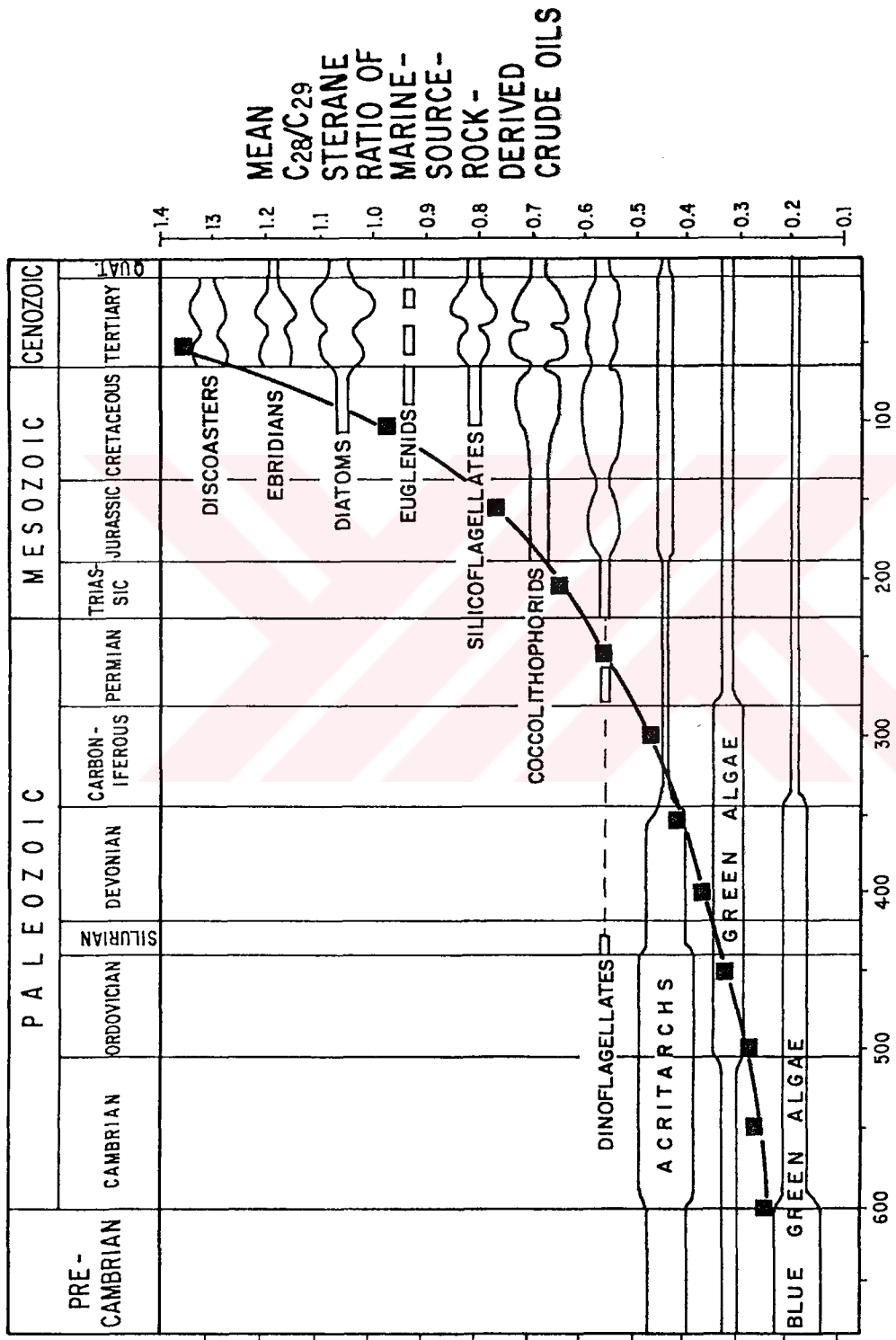


Figure 4.35 Geological distribution of important groups of phytoplankton (after Tappan and Loeblich, 1970) compared to the mean C₂₈/C₂₉ sterane ratio of marine source rock-derived crude oils (after Grantham and Wakefield, 1988).

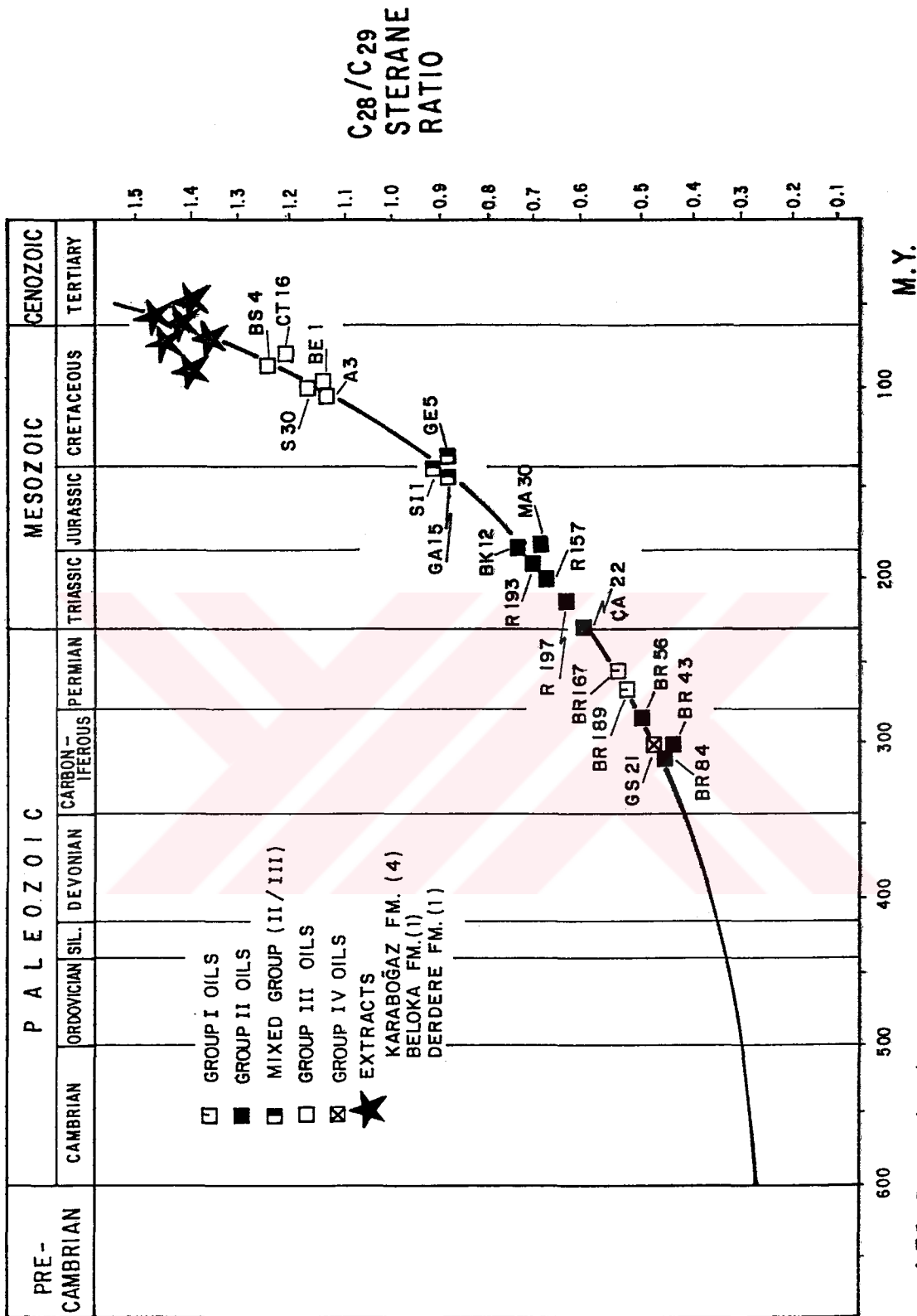


Figure.4.36 Determination of the age of the source rocks of the Turkish oils in terms of plotting C₂₈/C₂₉ sterane ratios on the Grantham and Wake field's (1988) diagram (modified from Gürgey and Harput (1990)).

that the source rocks which generated the Group III oils are most likely Cretaceous in age. Source rocks of the Group I, Group IV, and some oils of the Group II (e.g. BR84, BR43, and BR56) seem to be Paleozoic in age. Among these oils, the oil sample GS21 is the only oil which is known to be derived from Paleozoic aged Dadaş formation. Plotting of this oil in the Paleozoic region of Figure 4.36 confirms Robertson Research Co.,'s (1984) results. Further confirmation of the technique was made using the extract of the three suspected source rock candidates (Karaboğaz, Beloka, and Derdere formations) whose ages are already known to be Cretaceous. Indeed, when the C_{28}/C_{29} sterane ratios of the rock extracts was plotted in Figure 4.36 it was found that these extracts were generated from Cretaceous rock units. However, it seems that the Group I and some of the Group II oils appear to be generated from Paleozoic source rock which is problematic. Because, as discussed earlier, chemical composition of the Group I and II oils requires a source rock in evaporitic and calcareous character. Paleozoic section of SE Turkey comprises mostly clastics and do not contain evaporitic carbonates (Figure 1.4). One reason why the Group I and some of the Group II oils have low C_{28}/C_{29} ratios may be due to high concentration of C_{29} steranes in the microorganisms living in the special type of depositional environment of the source rocks. In evaporitic conditions (e.g. hypersaline conditions), only selective microorganisms can survive, for example halophilic bacteria may contain high concentrations of C_{29} steranes.

Beside the C₂₈/C₂₉ sterane ratios, examination of the 18 α Oleanane (XI) terpane biomarker in the crude oils in the presence or absence form was also tested to predict the age of the source rocks. This compound was first identified by Hills and Whitehead (1966) in an oil from the Niger Delta. Further work by several authors has suggested an origin from precursors in higher plants of the angiosperm (Ekweozor et al., 1979) evolution of which appeared to be started in the early Tertiary. In fact, this compound has been reported mainly in oils derived from Tertiary source rocks (Grantham et al., 1983). Careful examination of the m/z 191 mass fragmentograms revealed that this particular compound is not present in the Turkish oils. This suggests that none of the Turkish oils derived from the Tertiary rock units of SE Turkey. However, caution should be taken because any constraining marker, regardless of age, may not be found in a particular facies because the parent organisms are absent in those sediments. Thus, presence of a specific age correlation marker may be significant whereas its absence may not.

4.2. Possible Source Rocks of Each Correlated Group of Oils

In the previous sections, SE Turkey oils were characterized by applying conventional and statistical techniques to bulk and individual chemical parameters. This approach helped to separate the Turkish oils into four genetic groups with addition of a mixed type.

In the following section, the main distinguishing features of the oil groups obtained from the application of PCA to tri-tetracyclic terpanes, pentacyclic terpanes, tri-tetra-pentacyclic terpanes, steranes, and to the selected biomarker ratios will be interpreted in a combined manner. Then, these features will be used to predict source rock characteristics of the oils in terms of depositional environment, lithology, maturity, age and organic matter types. Consequently, using these source characteristics in addition to previously available geological and geochemical data on the some source rock candidates, the most possible source rock units which generated the each of the oil groups will be suggested.

4.2.1. Batman Area Oils (Group I Oils) and Their Possible Source Rocks.

The Group I oils (e.g. BR189 and BR167) are produced from Maastrichtian aged calcareous Garzan Formation. These oils, are geographically very close to the Group II oils in the Batman area. However, Figure 4.37 shows that they have distinct characteristics which make them to be considered under the different oil groups. Their geochemical features include high sulfur (4.3-4.6 wt %), and high asphaltene contents (28-55 %). The amount of saturates range from 9 to 24 % . The Pr/Phy ratios are about 0.61 which is within the range of those for the Group II and Group III oils.

DISTRIBUTION

GEOLOGICAL DATA

BATMAN AREA

AGE	LITHOLOGY	THICK- NESS m.	FORMATION	DEPOSITIONAL ENVIRONMENT	ORGANIC MATTER		
					TDC	TYPE	Tmax
CRETACEOUS-PALEOCENE		850	GERMAV	DEEP MARINE	VL	III	435
MAASTRICHTIAN		50	GARZAN	REEFAL/BANK	L	II	435
CENOMANIAN		40	KIRADAĞ	SHORELINE/FLUVI.	L	III	435
			DERDERE	SHELF LAGOONAL SHALLOW MARINE	H	I, II	438
APTIAN- CENOMANIAN		250	SABUNSUYU	LAGOONAL TO TIDAL FLAT	VL	-	-
JURASSIC- TRIASSIC		400		SEMI-RESTRICTED TO SHALLOW MARINE CARBONATE PLATFORM	VL	III	441
LOWER TRIAS		50	ULUDERE	SUBTIDAL-INTERTIDAL	-	-	-
UPPER PERMIAN		300	GOMANIBERİK	SHALLOW MARINE TO LAGOONAL	VL	III	451
			KAŞ	DELTA PLAIN	VL	III	453
OROVICIAN		100	BEDİMAN	DELTAIC-INTERDELTA	VL	II	452

IRAQ



43°00' 43°30' 44°00'

Figure 4.37

GROUP I OILS AND THEIR SOURCE ROCK I

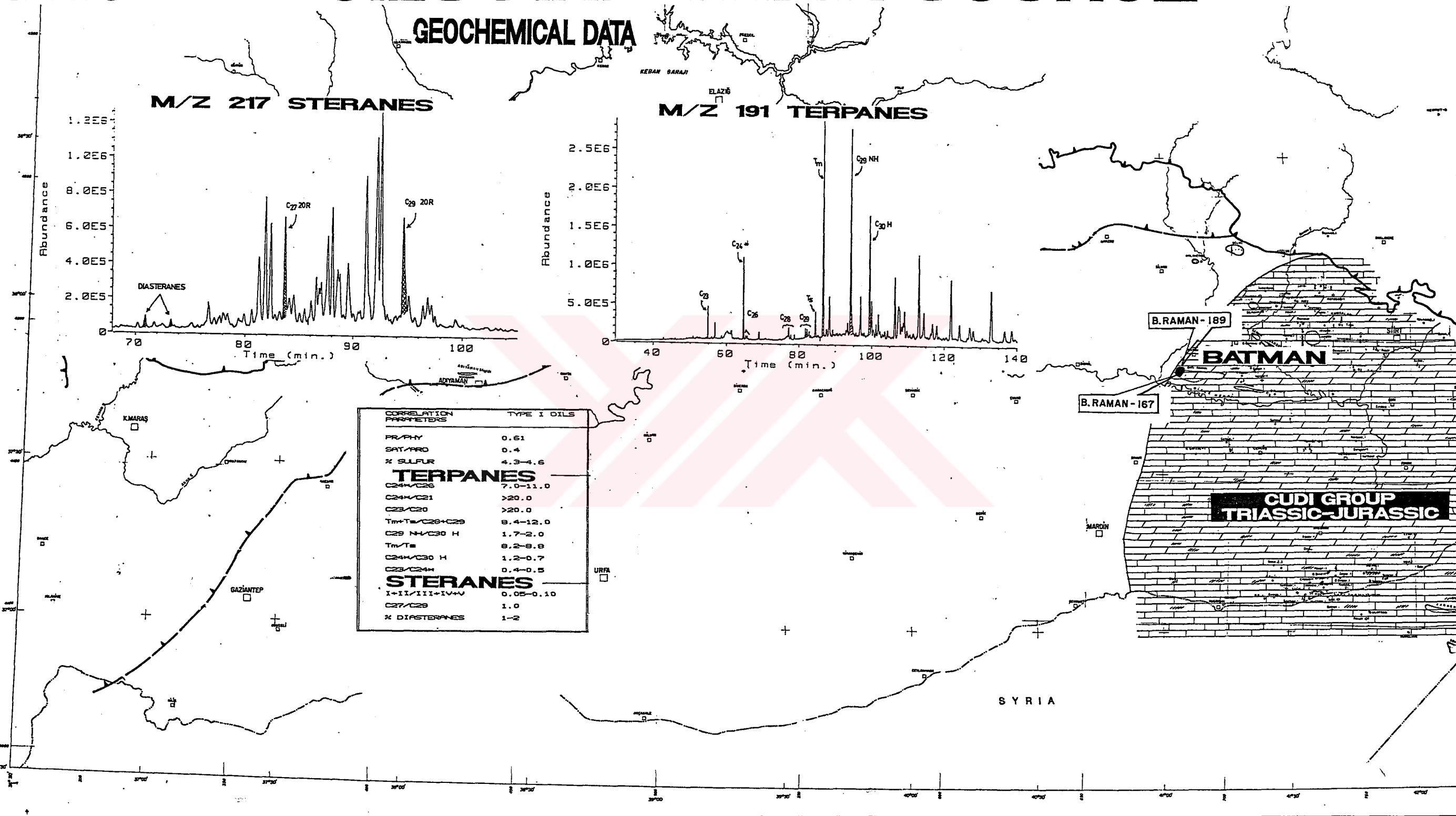


Figure 4.37 Batman area oils (Group I Oils) and their source rock distribution.

	Limestone		Silty marl
	Dolomitic Limestone		Silty shale
	Dolomite		Anhydrite
	Sandstone		Spheroidal forms
	Siltstone		Planktonic foraminifera
	Shale		Shell fragment
	Marl		

Figure_4.38 Symbols of rock used in this study.

In terms of steranes, the Group I oils are very similar to the Group II oils. For example, the C₂₇/C₂₉ regular sterane ratio is between the limits of those of the Group II oils (Table 4.1). These two groups also contain very low relative concentration of the diasteranes. The pentacyclic and tricyclic terpane distribution of the Group I oils, however, is significantly different than those of the Group II oils. The Group I oils contain abnormally low concentration of the 22R extended hopane epimers (peaks G, L, O, R, and T in Figure 3.3) and high concentrations of the T_m (peak B in Figure 3.3). The tricyclic terpanes are almost totally absent with the exception of the C₂₃ compound. The C₂₄ tetracyclic terpane is the dominant peak in this region of the m/z 191 mass fragmentograms

As discussed earlier, gas chromatogram of these oils do not carry any sign of biodegradation. However, sterane and terpane biomarkers suggest otherwise. In another words, these oils contain all the low molecular weight n-alkanes without any biodegradation but contain heavy molecular weight sterane and terpane compounds with biodegradation sign. Since bacteria consume low molecular weight compounds preferentially (Williams and Winters, 1969), present day composition of the Group I oils can be explained with a mixture of degraded oils with the normal oils. Hence, altered molecular composition of the Group I oils did not allow to predict the nature of their source rocks. Clearly, genetic relationship between the Group I and Group II oils requires further attention.

4.2.2. Batman-Nusaybin Area Oils (Group II oils) and Their Possible Source Rocks

The Group II Oils are found mainly in the Batman and Nusaybin areas (Figure 4.39) and include oils from the Batı Raman (e.g. BR43, BR56, BR84, BR47, BR211, BR176), Raman (e.g., R63, R157, R197, R193, R192, R151), Mağrip (e.g. MA30), Çamurlu (e.g. CA22), Batı Kozluca (e.g. BK12), and Güney Dinçer (e.g. GD3) oil fields. Oils of this group are accumulated in the Maastrichtian aged Garzan and Cenomanian aged Derdere Formations in the Batman and in the Maastrichtian aged Lower Sinan and Campanian aged Beloka Formations in the Nusaybin areas. Their geochemical characteristics include high sulfur contents (1.2-7.1 wt %), and high asphaltene contents (15-49 %), $\delta^{13}C$ values range from -27.30 per mil to -28.30 per mil for saturate hydrocarbons and from -27.12 per mil to -28.10 per mil for the aromatic hydrocarbons. The amount of saturates ranges from 9 to 33 % with NSO + Asphaltene components higher than aromatics. A close examination of the relative abundances of normal and branched alkanes shows a dominance of low molecular weight n-alkanes (around C_{15}, C_{17}), a slight even/odd n-alkane dominance, low Pr/Phy ratios (<0.83).

Distribution of the steranes and terpanes are different than the Group III oils. In terms of the steranes, the oils of Group II contain low concentration of diasteranes (Table 4.1) and show a dominance of C_{29} components over their C_{28} and C_{27} counterparts

DISTRIBUTION

GEOLOGICAL DATA

VAN GÖLÜ

BATMAN AREA

NUSAYBIN AREA

AGE	LITHOLOGY	THICKNESS m.	FORMATION	DEPOSITIONAL ENVIRONMENT	ORGANIC MATTER		
					TOC	TYPE	Tmax
CRETACEOUS - PALEOCENE		650	GERMAV	DEEP MARINE	VL	III	435
IAASTRICHIAN		50	GARZAN	REEFAL/BANK	L	II	435
		40	KIRADAG	SHORELINE/FLUV.	L	III	435
CENOMANIAN		150	DERDERE	SHOULDER LAGOON SHALLOW MARINE	-	-	-
APTIAN - CENOMANIAN		250	SABLINSUYU	LAGOONAL TO TIDAL FLAT	VL	-	-
JURASSIC - TRIASSIC		400		SEMI-RESTRICTED TO SHALLOW MARINE CARBONATE PLATFORM	VL	III	441
LOWER TRIAS		50	ULUDERE	SUBTIDAL-INTERTIDAL	-	-	-
UPPER PERMIAN		300	GOMANISIRIK	SHALLOW MARINE TO LAGOONAL	VL	III	451
			KAS	DELTA PLAIN	VL	II	453
ORDOVICIAN		100	BEDINAN	DELTAIC-INTERDELTA	VL	II	452

AGE	LITHOLOGY	THICKNESS m.	FORMATION	DEPOSITIONAL ENVIRONMENT	ORGANIC MATTER		
					TOC	TYPE	Tmax
EOCENE - OLIGOCENE		800		SHALLOW OPEN MARINE TO TIDAL FLAT	-	-	-
PALEOCENE - MAASTRICHIAN		350	GERMAV	DEEP MARINE	VL	III	430
			LOWER SINAN	SHOULDER MARGIN CARBONATE SANDS			
CAMPANIAN		100	BELOKA	SHALLOW OPEN MARINE	VL	III	430
ALBIAN - TURONIAN		400		RESTRICTED SEMI-RESTRICTED SHALLOW MARINE	-	-	-
TRIASSIC - JURASSIC		1300	YOLAÇAN	LAGOONAL TO SUPRATIDAL	-	-	-
			KOZLUCA				
			DİNÇER				
			TELHASAN				
			ÇAMURLU				
LOWER TRIAS			ULUDERE	CONTINENTAL	-	-	-
UPPER PERMIAN			GOMANISIRIK	LAGOONAL TO SUPRATIDAL	-	-	-
			KAS	TIDAL FLAT	-	-	-
ORDOVICIAN			BEDINAN	SHORELINE	H	II	440

0 10 20 30 40 km

Figure_4.39

GROUP II OILS AND THEIR SOURCE ROCK

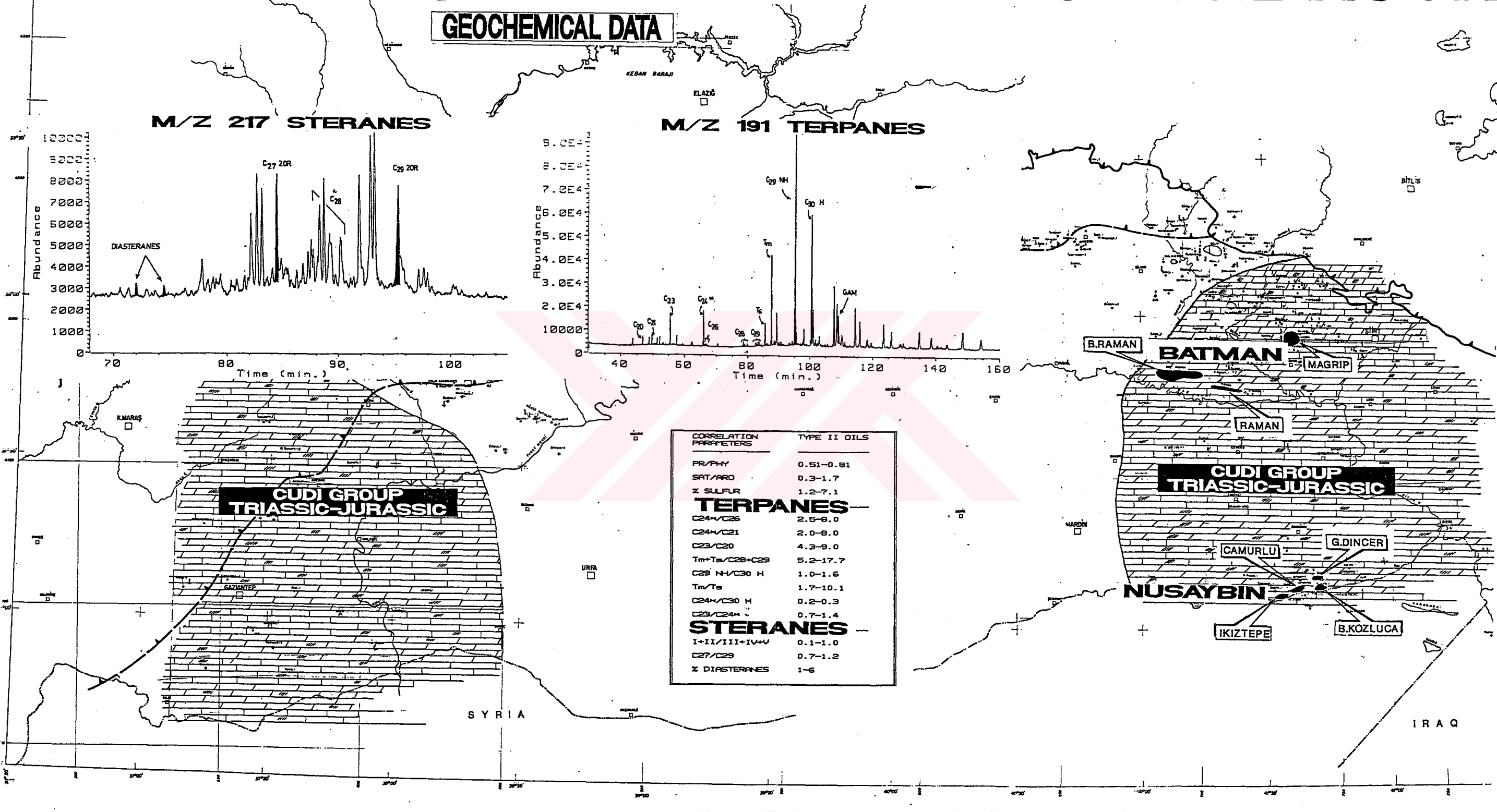


Figure 4.39 Batman - Nusaybin oils (Group II Oils) and their source rock distribution.

(Table 3.6). Most of these samples show an unusually low abundance of the $\alpha\alpha$ C₂₉ 20R components (Peak 22 in Figure 3.4) relative to $\alpha\alpha$ C₂₉ 20S components (peak 19 in Figure 3.4) and high abundances of the $\alpha\beta\beta$ components (peaks 9, 10, 16, 17, 20, and 21 in Figure 3.4) over the $\alpha\alpha$ components (peaks 8, 11, 15, 18, 19, and 22 in Figure 3.4). Also notable is the occurrence of C₃₀ steranes although in low concentrations only. In addition, the oils contain relatively high concentrations of low molecular weight steranes (pregnanes) relative to the C₂₇-C₂₉ regular steranes (Table 3.6).

The terpanes are also present in high concentrations as the steranes. Distribution of the tricyclic terpanes different from those of the oils of the Group III and Group IV in terms of their lesser abundance. They contain no tricyclic terpane lower than the C₂₃ (peak e in Figure 3.3). Overall, the characteristics of the m/z 191 mass fragmentograms for these oils include; a high concentration of Tm (peak B in Figure 3.3), and although in lower abundance, presence of gammacerane (peak GAM in Figure 3.3), very high Tm/Ts ratios (1.7-10.1), high C₂₄-tetracyclic terpane/C₃₀-H ratios (0.2-0.3), high C₂₉-NH/C₃₀-H ratios (1.0 - 1.6), and high Tm+Ts/C₂₈+C₂₉ ratios (5.2 - 17.7) (Table 4.1).

Depositional Environment: Presence of the C₃₀ steranes in the Group II oils was considered to be definitive indicator of source rock deposited in the marine environment (Moldowan et al., 1985). The high

sulfur contents, medium amount of saturates, a slight even over odd preference, and the predominance of phytane over pristane are all consistent with a hypersaline marine environment of deposition (Connan, 1984; ten Haven et al., 1985; Fu Jiamo et al., 1986). The origin of an even n-alkane dominance over odd ones associated with low Pr/Phy (<1) and high relative abundance of $C_{31}-C_{35}$ extended hopanes also indicate that the source rock was deposited under oxygen-deficient (anoxic) bottom waters (Connan et al., 1985; Moldowan et al., 1986; Fu Jiamo et al., 1986; Mello et al., 1988). The presence of abundant C_{21} pregnane and C_{22} homopregnane is consistent with hypersaline environment interpretation (Connan et al., 1985; ten Haven et al., 1988; Clark and Philp, 1989). The presence of gammacerane in all the Group II oils further support the hypersaline conditions (Philp, 1985; Moldowan et al., 1985). In the tricyclic region, the tricyclic terpanes are in very low abundance whereas the C_{24*} tetracyclic terpane is in significantly high concentration. This is an important evidence giving further information about the depositional environment of the source rock candidate. Connan (1984) found out that this compound occurs in the sediments of a sabkha environment in Guatemala. The high occurrence of the C_{24*}/C_{26} ratio (Table 4.1) has also been observed in an evaporative environment of the Spain Basin (Albaiges et al., 1985), Camague Basin, South France (Connan and Dessort, 1987), evaporate-carbonate rocks and oils of Sunniland formation of South Florida (Palacas et al., 1984), and Black Creek Basin of Alberta, Canada (Clark and

Philp, 1989). Since the source rock nature of the evaporate-carbonate sequences is a relatively new concept in general, source rock characteristics of such an environment will be briefly summarized below.

In years, organic matter of the evaporate-carbonate depositional settings has been thought to be well-aerated and hence, organic matter of this settings is not likely to be preserved. However, recent literature data showed that hypersaline seawater of evaporite-carbonate environment contain very limited amount of oxygen (Sammy, 1985). Thus, anoxic conditions necessary for the preservation of organic matter in this relatively shallow marine environment is formed spontaneously. If the salinity of the lower water mass were extremely high (e.g., 40 %), virtually all organic matter that sank into the lower water mass would become incorporated intact in the sediments because even sulfate reducing bacteria (e.g., sulfate reducing bacteria may decompose organic matter completely producing H_2S , CO_2 , and H_2O) could not exist because of the extreme salinity. Thus, much of the organic matter that rained into the deeper water zone in many evaporite environments would probably be preserved. Algae and bacteria which thrive in such environment of 40 to 250 % salinity tend to be large contributors to organic matter (Connan et al., 1985; Warren, 1986). Such a bottom environment may have been present in the Pennsylvanian Paradox basin, Utah, USA. Here, black carbonate rich shales interstratified with evaporites contains up to 15 % organic matter (Hite, 1970). As the salinity increases species diversity

decreases but the number and amount of individuals increased progressively (Kirkland and Evans, 1981; Sonnenfeld, 1985). Eventually, very unique kerogen composition specific to evaporate environments is formed.

Kerogen in the evaporate-carbonate environment is particularly sulfur rich and generates hydrocarbons much earlier than siliciclastic shales (Orr, 1986). This happens because, sulfur rich kerogens contain much S-C bonds which require less energy to cleave. This results in lower thermal stress necessary to produce hydrocarbons (Lewan, 1985). The presence of CaCO_3 in a source rock also lowers the activation energy necessary for oil generation (Eglinton et al., 1986). They also reported highest value of C29 20S/20S+20R sterane ratio in the presence of CaCO_3 relative to illite and montmorillonite. Hoering (1984) also observed an increased yield of hydrocarbons during pyrolysis experiment in the presence of CaCO_3 . Consequently, oils generated from this type of environments are usually sulfur rich, early mature, and heavy in character.

Petroleum source rocks in evaporate-carbonate depositional settings can better develop in transgressive facies (Malek and Aslani, 1980). The regressive facies, however, are favorably situated for development of leached secondary porosity. Moreover, the transgressive-regressive couplets, should be ideal sequences for petroleum generation and accumulation (Malek and Aslani, 1980). In the world, evaporate-carbonate rocks have been proved to

be the oil producers in a number of basins, for example, Paleozoic Salina Formation in the Michigan Basin (Rullkötter et al., 1985), Muskeg Formation in Black Creek Basin, Alberta, Canada (Jones and Philp, 1990), Triassic-Jurassic rocks in Italy (Mattavelli and Novelli, 1990).

Lithology: Very low relative abundance of diasteranes in the Group II oils suggests a source rock with carbonate lithology (Rubinstein et al., 1975; Sieskind et al., 1979). Similar features have been also observed in oils generated from evaporitic-calcareous source rocks (McKirdy et al., 1983; Fu Jiamo et al., 1986; Palacas et al., 1984). High T_m/T_s ratios, high $C_{29} \text{ NH}/C_{30} \text{ H}$ ratios further confirm the carbonate lithology of the source rock. High sulfur content associated with the high asphaltene content in these oils, however, strongly suggest a source rock with evaporate-carbonate lithology (Prof. Dr. R. P. Philp, University of Oklahoma, Personal communication, 1991).

Organic Matter Type: In all the Group II oils, the marine character of the organic matter in the source rock is confirmed by the presence of C_{30} -steranes, which are diagnostic marine organic matter markers. The dominance of C_{29} regular steranes over C_{27} and C_{28} counterparts associated with the dominance of low molecular weight n-alkanes are suggestive of the marine organic matter with algal input (Farrimond et al., 1989). The relative high abundance of the C_{31} - C_{35} extended hopanes in the Turkish oils may be due to some contribution to the sedimentary

organic matter by bacterial sources (Ourisson et al., 1979).

Maturity: It is almost certain that the Group II oils have expelled from relatively low mature source rocks. Majority of the Group II oils shows the C_{32} 22S/22S+22R hopane isomerization ratios near the equilibrium (0.60) suggesting that the source rock that generated these oils have an approximate vitrinite reflectance value of about 0.60 (Figure 4.6). The 20S/20S+20R sterane isomerization ratios (0.42-0.53) confirms the level of maturity suggested by hopane isomerization reactions and indicates a source rock at onset of oil generation phase. Low API gravity and high sulfur content of the Group II oils further support the immature nature of the their possible source rock.

Age: Application of Grantham and Wakefield's (1988) "biomarker dating method" to the Group II oils gave an age estimate of about Upper Carboniferous to Early Jurassic. This large range in age of the source rock seems erroneous and is probably related to a unique depositional environment where organisms are rich in C_{29} sterane thrive. This possibility probably was not considered by the Grantham and Wakefield (1988). As will be discussed later, several lines of evidence suggest that source of the Group II oils can not be Paleozoic in age.

Based on the source rock features described above, the oils belonging to the Group II oils are characterized

by a particular set of bulk and molecular features that are diagnostic of oils derived from an immature source rock deposited in an anoxic, hypersaline evaporate-carbonate depositional setting. In the Batman-Nusaybin area, the only rock stratigraphic unit which satisfies these conditions is the Triassic-Jurassic Cudi Group.

It is also probable that the evaporate-carbonate lithology as well as the higher abundances of S-C bonds in the kerogen matrix probably resulted in generation of the Group II oils at lower level of thermal maturity reflected by simply with low API gravities and high sulfur contents. These features significantly decreased the migration capability of the Group II oils. This implies that proposed source rock could be adjacent to the reservoir rocks of the Group II oils.

Localities of the Group II oils, limits of the Cudi Group, two stratigraphic columns from Batman and Nusaybin areas are given in Figure 4.39 where stratigraphic columns include lithology, depositional environment (O. Duran and N. Bozdoğan, TPAO Research Center, Personal Communication, 1991), total organic carbon (TOC), Tmax (maximum temperature on the apex of S2 peak), and organic matter types (İztañ and Soylu, 1991).

In the light of previous discussions of this study, Paleozoic siliciclastic rocks can easily be ruled out as possible source rocks because the composition of the Group II oils requires immature evaporate-carbonate

rock units. Cretaceous rock units can also be ruled out because the dominant lithology consists of carbonates, some shales, and marlstones which do not possess source rock potential in the Batman-Nusaybin area (Figure 4.39). The lower portion of the calcareous Derdere Formation has a thin (5-10m) spheroidal organic rich layer which is not believed to generate hydrocarbons equivalent to the amount the Group II oils have in the Batman area. For example, Batı Raman oil field contains 2,5 billion bbl original oil in place. In this respect, the thickness of Cudi Group reaches to 400m and 1300m in the Batman and Nusaybin areas respectively, therefore, it is a most possible source rock candidate for the Group II oils. However, source rock potential of the Cudi Group has not been extensively studied. Recent work by Salem (1984) covered the sedimentology and some organic geochemistry of the Cudi group showed that during deposition of Cudi Group, several 170 transgressive-regressive cycles were repeated in a sabkha environment and algal mats are often present in the evaporitic regressive sections.

Heavy character of the Group II oils, as previously discussed in Section 4.1.2.3 shows that these oils have not migrated long distances. When the distribution of the Cudi Group is taken into consideration (Figure 4.39) it is seen that there is no need for lateral long distance migration. However, vertical migration of hydrocarbons generated from the Cudi Group is necessary to fill the Beloka and Upper Sinan reservoirs in

Nusaybin area and the Garzan and Derdere reservoirs in the Batı Raman and Raman oil fields.

As in the case of SE Turkey, Triassic to Jurassic time slice in the Middle East is dominated by the accumulation of thick sequences of evaporates and carbonates (Kent and Worman, 1972). Although tremendous amount of oil is present in this region as yet, most of the source rocks for the Middle East oil have not been identified (Kirkland and Evans, 1981).

4.2.3. Kozluk-Adıyaman area oils (Group III Oils) and their possible source rocks

The Group III oils are found in Kozluk (S30, S5, BS4, CE16 KU1 oils) and Adıyaman (A3, CT16 oils) areas (Figure 4.40). They are accumulated in reservoirs ranging from Cenomanian to Upper Maastrichtian (Table 3.1). The bulk geochemical properties of these oils are moderate sulfur contents (0.61-2.92), low asphaltene contents (1.0-11.0), and show a slight predominance of even number n-alkanes over odd ones (Table 3.2).

Significant features of steranes are the high relative abundance of pregnanes and the low relative abundance of diasteranes (Table 3.6). Regular steranes show a dominance of aaa C₂₇ compounds over their C₂₉ counterparts. It is interesting to note that aaa C₂₈ steranes also dominate over the C₂₉ counterparts (Table 3.6). C₃₀ steranes were also recognized. In the

DISTRIBUTION

GEOLOGICAL DATA

WEST KOZLUK AREA EAST KOZLUK AREA

AGE	LITHOLOGY	THICKNESS m.	FORMATION	DEPOSITIONAL ENVIRONMENT	ORGANIC MATTER			AGE	LITHOLOGY	THICKNESS m.	FORMATION	DEPOSITIONAL ENVIRONMENT	ORGANIC MATTER			
					TOC	TYPE	T _{max}						TOC	TYPE	T _{max}	
Eocene	[Lithology]	350	GERCÜŞ	FLUVIAL	-	-	-	Eocene	[Lithology]	300	GERCÜŞ	FLUVIAL	-	-	-	
PALEOCENE	[Lithology]	330	UPPER SİNAN	INNER SHELF	-	-	-	PALEOCENE	[Lithology]	250	UPPER SİNAN	INNER SHELF	-	-	-	
		600	ANTAK	TRANSITIONAL TO FLUVIAL	-	-	-			200	UPPER GERMAV	OUTER SHELF	L	III	438	
CAMP.-MAAS.	[Lithology]	430	LOWER SİNAN	SHELF LAGOON TO SHALLOW MARINE	-	-	-	MAASTRICHTIAN	[Lithology]	170	LOWER SİNAN	INNER SHELF	-	-	-	
		20	L.GERMAV								170	LOWER GERMAV	DEEP MARINE	L	III	439
		270	GARZAN	REEFAL/BANK						100	GARZAN	BANK/REEFAL	L	III	435	
CAMPANIAN	[Lithology]	200	KIRADAĞ	TRANSITIONAL	H	III	440	CAMPANIAN	[Lithology]	70	KIRADAĞ	FLUVIAL	H	III	441	
		150	SAYINDERE	OPEN MARINE	H	II	432-447			170	BELOKA	INNER SHELF OUTER SHELF	L	II,III	440	
CENOMANIAN	[Lithology]	200	KARABOĞAZ	SHALLOW TO DEEPER MARINE	L	II	435	CENOMANIAN	[Lithology]	200	DERDERE	SHALLOW CARBONATE				
		200	DERDERE	SHELF LAGOON TIDAL FLAT	L	II	438			300	SABUNSUYU	PLATFORM				
APTIAN CENOMANIAN	[Lithology]	300	SABUNSUYU	LAGOONAL TO TIDAL FLAT	VL	?	440	LOWER TRIAS	[Lithology]	70	ULUDERE	SUBTIDAL - INTERTIDAL	-	-	-	
UPPER PERMIAN	[Lithology]	600	GOMANİBRİK	SHALLOW CARBONATE LAGUNAL	-	-	-	UPPER PERMIAN	[Lithology]	80	KAŞ	DELTAIC PLAIN	-	-	-	
UPPER SILURIAN	[Lithology]	70	DADAŞ	OPEN MARINE	-	-	-	ORDOVICIAN	[Lithology]	?	BEDİNAN	DELTAIC INTER DELTAIC	L	III	455	

FORMATION DEPOS

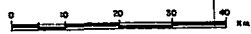
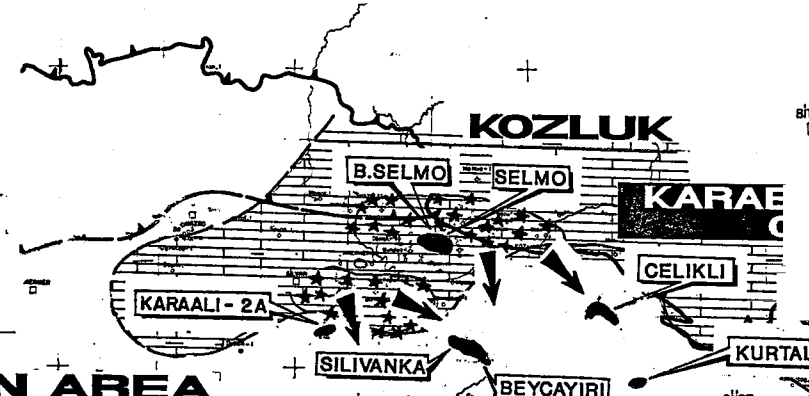
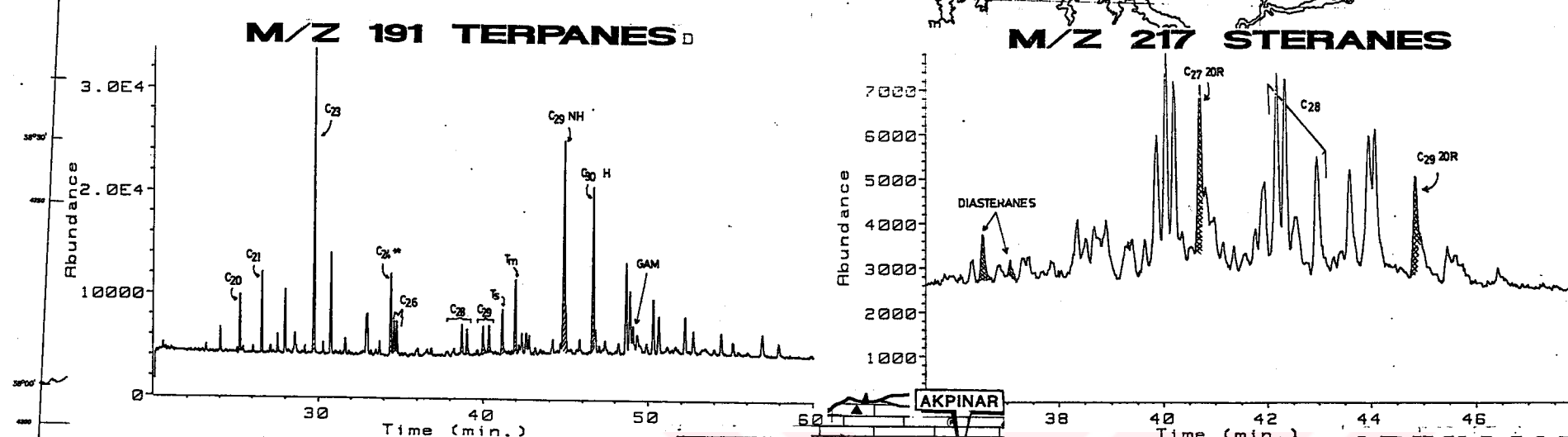


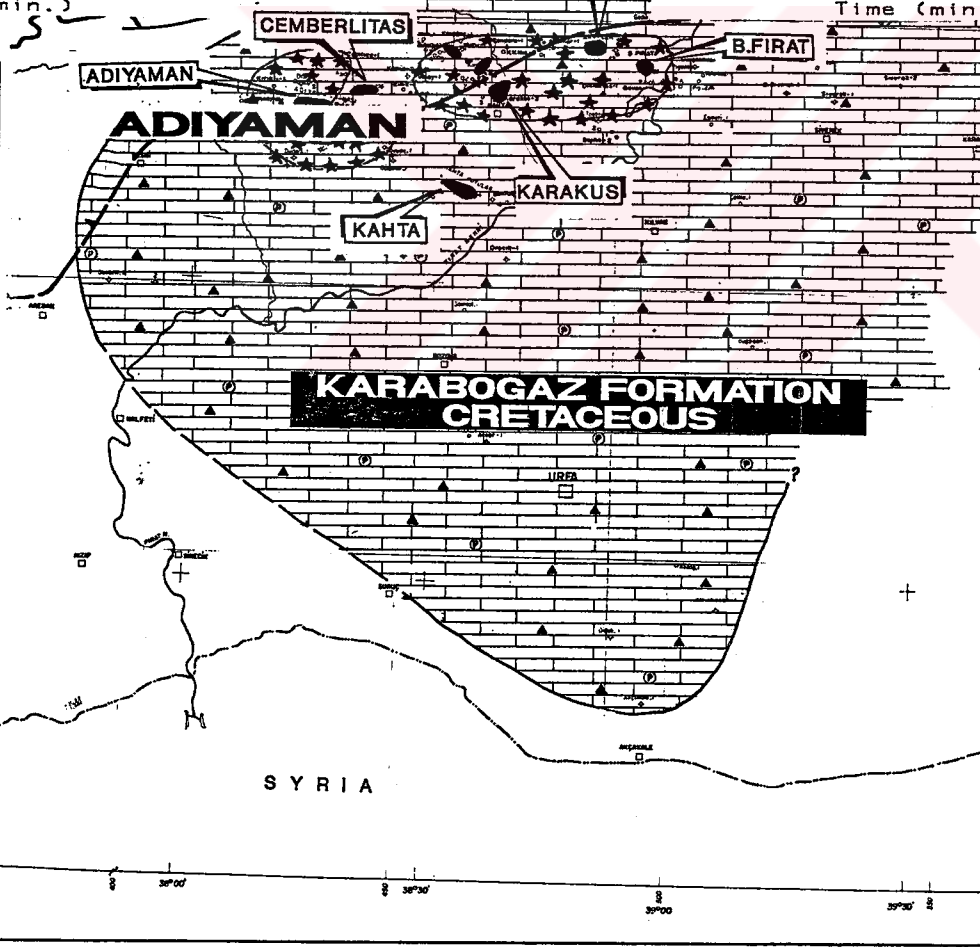
Figure_4.40

GROUP III OILS AND THEIR SOURCE ROCK

GEOCHEMICAL DATA



CORRELATION PARAMETERS	TYPE III OILS
PR/PHY	0.6-1.2
SAT/ARO	1.6-7.8
% SULFUR	0.6-3.0
- TERPANES -	
C24H/C26	0.8-1.7
C24H/C21	0.8-1.7
C23/C20	4.0-12.0
Tm+Ts/C28+C29	0.7-1.5
C29 NH/C30 H	0.8-1.3
Tm/Ts	0.9-4.5
C24H/C30 H	0.2-0.8
C23/C24H	2.8-3.7
- STERANES -	
I+II/III+IV+V	0.1-1.0
C27/C29	1.2-1.7
% DIASTERANES	3-12



AGE	LITHOLOGY	THICKNESS m.	FORMATION	DEPOSITIONAL ENVIRONMENT	ORGANIC MATTER
					TOC TYPE Tmax
MIDDLE-UPPER MAASTRICHTIAN		600	GERMAV	OUTER SHELF	V.L III 420
CAMPANIAN - MAASTRICHTIAN		1750	KASTEL	BASIN (DEEP MARINE)	- - -
		70	KARADUT		
		100	KASTEL		
CAMPANIAN		60	SAYINDERE	DEEP MARINE	- - -
TURONIAN - L. CAMPANIAN		5	KARABOGAZ	DEEP SHELF	V.H I,II 442
		10	KARABABA-C	LAGOONAL TO TIDAL FLAT	- - -
		30	KARABABA-B	SHALLOW OPEN MARINE	- - -
CENOMANIAN		20	KARABABA-A	INTRAPLAT FORM BASIN	V.H I,II 440
		70	DERDERE	LAGOONAL TO TIDAL FLAT	- - -
APTIAN		110	SABUNSUUYU	LAGOONAL TO TIDAL FLAT	- - -
LOWER TRIAS		5	AREBAN	SHORELINE	- - -
ORDOVICIAN			BEDINAN	SHALLOW MARINE	- - -
LOWER ORDOVICIAN			SEYDISEHIR	SHALLOW OPEN MARINE	- - -
UPPER CAMBRIAN			SOSINK	DELTA WITH TIDAL EFFECT	- - -
MIDDLE CAMBRIAN			KORUK	SHELF	- - -
LOWER CAMBRIAN			SADAN	NEARSHORE - BACKSHORE	- - -
PRE CAMBRIAN			TELBSANI	SHALLOW MARINE	- - -

★ KITCHEN AREA OF KARABOGAZ FOR
 ↗ MIGRATION PATHWAY

Figure_4.40 Adiyaman - Kozluk oils (Group III Oils) and their source rock distribution.

pentacyclic region of terpanes, the noteworthy feature is presence of gammacerane and high ratios of C_{35} to C_{34} (>1), high C_{29} NH/ C_{30} H ratios (0.84-1.27), and high Tm/Ts ratios ($>>1$). In the tricyclic region, C_{24} * tetracyclic terpene is not a major peak as in the Group I and Group II oils. Instead, C_{23} tricyclic terpene dominates the region. The C_{23}/C_{20} ratio is higher (3.95-12.26) whereas C_{24} */ C_{26} ratio is significantly lower (0.82-1.68) than the Group II oils.

Depositional Environment: The presence of C_{30} steranes is consistent with oils generated by marine source rocks (Moldowan et al., 1985). Unimodal distribution of n-alkanes maximizing on C_{15} - C_{21} region of the gas chromatograms support the marine origin. Many parameters indicate that source rock of the Group III oils deposited in anoxic conditions. Such parameters are low Pr/Phy ratios, and slight even/odd predominance in the n-alkanes (Table 3.1). The regular steranes show slight dominance of C_{28} odd components over their C_{29} counterparts. This has been reported to reflect the abundance of diatoms in the original organic matter of the source rock depositing probably in an upwelling environment (Volkman, 1986).

Organic Matter Type: In all of the Group III oils, marine character of the organic matter in the source rock is confirmed by the presence of C_{30} -Steranes (Moldowan et al., 1985). Dominance of C_{27} regular steranes over C_{29} counterparts and presence of substantial amount of Sulfur support to marine origin of organic matter. Presence of

large quantities of the C₂₈ regular steranes suggest diatomaceous organic matter input to the sediments. Bacterial input is also present due to high concentration of hopanes in these oils. Algal input is also present due to high concentration of low molecular weight n-alkanes.

Lithology: Stable carbon isotope ratio values being significantly heavier than those of the Group IV oils again suggests a source rock with carbonate lithology. Other parameters supporting this lithology are high sulfur contents, high asphaltene contents, negligible diasterane contents, low T_m/T_s ratios, high C₂₉ NH/C₃₀ H ratios (Table 4.10), and high concentration of low molecular weight pregnanes which are all consistent with the oils derived by 174 carbonate source rocks (Palacas et al., 1984; ten Haven et al., 1985; Talukdar et al., 1986). The dominance of the C₂₃ tricyclic terpane in the Group III oils is again common feature of oils derived from phosphate rich carbonate source rocks (Powell et al., 1975; Zumberge, 1987).

Maturity: Bulk composition and maturity sensitive biomarker parameters suggest that the Group III oils are found to be generated from marginally mature to mature source rocks.

Age: On the basis of the age controlled biomarker indicators, The Group III oils are most likely derived from the Cretaceous source rocks in the study area.

All the features mentioned above suggest a marine carbonate environment for the Group III oils based on the similarities between their specific chemical features and those of the well defined carbonate oils, for example; Sunniland oils in South Florida, USA (Palacas et al., 1984), La Luna oils, Venezuela (Talukdar et al., 1986;); Aquitane Basin oils, France (Connan et al., 1985); Australian oils (McKirdy et al., 1983). Based on the criteria given above, among those, Karaboğaz Formation of Campanian age would be a likely source rock candidate for the Adıyaman-Kozluk area oils. Other formations were ruled out on the basis of their organic richness, thickness, distribution, and lithology. The stratigraphic sections representing the Adıyaman and Kozluk areas in Figure 4.40 were compiled with the help of O. Duran and N. Bozdoğan (O.Duran and N.Bozdoğan, TPAO Research Center, Personal Communication, 1991). Average total organic carbon, organic matter type and Tmax values for the source rock candidates were also given on these stratigraphic sections (İztañ and Soylu, 1991).

Sabunsuyu Formation was not considered as a source rock for the Group III oils because it does not contain enough organic matter to generate oils. Derdere Formation of Cenomanian age is also widely distributed in the SE Turkey. This formation is composed of organic matter rich spheroidal facies just overlying the Sabunsuyu Formation but again it is too thin to be considered as a potential source rock for the Group III oils. However, some contributions from this formation into the oils of the

Group III seem possible. Turonian to Lower Campanian aged Karababa-A member of the Karababa Formation overlying the Derdere Formation in the Adıyaman area is also rich in organic matter (Soylu, 1991). However, the absence of Karababa-a member in the Kozluk area reduce the possibility of this unit as a source rock candidate for the Group III oils. Deeper marine facies of Beloka Formation of Campanian age in the Kozluk area also has some source potential. Again limited distribution of this facies in SE Turkey eliminates this rock unit as being a major source for the Group III oils which would possibly receive some hydrocarbons from this facies but only in the Kozluk area.

The Maastrichtian aged Kıradağ and Upper Maastrichtian-Paleocene aged Germav Formations were also ruled out because of their siliciclastic character and the unsuitable organic matter type of type III kerogen. This type of organic matter generates oil with high pristane to phytane ratio ($\gg 1$) and a bimodal distributed n-alkanes, and high C₂₉ regular steranes (Hughes and Holba, 1988). Obviously, none of the Kozluk-Adıyaman area oils possess these features.

The Campanian aged Karaboğaz Formation, therefore, is the most likely source for the Group III oils. This formation contains high organic carbon with right type of organic matter and it is mature enough to generate hydrocarbons in the Kozluk area (Figure 4.38). Mass-balance calculation made by İztan (1988) showed that

it is thick enough to generate hydrocarbons at least equivalent to the amount of hydrocarbons found in the Kozluk area. As discussed earlier in this section, biological marker geochemistry of the Group III oils suggested a phosphate and diatom rich carbonate source rock deposited in an upwelling environment. In fact, presence of various amounts of phosphatic material in the Karaboğaz Formation has been previously interpreted as a product of deposition in an upwelling environment (Wagner et al., 1986) Further, the occurrence of cherts in places 177 of Karaboğaz Formation (Wagner et al., 1986) could be interpreted as being formed by diagenesis of the diatoms. It is also evident from the age determinations of the Group III oils from C_{28}/C_{29} sterane ratios (Section 4.1.3) that age of the source rock candidate predicted to be Cretaceous. Therefore, it can be concluded that Karaboğaz Formation appears to be a reasonable choice for the source rock of the Group III oils in the Adıyaman-Kozluk area.

If the Karaboğaz Formation is responsible for the generation of the oils in the Kozluk area then present locations of the Çelikli, Silivanka, Beyçayırı, and Kurtalan oils require lateral-updip migration because of the fact that the Karaboğaz formation do not have source rock potential in this area. Therefore, one may speculate that hydrocarbons generated from the Karaboğaz Formation in the north migrated southward and filled the reservoirs of Çelikli, Silivanka, Beyçayırı, and Kurtalan oil fields (Figure 4.40). However, the possibility of this migration hypothesis still needs to be checked by estimation of

hydrocarbon generation and expulsion times of the Karaboğaz Formation and determining the timing of reservoir formation of the Çelikli, Silivanka, Beyçayırı, and Kurtalan oil fields.

In the Adıyaman area, on the other hand, the distribution of oil fields and kitchen areas (i.e., $TOC > 0.5$, $T_{max} > 435$, and organic matter type=I, II kerogen) of the Karaboğaz Formation overlap, therefore, there is no need for long distance migration.

Akpınar, Batı Fırat, Karakuş, and Kahta oils of the Adıyaman area and Karaali, and Tura oils of the Kozluk area shown in Figure 4.40 were not analyzed for the purpose of this study. However, they are believed to be generated from the Karaboğaz Formation.

4.2.4. Northern Diyarbakır Oils (Type IV oils) and Their Possible Source Rocks.

The Group IV oils are found in the northern Diyarbakır area (Figure 4.41) and produced from carbonate reservoirs of the Mardin Group of Turonian-Cenomanian age. Their geochemical features include low sulfur contents (0.41-0.91 %), relatively light $\delta^{13}C$ values from 29.10 per mil to -29.70 per mil for the saturate fraction and from -27.60 per mil to -28.50 per mil for the aromatic fraction (Table G). The compositional data show higher saturate (68-71 %) and lower asphaltene (4.8-5.0 %) contents relative to the Group I, II, and III oils.

DISTRIBUTION

GEOLOGICAL DATA

N. DIYARBAKIR AREA

KASTEL AREA

AGE	LITHOLOGY	THICKNESS m	FORMATION	DEPOSITIONAL ENVIRONMENT	ORGANIC MATTER			AGE	LITHOLOGY	THICKNESS m	FORMATION	DEPOSITIONAL ENVIRONMENT	ORGANIC MATTER		
					TOC	TYPE	Trace						TOC	TYPE	Trace
PALEOCENE		380	KAYAKÖY	TIDAL FLAT SHALLOW MARINE TO TRANSITIONAL				PALEOCENE		330	KAYAKÖY	SUPRATIDAL	-	-	-
CAMPANIAN - MAASTRICHTIAN		250	KASTEL					MAASTRICHTIAN		350	LOWER SINAN	SHALLOW CARBONATE PLATFORM (REFOIDAL)	-	-	-
		230	KARADUT	BASINAL	-	-	-								
		150	KASTEL		-	-	-								
CAMPANIAN		70	SAYINDERE	DEEP MARINE	-	-	-	CAMPANIAN - MAASTRICHTIAN		30	GARZAN		-	-	-
CENOMANIAN		150	DERDERE	SHALLOW CARBONATE PLATFORM DEPRESSION IN THE PLATFORM	-	-	-			160	KIRADAĞ	FLUVIAL	-	-	-
APTIAN- CENOMANIAN		280	SABUNSLUYU		SHALLOW CARBONATE PLATFORM	-	-		-		400	KASTEL	BASINAL	-	-
LOWER TRIAS		20	AREBAN	SHORELINE				CAMPANIAN		150	SAYINDERE	DEEP MARINE	H	I, II	435
MIDDLE DEVONIAN		115	KAYAYOLU	TIDAL FLAT- LAGUNAL	-	-	-		TURONIAN	20	KARABABA	LAGOONAL	VL	-	-
LOWER DEVONIAN		120	HAZRO	TIDAL FLAT- LAGUNAL	-	-	-		CENOMANIAN	130	DERDERE	SHALLOW MARINE	VL	-	-
UPPER SILURIEN			DADAŞ I	NEARSHORE SHALLOW MARINE RESTRICTED CONDITION	H	II, III	445	APTIAN - CENOMANIAN		230	SABUNSLUYU	SHALLOW MARINE TO TIDAL FLAT	VL	-	-
			DADAŞ II + III		vH	-	-			20	AREBAN	SHORELINE	-	-	-
			DADAŞ I						LOWER DEVONIAN	100	HAZRO	SHALLOW MARINE SHEET SANDS	-	-	-
			DADAŞ I					UPPER SILURIEN	80	DADAŞ II + III	NEARSHORE	H	I, III	443	
			DADAŞ I					ORDOVICIAN	70	BEDİNAN	NEARSHORE	-	-	-	

IRAQ



Figure_4.41

GROUP IV OILS AND THEIR SOURCE ROCK

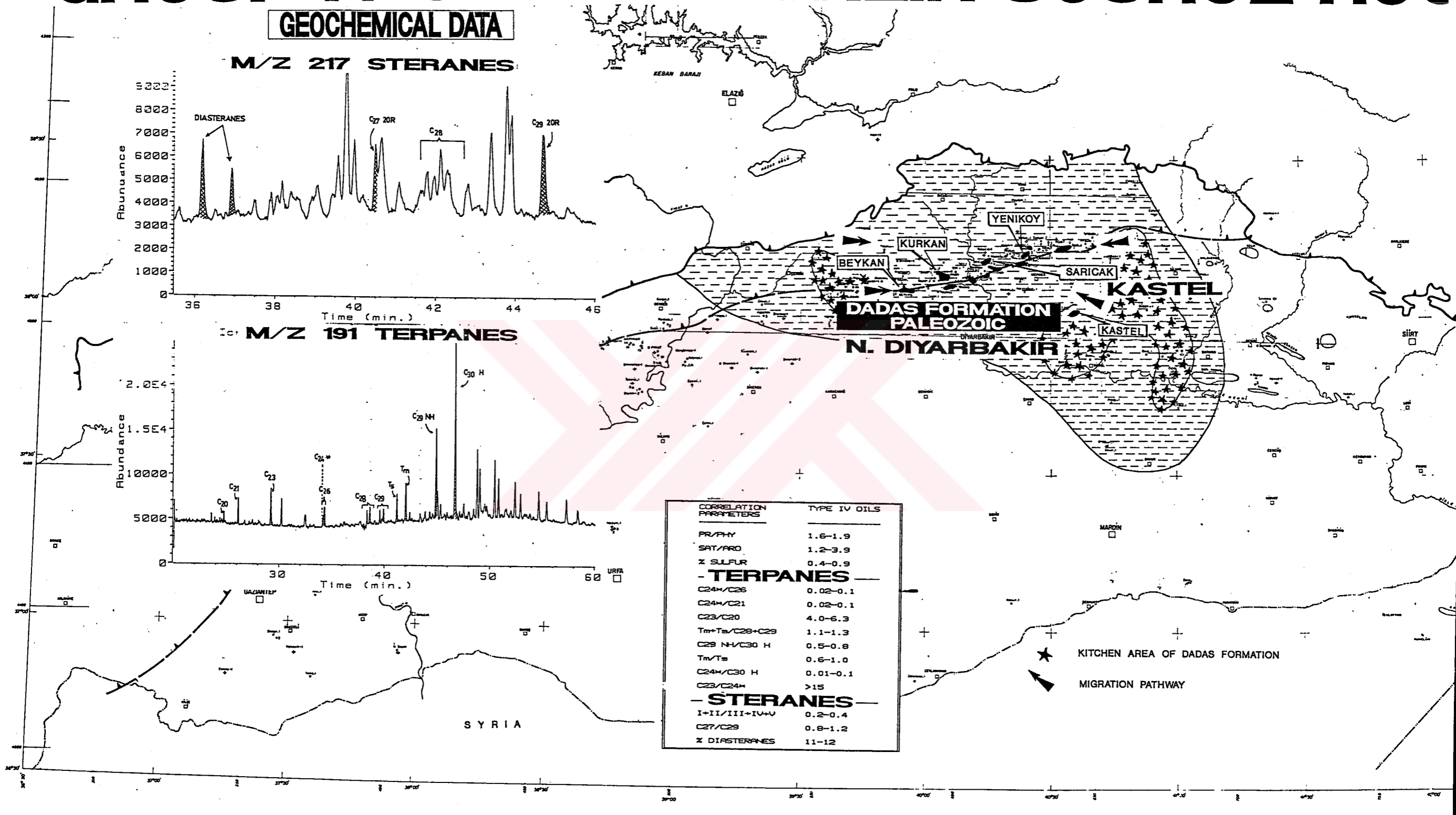


Figure_4.41 Northern Diyarbakir oils (Group IV Oils) and their source rock distribution.

Pristane to phytane ratios are significantly higher (1.50-1.91) compared to the other oil groups (Table 3.2).

Diasteranes, mainly *aaa* C₂₇ 20S and R isomers, are present in relatively higher amounts compared to the Group I, II, and III oils (Table 3.6). As for the Group I and II oils, the C₂₉ regular steranes are in high abundance and *aaa* C₂₇ to C₂₉ 20R sterane ratios vary between 0.81 and 1.18 (Table 3.6).

M/Z 191 mass fragmentograms (Figure 3.3, Appendix D) of the Group IV oils exhibit high relative abundances of the tricyclic terpanes. However, no C₂₄* tetracyclic terpane was detected in the Group IV oils. Thus, the C₂₄ tetracyclic to C₂₆ tricyclic ratio is significantly lower than the other oils (0.02-0.11) (Table E-5). The T_m/T_s ratio is relatively lower (0.57 - 1.01). The C₂₉ NH/C₃₀ H ratio is always smaller than 1 (Table E-5). Another noteworthy feature of the Group IV oils is the absence of gammacerane (peak GAM in Figure 3.3).

Depositional Environment: The biological marker distribution show characteristic features based on the occurrence or absence of specific compounds. For example, presence of the C₃₀ steranes, as in other oils, indicate definite marine origin of these oils (Moldowan et al., 1985). Absence of gammacerane, on the other hand, suggests a brackish water environment for the source of the Group IV oils rather than a hypersaline (salinity higher than normal sea water) environment. Absence of the C₂₄

tetracyclic terpane also confirms nonhypersaline depositional setting of the source rock. The high pristane/phytane ratios for the Group IV oils probably reflect the relationship between their precursors and the chemistry of environments (ten Haven and Sinighe, 1987) e.g. low salinity, rather than simply the anoxic/oxic condition of sedimentation. In a brackish water environment (salinity less than normal sea water), photosynthetic organisms containing phytol and tocopherols would be expected to be abundant. With an increase in salinity (higher Eh), however the bacterial population might be expected to increase in abundance. Thus the more saline the environment, the greater the potential for an increase in the concentration of phytane precursors. This may help explain the high predominance of pristane in a less saline environment compared with dominance of phytane in hypersaline environments (ten Haven et al., 1987). The low values of sulfur in the Group IV oils is also in agreement with their brackishwater origin since such property is primarily a function of the Eh-pH conditions and sulfide activity of the depositional environments (Orr, 1986).

Lithology: Presence of higher concentration of diasteranes in this group of oils together with low sulfur contents and high API gravity suggest predominantly siliciclastic mineral matrix in the source rocks (Sieskind et al., 1979; Rubinstein et al., 1979). A clastic source rock hypothesis also supported by the low $C_{29}NH/C_{30}H$ ratio being less than 1.

Organic Matter: The high saturate content and odd over even n-alkane predominance in the Group IV oils indicate some contributions from terrestrial land plants (Tissot and Welte, 1984) to depositional environment of their source rocks. The isotopically lighter values of $\delta^{13}C$ for saturate and aromatic fractions (Appendix G) also suggest principal lipid constituents, originating from terrestrial plants and/or freshwater algae. These are depleted in $\delta^{13}C$ relative to those of marine or saline plants (Moldowan et al., 1985). Presence of higher concentration of the regular C_{29} steranes also confirms some terrestrial organic matter input to the sedimentary organic matter. Beside terrestrial and algal organic matter, the source rock of the Group IV oils probably contain some bacterial input based on the fact that the C_{31} - C_{35} extended hopanes are in high concentrations.

Maturity: Bulk composition (high API gravity, low sulfur contents, high saturate content) suggested that the Group IV oils could be generated from mature source rocks. In contrast, biomarker maturity parameters suggested a marginally mature source rocks. One may further speculate that the Group IV oils contain some hydrocarbons generated from the lesser mature sediments.

Age: On the basis of the age controlled biomarker indicator in the GS21 oil of the Group IV oils suggest that these oils were derived from the Paleozoic source rocks.

Overall, the bulk and molecular features of the Group IV oils suggest siliciclastic rich source rock deposited in brackish to saline environment. Organic matter consists of mainly marine type but significant input of terrestrial type also exists. In the world, in a number of basins, siliciclastic rocks have been found to be oil generators. Well known examples are the Liassic, Oxfordian, and Kimmeridge shales, in the North Sea and Toarcian shales of SW-Germany, and Paris Basin, France (Mackenzie, 1984; Moldowan et al., 1985).

In view of the above discussion, among the other rock units present in the area, siliciclastic Upper Silurian aged Dadaş Formation seems the most likely source of the northern Diyarbakır area oils (Group IV oils) which was also assigned as a source rock for the northern Diyarbakır oils by Robertson Research Co., (1984). This study confirms Dadaş formation as a source for the Group IV oils and adds the KA2 oil to extend the Group IV oil distribution towards the Batman area. This study also brings the idea that especially brackish water facies of the Dadaş formation contributed to hydrocarbons into the Group IV oils. As seen in the stratigraphic columns of northern Diyarbakır region and Kastel-2 well (Figure 4.41), siliciclastic rock units dominate the Paleozoic section. As a conclusion, the Dadaş formation with its siliciclastic nature, nearshore depositional environment, high TOC content, and containing both type II (marine organic matter) and type III kerogen (terrestrial organic matter) is an ideal source rock candidate for the Group IV

oils. However, as mentioned earlier (Section 4.1.4.1), the Group IV oils are most likely commingled from the insitu generated hydrocarbons in the Cretaceous Mardin carbonates.

If the Northern Diyarbakır oils generated from the Dadaş Formation then present location of the Güney Sarıcak oil can be best explained by lateral-updip migration. The Dadaş Formation has two kitchen areas in the Northern Diyarbakır area (İzitan and Soylu, 1991). Migration of hydrocarbons generated in the kitchen areas probably migrated and filled the reservoir of the Güney Sarıcak oil fields. However, the possibility of the migration hypothesis should be checked by estimating hydrocarbon generation and expulsion time of the kitchen areas of the Dadaş Formation and determining reservoir forming time of the Güney Sarıcak oil field reservoirs. Beykan, Kurkan, and Yeniköy oils were also shown in Figure 4.41 although they were not analyzed for the purpose of this study. Because, they are believed to be generated from the Dadaş Formation (Robertson Research Co., 1984).

4.2.5. Mixed Origin Oils (Batman area Oils) and Their Possible Source Rock

Intermediate position of the GA15, GE12, and SI1 oils between the Group II and Group III oils provided strong evidence for a mixed source based on the several plots involving tricyclic terpanes, tetracyclic terpanes, pentacyclic terpanes, steranes, and several source

dependent biomarker ratios (see Chapter 4). This implies that the GA15, GE12, and SI1 oils comprise various contributions of the Group II and Group III oils. In other words, hydrocarbons generated from both the Campanian aged Karaboğaz Formation and the Triassic-Jurassic aged Cudi Group supply the GA15, GE12, and SI1 oils either in the reservoir or in the migration paths. Geographic location of the GA15 and GE12 and SI1 oils make a mixing hypothesis for these oils more reasonable (Figure 4.42).

Mixing of the generated hydrocarbons from the Karaboğaz Formation and Cudi Group most likely occurred in the reservoirs of Garzan (GA15), Germik (GE5), and Sinan (SI1) oils. Southward migration of hydrocarbons generated from the Karaboğaz Formation, as suggested for some of the Group III oils, may continue to migrate towards south and filled the Garzan, Germik and Sinan reservoirs. Hydrocarbons generated from the Cudi Group, however, needs only short distance vertical migration. Because, the distribution of the Cudi Group covers the location of the mixed oils. Confirmation of these migration hypothesis, however, should be made. Geologically, time of the reservoir forming processes of the mixed oils should be determined. Geochemically, timing of the oil generation in the both Karaboğaz Formation and Cudi Group should be estimated. Kitchen areas of the Cudi Group should be determined in order to explain better migration pathways for the mixed oils and also Group II oils.

CHAPTER V

CONCLUSIONS and RECOMMENDATIONS

The genetic classification of forty-four crude oils from Cretaceous reservoir rocks and their possible source rocks in SE Turkey were investigated by a variety of organic geochemical techniques with emphasis on sterane and terpane biological markers. Most of the data were evaluated using multivariate statistical analysis.

Results of this study showed that there are extra-immature, immature, moderately mature, and mature oils in SE Turkey. Thermal alteration process was not significant to prevent oil to oil correlation studies. Maturity sensitive biological markers suggested the maturity level of the oils equivalent to vitrinite reflectance value of 0.6-0.8. Biological degradation process appeared to be not altered the Turkish oils except in the case of two oils from the Batı Raman fields (Batman area). These oils displayed features of the mixing of degraded and normal crude oils. Crude oil alteration by secondary migration process was difficult to examine because source rock of these oils was not known at this stage.

Oil to oil correlations were carried out to classify the Turkish oils in SE Turkey genetically. The plot of stable carbon isotope ratios of saturate and aromatic fraction of the oils enabled to separate northern Diyarbakır oils (lighter values) from the rest of the oils (Batman-Nusaybin area oils). Multivariate statistical technique was applied to the five different biological marker data sets. This has led to the confirmation of four genetic oil groups (i.e., Batman, Batman-Nusaybin, Adıyaman-Kozluk, and Northern Diyarbakır oils) and the presence of oils of mixed origin.

The following parameters were found to be significant for the genetic classification of the Turkish oils.

i. The most diagnostic tri-tetracyclic terpene parameters of the Turkish oils were the C_{24} tetracyclic terpene, % tricyclic terpenes, % C_{19} , C_{22} , and C_{23} tricyclic terpenes.

ii. The most diagnostic pentacyclic terpene parameters of the Turkish oils were % B1 (unidentified pentacyclic compound), C_{29} moretane, 17 α (H) 22,29,30-Trisnorhopane (Tm), 18 α (H) 22,29,30-Trisnorhopane (Ts), 17 α (H), 21 β (H) 30-norhopane, and 17 α (H), 21 β (H) 30-hopane.

iii. In addition to parameters mentioned above, the most diagnostic tri-tetra-pentacyclic terpane parameters were % C₃₁-C₃₅ extended hopanes.

iv. The most diagnostic pregnane-diasterane-regular sterane parameters were % C₂₇-C₂₉ regular steranes, C₂₂ homopregnane (IV), C₂₁ pregnane (II), and diasteranes.

v. The most diagnostic selected biomarker ratios were the Sat/Aro, I+II/III+IV+V (pregnanes), C₂₇/C₂₉ (regular steranes), Tm+Ts/C₂₈+C₂₉ (pentacyclic/tricyclic terpanes), Tm/Ts (pentacyclic terpanes), C_{24*}/C₂₆ (tetracyclic/tricyclic terpanes), C₂₉ NH/C₃₀ H (pentacyclic terpanes), C₂₄/C₂₁ (tetracyclic/tricyclic terpanes), and C₂₃/C₂₀ (tricyclic terpanes) ratios. The % S (sulfur) was also included in the selected biomarker ratio input due to its obvious significance for the Turkish oils.

The investigation of the age related biomarkers in the oils showed that the Turkish oils were derived from the source rocks of three distinct ages: Cretaceous; Paleozoic; Triassic-Jurassic.

Finally, an attempt was made to conduct source rock-oil correlations by comparing the features such as depositional environment, lithology, organic matter type, maturity, and age of the previously known potential source rocks with those of the oils suggested by biological markers. On the basis of this approach, the following source rock-oil correlations were made (Figure 4.43): The

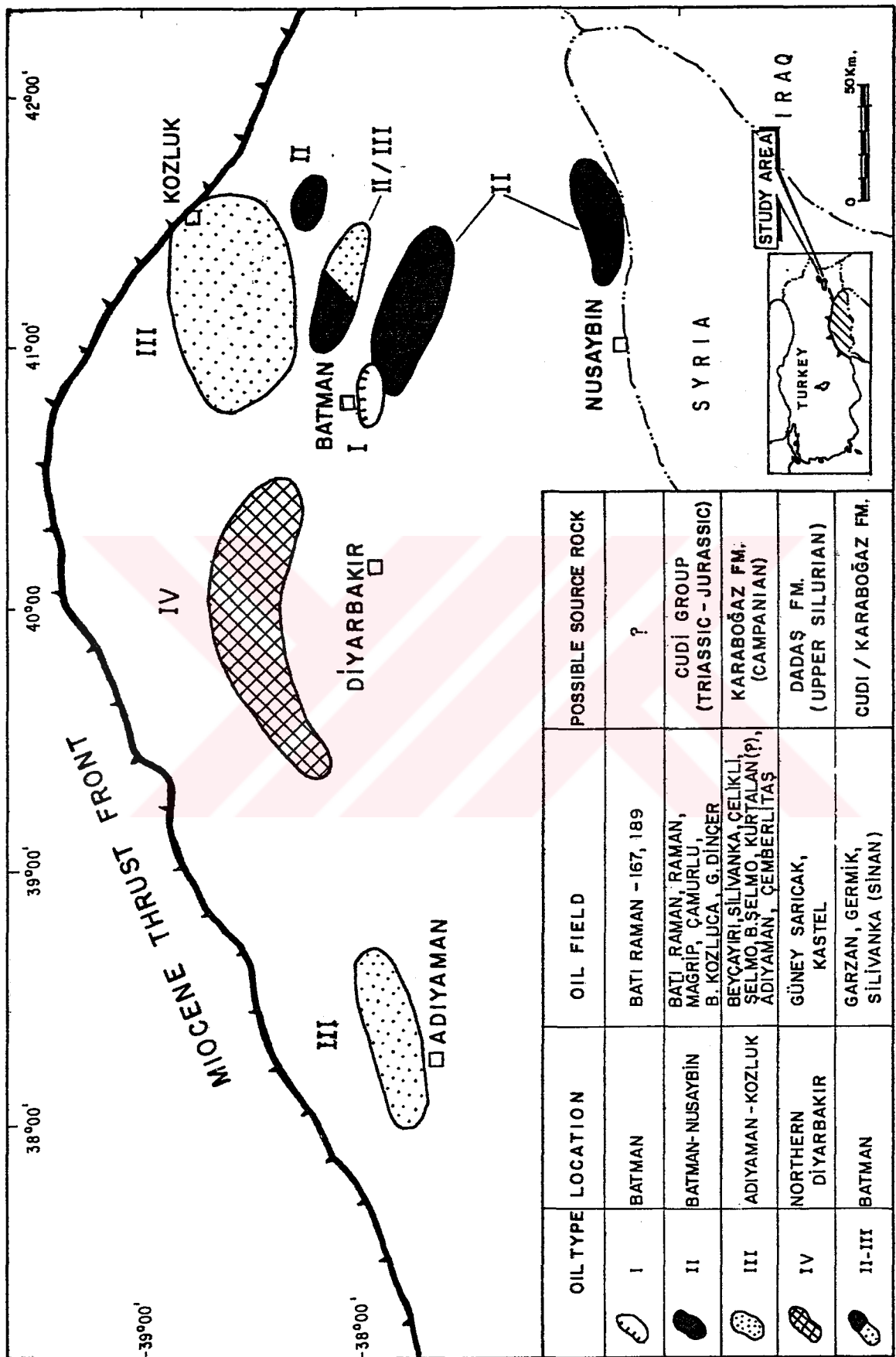


Figure - 4.43 Oil groups and their distribution in the SE Turkey.

oils seem to be divided into four groups in addition to a fifth group of oils of a mixed origin. Group I oils (Batman area oils) are sulfur rich, immature-heavy oils and exhibit different geochemical characteristics (high C₂₄ tetracyclic terpane peak and very high 18 α (H) Trisnorhopane T_m peak) from nearby Group II oils. They show the features of a mixture of degraded oils with the 190 normal oils. Altered molecular composition prevents to predict nature of their source rocks.

Group II oils (Batman-Nusaybin area oils) are sulfur-rich, immature-heavy oils and contain very low diasteranes and tricyclic terpanes but high C₂₄* tetracyclic terpane. These oils are most likely derived from an evaporite-carbonate source rock deposited in an extremely anoxic, hypersaline water column. In the interest area, The Triassic-Jurassic Judi Group is the only rock unit which satisfies these requirements.

Group III oils (Adiyaman-Kozluk area oils) exhibit a large range of characteristics under the influence of maturity especially in the Kozluk area. They include both sulfur-rich, marginally-mature oils and sulfur-poor, mature-light oils. High concentration of tricyclic terpanes in particular C₂₃ tricyclic terpane and diasteranes are the main features of these oils. They are most likely derived from a carbonaceous marine source rock deposited under an anoxic and saline water column. The source rock for these oils is most likely Campanian aged Karaboğaz formation.

Group IV oils (Northern Diyarbakır oils) are sulfur-poor and mature-light oils which are significantly different from the other oil groups by having higher concentration of diasteranes, low ratios of C₂₉ norhopane to C₃₀ hopane ratios (<1) and not having C₂₄* tetracyclic terpane compound. These oils are most likely derived from siliciclastic source rocks deposited in suboxic-anoxic, and brackish water column. The suspected source rock is most likely Upper Silurian aged Dadaş formation.

The oil group with a mixed origin shows the characteristics of both Group II and Group III oils. This suggests that mixing of hydrocarbons generated from the Karaboğaz formation and the Cudi Group have been occurred either in the reservoir during accumulation or in the carrier beds during secondary migration.

Under the light of this study, by no means that exact source rocks were established, therefore, detailed studies are recommended for further source rock-oil correlations in SE Turkey.

The parameters outlined above may serve as a reference information for grouping of the oils to be discovered in future.

In order to confirm possibility of suggested oil migrations, timing of hydrocarbon generation and structural configuration of reservoir rocks in SE Turkey should be established.

Grantham and Wakefield's (1988) "source rock age dating curve" should be verified and/or modified for the source rocks of SE Turkey.



REFERENCES

Ala, M. A., and Moss, B.C., 1979. "Comparative petroleum geology of Southeast Turkey and Northeast Syria", Journal of Petroleum Geology, Vol. 1, pp. 3-27.

Albaiges, J., Algaba, J., Clavell, E., and Grimalt, J., 1985. "Petroleum geochemistry of the Tarragona Basin (Spanish Mediterranean off-shore)", In: Advances in Organic Geochemistry. Leythausser, D., and Rullkötter, J., (eds), pp. 441-450.

Alexander, R., Kagi, R.I., and Woodhose, G.H., 1981. "Geochemical correlation of Windalia oil and extracts of Winning Group (Cretaceous) potential source rocks, Barrow subbasin, Western Australia", Bulletin of American Association of Petroleum Geologist, Vol. 65, pp. 235-250.

Aquino Neto, F.R., Trendel, J.M., Restle, A., Albrecht, P., and Connan, J., 1981. "Occurrence and formation of tricyclic and tetracyclic terpanes in sediments and petroleum". In: Advances in Organic Geochemistry, 1981. M. Bjoroy et al. (eds). pp. 659-667.

Barker, C., 1979. Organic Geochemistry in Petroleum Exploration American Association of Petroleum Geologist, Educational Short Course Note Series, No. 10, 159 p.

Bockmeulen, H., Barker, C., and Dickey, P.A., 1983. "Geology and geochemistry of crude oils, Bolivar Coastal Fields, Venezuela", Bulletin of American Association of Petroleum Geologist, Vol. 67, pp.242-260.

Bozdoğan, N., and Erten, T., 1990. "Mardin yükseliminin yaşı ve etkileri, GD Anadolu", Türkiye 8. Petrol Kongresi, 1989, Ankara, p.207-227.

Brooks, W.P., Fowler, G.M., and Macqueen, W.R., 1988. "Biological marker and conventional organic geochemistry of oil sands/heavy oils, Western Canada Basin", Organic Geochemistry, Vol. 12, pp. 519-538.

Buchanan, R., 1974. "Hydrocarbon generation and entrapment in the Shell oil field area of southeast Turkey", N. V. Turkish Shell Petroleum Engineering Note # 40, Ankara, Turkey (unpublished).

Calvin, M., 1963. Chemical Evolution, Oxford University Press, Oxford.

Carlson, R. M. K., and Chamberlain, D. E., 1986. "Steroid biomarker-clay mineral adsorption free energies: implications to petroleum migration indices", In: Advances in Organic Geochemistry, 1985. Leythauser, D., and Rullkötter, J., (eds), Pergamon Press, Oxford, pp. 163-180

Chevron Oil Co., 1987. "Oil to oil correlations determined from routine analysis of oils from Southeast Turkey". Chevron Oil Field Research Company, La Habra, California. Unpublished Report.

Christie, H.O., Esbensen, K., Meyer, T., and Wold, S., 1984. "Aspects of pattern recognition in organic geochemistry", Organic Geochemistry, Vol. 6, pp. 885-891.

Clark, P. J, and Philp, R. P., 1989. "Geochemical characterization of evaporite and carbonate depositional environments and correlation of associated oils in the Black Creek Basin, Alberta", Bulletin of Canadian Petroleum Geologist, Vol. 37, pp. 401-416.

Clayton, A. W., 1989. "Geochemical evidence for Paleozoic oil in Lower Cretaceous sandstone, Northern Denver Basin", American Association of Petroleum Geologist, Vol. 73, pp. 977-988.

Connan, J., 1984. "Biodegradation of crude oil in reservoirs", In: Advances in Petroleum Geochemistry. Brooks J., and Welte, D. H., (eds), Vol. 1, pp. 299-335. Academic Press London.

Connan, J., Bouroulllec, J., Dessort, D., and Albrecht, P., 1985. "The microbial input in carbonate-anhydrite facies of a sabkha palaeoenvironment from Guatemala: a molecular approach", In: Advances in Organic Geochemistry, 1985. Leythauser, D., and Rullkötter, K., (eds), pp. 29-50.

Connan, J., and Dessort, D., 1987. "Novel family of hexacyclic hopanoids alkanes (C32-C35) occurring in sediments and oils from anoxic paleoenvironments", Organic Geochemistry, vol. 11, pp. 103-113.

Curiale, A. J., 1983. "Petroleum occurrences and source rock potential of the Quachita Mountains, southeastern Oklahoma", Oklahoma Geological Survey, Bull., 135, 65p.

Davis, C. J., 1973. Statistic and Data Analysis in Geology, John Wiley and Sons, Newyork, 550 p.

Dembicki, H., Meinschein, W. G., and Hattin, D. E., 1976. "Possible ecological and environmental significance of the predominance of even-carbon number C20-C30 n-alkanes", Geochimica et Cosmochimica Acta, vol. 40, pp. 203-208.

Didyk, B.M., Simoneit, B. R. T., Brassell, S. C., and Eglinton, G., 1978. "Organic geochemical indicators of paleoenvironmental conditions of sedimentation", Nature, Vol. pp. 1041-1052.

Duran, O., Şemşir, D., and Perinçek, D., 1988. "Güneydoğu Anadolu'da Midyat ve Silvan Gruplarının stratigrafisi, sedimentolojisi, ve petrol potansiyeli", Türkiye Petrol Jeologları Derneği Bülteni, Cilt 1/2, sayfa 99-126.

Ediger, Ş. V., Gürgey, K., and Batı, Z., 1990. "An example to the application of the cluster and PCA analyses in Paleopalynological biostratigraphy from the northern Thrace basin", Doğa, Tr. J. of. Engineering and Environmental Sciences, Vol. 14, pp. 393-401.

Eglinton, T., Rowland, S., Curtis, S., and Douglas, A., 1986. "Kerogen-mineral reactions at raised temperatures in the presence of water", In Advances in Organic Geochemistry, 1985. Leythausen, D., and Rullkötter, J., (eds). Pergamon Press, Oxford, pp. 1041-1052.

Ekweozor, C. M., Okogun, J. I., Ekong, D. E. U., and Maxwell, J. R., 1979. "Preliminary organic geochemical studies of samples from the Niger Delta (Nigeria). I. Analysis of crude oils from triterpanes", Chemical Geology, vol. 27, pp. 29-37.

Engel, H. M., Imbus, W. S., and Zumberge, E. J., 1988. "Organic geochemical correlation of Oklahoma crude oils using R- and Q-mode factor analysis", Organic Geochemistry, vol. 12, pp. 157-170.

Englinton, G., and Calvin, M., 1967. Chemical fossils, vol. 216, pp. 32-43.

Erdoğan, L. T., and Akgül, A., 1981. "An oil migration and re-entrapment model for the Mardin Group reservoirs of southeast Anatolia", Journal of Petroleum Geology, Vol. 4, pp. 57-75.

Eseller, G., 1986. "The geology of the Mağrip and Çelikli oil fields (southeastern Turkey) and evaluation of carbonate reservoirs using well logs", PhD. Thesis, University of London, 304 p.

Evans, C. R., Rogers, M. A., Bailey, N. J. L., 1971. "Evolution and alteration of petroleum in western Canada", Chemical Geology, vol. 8, pp. 147-170.

Exxon Production Co., 1988. "Geochemistry of Şelmo field crude oil and diesel from the Batman and Mersin refineries, Turkey", TPAO Arş. Merk. Report No: 2506, 102p.

Fowler, M. G., and Douglas, A. G., 1987. "Saturated hydrocarbon biomarkers in oils of Late Precambrian age from eastern Siberia", Organic Geochemistry, vol. 11, pp. 201-213.

Farrimond, P., Eglinton, G., Brassell, C. S., and Jenkyns, C. H., 1989. "Toarcian anoxic event in Europe: an organic geochemical study", Marine and Petroleum Geology, vol. 6, pp. 136-146.

Fu Jiamo, G. S., Pingan, P., Brasell, S. C., Englinton, G., and Jigang, J., 1986. "Peculiarities of salt lake sediments as potential source rocks in China", in Advances in Organic geochemistry, 1985. Leythauser, D., and Rullkötter, K., (eds), pp. 119-127. Pergoman Press, Oxford.

Gagosian, R. B., 1983. "Review of marine organic geochemistry", Reviews of Geophysics and Space Physics, Vol. 21, pp. 1245-1258.

Govett, S. J. G., 1983. Handbook of Exploration Geochemistry: Statistics and Data Analysis in Geochemical Prospecting, Vol. 2, Elsevier, 437 p.

Grantham, P. J., Posthuma, J., and Baak, A., 1983. "Triterpenoids in a number of far eastern crude oils", In: Advances in Organic Geochemistry, 1981. Bjoroy et al., (eds), pp. 675-683.

Grantham, J. P., 1986. "The occurrence of unusual C27 and C29 sterane predominance in two types of Oman crude oils", Organic Geochemistry, Vol. 1, pp. 1-10.

Grantham, J. P., and Wakefield., 1988. "Variations in the sterane carbon number distributions of marine source rock derived crude oils through geological time", Organic Geochemistry, Vol. 12, pp. 61-73.

Gussow, W. C., 1954. "Differential entrapment of oil and gas-A fundamental principle", Bulletin of American Association of Petroleum Geologist, vol. 38, pp. 816-853.

Gürgey, K., 1983. "Characterization of crude oils and some potential source rocks from SE-Turkey", M.S. Thesis, University of Tulsa, 105p.

Gürgey, K., 1987. "Petroleum geochemistry of the southeast Turkey (District X)", Proceedings, 7th Biannual Petroleum Congress of Turkey, pp. 415-426, April 6-10, Ankara.

Gürgey, K., 1989. "Application of principal component analysis to correlation of SE-Turkey oils", 14th International Meeting on Organic Geochemistry, Abstract No: 158, Paris, September 18-22.

Gürgey, K., and Harput, A., 1990. "Estimated age of the source rocks of southeast Turkey oils using sterane carbon distributions", Proceedings 8th Biannual Petroleum Congress of Turkey, April 16-20, Ankara, pp. 62-78.

Gürgey, K., and Sayılı, S., 1990. "Organic geochemistry of the Marmara Sea Holocene sediments", IESCA, izmir (in press).

Harput, B., Soylu, C., Harput, A., Ertürk, O., 1986. "IX Bölge tortullarının kaynak kaya değerlendirilmesi ve havza petrolerinin oluşum-göç dinamiğine yaklaşımlar", TPAQ Araş. Merk. Rapor No: 913 (unpublished).

ten Haven, L., de Leeuw, W. J., and Schenk, A. P., 1985. "Organic geochemical studies of a Messinian evaporitic basin, northern Apennines (Italy) I: Hydrocarbon biological markers for a hypersaline environment", Geochimica et Cosmochimica Acta, Vol. 49, pp. 2181-2191.

ten Haven, L., de Leeuw, W. W. J., Rullkötter, J., and Sinnighe, D. S. J., 1987. "Restricted utility of the pristane/phytane ratio as a paleoenvironmental indicator", Nature, Vol. 330, pp. 641-642.

ten Haven, L., de Leeuw, W. J., Sinnighe D. S. J., Schenck, A. P., Palmer, E. S., and Zumberge, E. J., 1988. "Application of biological markers in the recognition of paleohypersaline environments", In: Lacustrine Petroleum Source Rocks, Fleet, J. A., Kelts, K., and Talbot, R. M., (eds.). Blackwell Scientific Publications, Oxford, pp. 123-130.

Hills, I. R., and Whitehead, E. V., 1966. "Triterpanes in optically active petroleum distillates", Nature, Vol. 209, pp. 977-979.

Hite, R. J., 1970. "Shelf carbonate sedimentation controlled by salinity in the Paradox basin, southeast Utah", In: Third Symposium On Salt, Northern Ohio Geol Society, vol. 1, pp. 48-66.

Hoering, T. C., 1984. "Thermal reactions of kerogen with added heavy water and pure organic substances", Organic Geochemistry, vol. 5, pp. 267-278.

Horstink, J., 1980. "Oil exploration in southeast Turkey thrust belt", Exp. 22-1, N.V. Turkse Shell, pp. 1-20 (unpublished).

Huang, W., and Meinschein, W. G., 1976. "Sterol as source indicators of organic materials in sediments", Geochimica et Cosmochimica et Cosmochimica Acta, Vol. 40, pp. 323-330.

Hughes, B.W., and Holba, G. A., 1988. "Relationship between crude oil quality and biomarker patterns", Organic Geochemistry, Vol. 13, PP. 15-30.

Hunt, M. J., 1979. Petroleum Geochemistry and Geology, W. H. Freeman and company, San Francisco, 617 p.

Illich, A. H., Havey, R. F., and Mundoza, M., 1981. "Geochemistry of oil from Santa Cruz Basin, Bolivia: Case Study of migration-fractionation", Bulletin of American Association of Petroleum Geologist, Vol. 65, pp. 2388-2402.

Illich, H. A., 1983. "Pristane, phytane and lower molecular weight isoprenoids in oils", Bulletin of American Association of Petroleum Geologist, Vol. 67, pp. 385-395.

İzitan, H., 1987. X. "Bölge Karaboğaz Formasyonu'nun kaynakkaya potansiyeli", TPAO Arş. Merk., Rapor No: 1113 (unpublished).

İzitan, H., 1988. "X. Bölgede Karaboğaz Formasyonundan türeyen petrol miktarının hesaplanması", TPAO Arş. Merk. Rapor No: 1337 (unpublished).

İzitan, H., and Soylu, C., 1991. "Güneydoğu Anadolu bölgesinin organik jeokimyasal değerlendirilmesi, Kaynak kayalar-Cilt I", TPAO Arş. Merk. Rapor No: 1599 (unpublished).

Kent, P. E., and Warman, H. R., 1972. "An environmental review of the world's richest oil-bearing region; The Middle East, Proceedings 24th International Geology Congress, Section 5, pp. 142-152, Montreal.

King, D. J., and Claypool, E.G., 1983. "Biological marker compounds and implications for generation and migration of petroleum in rocks of the Point Conception deep-stratigraphic test well, OCS-Cal 78-164 NO: 1 Offshore California", In: Petroleum Generation and Occurrence in the Miocene Monterey Formation, California. Isaacs et al., (eds), SEPM Pacific Section, pp. 191-200.

Kirkland, W. D., and Evans, R., 1981. "Source-rock potential of evaporitic environment", Bulletin of American Association Petroleum Geologist, Vol. 65, pp. 181-182.

Köylüođlu, M., 1986. "Güneydođu Anadolu otokton birimlerinin kronostratigrafisi, mikrofasiyes ve mikrofosilleri", TPAO Eđitim Yayınları, No: 9, Ankara, 52p.

Kvalheim, M. O., 1985. "Scaling of analytical data", Analytica Chimica Acta, Vol. 177, pp. 71-79.

Kvalheim, M.O., and Telnaes, N., 1986. "Visualizing information in multivariate data: Applications to petroleum geochemistry, Part 2. Interpretation and correlation of North Sea Oils by using three different biomarker fractions", Analytica Acta, Vol. 191, pp. 97-110.

Johns, B. R., 1986. Biological Markers in the Sedimentary Record. Methods in Geochemistry and Geophysics, 24, 364p.

Jones, J.P., and Philp, P.R., 1990. "Oils and source rocks from Pauls Valley, Anadarko Basin, Oklahoma, U.S.A.", Applied Geochemistry, Vol. 5, pp. 429-448.

Jöreskog, K.G., Klowan, J.E., and Reyment, R.A., 1976. Geological Factor Analysis, Elsevier, Amsterdam, 178 p.

Lebküchner, R. F., Orhun, F., and Wolf, M., 1972. "Asphaltic substances in southeast Turkey", Bulletin of American Association of Petroleum Geologist, Vol. 56, pp. 1939-1964.

Leythauser, D., Bjoroy, M., Mackenzie, A. A., Schaefer, R. G., and Altebaumer, F. J., 1983. "Recognition of migration and its effect within two boreholes in shale/sandstone sequence from Svalbard, Norway", In: Advances in Organic Geochemistry, 1981. Bjoroy, M., et al (eds), Wiley, Chichester, pp. 136-146.

Lewan, M.D., 1985. "Evaluation of petroleum generation by hydrous pyrolysis experimentation", Phil. Tran. R.Soc. London, A., Vol. 315, pp. 123-134.

Longman, W. M., and Palmer, E.S., 1987. "Organic geochemistry of Mid-continent Middle and Late Ordovician oils", Bulletin of American Association of Petroleum Geologist, Vol. 71, pp. 938-950.

Mackenzie, A.S., 1984. Applications of biological markers in Petroleum Geochemistry. Brooks, J., and Welte, D. (eds.), Academic Press, London, Vol. 1, pp. 115-214.

Mackenzie, S. A., Rullkötter, J., Welte, D. H., and Mackiewicz, F., 1985. "Reconstruction of oil formation and accumulation in North Slope, Alaska, using quantitative gas chromatography-mass spectrometry", In: Alaska North Slope Oil/Rock Correlation Study. Magoon, B. L., and Claypool, E. G., (eds), AAPG Studies in Geology # 20, pp. 319-379.

Malek-Aslani, M., 1980. "Environmental and diagenetic controls of carbonate and evaporate source rocks", Gulf Coast Association Geological Transaction, Vol. 30, pp. 445-458.

Mattavelli, L., and Novelli, L., 1990. "Geochemistry and habitat of the oils in Italy", Bulletin of American Association of Petroleum Geologist, vol. 74, pp. 1623-169.

McKirdy, D. M., Aldridge, A. K., and Ypma, P. J. M., 1983. "A geochemical comparison of some crude oils from Pre-Ordovician carbonate rocks", In: Advances in Organic Geochemistry. Bjoroy, et al., (eds), Wiley Chichester, pp. 99-107.

Mello, R. M., Garliane, C. P., Brasell, C. S., and Maxwell, R. J., 1988. "Geochemical and biological marker assessment of depositional environments using Brazilian offshore oils", Marine and Petroleum Geology, vol. 5, pp. 205-223.

Moldowan, M.C., Sundaraman, P., Schoell, M., 1986. "Sensitivity of biomarker properties to depositional environment and/or source input in the Lower Toarcian of SW Germany", Organic Geochemistry, Vol. 10, pp.915-926.

Moldowan, M. J., Seifert, K. W., and Gallegos, J. M., 1985. "Relationship between petroleum composition and depositional environment of petroleum source rocks", Bulletin of American Association of Petroleum Geologist, Vol. 69, No. 8, pp. 1255-1268.

Nwachukwu, O. S., 1976, "Approximate geothermal gradients in Niger Delta Sedimentary Basin", Bulletin of American Association of Petroleum Geologist, Vol. 60 pp. 1073-1077

Ourisson, G., Albrecht, P., and Rohmer, M., 1979. "Paleochemistry and biochemistry of a group of natural product: the hopanoids", Pure and Applied Chemistry, Vol. 51, pp. 709-729.

Ourisson, G., Albrecht, P., Rohmer, M., 1984. "The microbial origin of fossil fuels", Scientific American, Vol. 251, pp. 44-51.

Oro, J., Torhabene, T. G., Nooner, D. W., and Gelpi, E., 1967. "Aliphatic hydrocarbons and fatty acids of some marine and freshwater organisms", Journal of Bacteriology, Vol. 93, pp. 1811-1817.

Orr, W. L., 1974. "Changes in sulfur content and isotopic ratios of sulfur during petroleum maturation study of Big Horn Basin Paleozoic oils", Bulletin of American Association of Petroleum Geologist, Vol. 58, pp. 2295-2318.

Orr, W. L., 1978. "Sulfur in heavy oils, oil shales", In: Oil Sand and Oil Shale Chemistry. Strauss, D., and Lowan, E., (eds.), Verlag Chemie Int., pp. 223-243.

Orr, W. L., 1986. "Kerogen/asphaltene/sulfur relationships in sulfur-rich Monterey oils", In: Advances in Organic Geochemistry, 1985. Leythausen, D., and Rullkötter, S., (eds), vol. 10, pp. 499-516.

Palacas, G. P., Anders, D. E., and King, J. D., 1984. "South Florida Basin- A prime-example of carbonate source rocks of petroleum", In: Petroleum Geochemistry and Source Rock Potential of Carbonate Rocks, I.G. Palacas (ed.). AAPG Studies in Geology 18, pp. 71-96.

Palacas, G. P., 1984. "Carbonate rocks as sources of petroleum: Geological and chemical characteristics and oil source rock correlations", 11th World Petroleum Congress Proceedings (1983), Vol. 2, pp. 31-42.

Patterson, G. W., 1971. "The distribution of sterols in algal lipids", Nature, Vol. 4, pp. 120-127.

Perinçek, D., 1991. "Hakkari ili ve dolayının stratigrafisi, Güneydoğu Anadolu, Türkiye", Türkiye Petrol Jeologları Derneği Bülteni, cilt. 2, sayfa. 21-68.

Peters, E. K., Moldowan, M. J., Driscalle, R. A., and Demaison, J. M., 1989. "Origin of Beatrice oil by co-sourcing from Devonian and Middle Jurassic source rocks, Inner Moray Firth, United Kingdom", Bulletin of American Association of Petroleum Geologist, vol. 73, pp. 454-471.

Philippi, G. T., 1977. "On the depth, time, and mechanism of origin of the heavy to medium gravity naphenic crude oils", Geochimica et Cosmochimica Acta, vol. 41, pp. 33-52.

Philp, P. R., 1985. Fossil Fuel Biomarkers-Applications and Spectra. Methods in Geochemistry and Geophysics, Vol. 23, 294 p.

Philp, P. R., and Gilbert, T. D., 1985. "Biomarker distribution in Australian oils predominantly derived from terrigenous source material", In: Advances in Organic Geochemistry, Leythausen, D., and Rullkötter, J., (eds.), Oxford, Pergamon, pp. 73-84.

Philp, P. R., and Zhaoan, F., 1987. "Geochemical investigation of oil and source rocks from Qianjiang depression of Jiangnan Basin, terrigenous saline basin, China", Organic Geochemistry, vol. 11, pp. 549-562.

Powell, T. G., and McKirdy, D. M., 1973. "Relationship between ratio of pristane to phytane, crude oil composition and geological environment in Australia", Nature, Vol. 243, pp. 37-39.

Powell, T.G., Cook, P.J., and McKirdy, D.M., 1975. "Organic geochemistry of phosphorites: Relevance to Petroleum genesis", Bulletin of Association of American Petroleum Geologist, Vol. 69, pp. 619-632.

Qygaard, K., Grahl-Nielsen, O., and Ulvoen, S., 1984. "Oil/oil correlation by aid of chemometrics", Organic Geochemistry, vol. 6, pp. 561-567.

Reed, W.E., 1977. "Molecular compositions of weathered petroleum and comparison with its possible source", Geochimica et Cosmochimica Acta, Vol. 41, pp. 237-247.

Rigo de Righi, M., and Cortesini, A., 1964. "Gravity tectonics in foothills structure belt of Southeast Turkey", Bulletin of Association of American Petroleum Geologist, Vol. 48, No. 12, pp. 1011-1032.

Robertson Research Co., 1984. "The petroleum geochemistry of source rocks and oils in Southeast Anatolia, Turkey", TPAO Ars. Merk. Report, Vol. 1, 100 p.

Rohrback, B. G., 1983. "Crude oil geochemistry of the Gulf of Suez", In: Bjoroy, M., et al., (eds). Advances in Organic Geochemistry, John Wiley and Sons. Ltd., pp. 39-48.

Rubinstein, I., Sieskind, O., and Albrecht, P., 1975. "Rearranged sterenes in a shale: occurrence and simulated formation", Journal of Chemical Society Perkin, vol. 1, pp. 1833-1843.

Rullkötter, J., and Wendisch, D., 1982. "Microbial alteration of 17(H) Hopanes in Madagascar asphalts: removal of C-10 methyl group and ring opening", Geochimica et Cosmochimica Acta, Vol. 46, pp. 1545-1553.

Rullkötter, J., Meyers, A. P., Schaefer, R., and Dunham, K., 1985. "Oil generation in the Michigan Basin: A biological marker and carbon isotope approach", In: Advances in Organic Geochemistry, Eds Leythauser and Rullkötter, J., Vol. 10 pp. 359-375.

Rullkötter, J., and Marzi, R., 1988. "Natural and artificial maturation of biological markers in a Toarcian Shale from Northern Germany", In: Advances in Organic Geochemistry, Mattavelli, L., and Novelli, L.,(eds.), Pergoman Press, Oxford, pp. 639-645.

Sajgo, C., 1984. "Organic geochemistry of crude oils from Southeast Hungary", Organic Geochemistry, Vol. 6, pp. 569-578.

Salem, R., 1984. "Geology and hydrocarbon evaluation of the Cudi Group sequence (Triassic-Jurassic) in Southeast Turkey", TPAO Ars. Merk. Report No. 1968.

Sammy, N., 1985. "Biological systems in northwestern Australian solar salt and fields", Proc. 6 th International Symp. on Salt: Salt Institute, Alexandria, Va., Vol.1, pp. 207-215.

Savcı, H., 1983. "Geochemical characterization of oil types and the Germav formation, southeastern Turkey", Ms Thesis, University of Tulsa, 146p.

Seifert, W. K., and Moldowan, J. M., 1978. "Applications of steranes, terpanes and monoaromatics to the maturation, migration and source of crude oils", Geochimica et Cosmochimica Acta, Vol. 42, pp. 77-95.

Seifert, W. K., and Moldowan, J. M., 1979. "The effect of biodegradation on steranes and terpanes in crude oils", Geochimica et Cosmochimica Acta, Vol. 45, pp. 783-794.

Seifert, W. K., and Moldowan, J. M., 1981. "Paleoreconstruction by biological markers", Geochimica et Cosmochimica Acta, Vol. 45, pp. 783-794.

Sieskind, O., Joly, G., and Albrecht, P., 1979. "Simulation of the geochemical transformation of sterols: superacid effect of clay minerals", Geochimica et Cosmochimica Acta, Vol. 43, pp. 1675-1679.

Silverman, S. R., 1965. "Migration and segregation of oil and gas", In: Fluids in Sub-surface Environment. Young, A., and Galley, E.J., (eds), AAPG Memoir 4, Tulsa, pp. 52-65.

Simoneit, B. R. T., Holpern, H. I., and Didyk, M. B., 1980. "Lipid productivity of a high Andean Lake", In: Biochemistry of ancient and modern environments, Canberra, Trudniger, A.P., Walter, R.M., and Ralph, J.B., (eds.). Australian Academy of Sciences pp. 201-210.

Sofer, Z., 1984. "Stable carbon isotope composition of crude oils: Application to source depositional environments and petroleum alteration", Bulletin of American Association of Petroleum Geologist, Vol. 68, pp. 31-49.

Sofer, Z., Leenheer, J. M., Palmer, E. S., and Zumberge, E. J., 1985. "Geochemical correlation of oils and source rocks, North slope of Alaska: USGS Interlaboratory Comparison Study", In: Alaska North slope oil/rock correlation study, Magoon, B.L., and Claypool, E.G., (eds.), AAPG Studies in Geology # 20, pp. 185-201.

Sonnenfeld, P., 1985. "Evaporites as oil and gas source rocks", Jour. of Petroleum Geology, Vol. 8, No. 3, pp. 253-271.

Soylu, C., 1991. "Oil source rocks in the Adıyaman area, southeast Turkey", Journal of Southeast Asian Earth Sciences, vol. 5, pp. 429-439.

Stahl, W. J., 1978. "Source rock-crude oil correlation by isotope-type-curves", Geochimica et Cosmochimica Acta, vol. 42, pp. 1573-1577.

Sungurlu, O., 1974. VI. "Bölge kuzey sahalarının jeolojisi", Türkiye 2. Petrol Kongresi, pp. 85-107.

Tappan, H., and Loeblich, A., 1973. "Evolution of the oceanic plankton", Earth Science Review, Vol. 9, pp. 207-240.

Telnaes, N., and Dahl, B., 1985. "Oil-oil correlation using multivariate techniques", Organic Geochemistry, Vol. 10, pp. 425-432.

Temple, P. G., and Perry, J. L., 1962. "Geology and oil occurrence, southeast Turkey", Bulletin of American Association of Petroleum Geologist, vol. 46, pp. 1596-1612.

Tissot, B., and Welte, D., 1984. Petroleum Formation and occurrence. Second edition, Springer-Verlang, 699 p.

Talukdar, S., Gallango, O., and Lien, A. C., 1986.

"Generation and migration of hydrocarbons in the Maracaibo Basin, Venezuela; An integrated basin study", In: Advances in Organic Geochemistry, In: Leythausser, D., and Rullkötter, J., (eds.), Pergamon, pp. 261-280.

Trebs, A., 1936. "Chlorophyll-und haminderivate in organischen mineralsstoffen", Annual Chemistry., vol. 49, pp. 682-686.

Volkman, J. K., 1986. "A Review of sterol markers for marine and terrigenous organic matter", Organic Geochemistry, Vol. 9, pp. 83-99.

Volkman, J. K., 1988. "Biological marker compounds as indicators of the depositional environments of petroleum source rocks", In: Lacustrine Petroleum Source Rocks. Kelts, K., and Talbot, M. R., (eds). Geological Society Special Publication, No: 40, pp. 103-122.

Williams, J. A., and Winters, J. C., 1969. "Microbial alteration of crude oil in the reservoir", In: Symp. Pet. Transformations in Geology, Env. Am. Chem. Soc. Nat. Meeting, Preprints, vol. 14, pp. 22-31ç

Wagner, C. W., Soylu, C., and Pehlivan, M., 1986. "Oil habitat of the Adıyaman area, southeast Turkey: a joint geological- geochemical study", TPAO Arş. Merk. Report No: 2139 (unpublished).

Waples, W. D., 1981. Organic Geochemistry for Exploration Geologists. Burgess Publishing Company, 151 p.

Waples, W. D., and Machihara, T., 1990. "Application of sterane and triterpane biomarkers in petroleum exploration", Bulletin of Canadian Petroleum Geology, Vol. 38, pp. 337-380.

Warren, K. J., 1986. "Shallow water evaporitic environments and their source rock potential", Journal of Sedimentary Petrology, Vol. 56, pp. 442-554.

Wingert, S. W., and Pomerantz, M., 1986. "Structure and significance of some twenty-one and twenty-two carbon petroleum steranes", Geochimica et Cosmochimica Acta, Vol. 50, pp. 2763-2769.

Zhusheng, J., Philp, R. P., and Lewis, A. C., 1988. "Fractionation of biological markers in crude oils during migration and effects on correlation and maturation parameters", In: Advances in Organic Geochemistry, Vol. 13, pp. 561-571.

Zumberge, J. E., 1983. "Tricyclic diterpane distributions in the correlation of Paleozoic oils from the Williston Basin", In: Advances in Organic Geochemistry, Bjoroy, M. et al.(eds.), pp. 738-745.

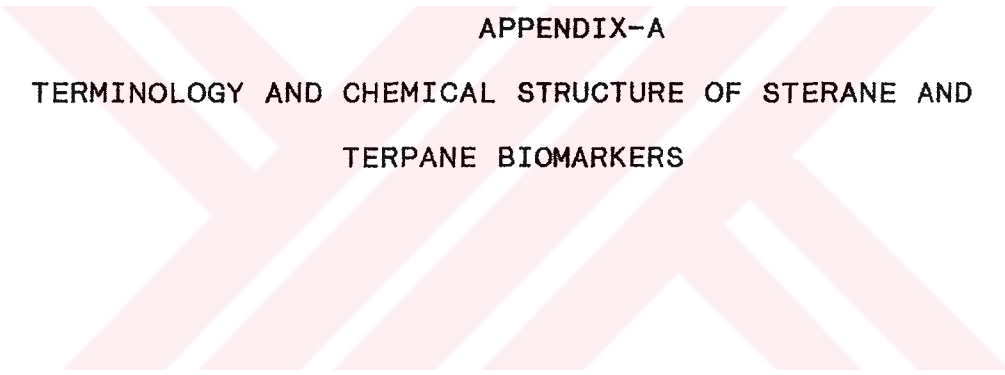
Zumberge, J. E., Palmer, S. E., and Schiefebein, C., 1984. "Kinetics of sterane and hopane epimerization: Laboratory simulation by hydrous pyrolysis", Geol. Soc. Amer. Abstr., Reno, Nevada.

Zumberge, J. E., 1987. "Prediction of source rock characteristics based on terpane biomarkers in crude oils: A multivariate statistical approach", Geochimica et Cosmochimica Acta, Vol. 51, pp. 1625-1637.





APPENDICES



APPENDIX-A
TERMINOLOGY AND CHEMICAL STRUCTURE OF STERANE AND
TERPANE BIOMARKERS

APPENDIX A
TERMINOLOGY AND CHEMICAL STRUCTURE OF VARIOUS
STERANES AND TERPANE BIOMARKERS

The precise number of carbon atoms in a given cyclic biomarker varies considerably as a result of differences in source material, effects of diagenesis, thermal maturity, and biodegradation. Names like "terpane" tell us only that there are approximately $3 \times 10 = 30$ carbon atoms in the compound. The ring structures themselves seldom account for the carbon atoms. For example, a four-ring sterane contains only 17 carbon atoms in the ring structure; the remaining dozen or so carbons are attached to the ring structure in various groups or side chains. Each carbon atom in a sterane or terpane molecule is numbered for easy reference (Figure 1.5).

The numbering system indicates the location of side chains. For example, the two terpanes III and V differ by only methyl groups at C₂₂, C₂₉, and C₃₀. In compound III, the methyl groups have been replaced by hydrogen atoms. Compound V is a member of a class of compounds called "hopanes", and itself is called the "C₃₀ hopane" or often simply "hopane". In one naming system compound III can be referred to as the 22,29,30-trisnorhopane, where the prefix "nor" means that

one methyl group is missing, and "22,29,30" indicate which methyl groups are absent.

The numbering system also indicates where stereochemical changes occur. "Stereochemistry" refers to the spatial relationship of atoms in a molecule. The ring system of cyclic biomarkers are often reasonably flat, resembling perhaps a piece of corrugated sheet metal. Wherever two rings are joined, each of the joining atoms is attached to three other carbon atoms in the ring structure. Its fourth bond usually to a hydrogen atom or to the carbon of methyl (CH₃-group) can point either up or down with respect to the plane of the rings. Substituents that point down are called "alpha" (α); those that point up are called "beta" (β).

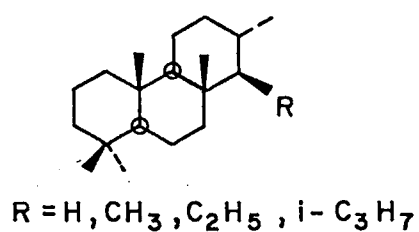
There are two systems for indicating alpha -beta stereochemistry. In one system, which can be used for any group attached to the ring system, we indicate an upward direction (toward the viewer) by drawing the bond as a wedge. If the group points down, the bond is drawn as a dashed or dotted line. The other system is only used to indicate the stereochemistry of hydrogen atoms. A hydrogen atom in the alpha position (pointing down) is shown by an open circle at the point of attachment, whereas a hydrogen in the beta position (pointing up) is represented by a solid circle. The two systems are often mixed.

Other aspects of stereochemistry can also be important. If four different substituents are attached to

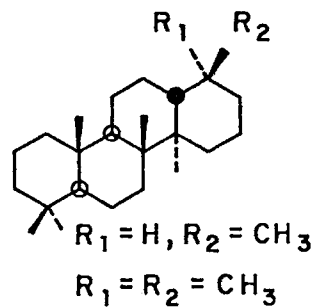
a particular carbon atom (for example, C₂₂ in the terpane molecule and C₂₀ in the sterane molecule in Figure 1.5), that atom is called "asymmetric" carbon atom. The configuration at any asymmetric centre outside the ring structure to as "R" or "S". The most important configurational differences in R and S epimers are those occurring in the side chain at C₂₀ (20R and 20S) in steranes and C₂₂ (22R and 22S) in terpanes containing more than thirty carbon atoms.



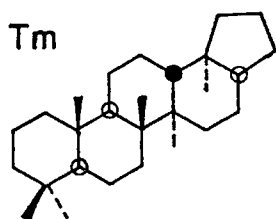
I
PEAKS; $\alpha \dots k 2$
TRICYCLIC TERPANES



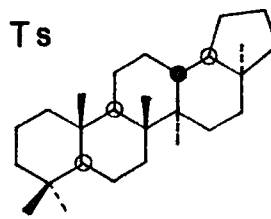
II
PEAK; TC*
TETRACYCLIC TERPANES

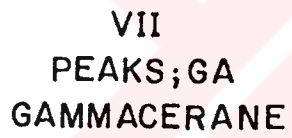
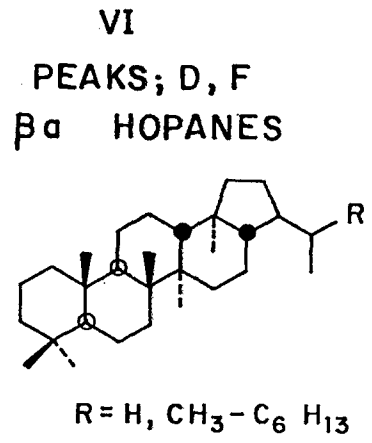
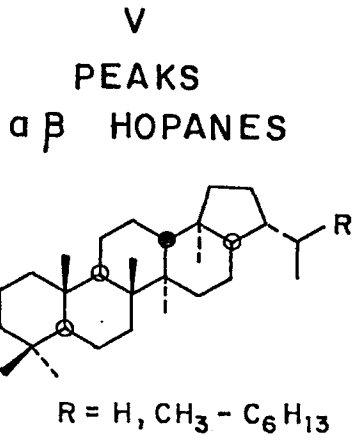


III
PEAK; B
17 α (H), 22, 29, 30
TRISNORHOPANE

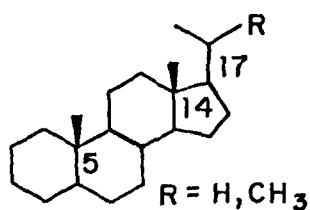


IV
PEAK; A
18 α (H), 22, 29, 30
TRISNORNEOHOPANE

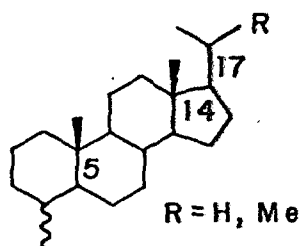




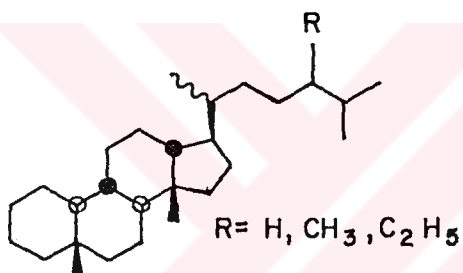
IX
PEAKS; 2, 3, 5
PREGNANES AND
HOMOPREGNANES



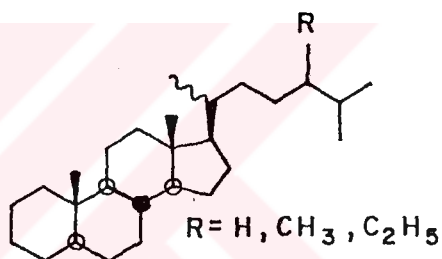
X
PEAKS; 4
METHYLPREGNANES



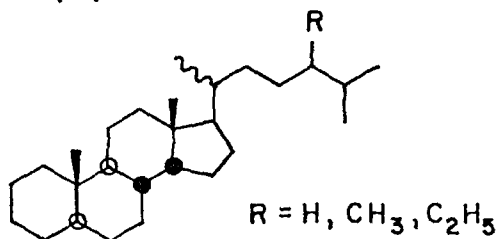
XI
PEAKS; 1, 2
DIASTERANES



XII
PEAKS; 8, 11, 15, 18, 19, 22
α α α STERANES



XIII
PEAKS; 9, 10, 16, 17, 20, 21
α β β STERANES



APPENDIX-B

MULTIVARIATE STATISTICAL ANALYSIS

APPENDIX B
MULTIVARIATE DATA ANALYSIS

Among the several statistical techniques, principal component analysis (PCA), also known as factor analysis, is now a well-established tool for the interpretation of a multivariate large data sets. The method is well documented with numerous geological and geochemical texts (Davis, 1973; Joreskog, 1976). Application of PCA to petroleum geochemistry, in particular, to oil to oil correlations is also widely used (Qygaard et al., 1984; Telnaes and Dahl, 1985; Kvalheim and Telnaes, 1986; Zumberge, 1987; Engel et al., 1988; Gurgey, 1989). Hence, the following is a brief description of the steps necessary to understand interpretation of PCA results in the present study.

PCA method and computer program of Davis (1973) implemented to WAX 11/780 system was applied to the sets subsequent to the data standardization (i.e., the mean is subtracted from each corresponding value of variable and divided by the standard deviation). The new variables will then have a mean of zero and variance of one. The procedure is very useful when the variables are expressed in different units of measurements (e.g., % sulfur content, pristane/phytane ratio).

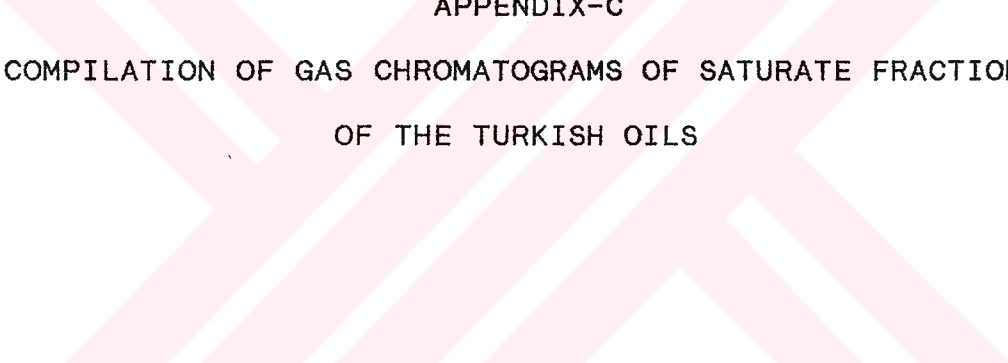
The major step in PCA is the extraction of the eigenvectors from the correlation matrix to get uncorrelated new variables called "principal components" (PCs) or "factors". Since the PCs are linear combinations of all the original variables, they can be viewed as composite average variables, located in the directions explaining most of the variation in the data set. If the original variables are highly correlated the first few PCs explain most of the total variance.

Score Plot: As discussed in Chapter 4, one of the nice features of PCA is that nearly every result can be represented graphically. The scores along the PCs reveal the relationships among the samples (R-Mode factor analysis) this information is displayed in a score plot where similar samples group together in clusters.

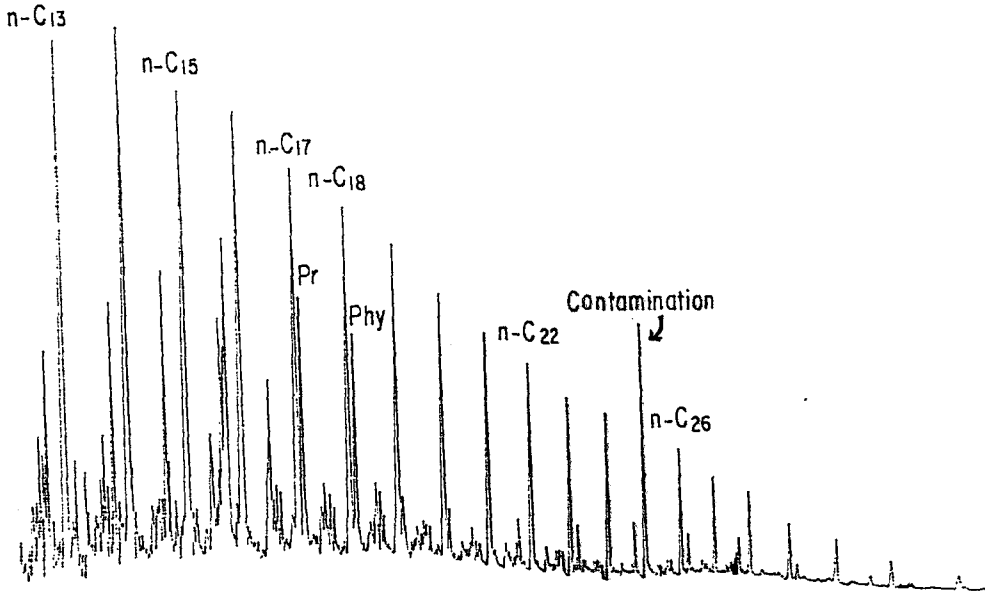
Loading Plot: Interpretation of a single PC and the features of a PC model is possible through the connection to the original variables. A loading plot displays both the importance of each variable to the interpretation of a PC and the relationship among variables in that PC (Q-Mode factor analysis). First, a variable's contribution to a PC is directly proportional to the squared loading. Thus, the distance of a variable to the origin along a PC is a quantitative measure of the importance of that variable in the PC. A variable near the origin carries little or no information in the PC, while a large distance from the origin (e.g. high loading) means that the variable is important in the interpretation of

the PC. Second, the mutual location of the variables reflects the coherences among them. Variables grouped together hold the same information in the PC. Also variables located on the same side of the origin are positively correlated, while variables located on opposite sides are negatively correlated. The larger the separation of two negatively correlated variable, the stronger is the negative correlated.

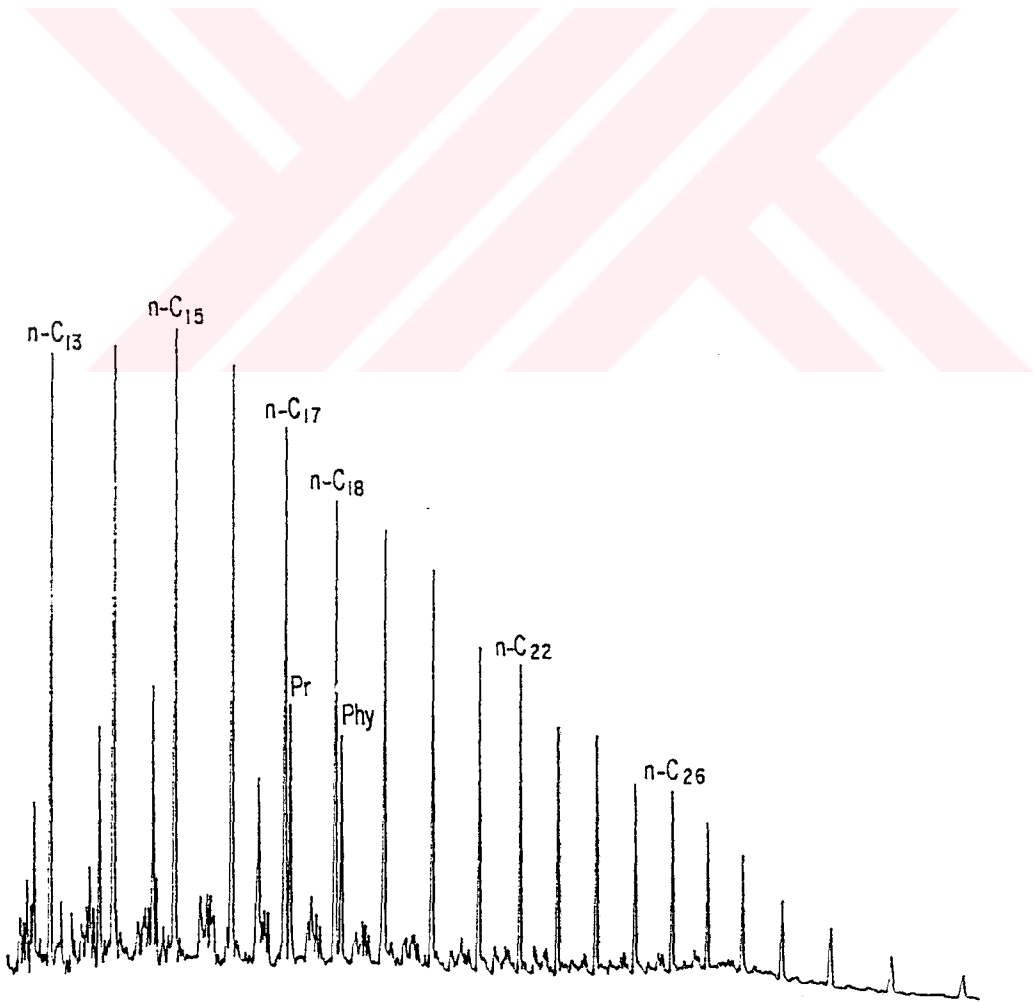




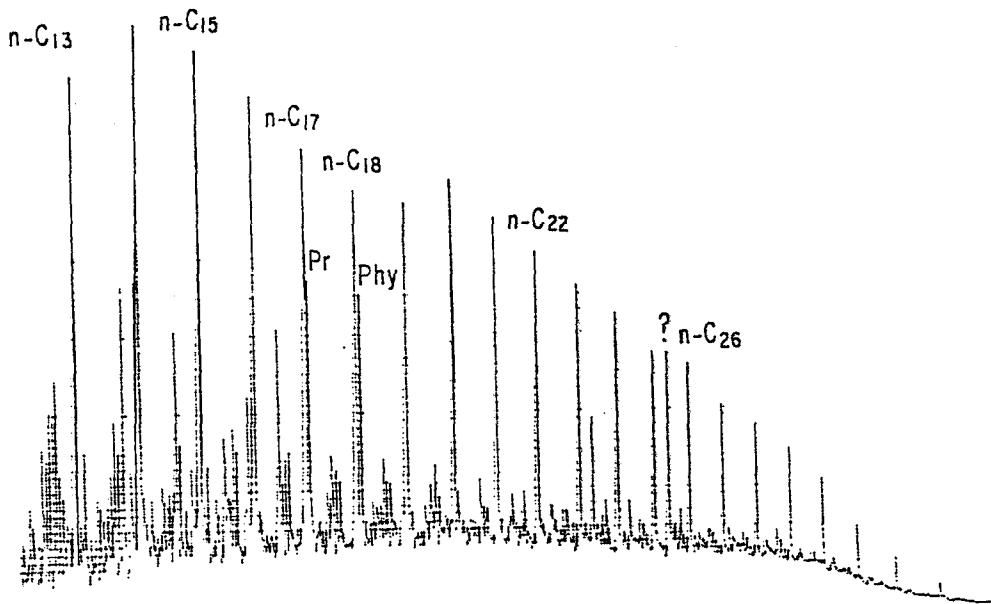
APPENDIX-C
COMPILATION OF GAS CHROMATOGRAMS OF SATURATE FRACTION
OF THE TURKISH OILS



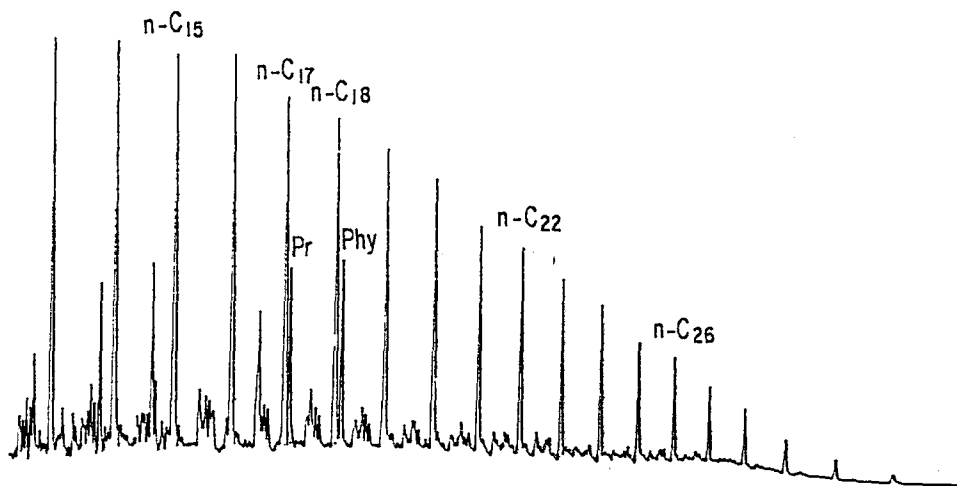
Figure_C.1 Gas chromatogram of the saturate fraction of Çelikli_18 (CE18) oil.



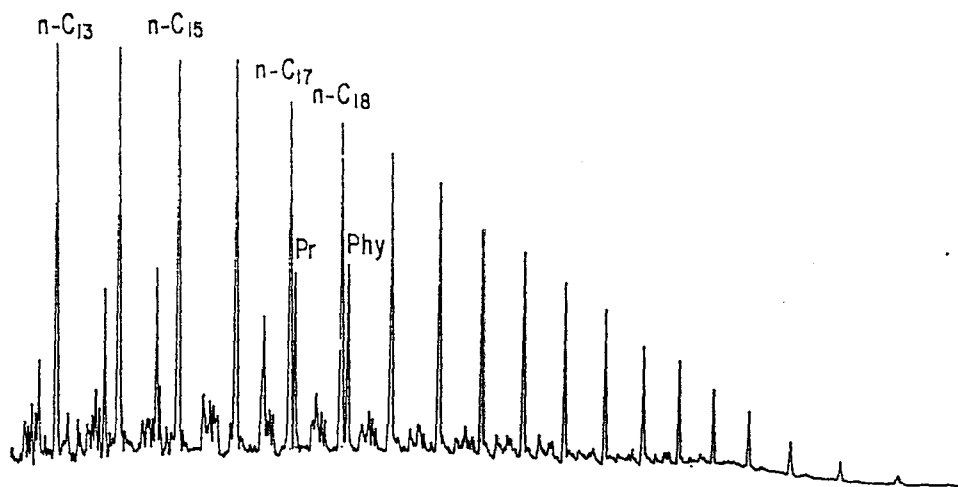
Figure_C.2 Gas chromatogram of the saturate fraction of Çelikli_16 (CE16) oil.



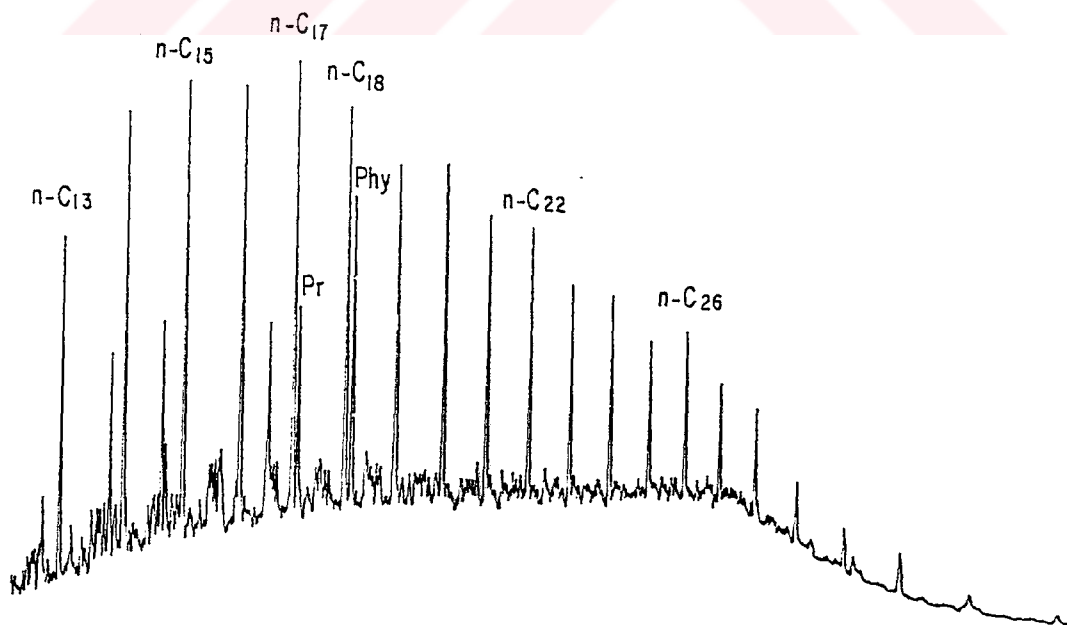
Figure_C.3 Gas chromatogram of the saturate fraction of Şelmo_5 (S5) oil.



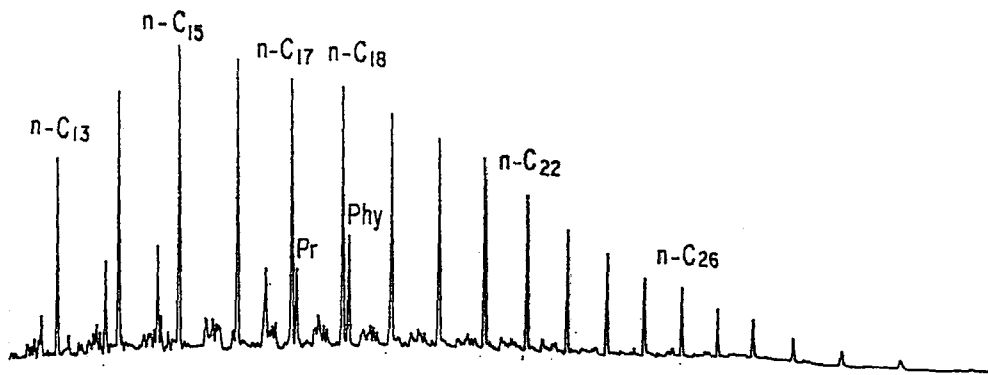
Figure_C.4 Gas chromatogram of the saturate fraction of Batı Şelmo_4 (BS4) oil.



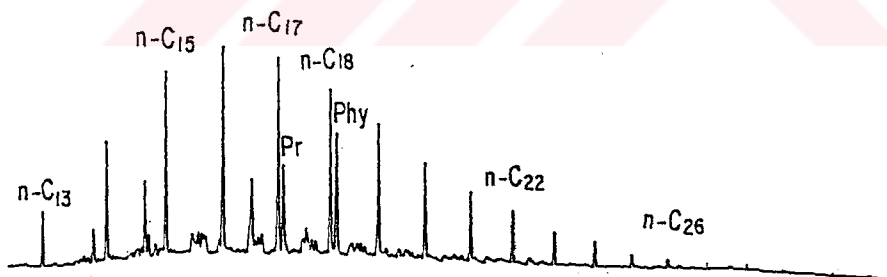
Figure_C.5 Gas chromatogram of the saturate fraction of Batı Şelmo_103 (BS103) oil.



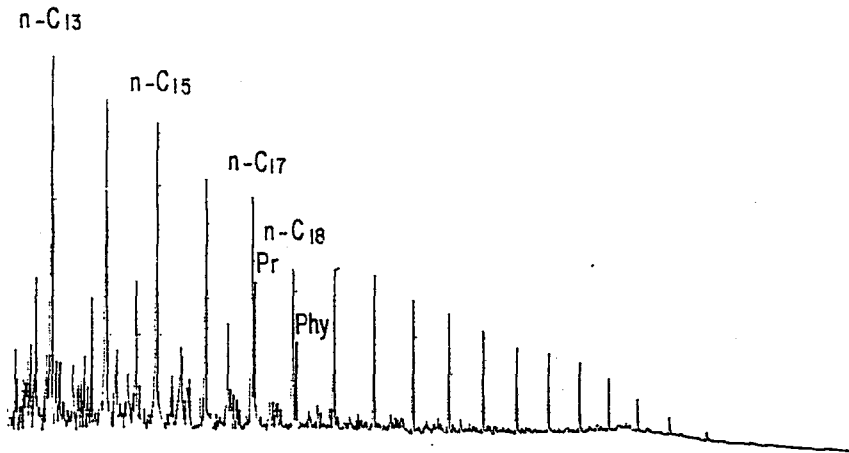
Figure_C.6 Gas chromatogram of the saturate fraction of Sinan_13 (S113) oil.



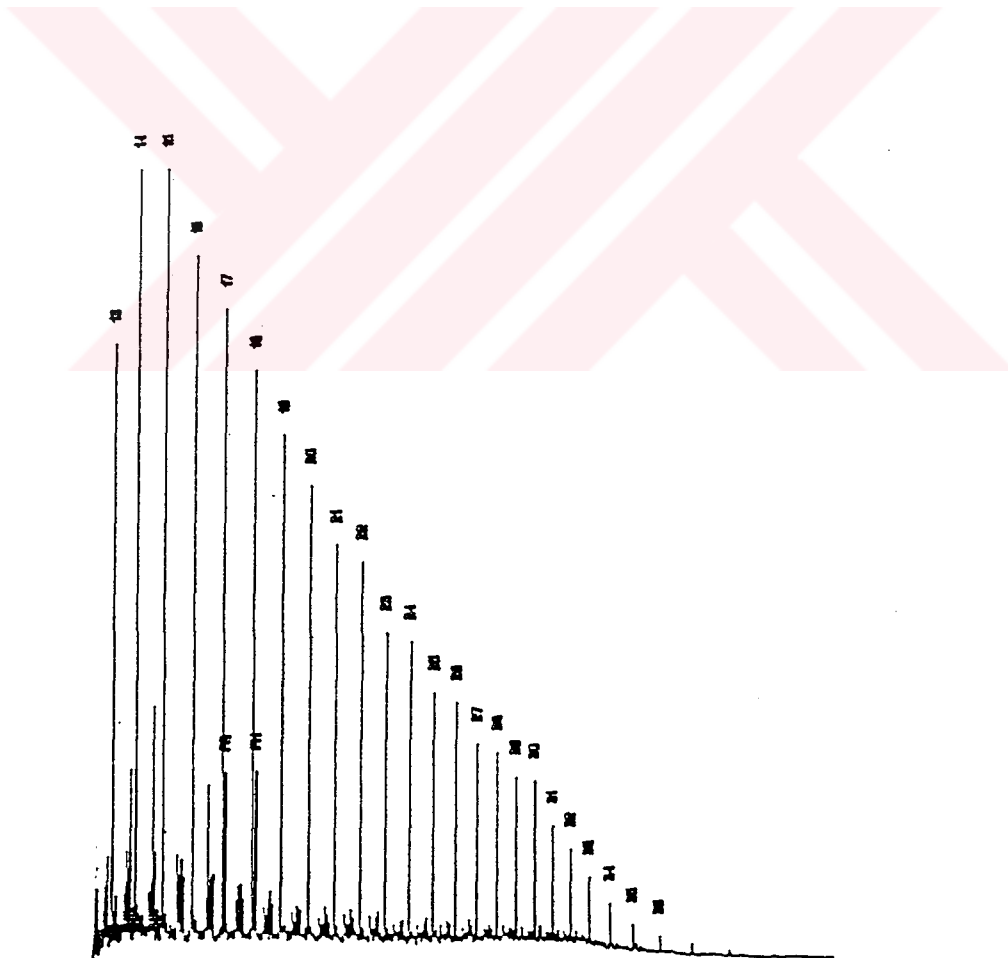
Figure_C.7 Gas chromatogram of the saturate fraction of Silivanka_30(S30)oil.



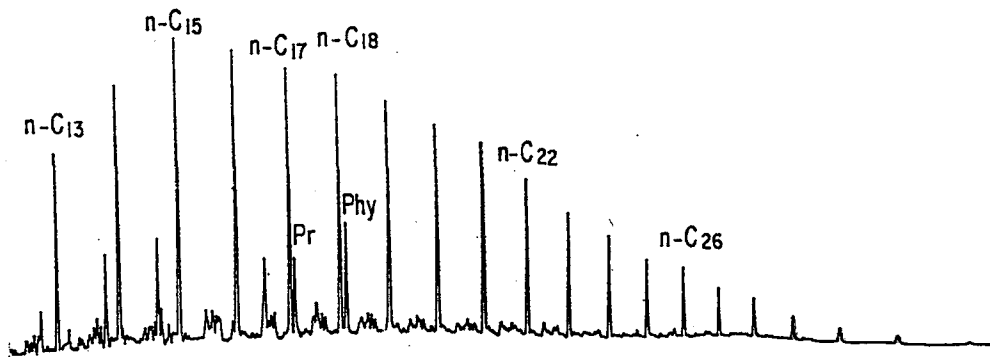
Figure_C.8 Gas chromatogram of the saturate fraction of Sinan_1(SII)oil.



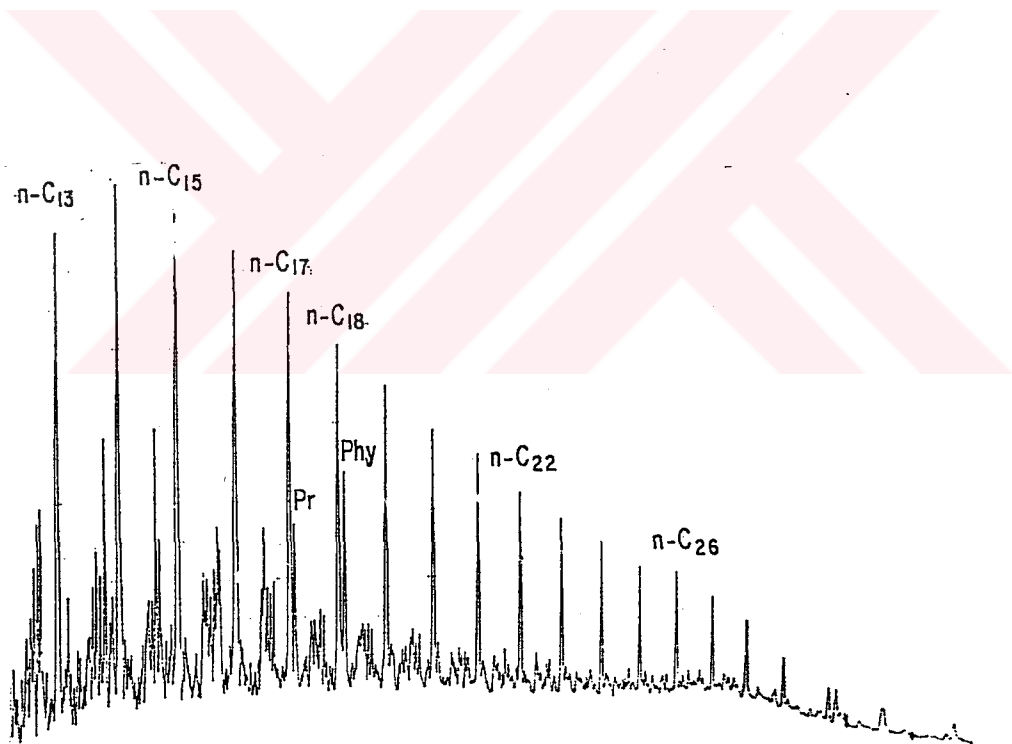
Figure_C.9 Gas chromatogram of the saturate fraction of Kastel 2 (KA2) oil.



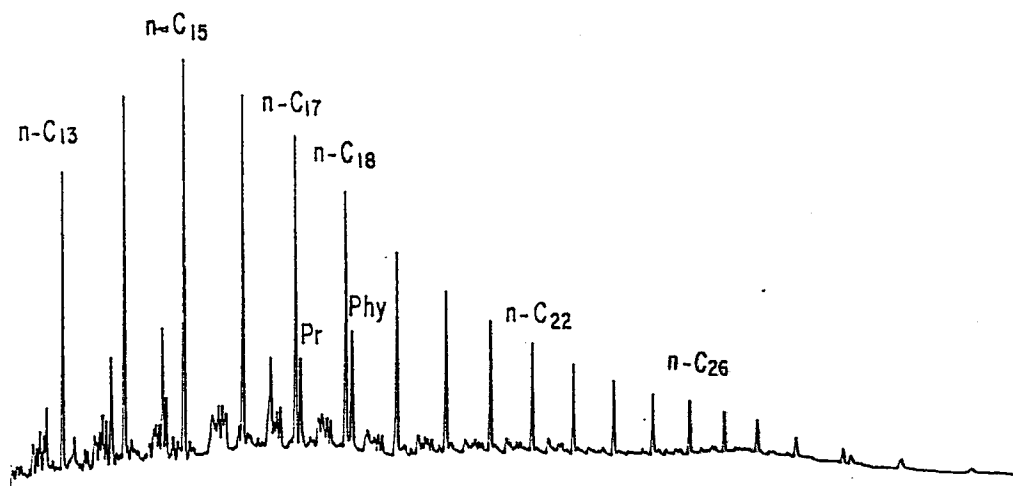
Figure_C.10 Gas chromatogram of the saturate fraction of Kurtalan_1 (KU1) oil.



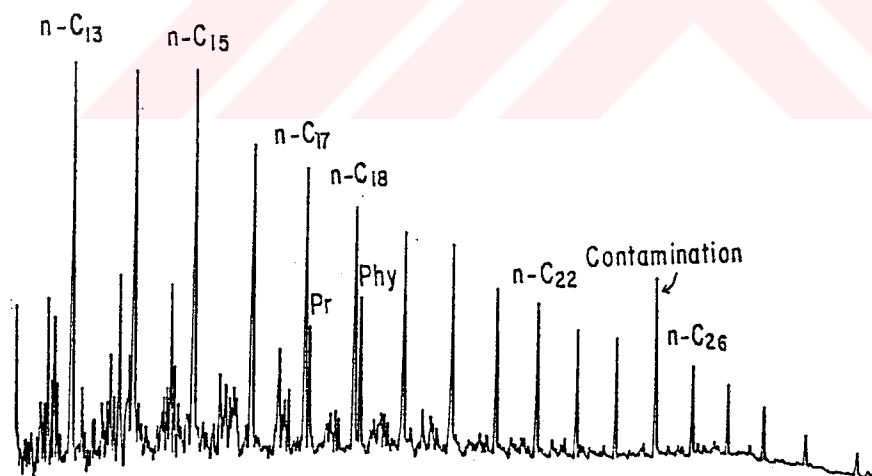
Figure_C.11 Gas chromatogram of the saturate fraction of Beyçayırı_1 (BE1) oil.



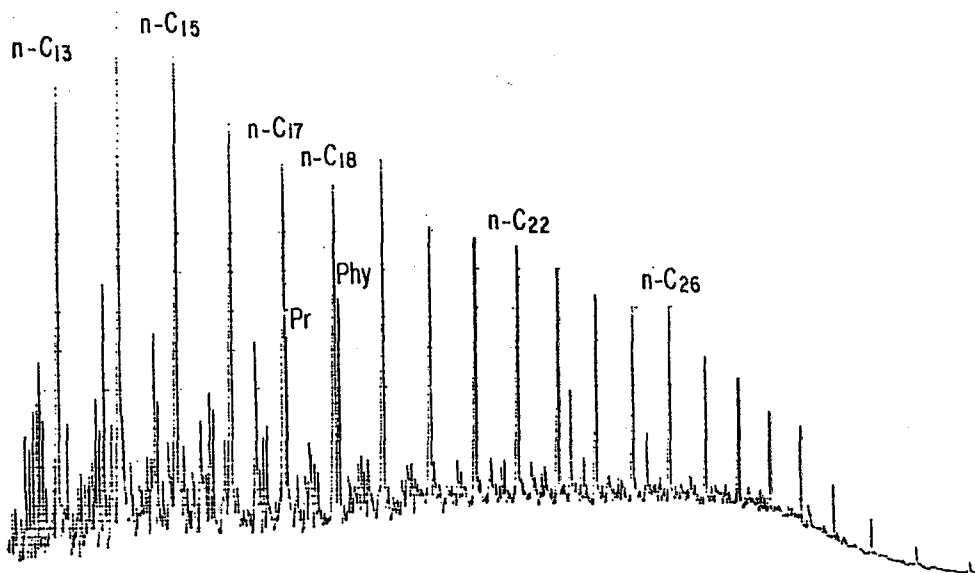
Figure_C.12 Gas chromatogram of the saturate fraction of Magrip_53 (MA53) oil.



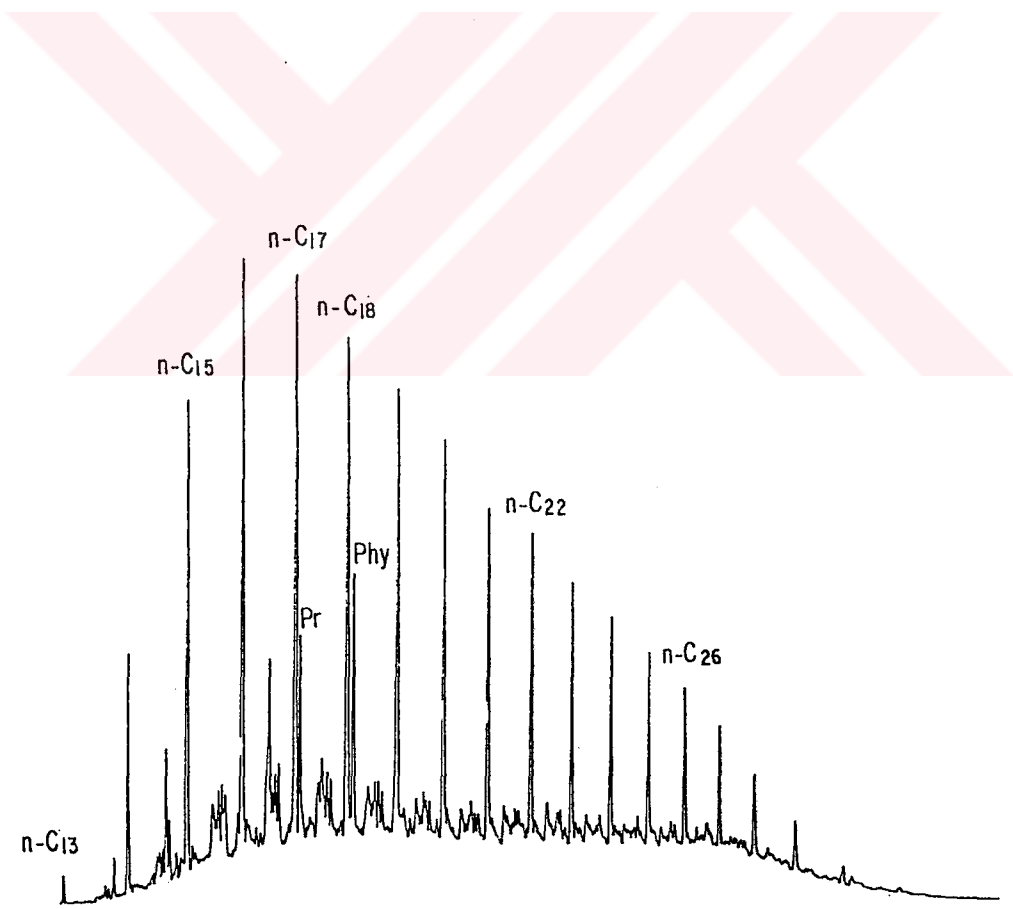
Figure_C.13 Gas chromatogram of the saturate fraction of Magrip_30 (MA30) oil.



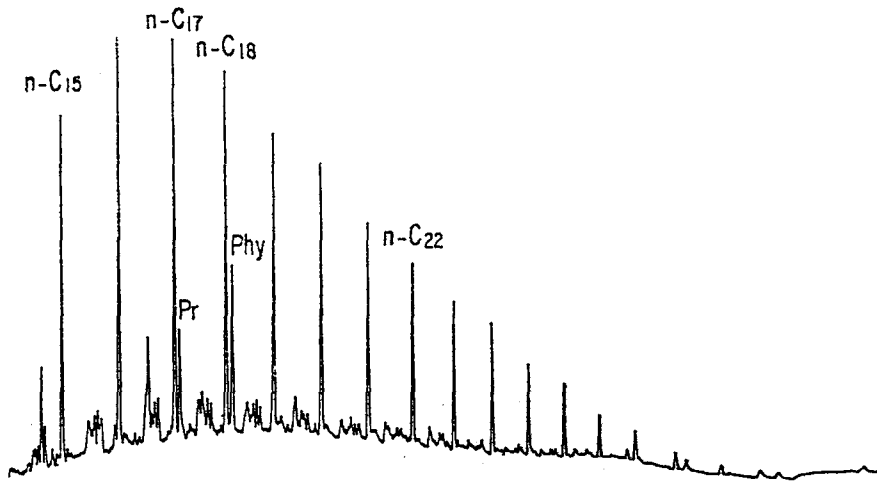
Figure_C.14 Gas chromatogram of the saturate fraction of Garzan_17 (GA17) oil.



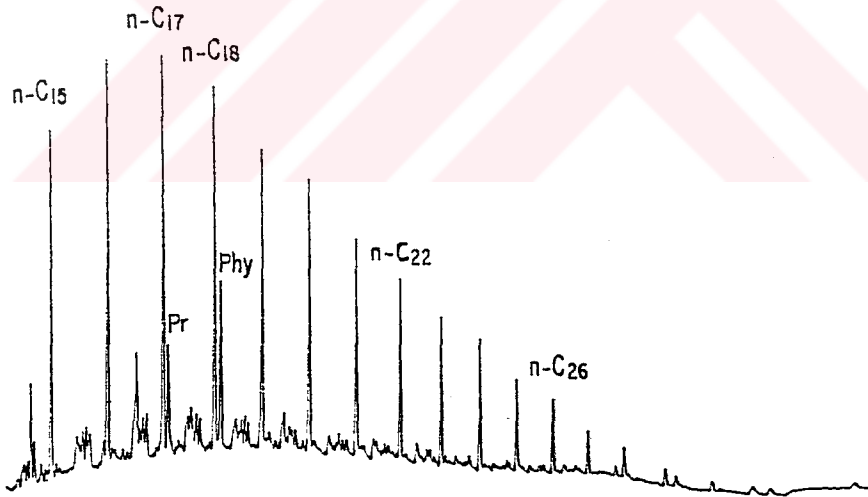
Figure_C.15 Gas chromatogram of the saturate fraction of Garzan_90 (GA90) oil.



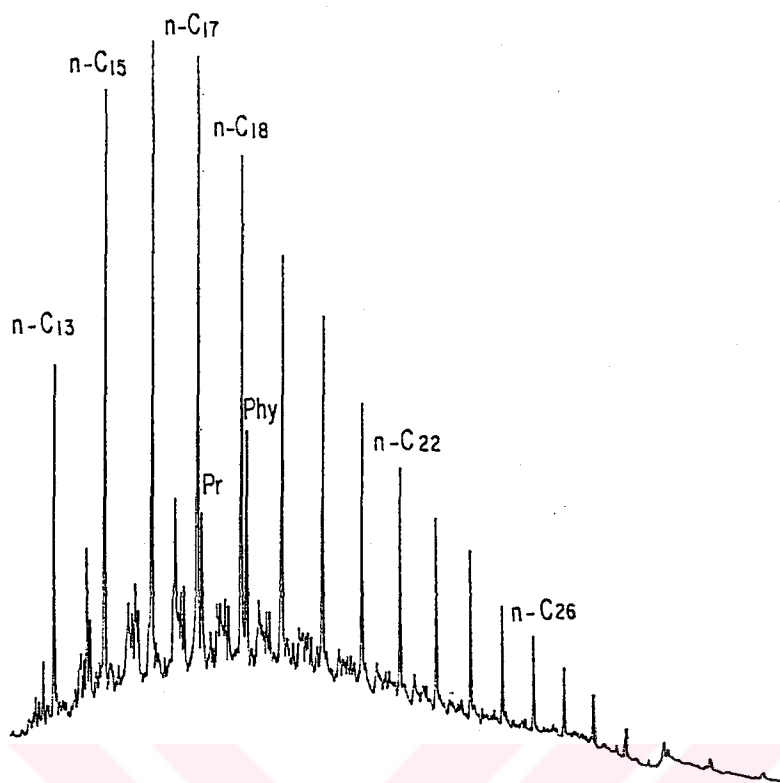
Figure_C.16 Gas chromatogram of the saturate fraction of Garzan_15 (GA15) oil.



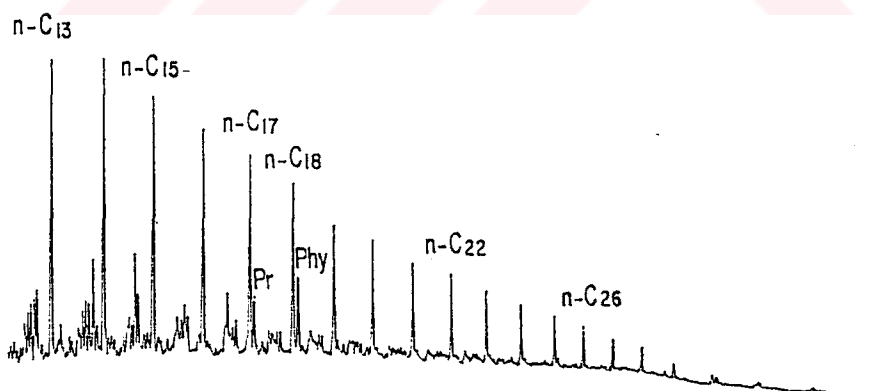
Figure_C.17 Gas chromatogram of the saturate fraction of Germik_12 (GE12) oil.



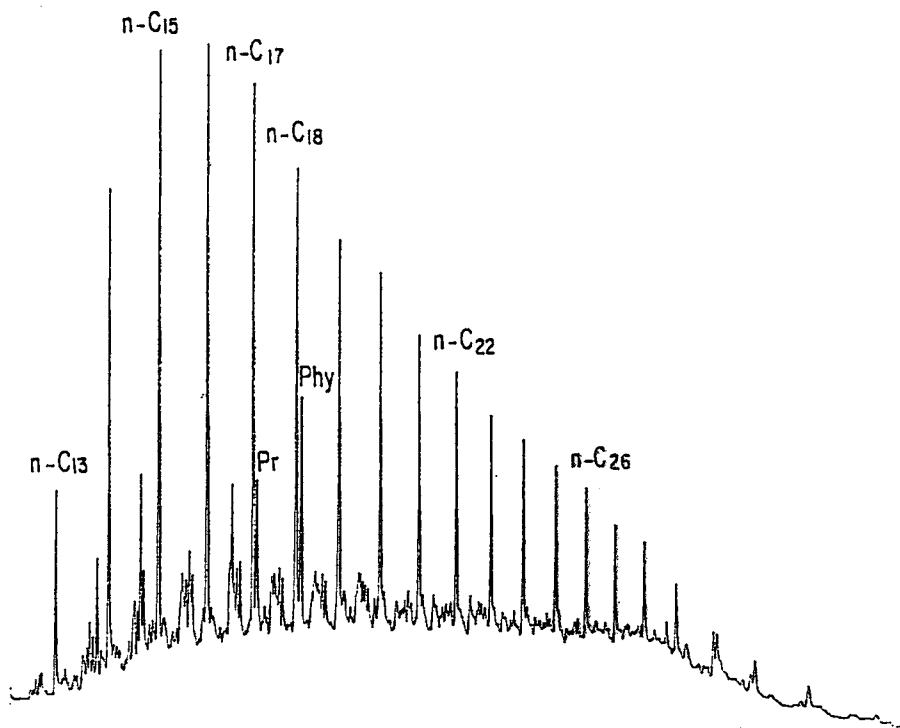
Figure_C.18 Gas chromatogram of the saturate fraction of Germik_5 (GE5) oil.



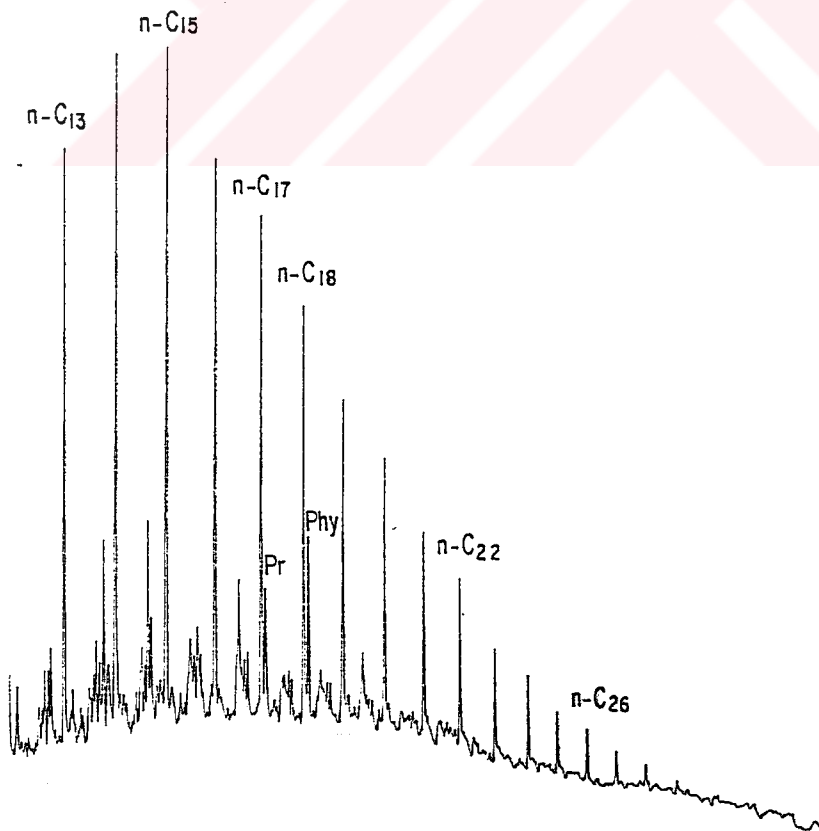
Figure_C.19 Gas chromatogram of the saturate fraction of Raman_87 (R87) oil.



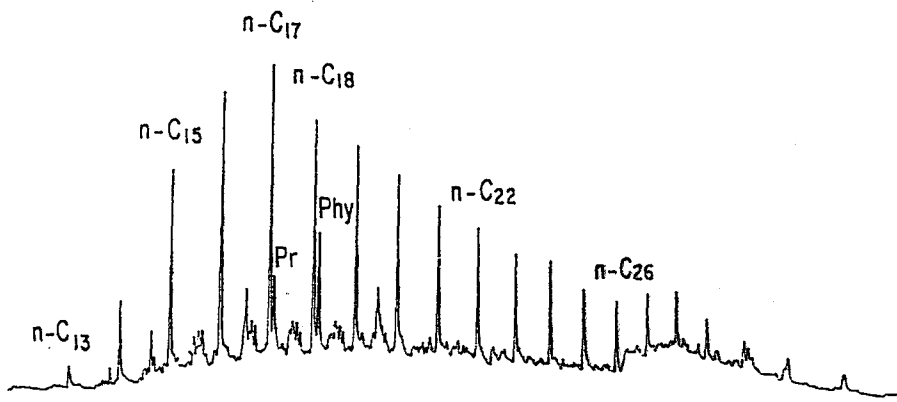
Figure_C.20 Gas chromatogram of the saturate fraction of Raman_192 (R192) oil.



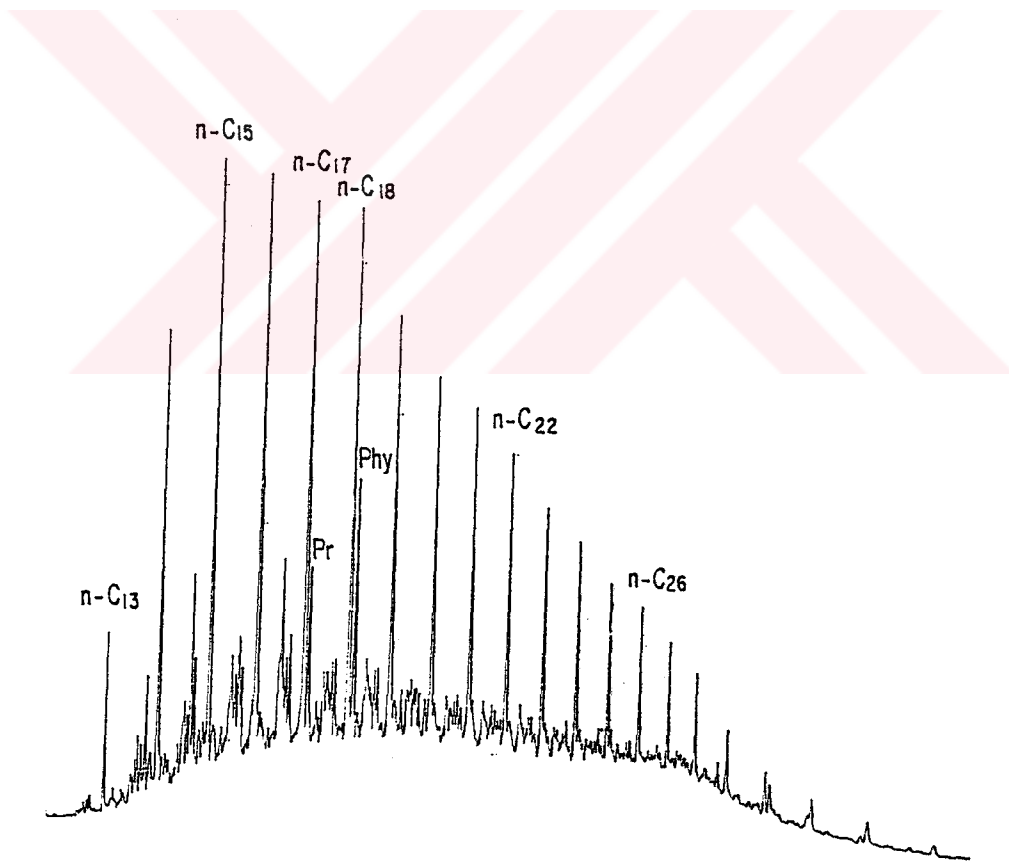
Figure_C.21 Gas chromatogram of the saturate fraction of Raman_157 (R157) oil.



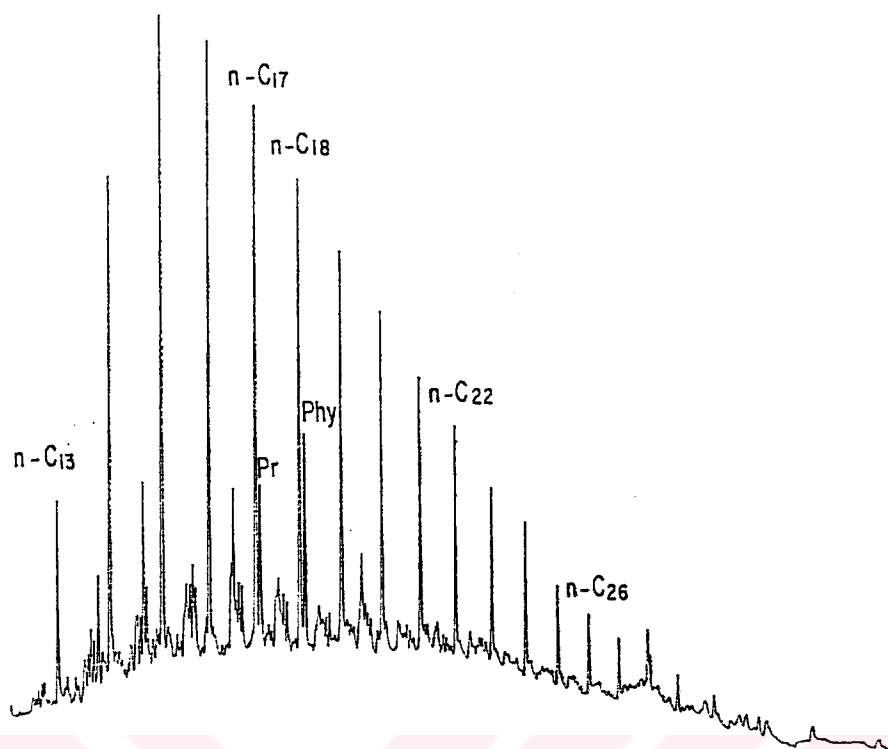
Figure_C.22 Gas chromatogram of the saturate fraction of Raman_63 (R63) oil.



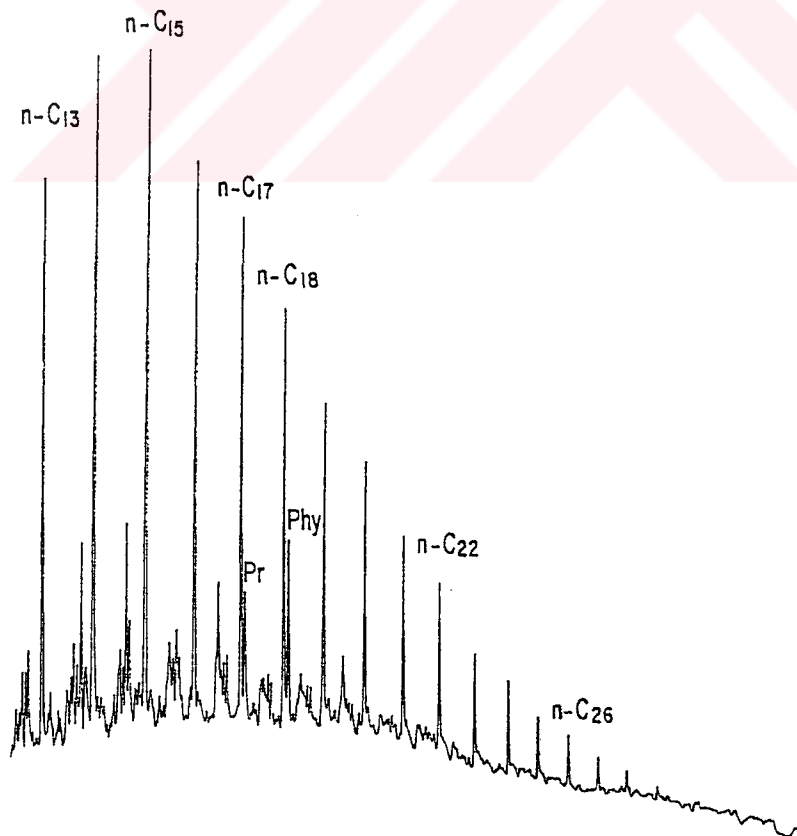
Figure_C.23 Gas chromatogram of the saturate fraction of Raman_193 (R193) oil.



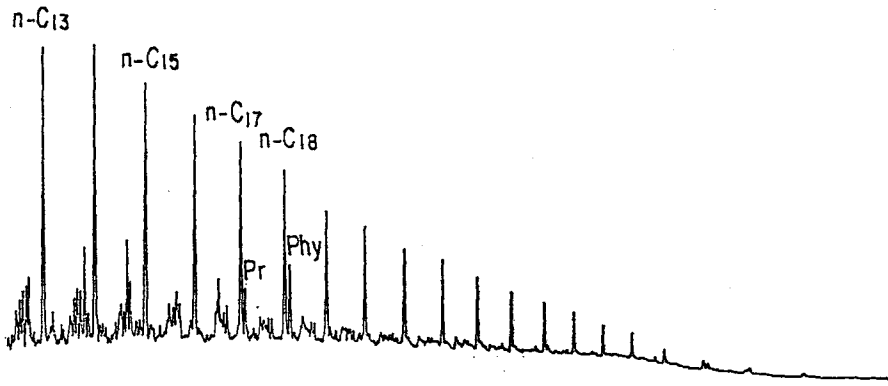
Figure_C.24 Gas chromatogram of the saturate fraction of Raman_151 (R151) oil.



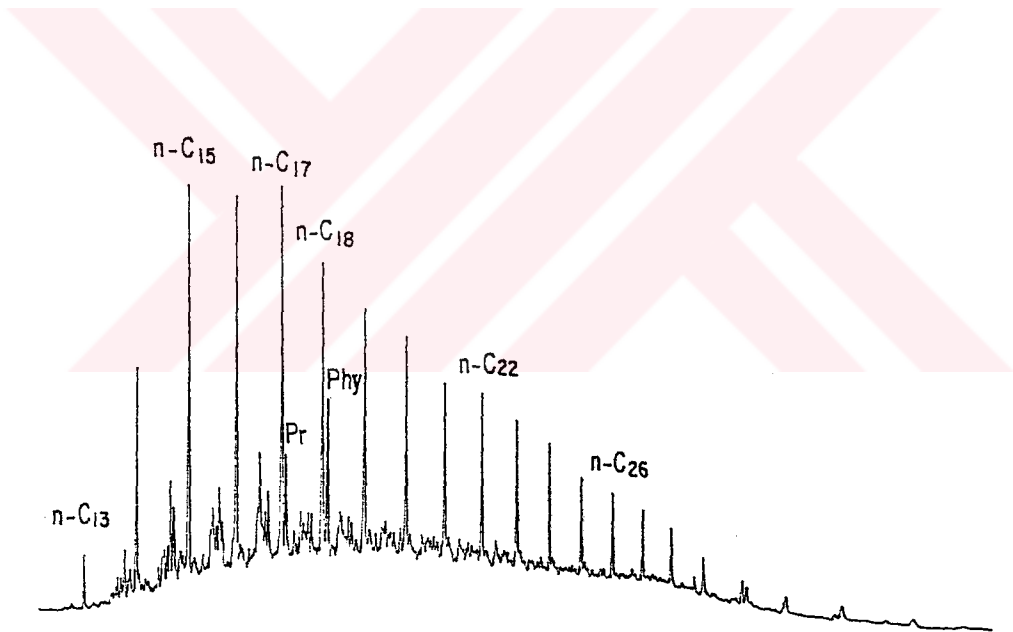
Figure_C.25 Gas chromatogram of the saturate fraction of Raman_197 (R197) oil.



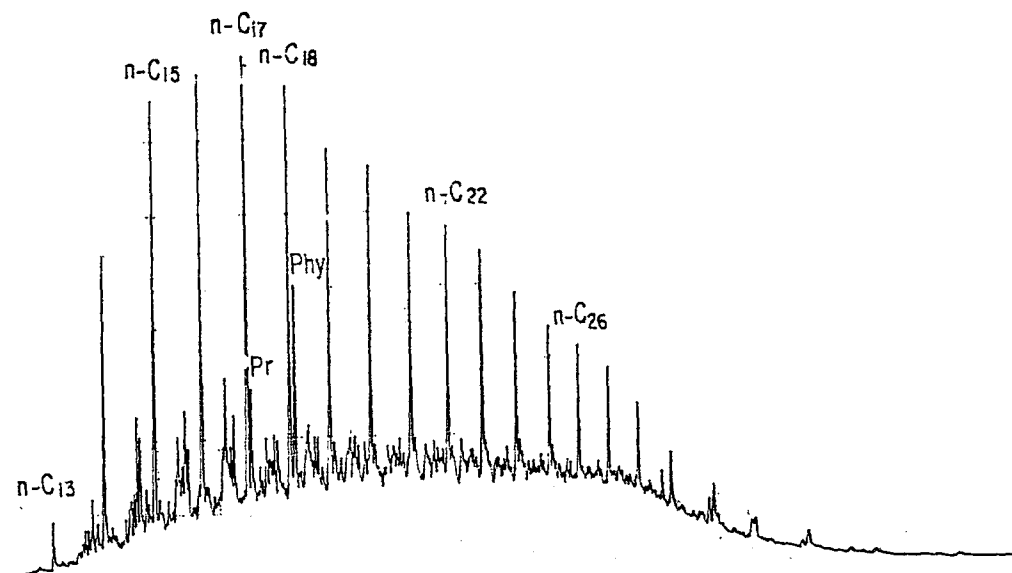
Figure_C.26 Gas chromatogram of the saturate fraction of Raman_84 (R84) oil.



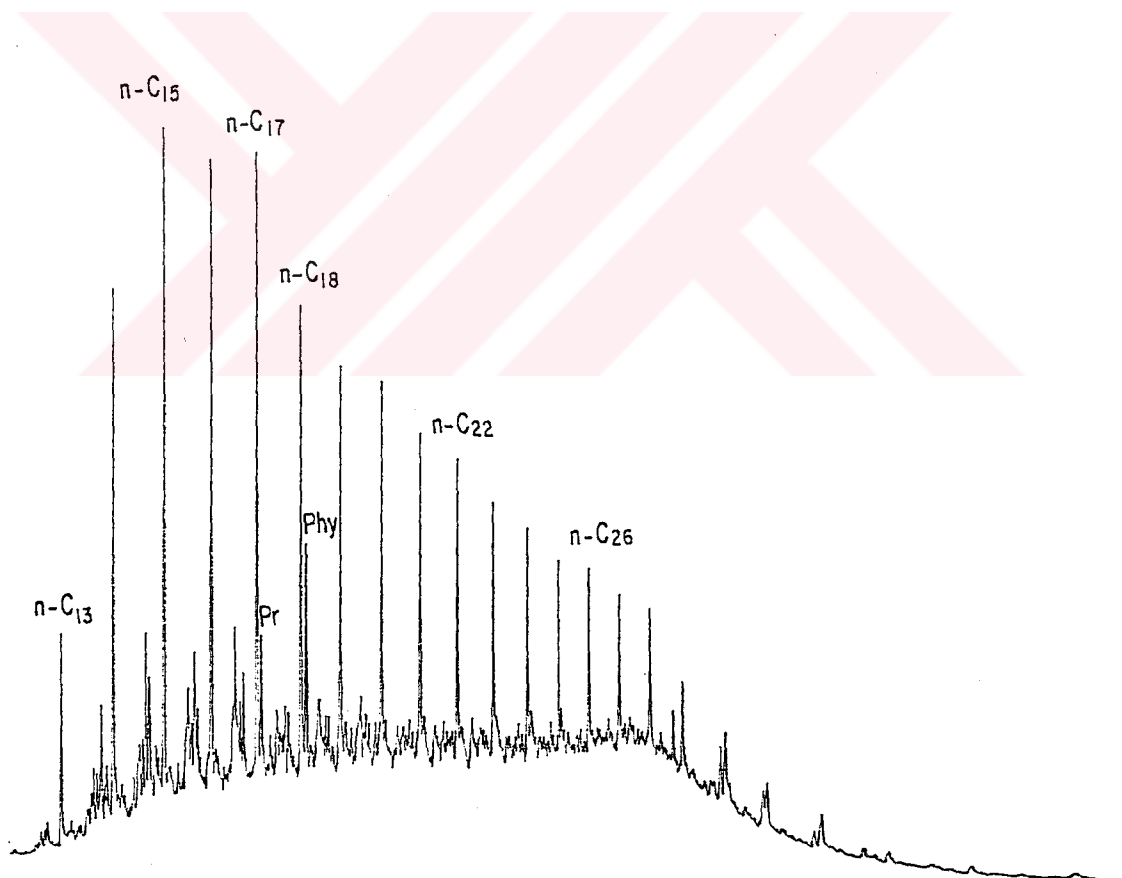
Figure_C.27 Gas chromatogram of the saturate fraction of Raman_93 (R93) oil.



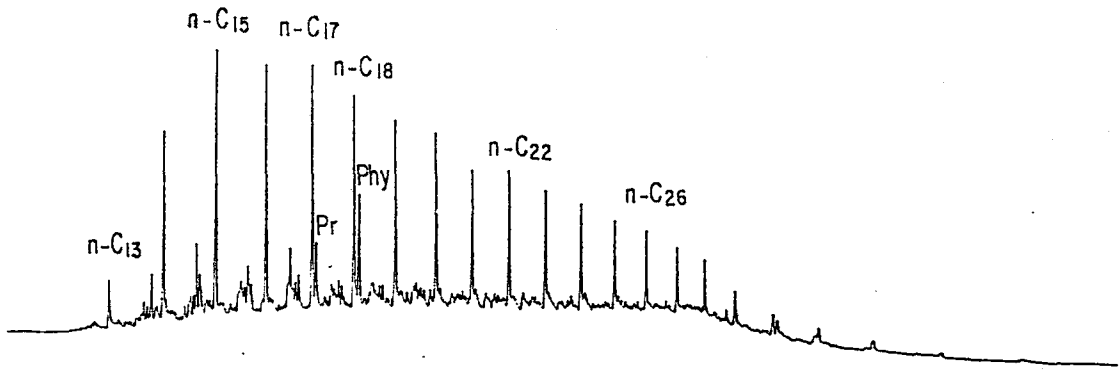
Figure_C.28 Gas chromatogram of the saturate fraction of Batı Raman_47 (BR47) oil.



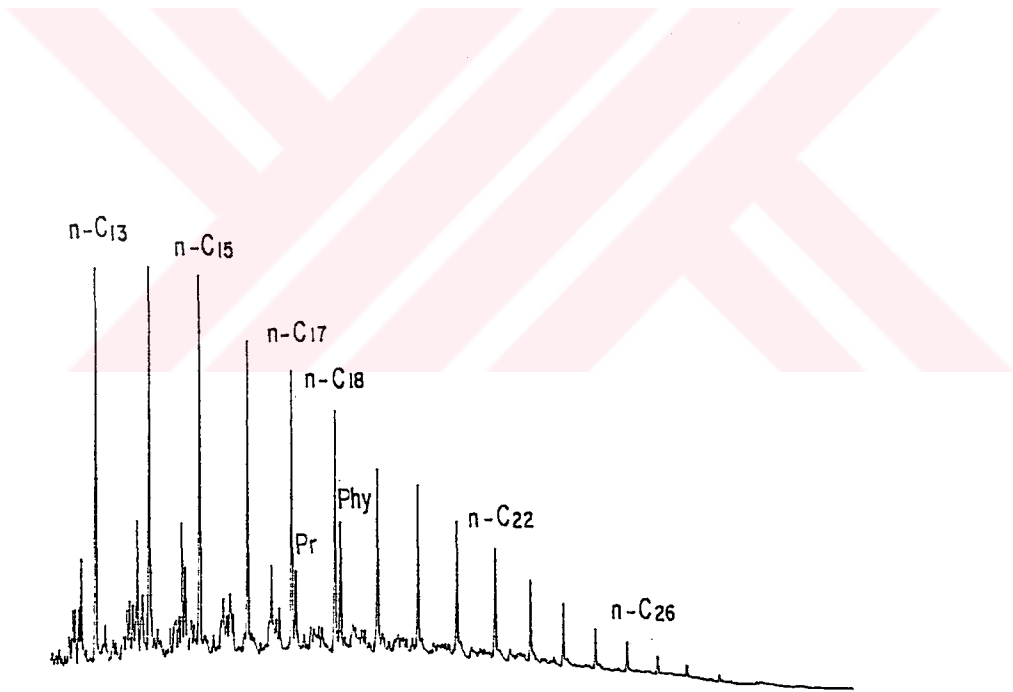
Figure_C.29 Gas chromatogram of the saturate fraction of Bati Raman_56 (BR56) oil.



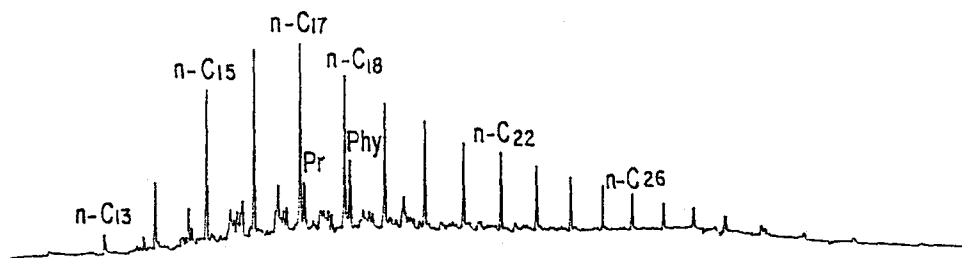
Figure_C.30 Gas chromatogram of the saturate fraction of Bati Raman_84 (BR84) oil.



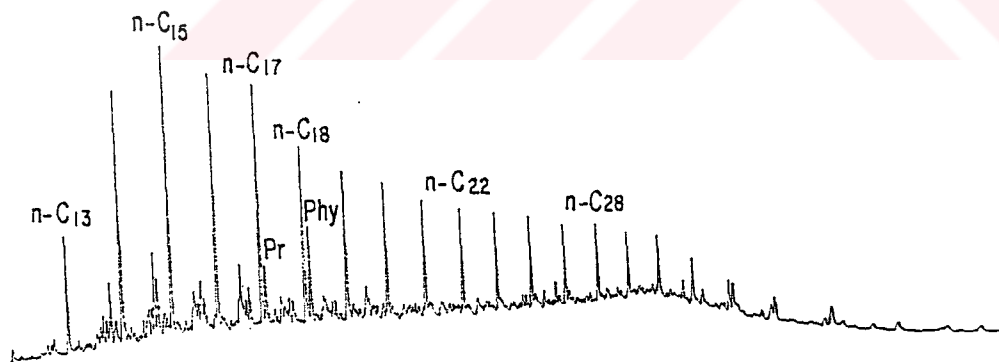
Figure_C.31 Gas chromatogram of the saturate fraction of Batı Raman_43(BR43)oil.



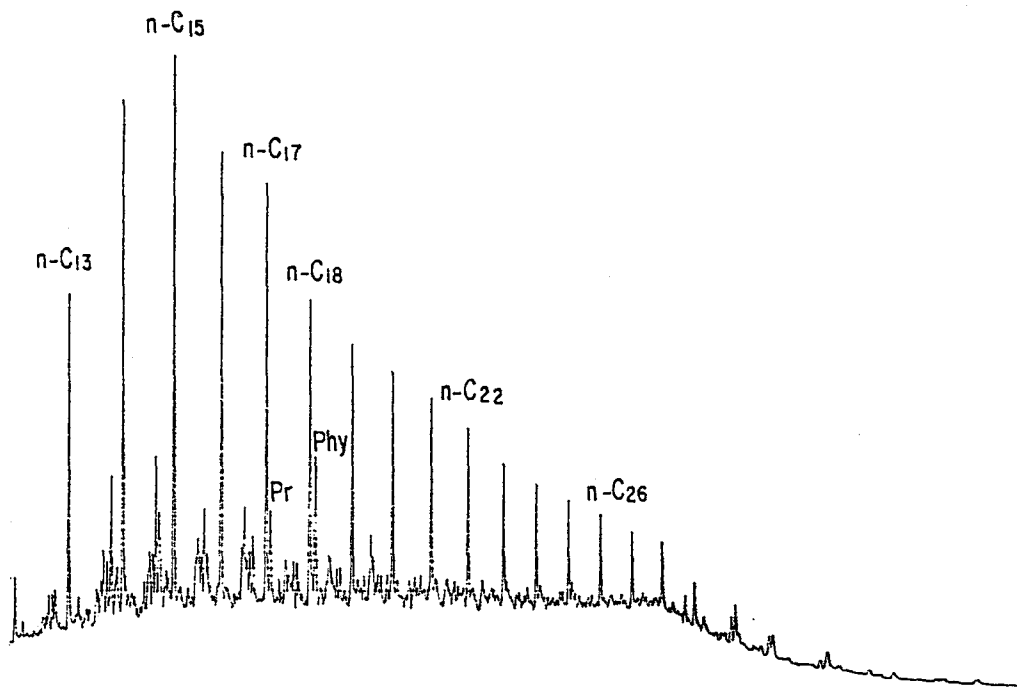
Figure_C.32 Gas chromatogram of the saturate fraction of Batı Raman_211 (BR211)oil.



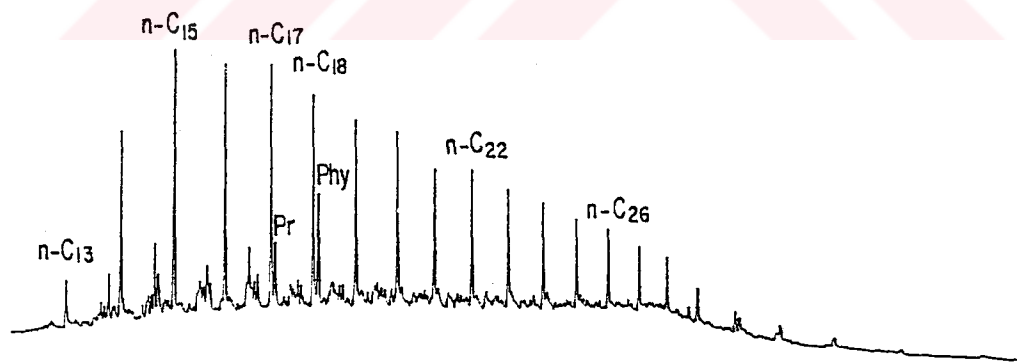
Figure_C.33 Gas chromatogram of the saturate fraction of Bati Raman_193 (BR193) oil.



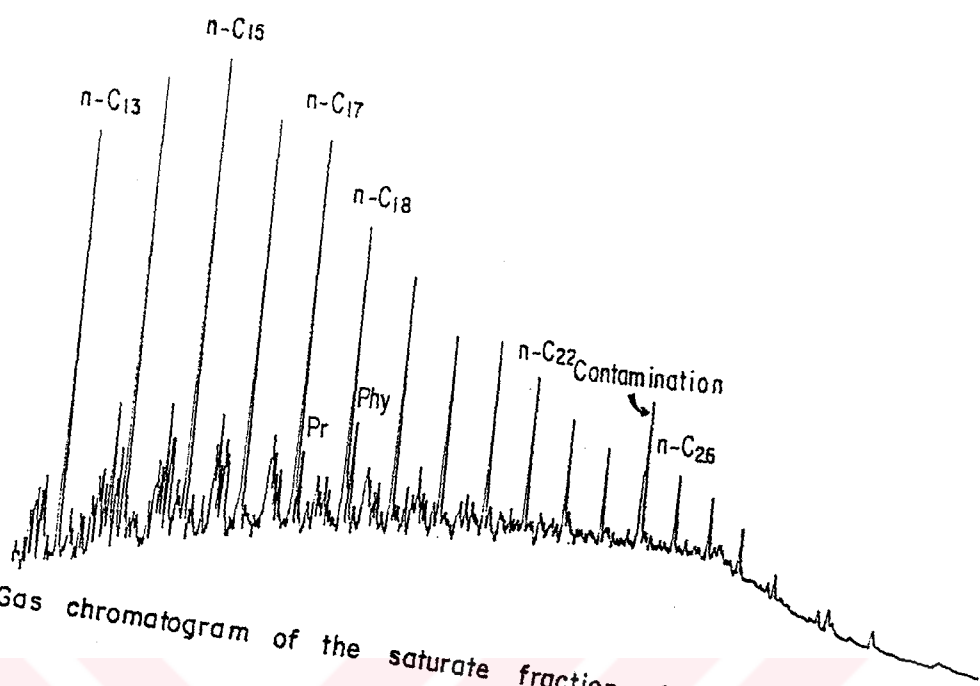
Figure_C.34 Gas chromatogram of the saturate fraction of Bati Raman_189 (BR189) oil.



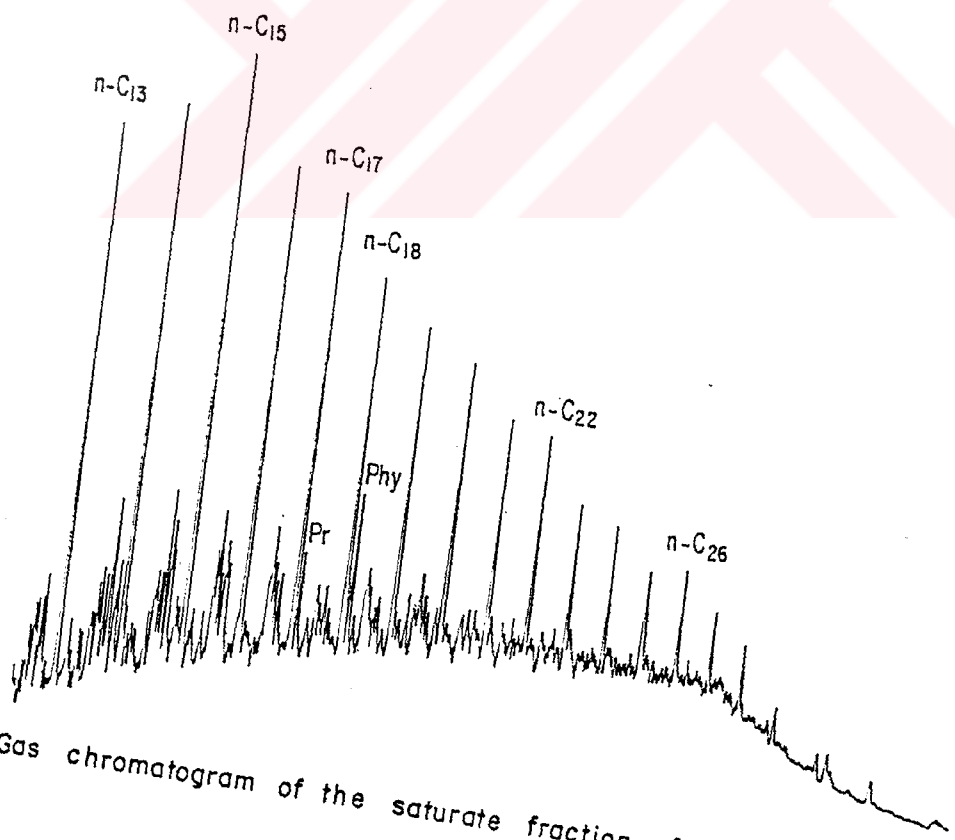
Figure_C.35 Gas chromatogram of the saturate fraction of Batı Raman_167 (BR167) oil.



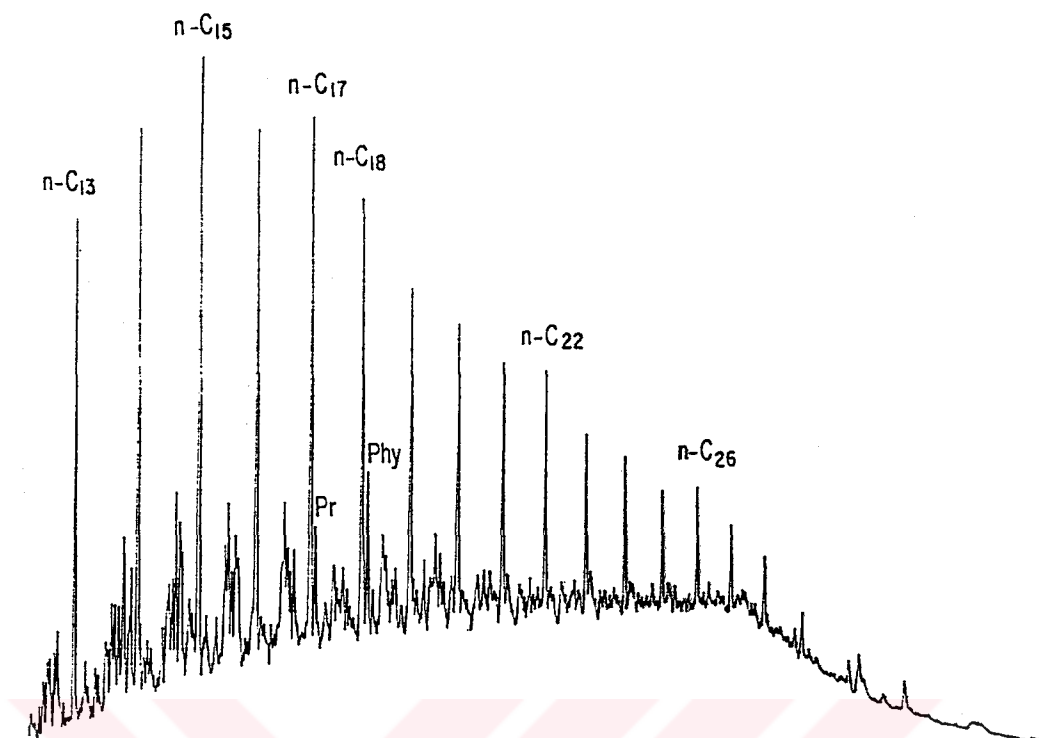
Figure_C.36 Gas chromatogram of the saturate fraction of Batı Raman_176 (BR176) oil.



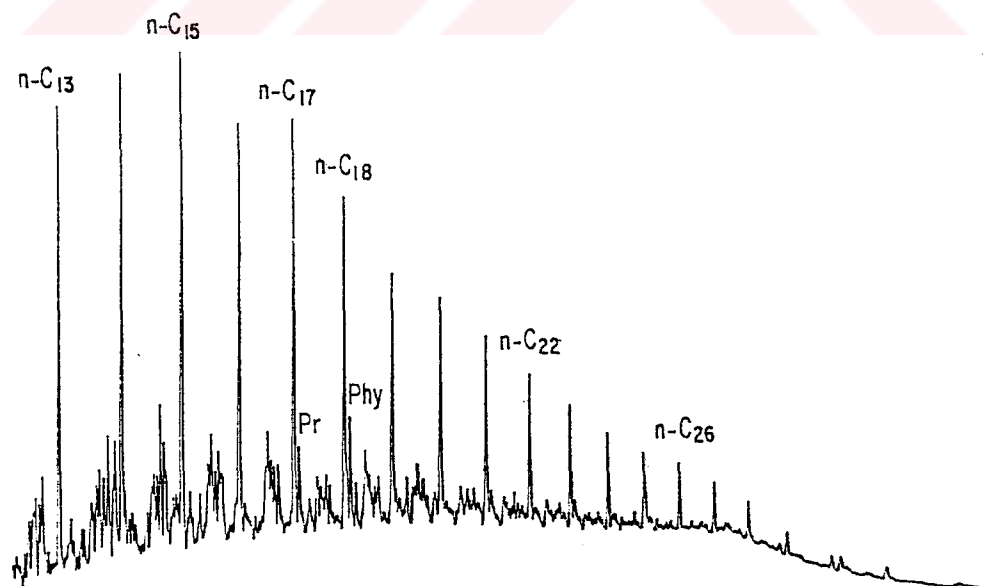
Figure_C.37 Gas chromatogram of the saturate fraction of Çamurlu_2 (CA2) oil.



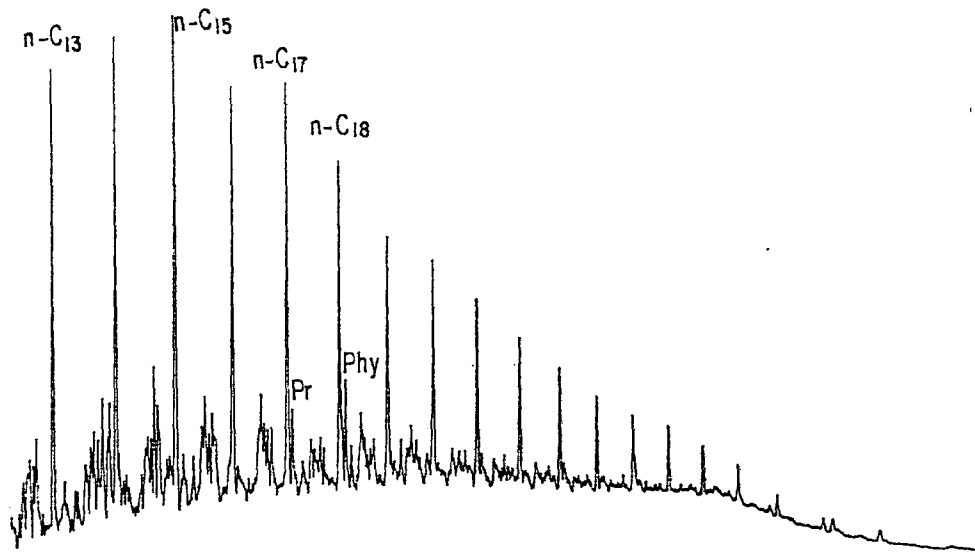
Figure_C.38 Gas chromatogram of the saturate fraction of Çamurlu_22 (CA22) oil.



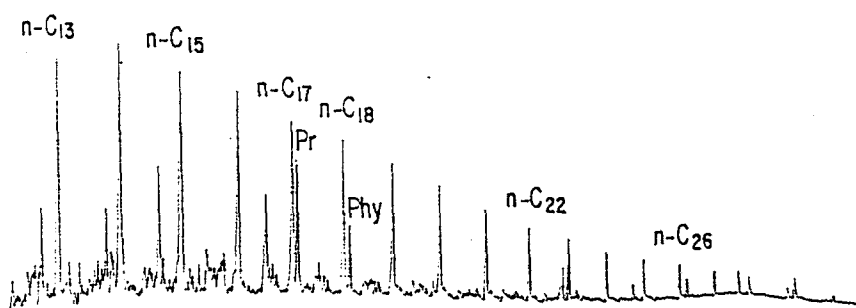
Figure_C.39 Gas chromatogram of the saturate fraction of Batı Kozluca_12 (BK12) oil.



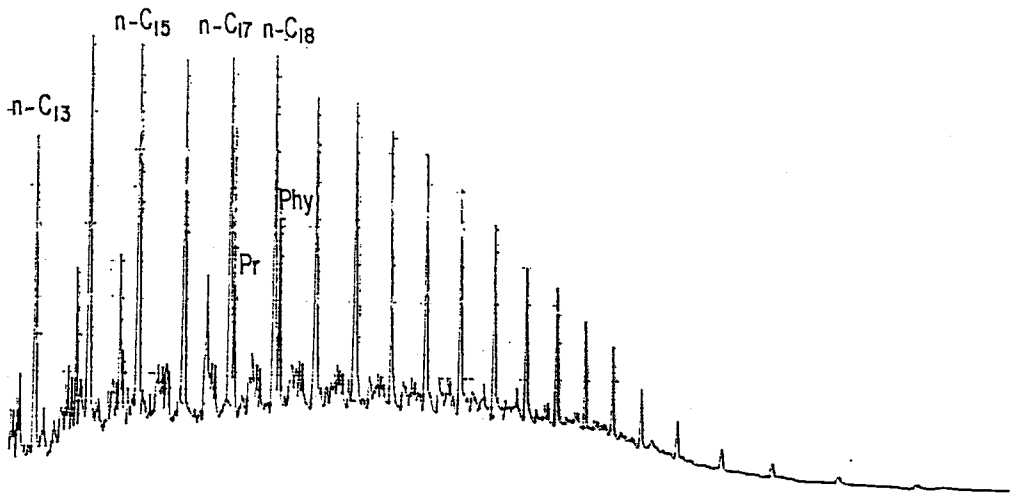
Figure_C.40 Gas chromatogram of the saturate fraction of Güney Dinçer_3 (GD3) oil.



Figure_C.41 Gas chromatogram of the saturate fraction of Güney Dincer_15 (GD15) oil.



Figure_C.42 Gas chromatogram of the saturate fraction of Güney Sarıcağ_21 (GS21) oil.



Figure_C.43 Gas chromatogram of the saturate fraction of Adiyaman_3 (A3) oil.

APPENDIX-D

COMPILATION OF M/Z 191 (TERPANE) MASS FRAGMENTOGRAMS OF
BRANCH/CYCLIC FRACTION OF THE TURKISH OILS

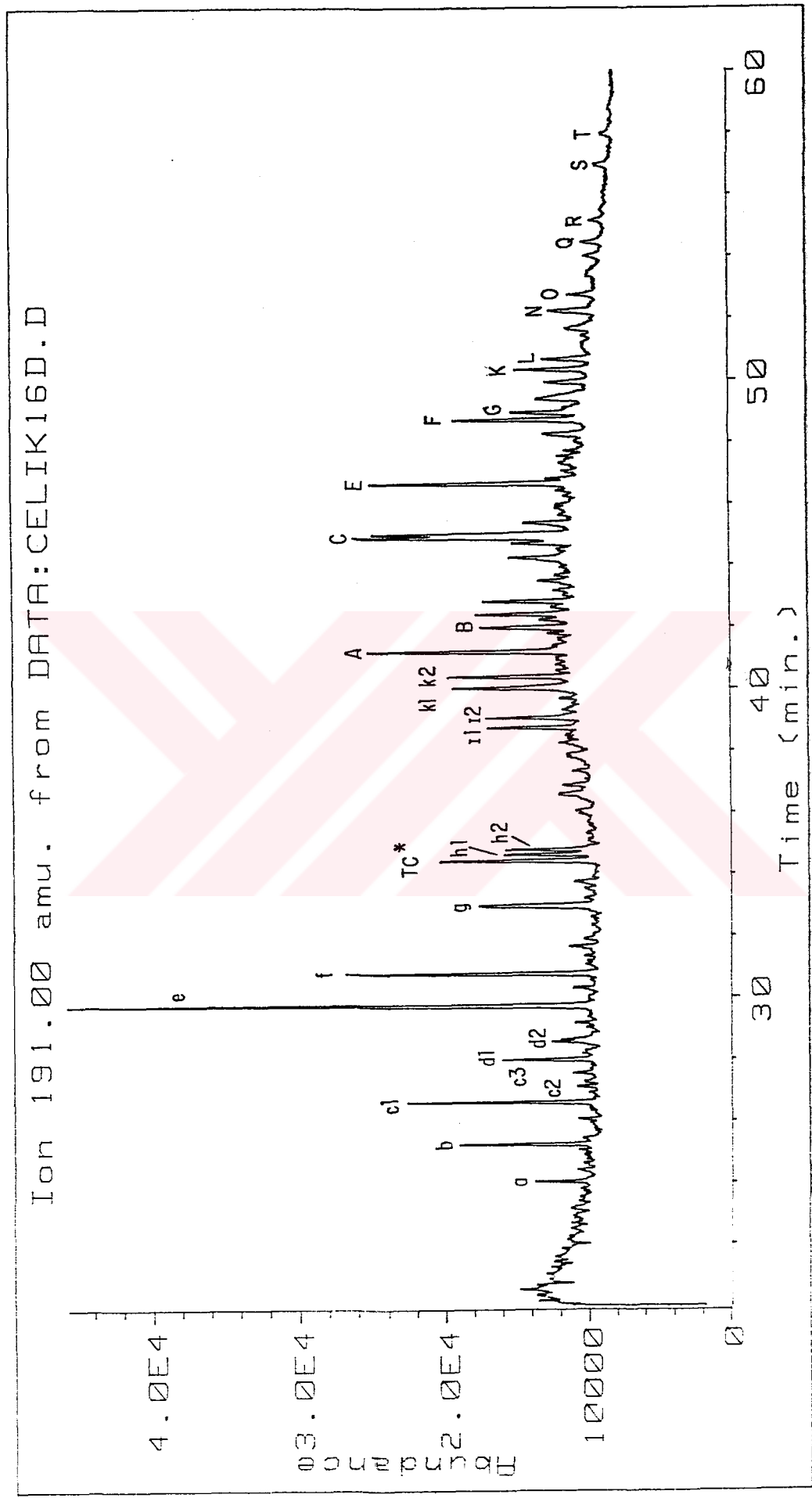


Figure - DI M/Z 191 mass fragmentogram of the ÇelikII_16 (CE16) oil.

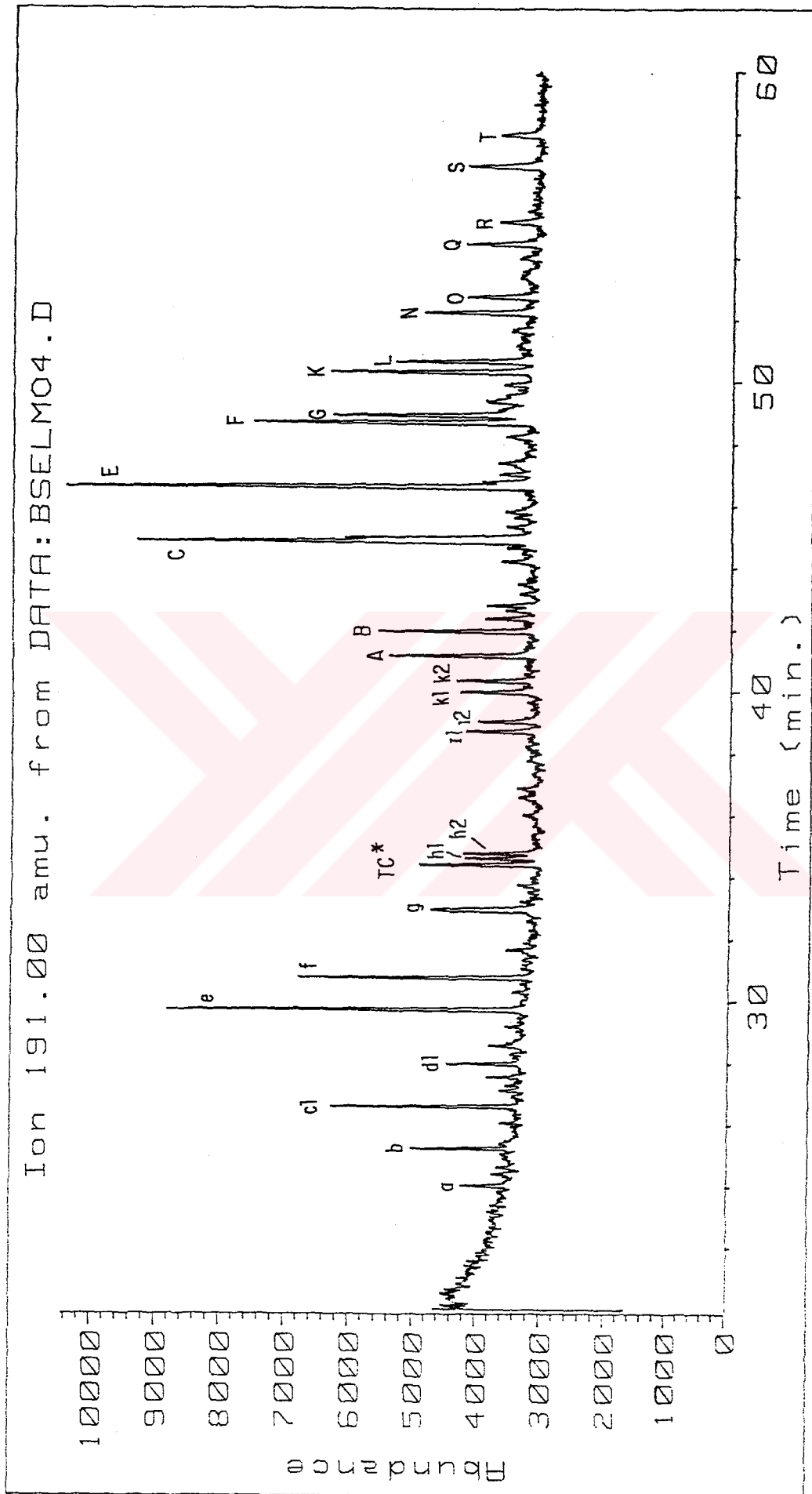


Figure -D.2 M/Z 191 mass chromatogram of the Batı Şelmo_4 (BS4) oil.

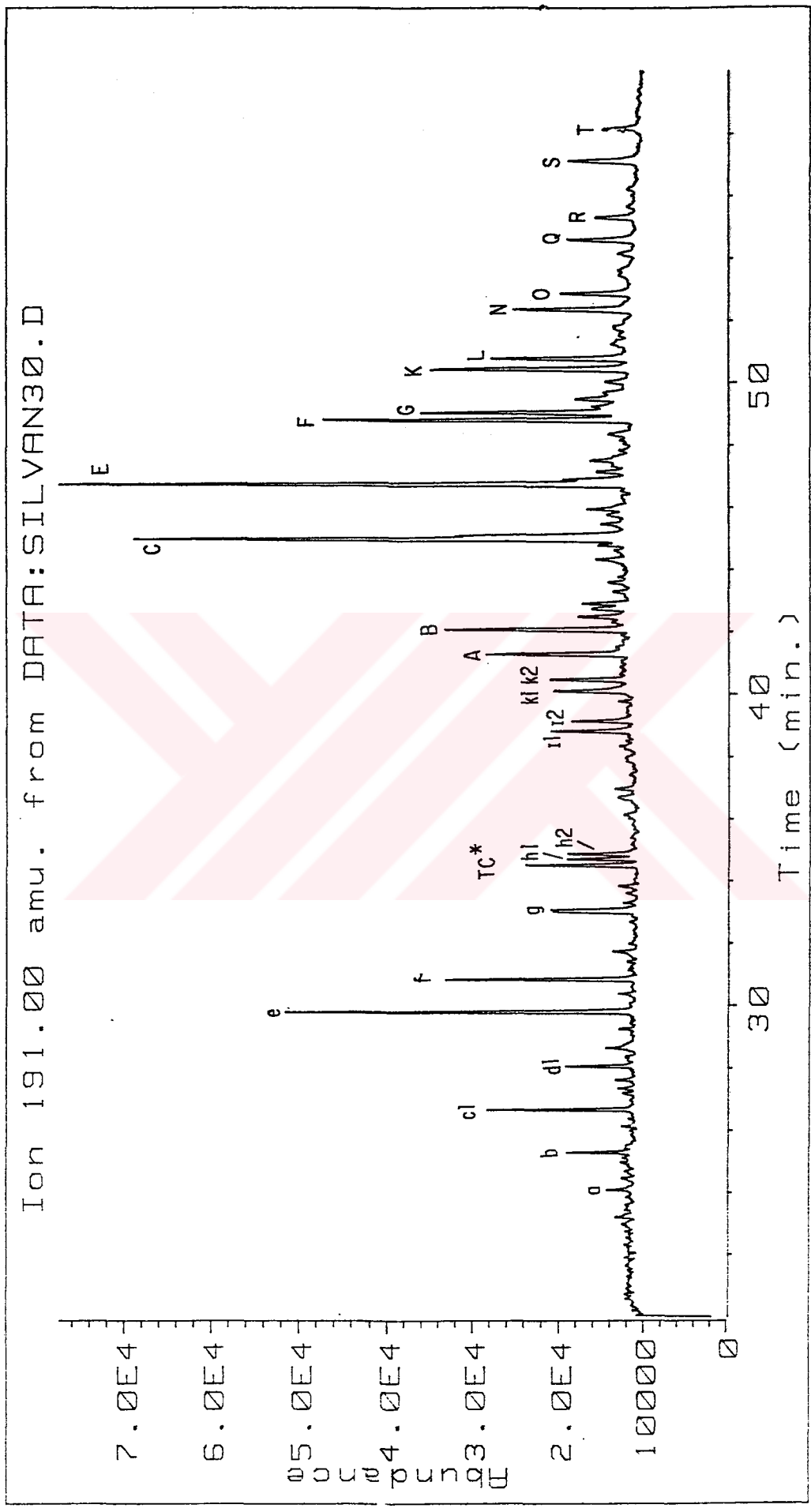
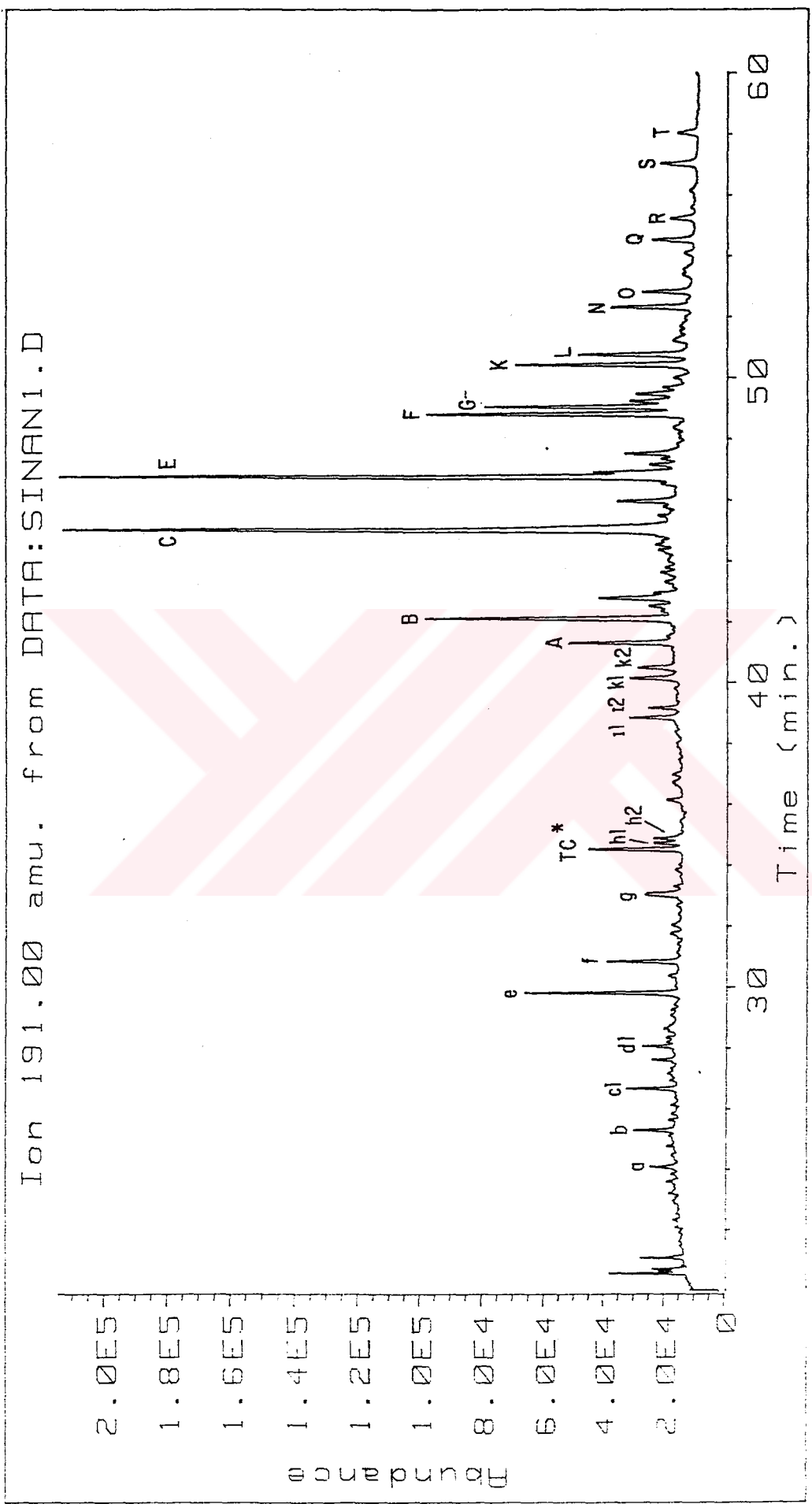
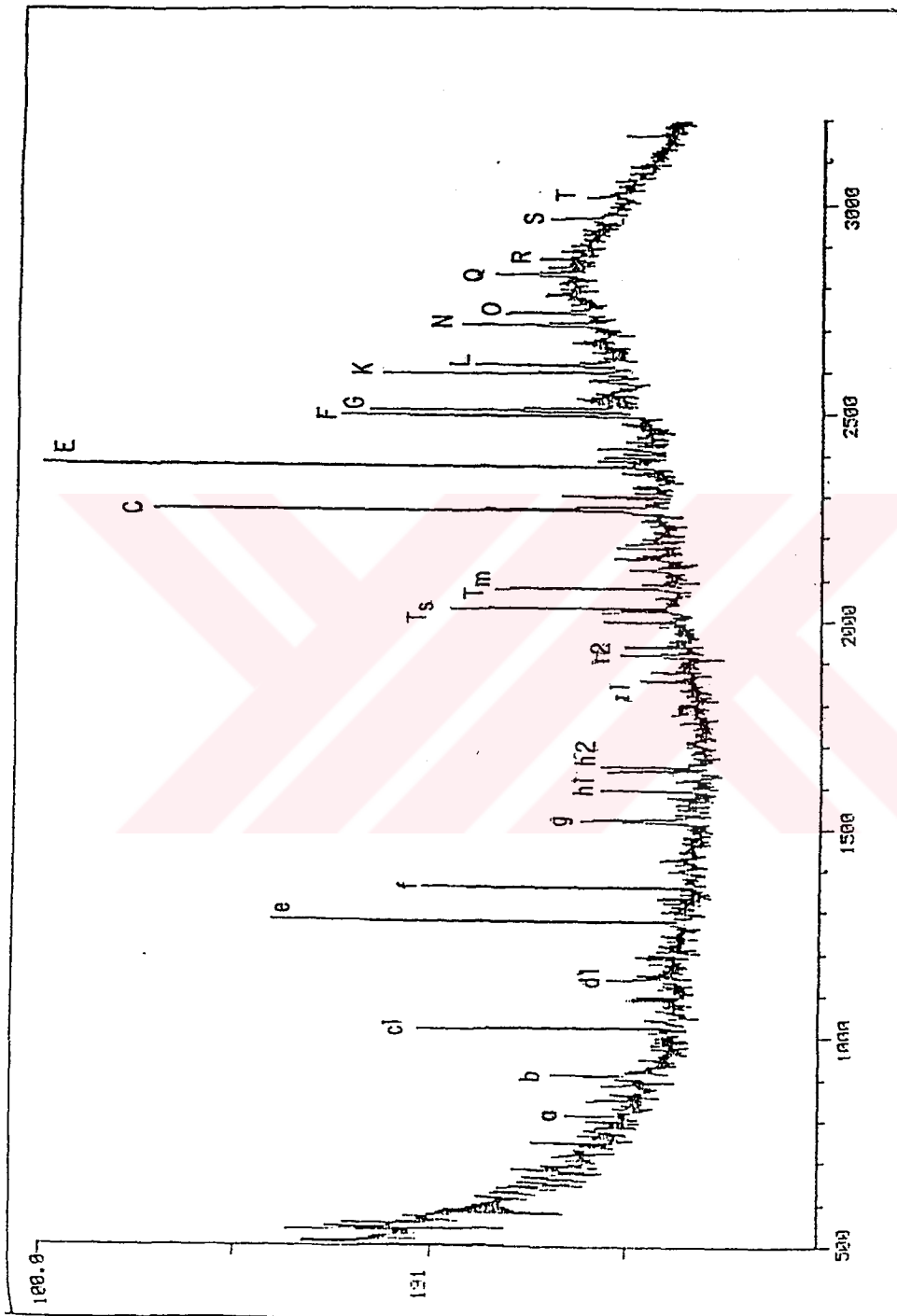


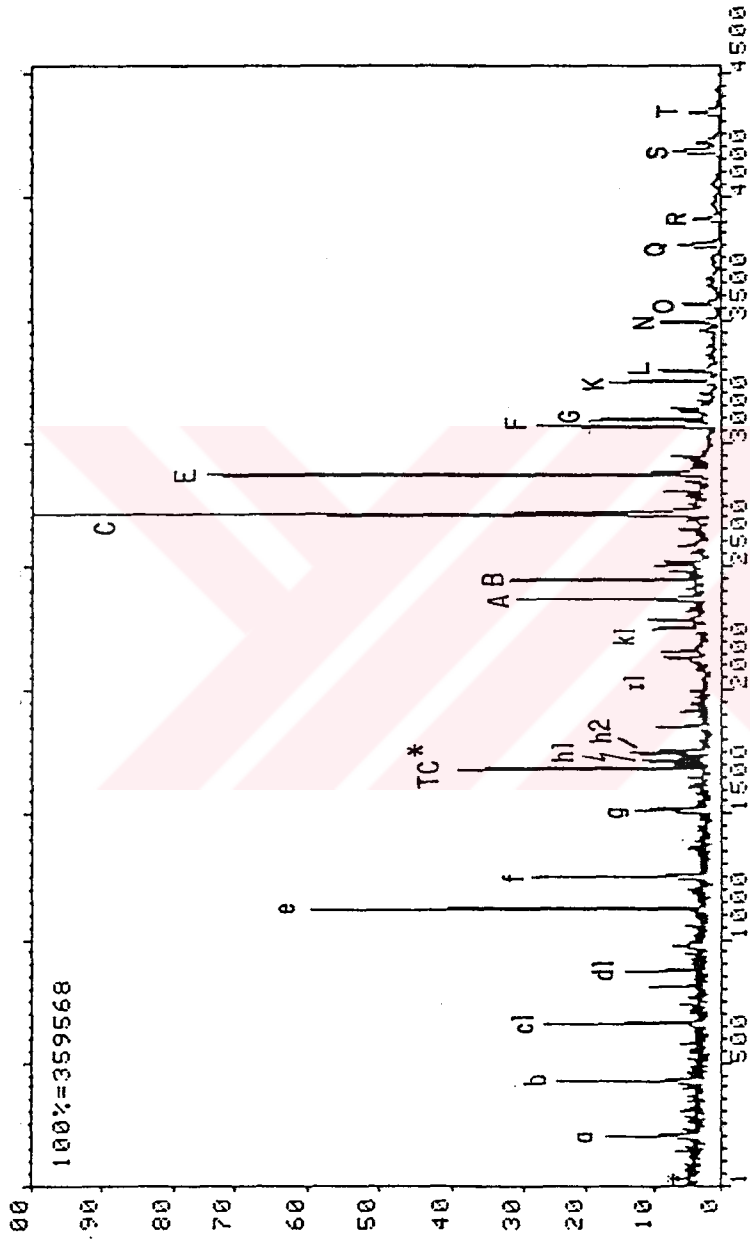
Figure .D.3 M/Z 191 mass fragmetogram of the Silivanka_30 (S30) oil.



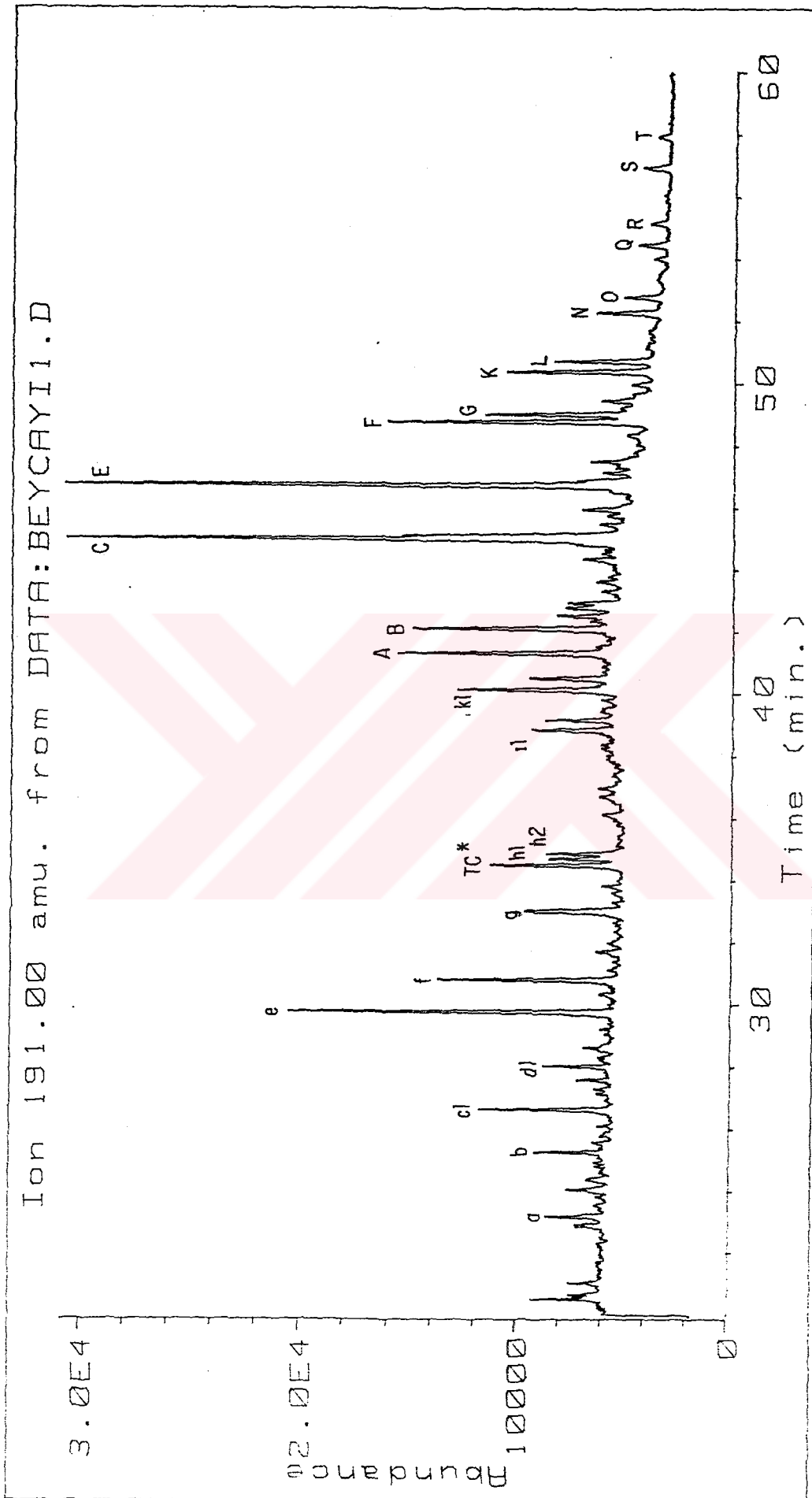
Figure_D.4 M/Z 191 mass fragmentogram of the Sinan_1 (S11) oil.



Figure_D.5 M/Z 191 mass fragmentogram of the Kaste1.2 (KA2) oil.



Figure_D.6 M/Z 191 mass fragmentogram of the Kurtalan_1 (KUI) oil.



Figure_D.7 M/Z 191 mass fragmentogram of the Beyçayırı_1 (BE1) oil.

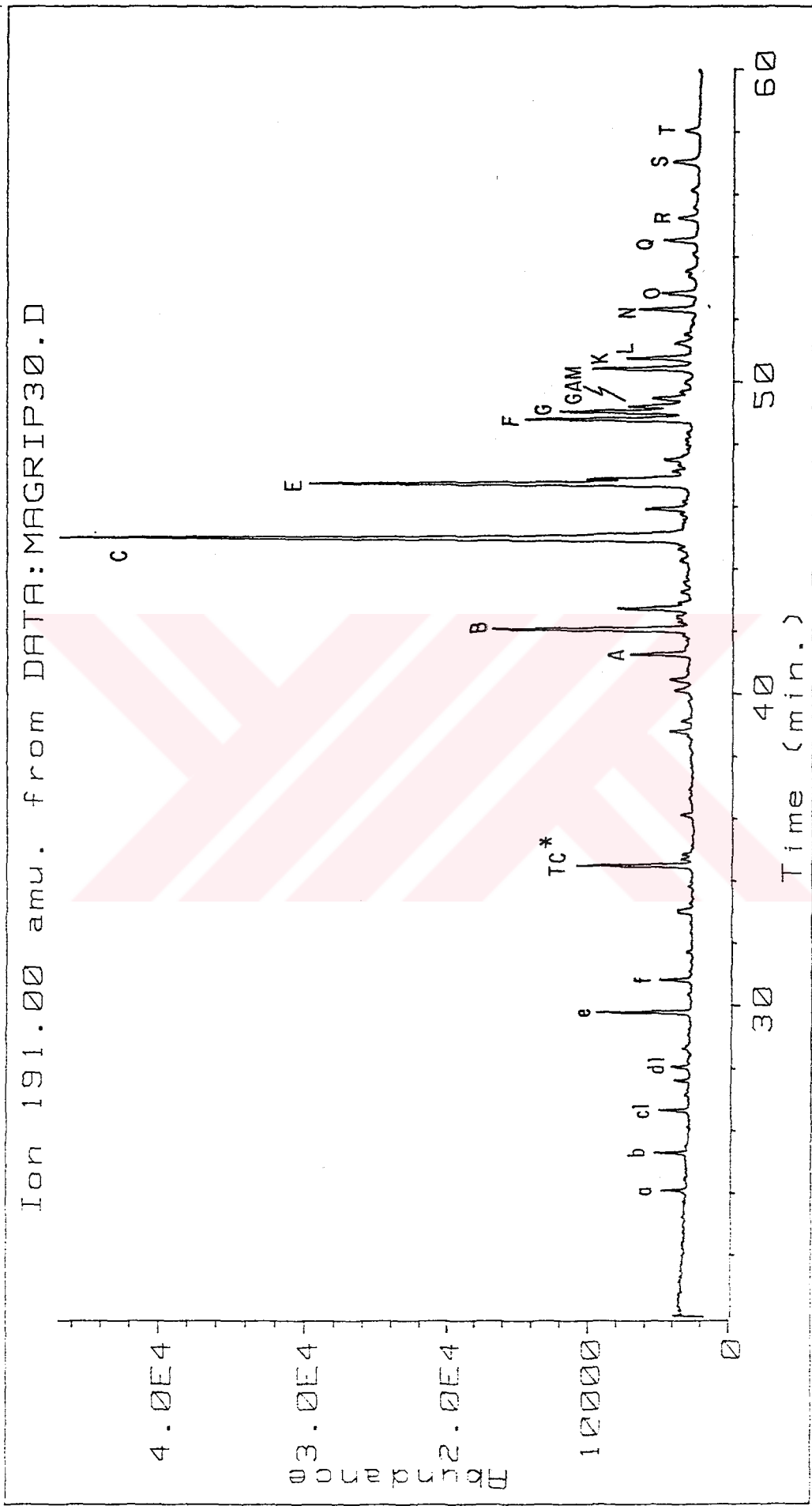
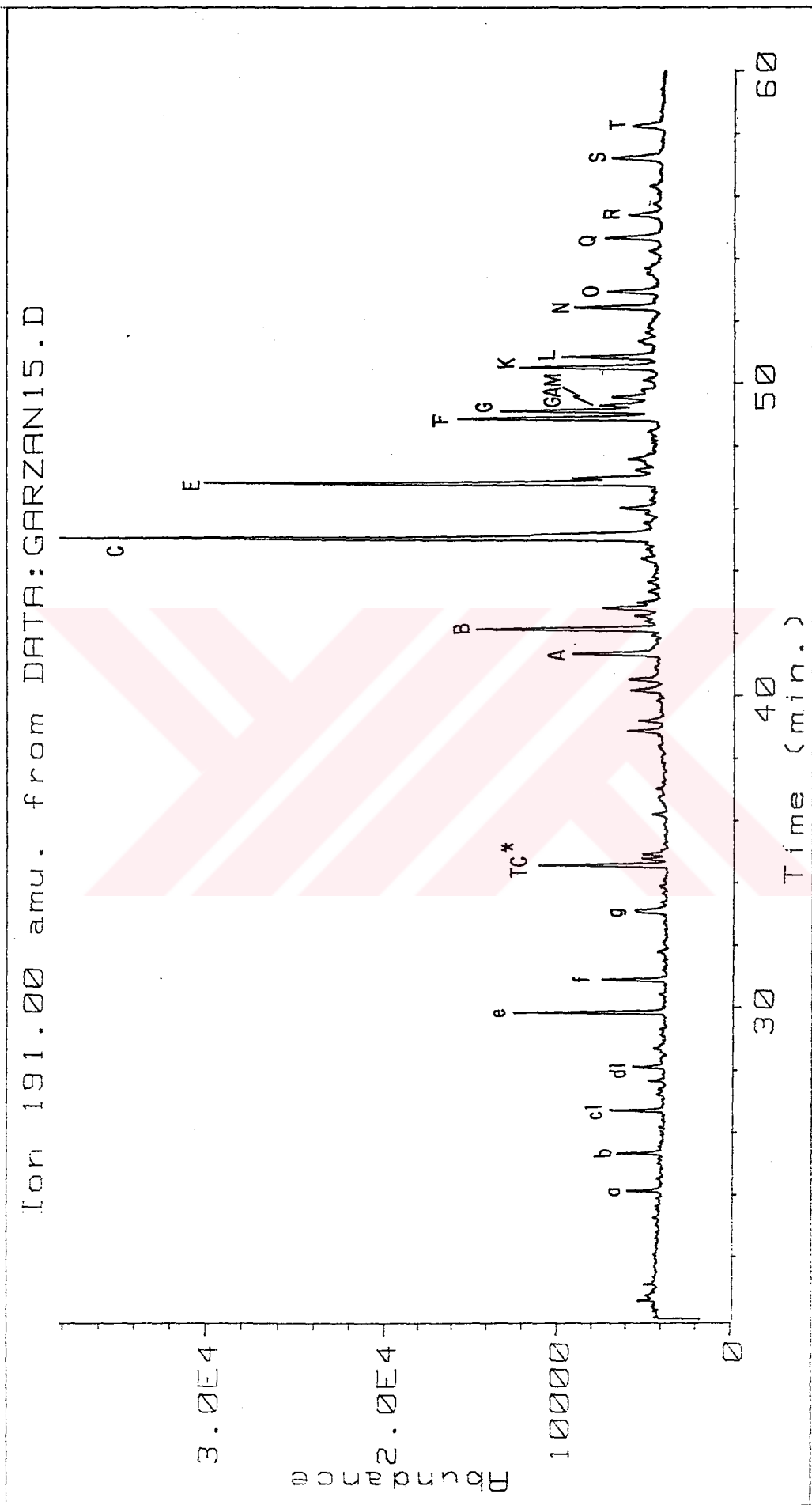


Figure -D.8 M/Z 191 mass chromatogram of the Magrip-30 (MA30) oil.



Figure_D.9 M/Z 191 mass chromatogram of the Garzan_15 (GA15) oil.

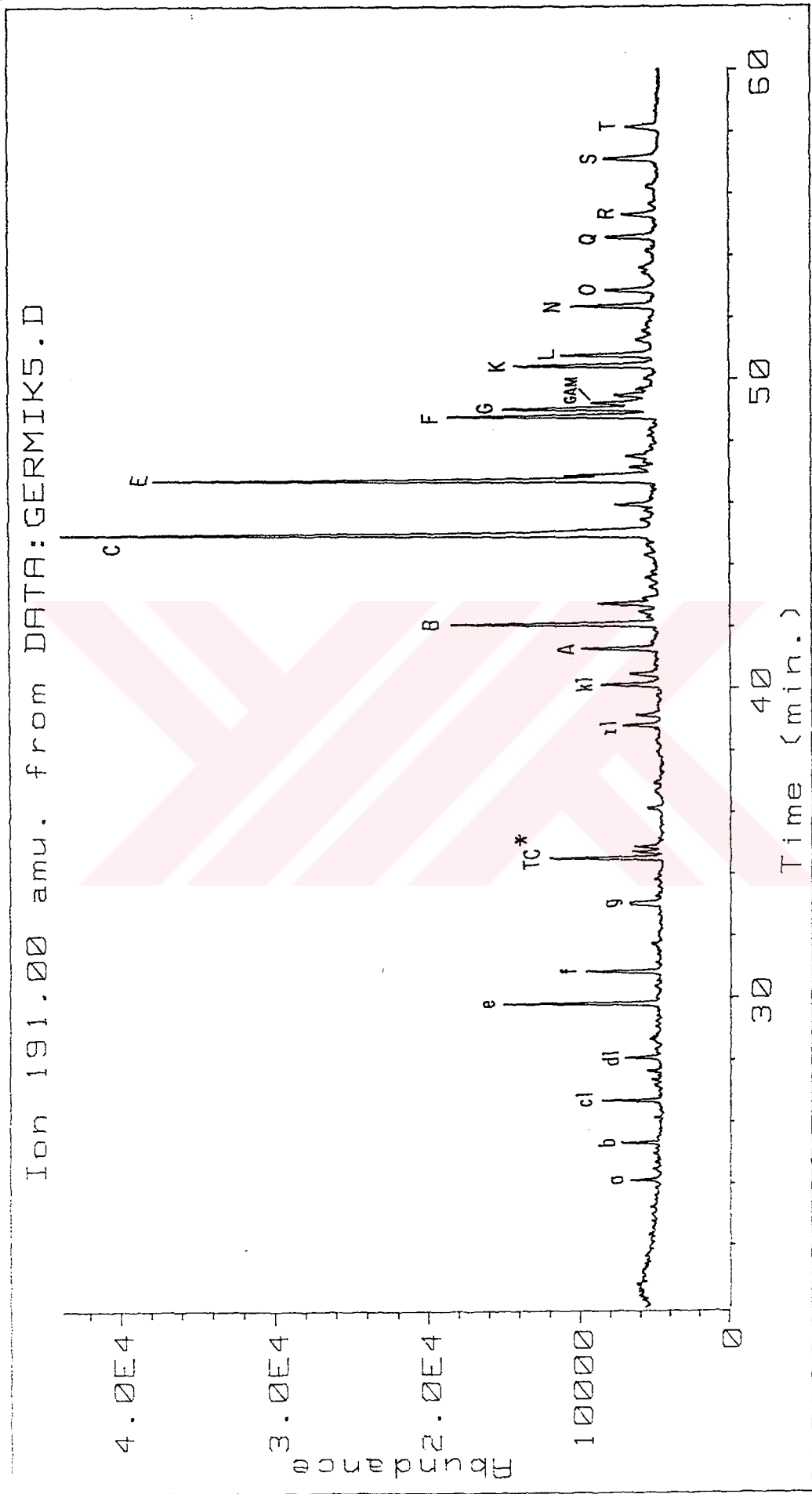
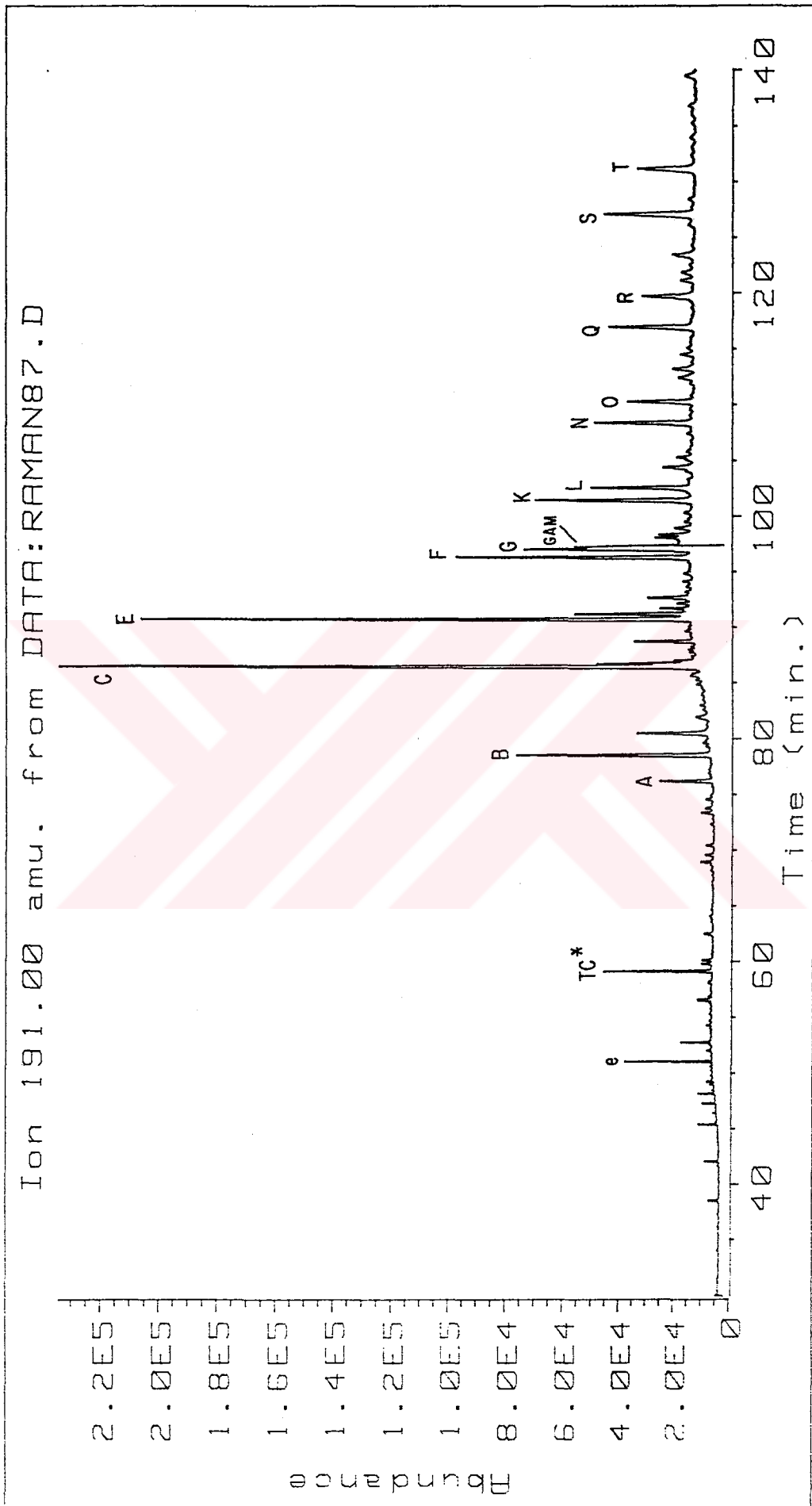
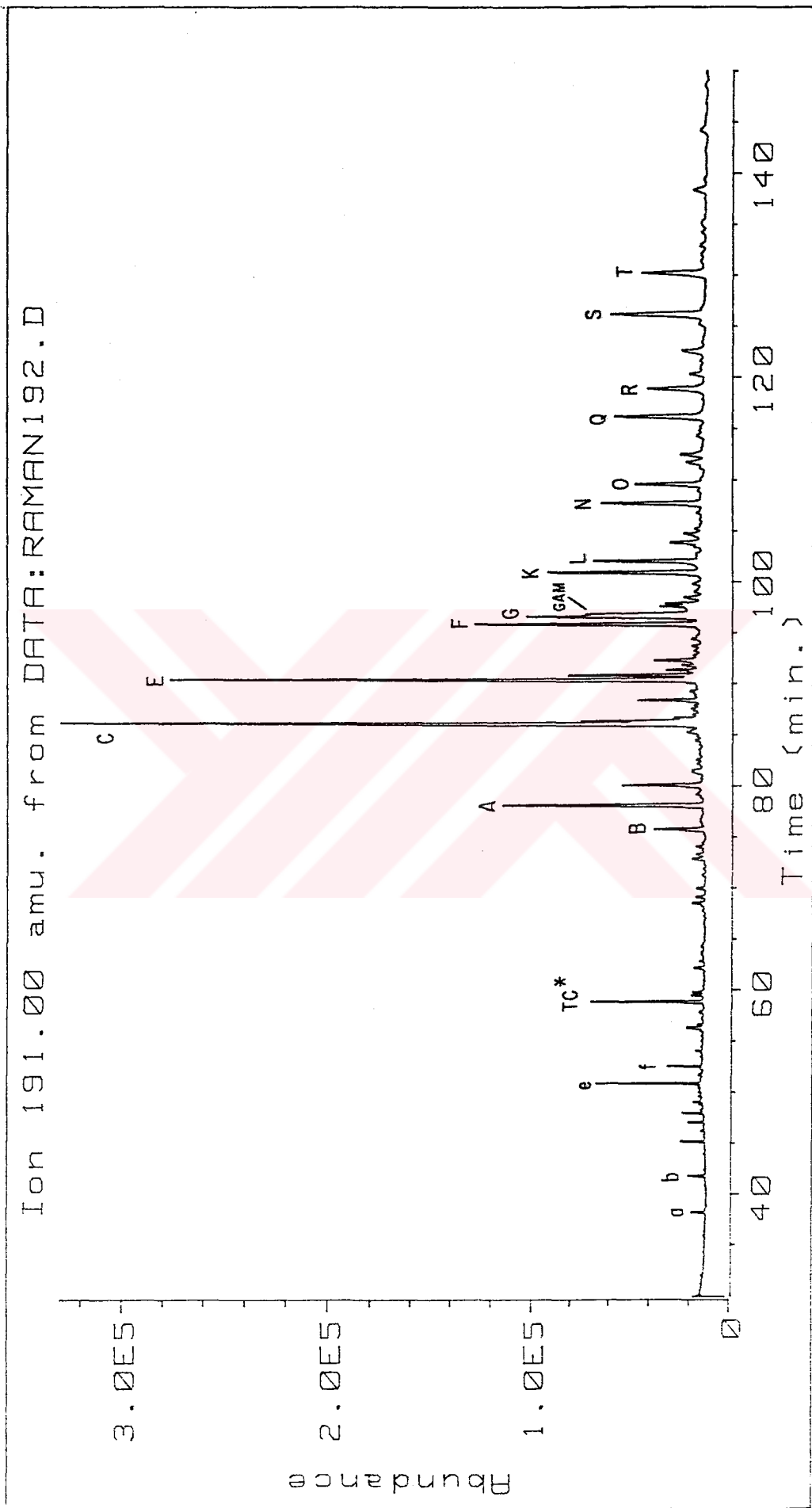


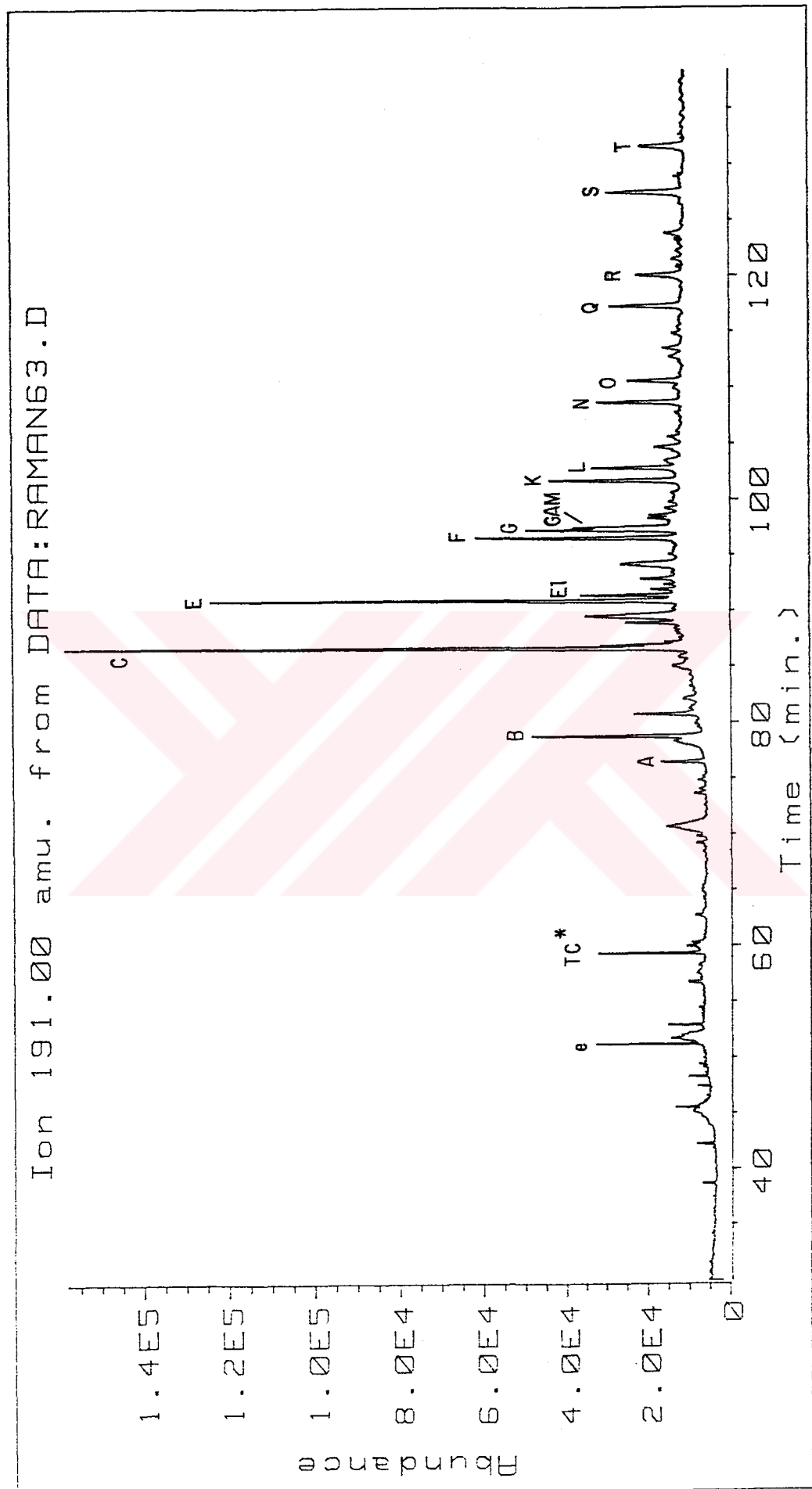
Figure .D.10 M/Z 191 mass fragmentogram of the Germik_5 (GE5) oil.



Figure_D.11 M/Z 191 mass chromatogram of the Raman_57 (R57) oil.



Figure_D.12 M/Z 191 mass fragmentogram of the Raman_192 (R192) oil.



Figure_D.13 M/Z 191 mass fragmentogram of the Raman_63 (R63) oil.

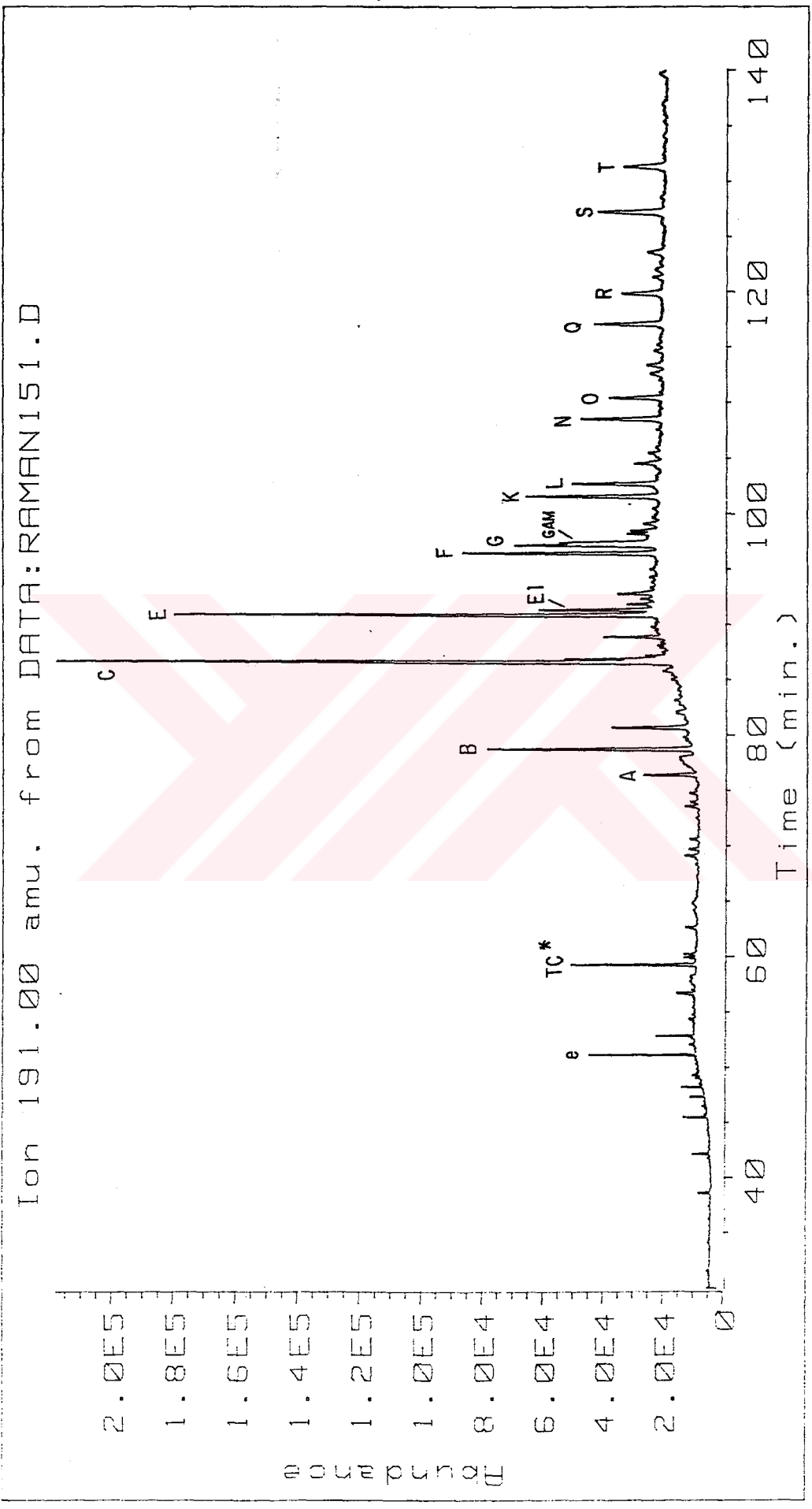


Figure - D.14 M/Z 191 mass fragmentogram of the Raman_151(R151) oil.

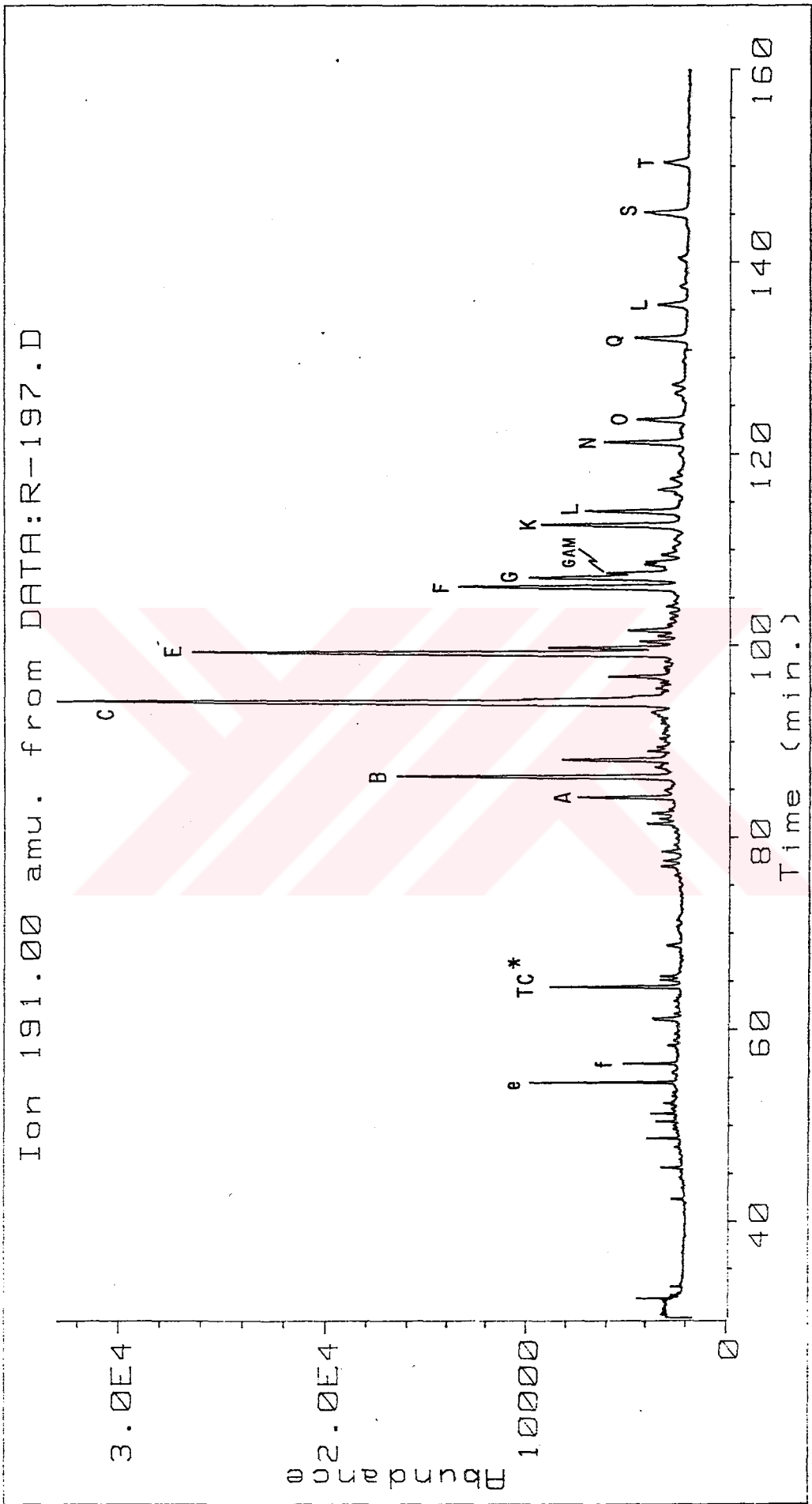
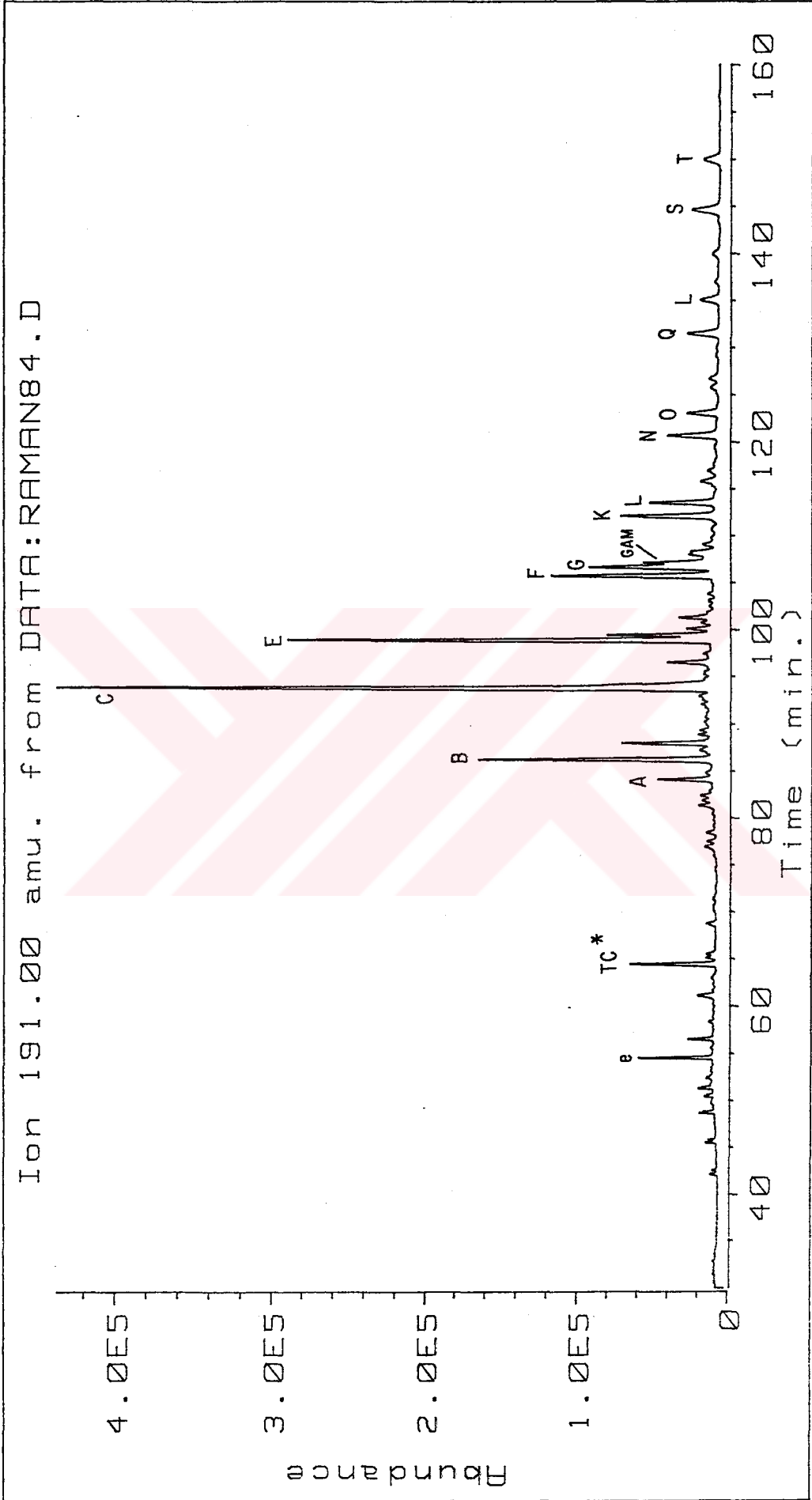
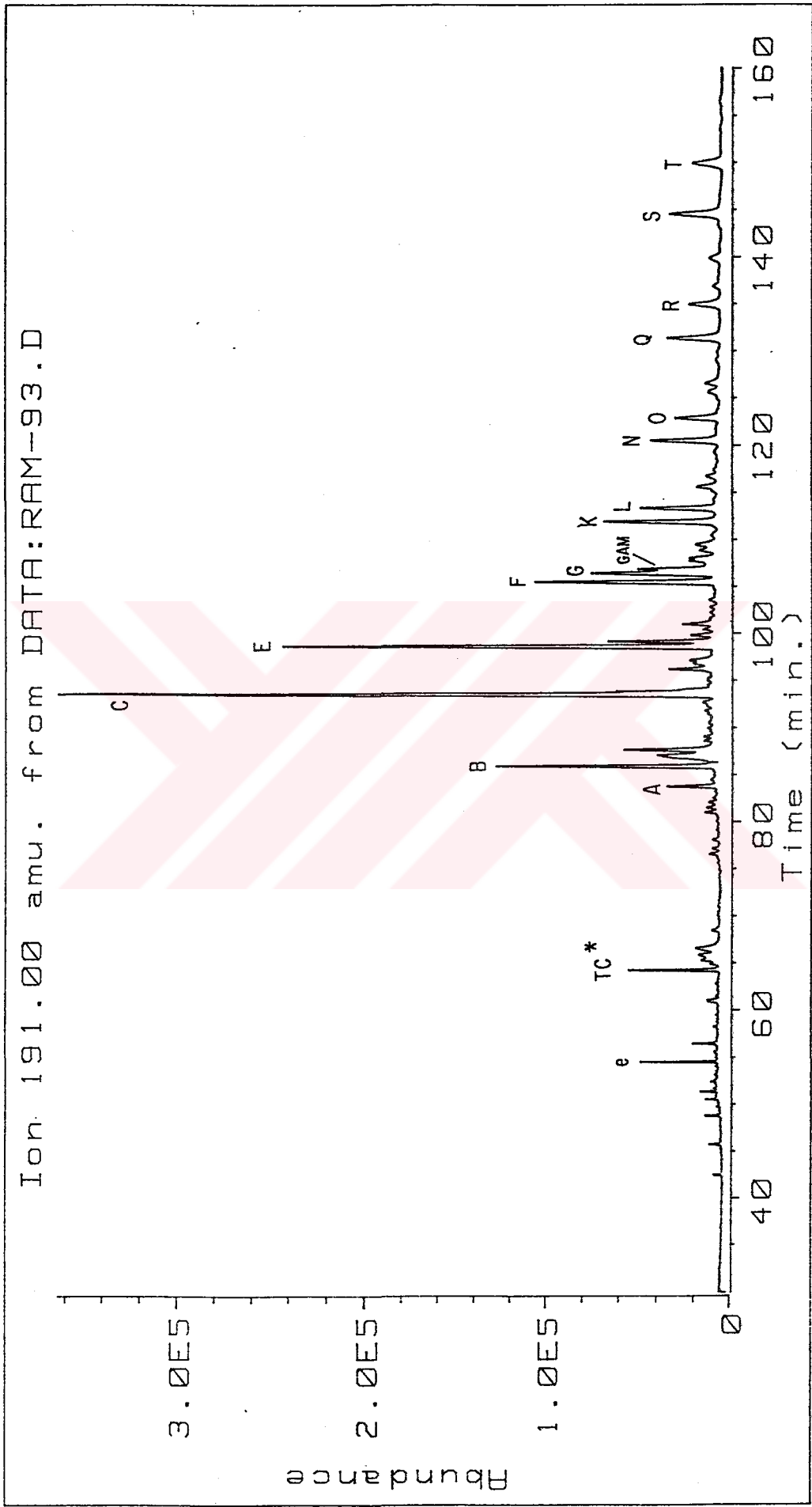


Figure - D.15 M/Z 191 mass fragmentogram of the Raman_197 (R197) oil.



Figure_D.16 M/Z 191 mass fragmentogram of the Raman_84 (R84) oil.



Figure_D.17 M/Z 191 mass fragmentogram of the Raman_93 (R93) oil.

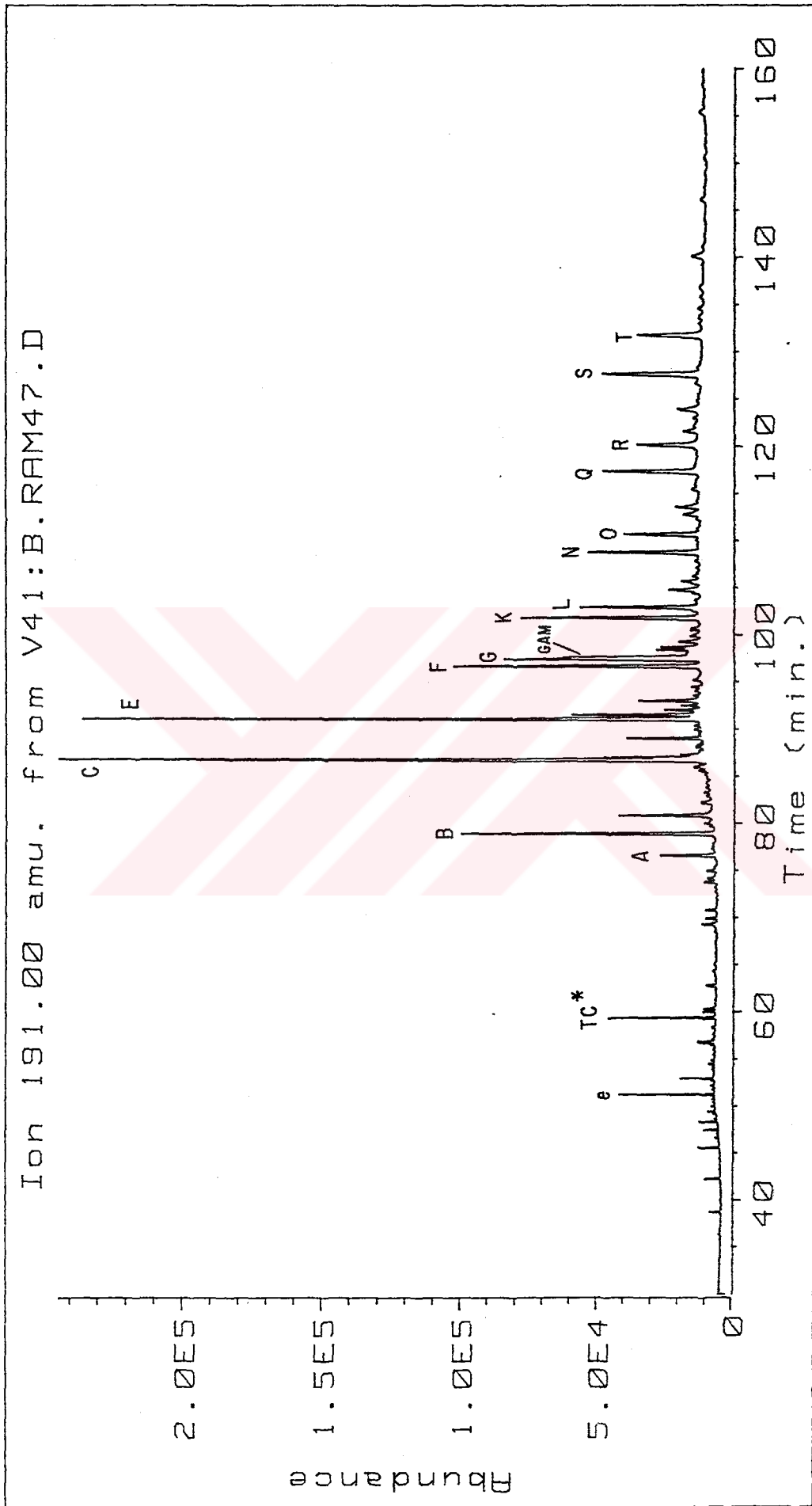


Figure-D.18 M/Z 191 mass fragmentogram of the Bati Raman_47 (BR47) oil.

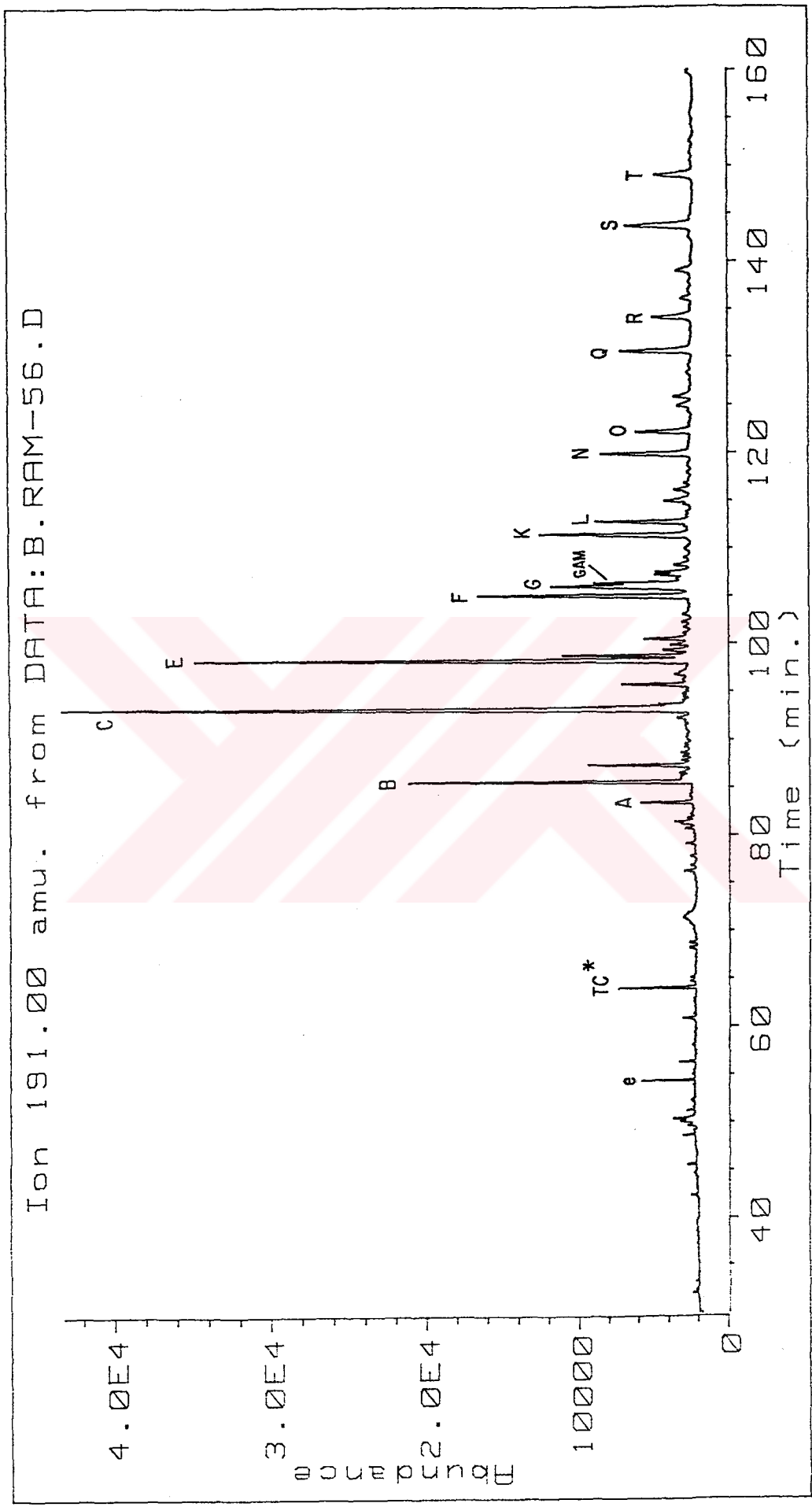


Figure-D.19 M/Z 191 mass chromatogram of the Bati Raman_56 (BR56) oil.

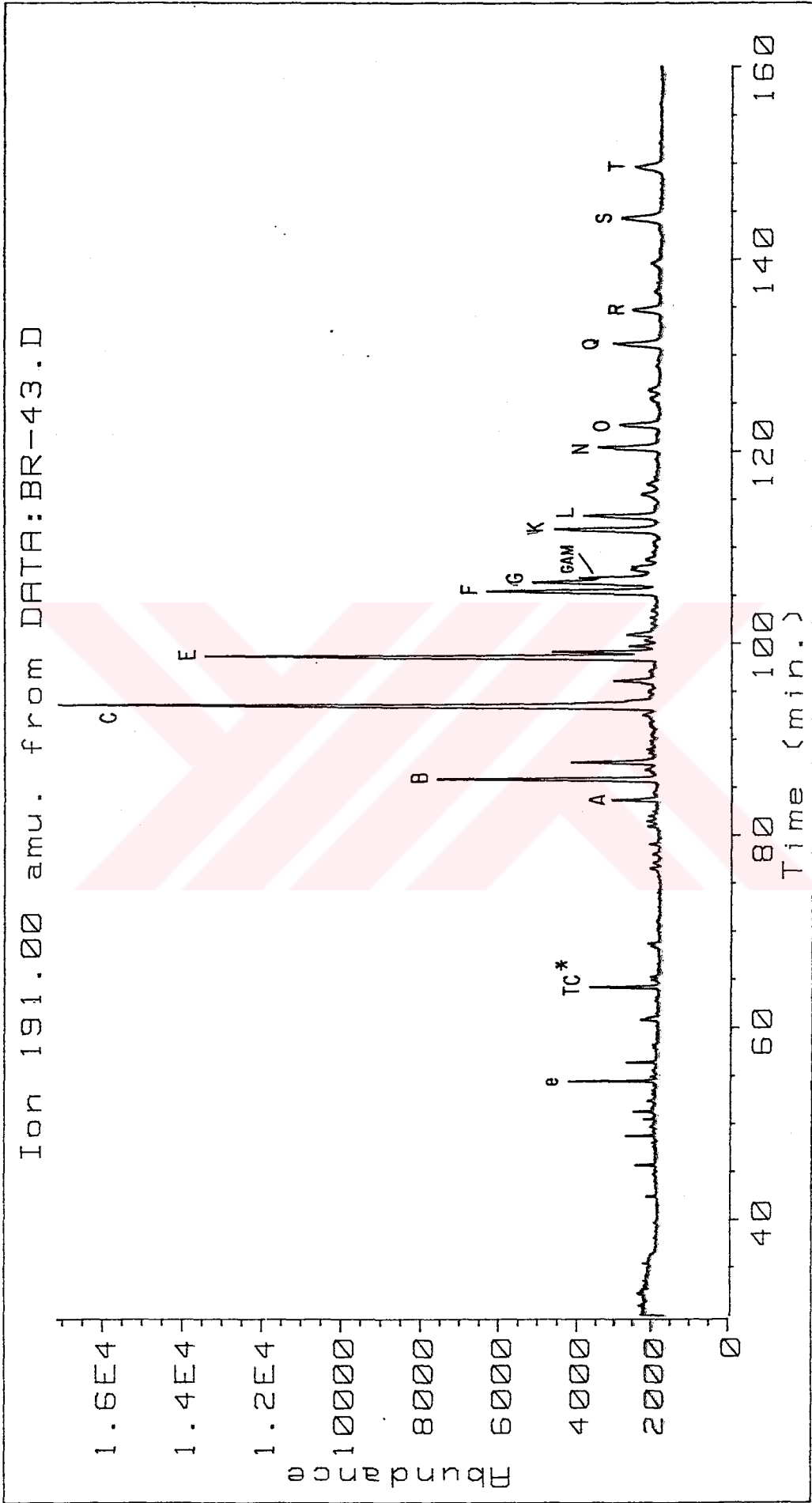


Figure -D.21 M/Z 191 mass fragmentogram of the Bati Raman_43 (BR43) oil.

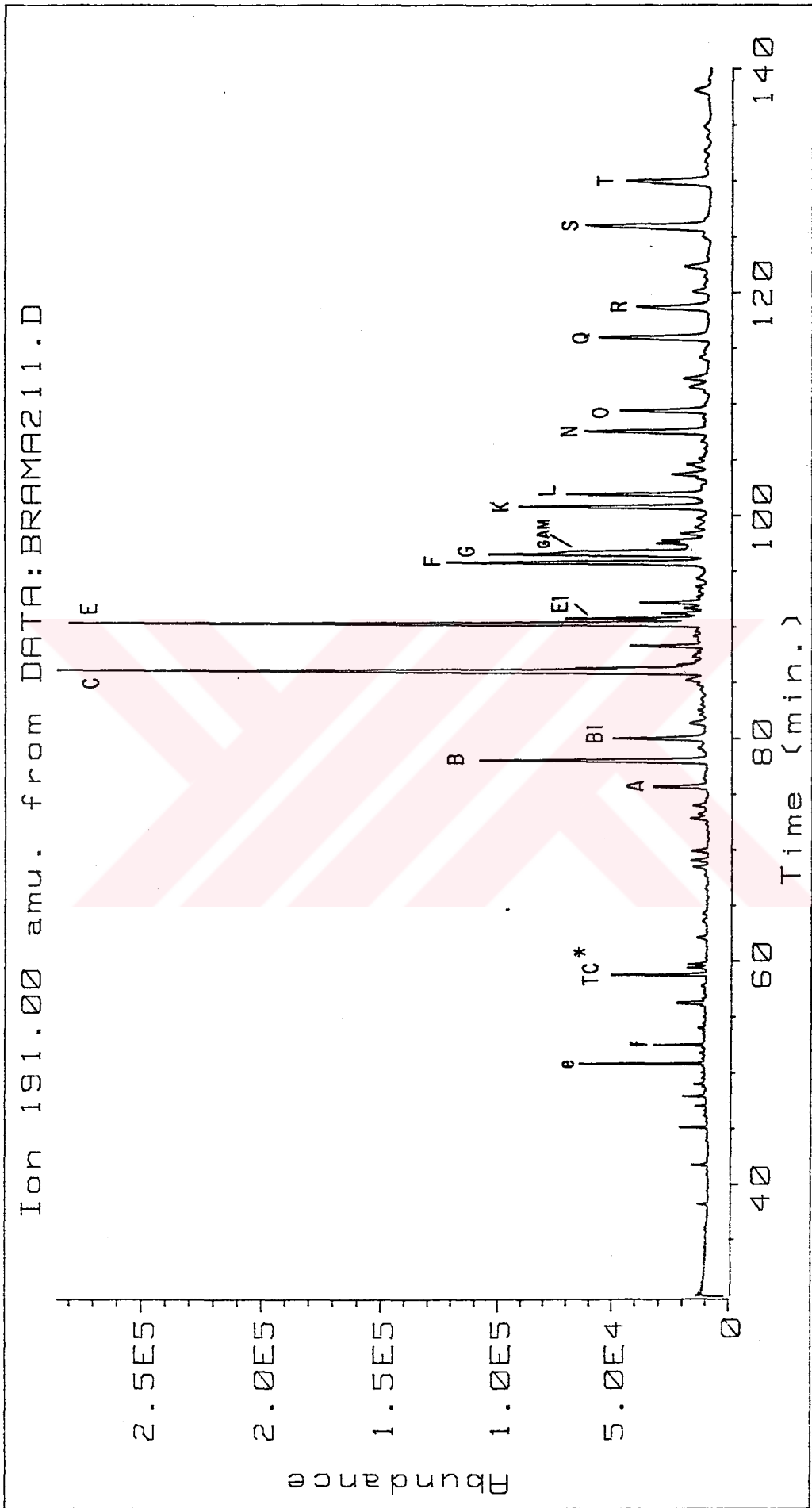


Figure .D.22 M/Z 191 mass fragmentogram of the Bati Raman_211 (BR211) oil.

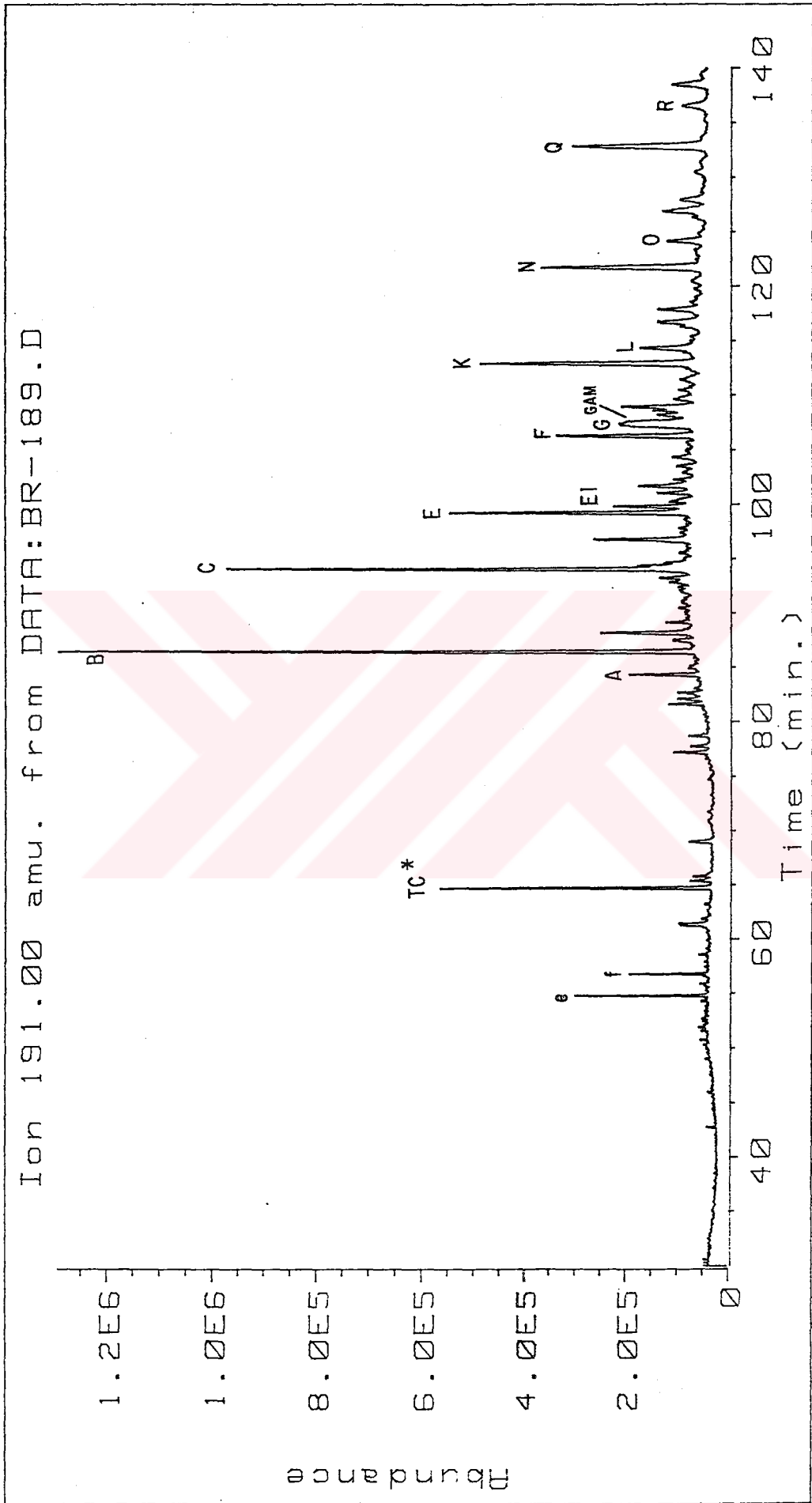
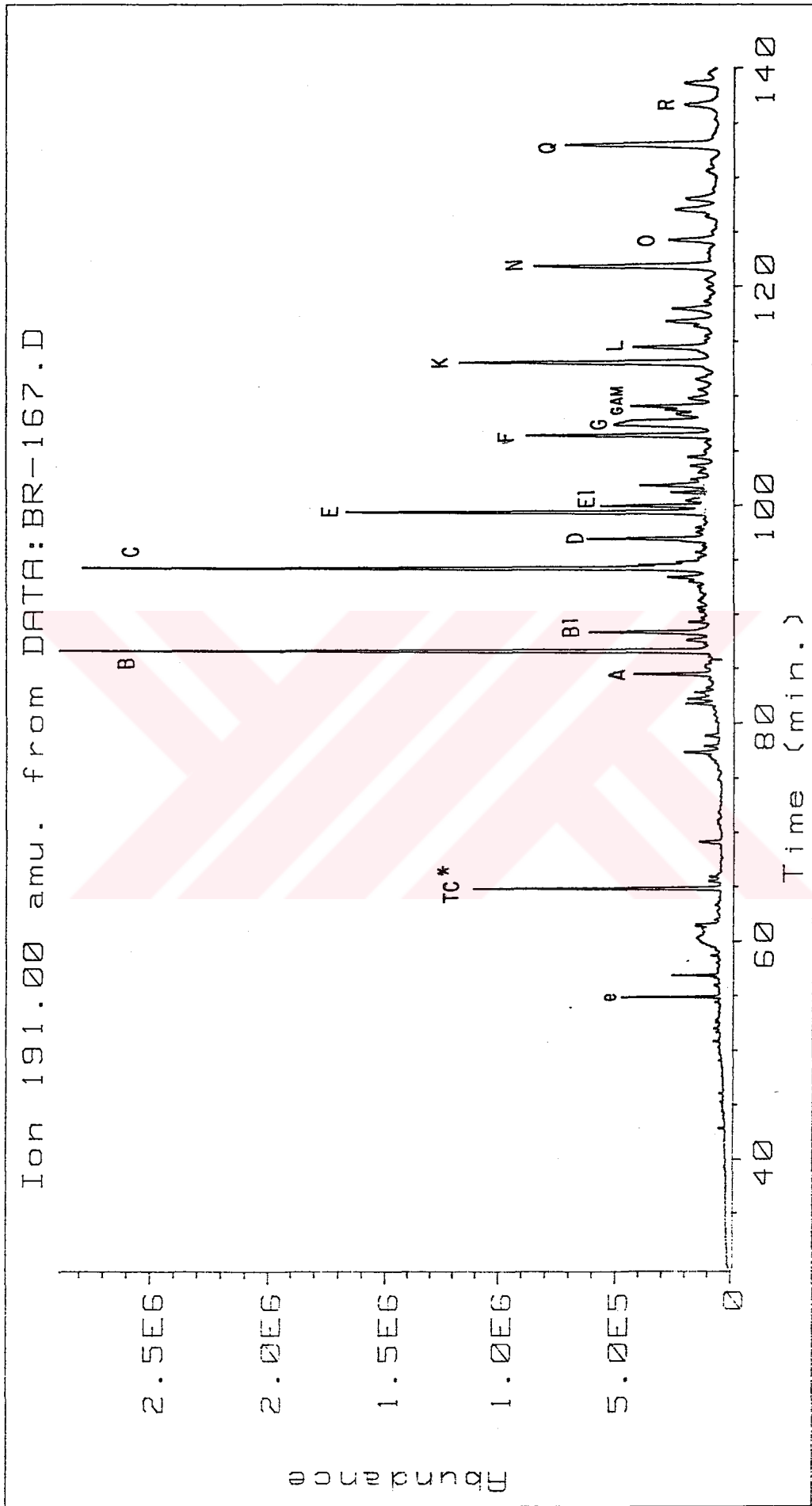


Figure D.23 M/Z 191 mass fragmentogram of the Bati Raman-189 (BR189) oil.



Figure_D.24 M/Z 191 mass fragmentogram of the Bati Raman_167 (BR167) oil.

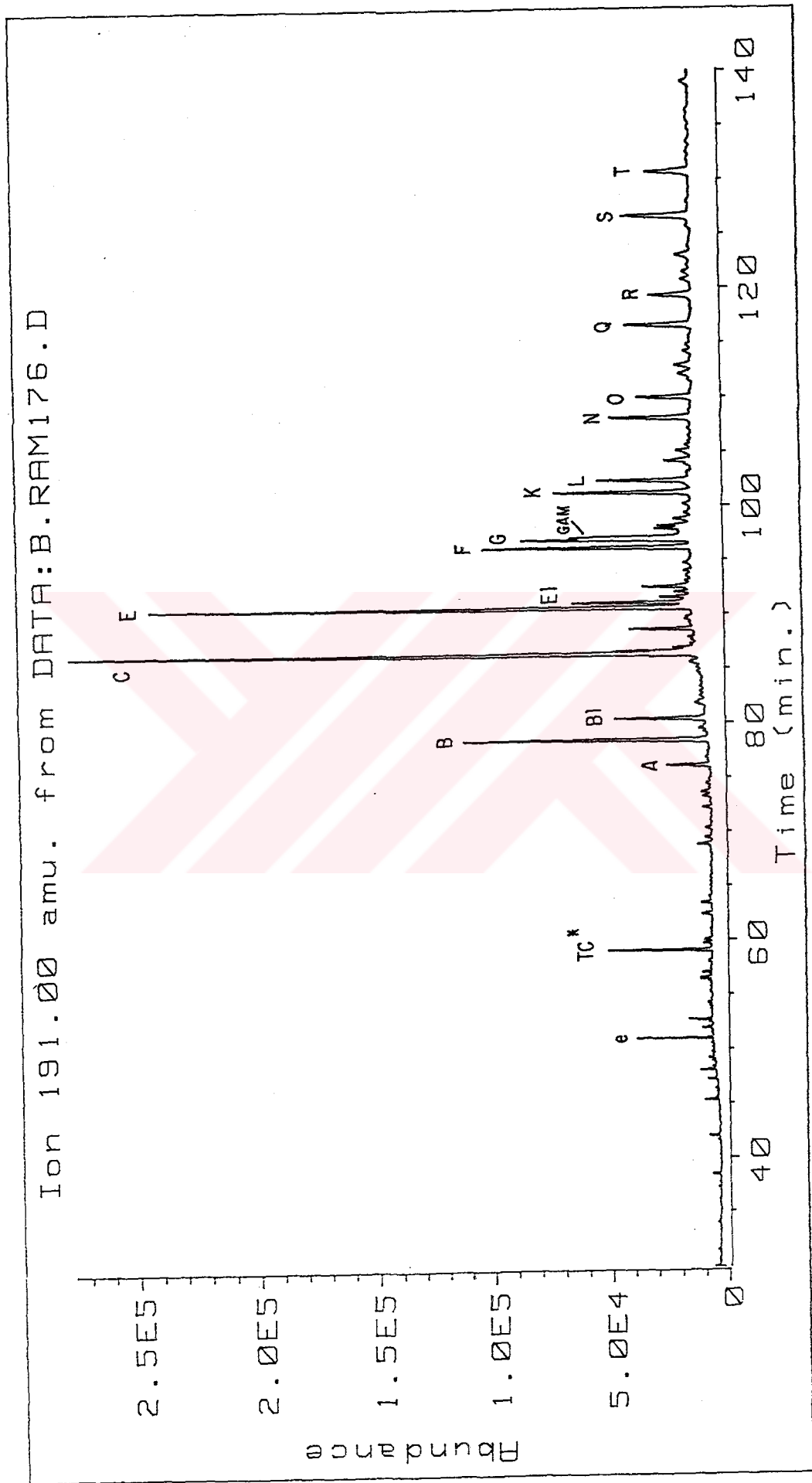
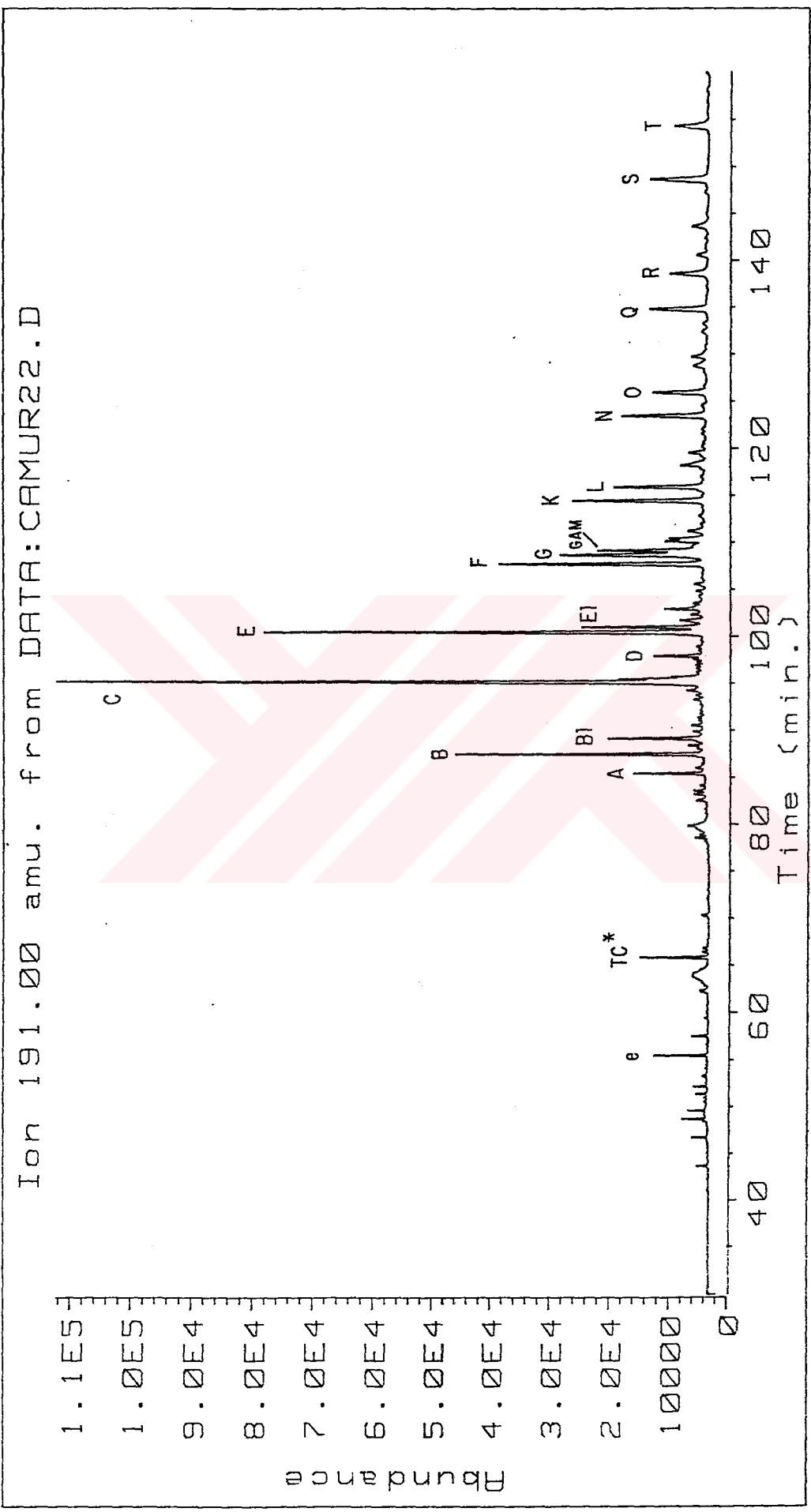
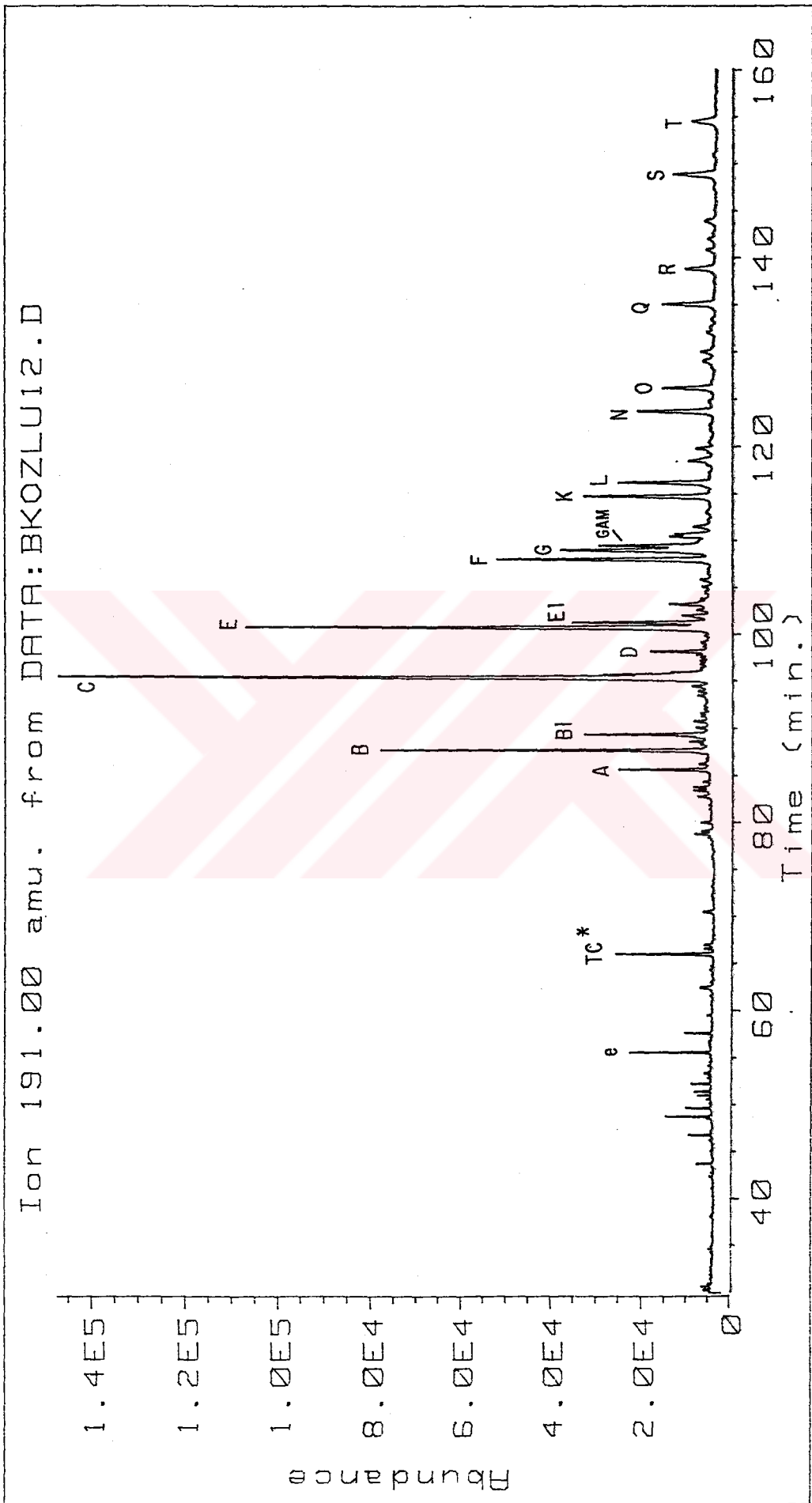


Figure - D.25 M/Z 191 mass fragmentogram of the Bati Raman-176 (BR176) oil.



Figure_D.26 M/Z 191 mass fragmentogram of the Çamurlu_22 (CA22) oil.



Figure_D.27 M/Z 191 mass chromatogram of the Batı Kozluca_12 (BK12) oil.

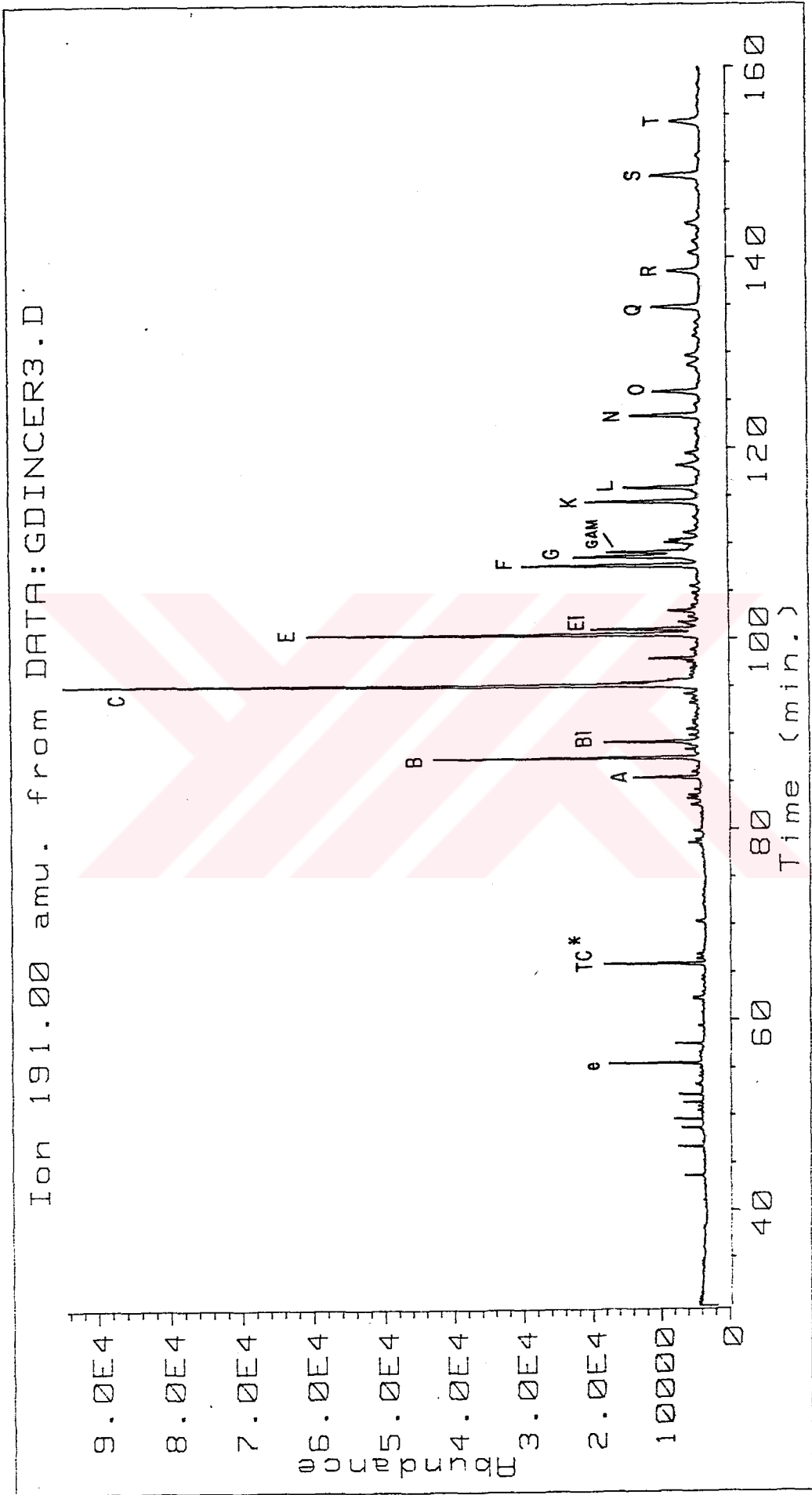
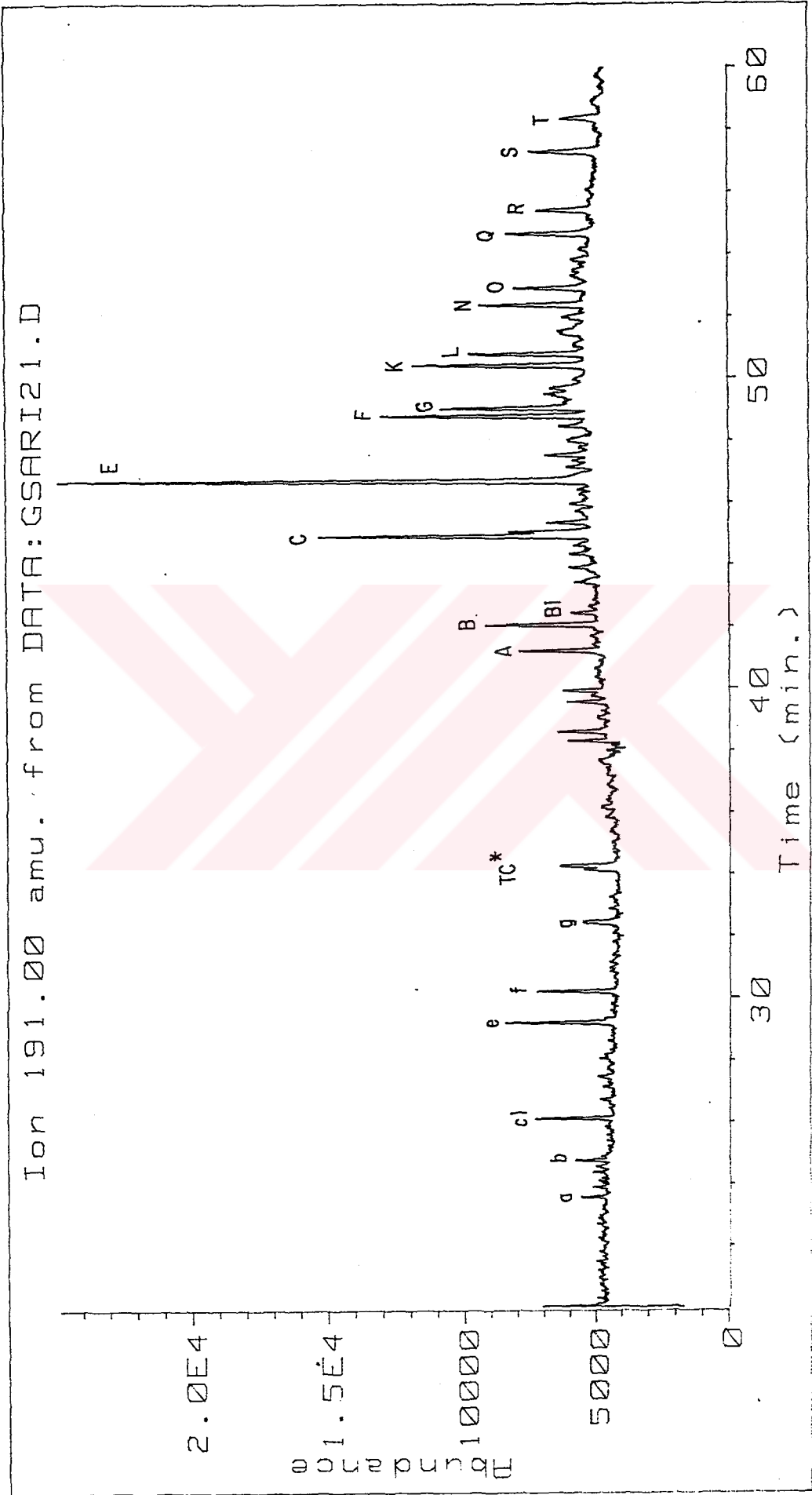
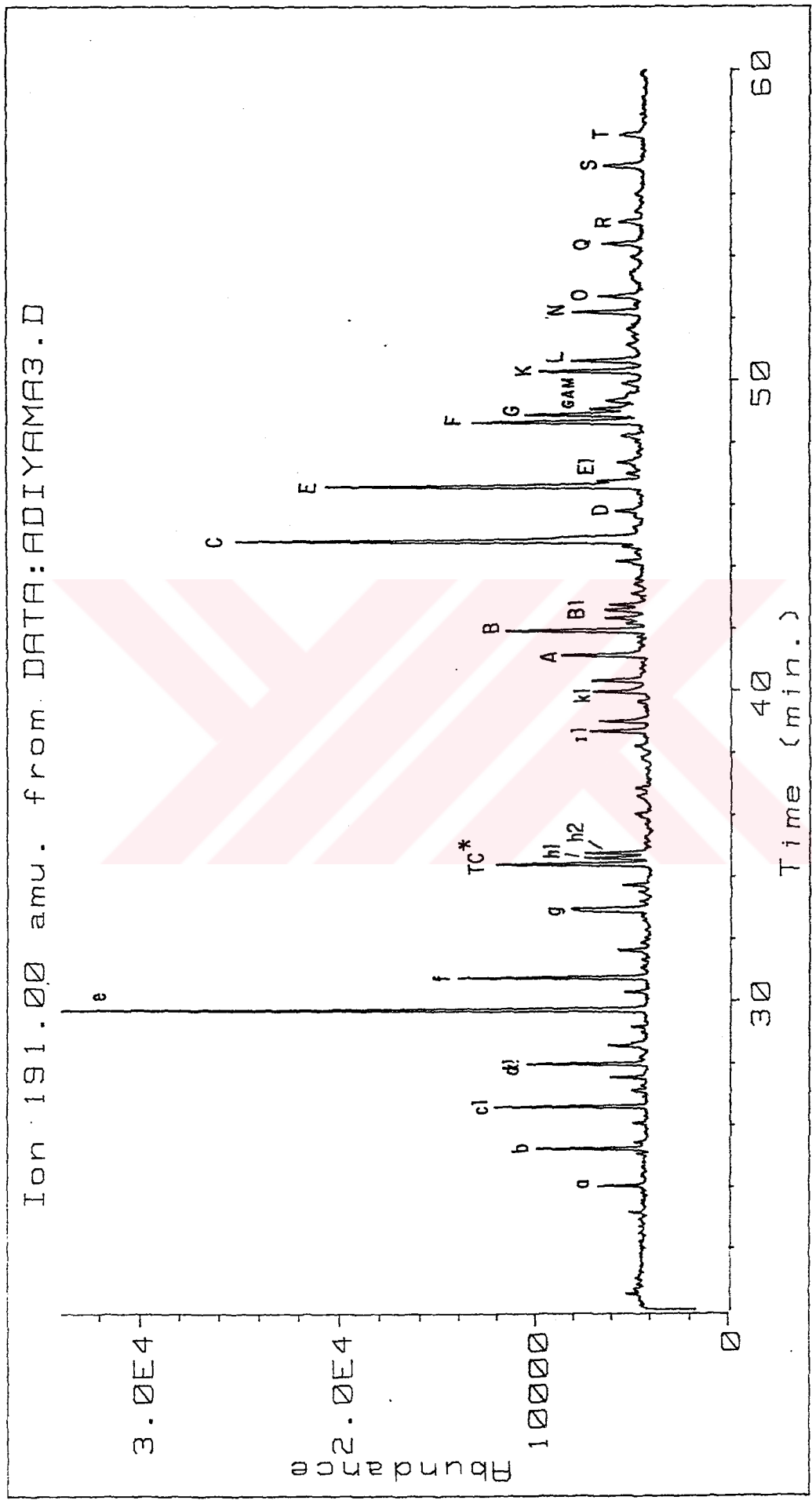


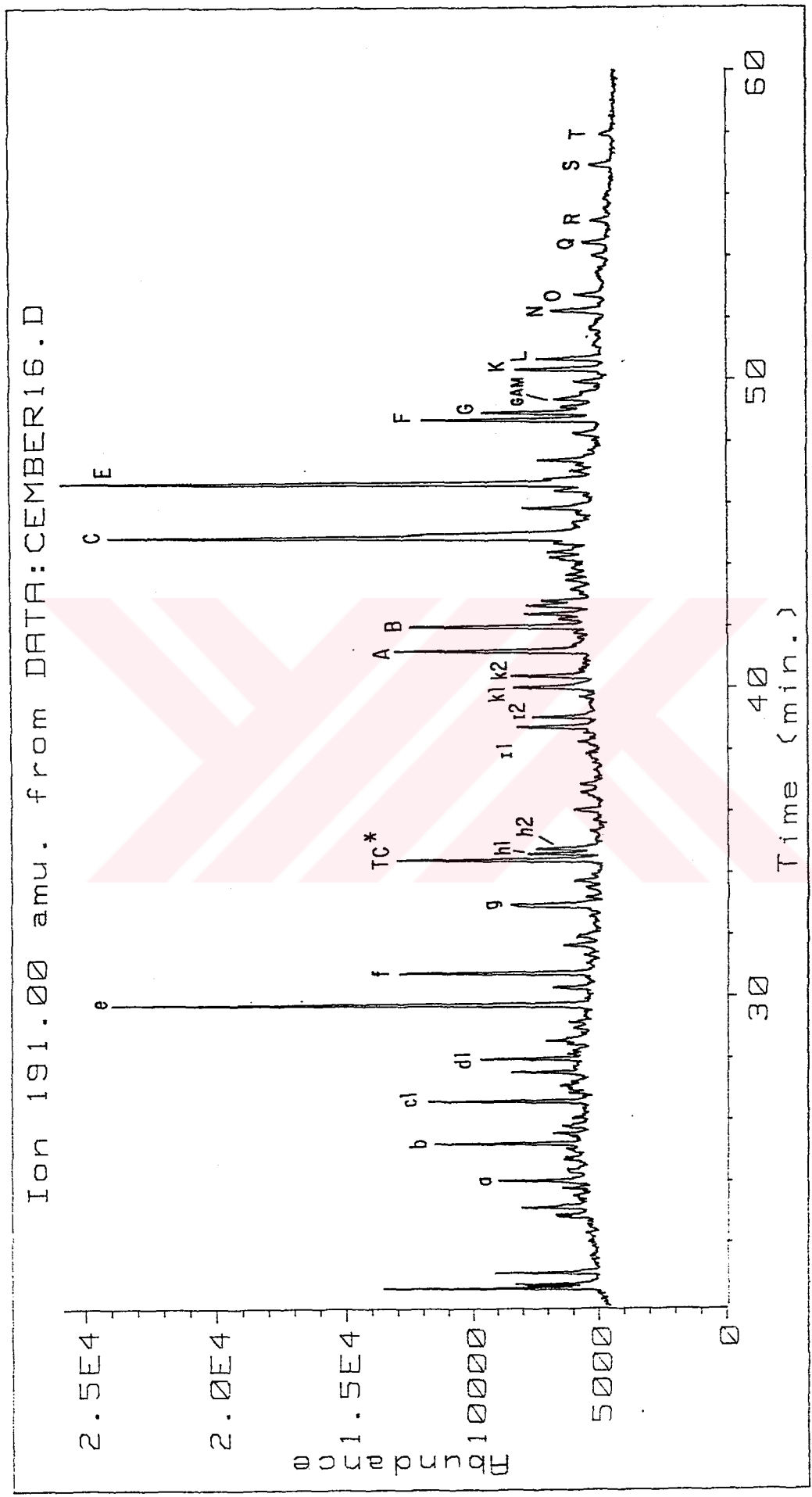
Figure _D.28 M/Z 191 mass fragmentogram of the Güney Dincer_3 (GD3) oil.



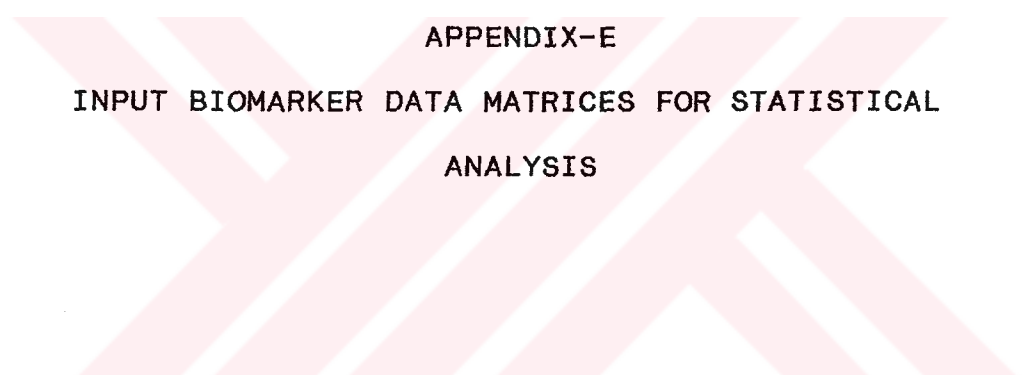
Figure_D.29 M/Z 191 mass fragmentogram of the Güney Sarıcaç_21 (GS21) oil.



Figure_D.30 M/Z 191 mass fragmentogram of the Adiyaman_3 (A3)oil.



Figure_D.31 M/Z 191 mass fragmentogram of the Çemberlitaş_16(CT16) oil.



APPENDIX-E
INPUT BIOMARKER DATA MATRICES FOR STATISTICAL
ANALYSIS

Table-E.1 Normalized molecular distribution of tri-tetra-pentacyclic terpanes.

OILS	a*	b	cl	dl.	e	f	g	TC*	hl+h2	kl+k2	ll+l2+	A	B	C	E	F+G+K+L+N+O+P Q+R+S+T
1 ÇE16	0.9	2.2	3.2	1.5	8.8	4.2	2	2.7	3	7	3.3	1.4	3.6	3.5	7.5	
2 BS4	0.8	1.6	3.1	1.2	5.9	3.7	1.7	2	2.6	4.6	2.4	2.6	6.5	7.8	20	
3 S30	0.4	1.1	2.4	1.2	5.8	3.1	1.9	1.9	2.3	4.7	2.2	3	8.1	9.4	20.4	
4 SI1	0.4	0.7	0.8	0.5	2.6	1.2	0.6	1.6	0.9	2.6	1.8	4.2	10.1	10.2	16.5	
5 KA2	0.7	1.4	3.5	1	5.8	3.8	1.7	0.4	2.8	3.3	1.1	3.1	7.1	8.5	19.7	
6 KUI	1.3	1.9	2.1	1	5.2	2.3	1	3.2	1.7	2.5	2.5	2.5	8.8	6.5	9.4	
7 BE1	0.6	1.1	2.2	1.1	5.4	3	1.6	2.2	2.4	6.2	3.5	3.3	9.1	9.4	14	
8 MA30	0.4	0.5	0.5	0.3	1.6	0.5	0.25	1.9	0.3	1.1	0.95	3.2	10.3	6.3	10.4	
9 GA15	0.5	0.7	0.9	0.5	2.5	1	0.5	2.1	0.7	1.9	1.4	3	9.9	7.5	14.6	
10 GE5	0.5	0.6	1	0.55	2.6	1.25	0.5	1.9	0.9	2.4	1.2	3.4	9.8	8.3	14.4	
11 R87	0.2	0.3	0.4	0.3	1.5	0.5	0.25	1.6	0.3	0.4	0.9	3.3	10.6	9.1	18.6	
12 RI92	0.25	0.3	0.4	0.35	1.7	0.5	0.3	1.9	0.4	0.4	0.8	3.4	10.5	8.7	18.7	
13 R63	0.2	0.35	0.35	0.4	1.8	0.6	0.2	1.8	0.4	0.6	0.8	2.9	10.4	7.8	16	
14 RI51	0.3	0.4	0.7	0.4	2.7	1	0.5	3.1	0.6	0.9	1.4	5.1	14.8	11.6	22.1	
15 RI97	0.25	0.4	0.6	0.4	2.5	0.9	0.5	2.2	0.7	0.9	1.6	4.7	10.2	8	14.6	
16 R84	0.15	0.15	0.2	0.1	1.3	0.45	0.3	1.5	0.3	0.5	0.9	3.9	10.8	7.1	10.1	
17 R93	0.15	0.2	0.3	0.3	1.3	0.45	0.2	1.5	0.5	0.4	0.8	3.6	10.8	7.2	14.4	
18 BR47	0.2	0.25	0.35	0.3	1.6	0.65	0.3	1.8	0.4	0.7	0.9	4.2	10.6	10.2	20.4	
19 BR56	0.15	0.15	0.2	0.4	0.9	0.3	0.2	1.3	0.2	0.5	0.9	4.8	10.5	8.2	16.2	
20 BR84	0.1	0.15	0.18	0.2	1	0.3	0.15	1.4	0.2	0.3	0.8	4.5	10.4	8.5	17.4	
21 BR43	0.2	0.4	0.5	0.4	1.5	0.5	0.3	1.25	0.2	0.4	0.8	3.8	9.8	7.5	12.4	
22 BR211	0.15	0.25	0.5	0.4	2.1	0.8	0.5	1.5	0.6	0.9	0.9	3.8	10.6	10.4	23.4	
23 BR189	0.15	0.1	0.1	0.1	2.3	1.3	0.5	4.6	0.7	1.4	1.2	10.6	7.6	4	15.9	
24 BR167	0.1	0.1	0.1	0.1	1.6	0.8	0.4	4.1	0.4	1	1.3	10.7	10.2	6	19.4	
25 BR176	0.15	0.2	0.25	0.25	1.3	0.4	0.2	1.8	0.3	0.4	0.75	4.2	10.7	9.2	16.3	
26 CA22	0.2	0.3	0.3	0.2	0.9	0.3	0.1	1.1	0.2	0.6	1.2	4.1	10.6	7.3	14.5	
27 BK12	0.3	0.4	0.45	0.35	1.4	0.5	0.25	1.7	0.2	0.7	1.5	5.5	10.7	7.8	14.1	
28 GD3	0.35	0.45	0.5	0.4	1.6	0.5	0.2	1.7	0.2	0.6	1.1	4.5	10.6	6.6	12.8	
29 GS21	0.4	0.6	1.3	0.2	1.9	1.4	1.6	0.1	1.6	3	1.4	1.9	4.5	8.8	17.6	
30 A3	0.8	2.6	2	9.7	3.2	1.3	2.6	2.6	2	2.6	1.4	2.4	6.8	5.3	11.6	
31 ÇE16	1.5	2.5	2.7	1.7	8	3.3	1.5	3.5	2.1	5	3.3	3	8	8.9	9.7	

*Corresponds to the peaks labelled in Figure 3.3 and described in Table 3.4.

Table_E.2 Normalized molecular distribution of tri_tetracyclic terpanes.

OILS	a*	b	cl	c2	c3	d1	d2	e	f	g	TC*	h1	h2
1 ÇE15	3.4	7.6	11.1	1.1	1.1	5.2	1.4	29.9	14.4	6.5	8.9	4.8	4.8
2 8S4	3.6	7.2	11.4	1.4	2.5	5.4	1.8	25.4	16.4	7.2	8.6	4.6	4.6
3 530	2.3	5.2	12.1	1.1	1.6	5.5	2.3	28.2	15.2	6.8	9.1	5.5	5.5
4 511	4.6	6.8	8.7	0.9	3.7	5.3	1.2	26.6	12.4	5.9	15.8	3.9	4.1
5 KA2	4.1	6.1	16.1	0.9	2.3	4.2	1.8	26.2	17.5	7.8	0.9	6.1	5.9
6 KUI	6.2	9.3	10.1	1.1	3.4	5.1	1.1	24.5	11.1	4.8	16.1	3.7	3.7
7 BE1	3.1	5.3	10.6	2.8	5.3	5.3	1.6	25.2	14.1	7.4	10.3	4.3	5.1
8 MA30	6.4	8.1	7.4	1.1	3.7	4.1	1.3	23.2	8.1	3.7	28.3	2.4	2.4
9 GA15	5.5	7.1	9.1	1.3	2.9	5.2	1.6	25.2	10.6	3.5	21.1	3.5	3.5
10 GE5	4.9	6.1	9.7	1.3	2.3	5.5	1.3	24.5	12.1	5.2	18.1	4.5	4.5
11 R87	3.2	4.2	5.8	1.3	3.8	4.8	1.9	25.3	8.3	3.8	31.7	2.9	2.9
12 R192	3.8	4.4	6.2	1.1	4.1	5.4	2.2	26.3	8.6	3.8	28.6	2.8	2.6
13 R63	3.7	4.7	6.2	0.9	3.7	5.3	2.2	26.5	9.1	4.1	27.3	3.4	2.8
14 R193	5.2	5.5	6.7	1.2	4.3	4	2.2	28.4	10.7	5.2	22.1	2.2	2.4
15 R151	2.9	4.2	6.2	1.3	3.9	5.2	1.9	25.6	8.9	4.2	29.8	2.9	2.9
16 R197	3.3	5.2	7.7	1.1	3.9	9.6	4.1	31.6	11.4	4.1	14.3	1.8	1.8
17 R84	2.8	3.8	5.6	0.9	3.1	5.1	2.2	26.6	9.4	5.6	30.7	2.8	2.2
18 R93	3.1	4.3	5.6	0.9	4.1	5.8	1.9	26.3	8.6	4.3	30.6	1.9	2.8
19 BR47	3.2	4.4	5.7	1.2	4.1	5.3	2.3	25.2	9.1	4.4	28.4	3.2	3.2
20 BR56	3.3	4.2	5.4	2.9	6.3	3.8	1.7	22.5	7.1	5.4	33.3	2.1	2.1
21 BR84	3.2	4.1	4.6	0.9	3.7	4.6	1.8	25.3	6.9	3.2	36.9	2.3	2.3
22 BR43	3.5	6.6	9.2	1.3	3.9	6.1	2.2	26.6	9.2	5.2	21.8	2.2	2.2
23 BR211	2.5	3.7	6.5	0.6	2.5	5.5	2.5	28.6	11.4	6.2	21.5	4.3	4.3
24 BR189	0.5	0.5	0.5	0.5	0.5	0.5	0.5	23.2	13.6	5.1	47.7	3.6	3.6
25 BR167	0.5	0.5	0.5	0.5	0.5	0.5	0.5	21.8	10.4	33.6	55.4	2.6	2.6
26 BR176	2.1	3.6	5.1	1.1	3.6	5.1	1.8	25.4	7.6	3.6	34.9	2.8	2.5
27 ÇA22	5.4	6.9	7.2	1.1	4.7	5.8	1.8	23.2	7.2	3.6	29.1	2.2	1.8
28 8K12	4.9	6.9	7.5	1.4	4.9	5.8	2.1	22.8	7.9	3.5	27.3	2.6	2.3
29 603	5.4	6.8	7.7	1.2	5.1	6.3	1.8	24.7	7.4	2.9	27.1	1.8	1.8
30 6S21	5.2	6.7	15.9	2.1	2.1	2.8	2.1	21.6	15.9	7.2	0.01	6.7	11.9
31 A3	2.9	6.9	9.5	0.7	2.2	7.3	1.8	35.4	11.7	4.7	9.5	3.6	3.6
32 ÇT16	5.3	9.1	9.9	0.7	4.1	5.9	1.7	27.1	11.7	5.3	12.3	4.1	3.3

* Corresponds to the peaks labelled in Figure 3.3 and described in Table 3.4.

Table_E.3 Normalized molecular distribution of pentacyclic terpanes.

OILS	A*	B	BI	C	D	E	E1	F	G	H	K	L	N	O	Q	R	S	T
1 GE16	16.2	7.3	1.1	16.8	0.8	16.2	2.1	0.6	10.5	5.3	5.9	5.3	5.1	2.2	1.7	1.1	1.1	0.8
2 BS4	5.9	6.4	1.1	16.1	0.7	19.1	0.7	1.1	11.1	7.4	8.1	5.7	4.4	3.1	3.1	1.7	3.1	1.7
3 S30	5.2	6.8	1.1	17.8	1.1	21.1	1.1	0.7	11.3	7.1	7.4	5.1	4.3	2.5	2.5	1.4	2.5	1.4
4 S11	3.9	9.1	2.4	21.6	2.2	22.1	1.5	1.7	9.1	6.5	6.3	3.9	3.9	1.7	1.5	0.9	1.3	0.6
5 KA2	7.5	6.1	1.8	16.4	1.2	19.6	0.2	2.1	9.4	8.7	8.1	5.1	4.8	3.1	2.8	1.8	2.3	1.4
6 KUI	7.9	8.2	1.9	27.8	1.6	20.9	1.6	1.3	7.6	5.1	4.4	2.2	2.5	1.6	1.6	1.3	1.6	0.9
7 BE1	8.6	8.1	1.5	22.1	1.5	23.1	1.1	1.2	10.1	5.6	5.8	3.9	2.4	1.5	1.2	0.7	1.2	0.5
8 MA30	3.1	9.8	3.3	30.6	2.1	19.1	2.7	0.6	8.1	5.6	4.8	3.1	2.7	1.5	1.5	0.9	1.2	0.6
9 GA15	3.7	7.9	2.1	25.4	1.3	19.6	2.1	0.8	8.6	6.1	5.8	3.9	3.7	2.1	2.4	1.3	2.1	1.3
10 GE12	3.1	8.5	2.3	24.6	1.5	20.9	2.5	0.8	8.5	5.5	5.8	3.8	3.5	2.1	2.1	1.3	2.3	1.3
11 R87	1.9	6.9	4.6	21.9	2.1	19.1	3.8	1.5	8.1	5.6	5.4	3.5	3.5	2.3	2.9	1.9	3.1	2.1
12 R192	1.7	7.3	2.8	22.3	2.1	18.5	4.5	1.5	7.9	6.2	5.5	3.6	3.6	2.3	2.9	1.9	3.2	2.1
13 R63	1.9	7.1	2.6	25.1	2.2	19.1	3.6	1.2	8.2	6.1	5.3	3.4	3.4	2.2	2.9	1.7	2.9	1.9
14 R151	2.1	7.9	3.1	23.7	2.3	18.6	6.7	1.4	7.4	5.3	5.1	3.3	3.1	1.9	2.6	1.4	2.6	1.6
15 R197	3.6	10.5	4.1	23.1	2.3	18.2	4.3	1.6	8.4	5.5	5.2	3.6	3.1	1.6	1.8	0.9	1.6	0.9
16 R84	2.4	10.6	4.1	29.1	1.9	19.2	4.6	1.3	7.3	5.4	4.3	2.7	2.2	1.4	1.1	0.8	1.1	0.5
17 R93	2.1	9.3	2.6	27.9	1.6	18.4	4.1	1.1	7.5	4.9	4.7	3.1	2.8	1.8	2.3	1.3	2.1	1.3
18 BR47	1.8	8.5	3.1	20.9	2.4	19.9	3.9	2.1	8.1	6.1	5.9	1.8	3.5	2.4	3.1	2.1	3.1	2.1
19 BR56	1.9	10.5	3.6	22.3	2.4	17.6	4.3	1.5	7.5	4.9	5.4	3.4	3.2	1.9	2.6	1.3	2.4	1.3
20 BR84	1.8	9.1	3.2	21.1	2.1	17.1	4.1	1.4	8.1	5.5	5.9	4.1	4.1	2.6	3.2	2.1	3.1	2.1
21 BR43	2.1	9.8	4.1	25.8	1.9	19.7	4.1	1.1	7.4	5.3	4.5	3.5	2.7	1.9	2.1	1.3	1.9	1.1
22 BR211	1.7	7.1	2.8	19.5	2.2	19.1	3.7	1.8	7.9	6.4	5.7	4.2	3.7	2.6	3.3	2.1	3.7	2.6
23 BR189	2.7	23.8	3.7	17.3	3.6	9.1	2.5	1.6	5.2	2.5	8.1	1.8	5.8	1.1	4.9	0.9	5.2	0.9
24 BR167	2.5	20.6	3.7	19.4	3.7	11.5	3.1	1.9	5.8	2.9	7.9	2.3	5.6	1.3	4.8	1.1	5.1	1.1
25 BR176	1.7	9.1	3.3	23.1	2.4	20.1	4.1	1.5	7.8	6.3	5.1	3.3	2.8	2.1	2.4	1.5	2.4	1.5
26 CA22	2.6	9.7	3.6	24.9	1.7	17.1	4.5	1.4	8.1	5.4	5.2	3.5	3.3	1.9	2.1	1.4	2.1	1.4
27 BK12	3.3	12.1	4.4	23.3	2.1	16.7	4.6	1.1	7.7	4.8	4.6	3.3	2.6	1.8	2.1	1.1	1.5	0.9
28 GD3	2.8	11.4	4.1	26.6	2.1	16.7	4.6	1.1	7.6	4.6	4.8	3.1	2.8	1.8	2.1	1.3	2.1	1.1
29 GS21	4.1	5.4	0.3	12.9	0.6	24.9	0.01	2.1	9.7	6.6	8.3	5.4	4.7	3.4	4.1	2.6	3.2	1.7
30 A3	4.9	8.2	2.1	23.1	1.3	18.2	1.5	1.1	10.1	6.2	5.9	4.1	3.9	2.3	2.3	1.3	2.3	1.3
31 CT16	9.2	8.5	2.8	21.7	2.8	24.5	0.9	2.1	8.5	4.8	3.9	3.1	2.5	1.4	1.1	0.8	0.8	0.6

* Corresponds to the peaks labelled in Figure 3.3 and described in Table 3.4.

Table E.4 Normalized molecular distribution of steranes.

OILS	I*	II	III	IV	V	1	2	8	9	10	11	15	16	17	18	19	20	21	22
1 CE16	0.78	3.52	7.94	1.04	4.04	7.16	4.56	5.21	10.29	6.77	5.86	2.99	7.29	8.59	4.04	3.78	5.60	6.38	4.17
2 S5	10.00	4.05	5.95	0.81	2.16	4.59	2.70	4.59	8.11	5.14	5.14	2.97	6.76	7.57	4.32	5.14	7.57	7.57	4.86
3 8S4	0.81	6.03	9.93	0.98	4.07	6.19	4.07	5.37	9.28	6.68	5.54	3.26	6.84	7.00	4.23	4.07	5.37	6.03	4.23
4 S30	0.66	3.98	8.09	1.06	4.11	4.64	2.92	5.31	10.61	6.90	6.10	3.05	7.03	7.96	4.51	4.91	6.37	6.50	5.31
5 S11	4.66	1.93	5.46	0.68	3.07	3.30	1.71	5.92	9.67	6.83	6.71	2.50	6.60	7.39	4.32	6.37	8.08	7.96	6.83
6 KA2	1.17	6.61	14.40	1.17	5.06	6.81	4.47	3.11	7.78	7.39	3.89	1.75	7.39	4.86	1.75	3.11	8.75	7.20	3.31
7 KUI	1.25	6.00	21.25	2.50	5.25	5.75	3.50	4.25	8.00	6.00	5.50	2.25	4.75	4.50	2.00	3.50	5.00	4.25	4.50
8 BE1	2.30	3.25	7.32	0.81	3.39	4.20	2.71	6.10	10.16	7.32	6.78	3.39	7.45	7.45	4.20	4.88	6.78	6.37	5.15
9 MAS0	0.50	2.15	13.41	2.98	5.13	1.99	1.32	4.47	7.45	5.79	6.29	2.98	5.30	5.79	3.15	6.29	8.28	8.11	8.61
10 GA15	0.80	2.87	11.32	2.07	3.99	3.19	2.07	4.94	8.93	6.22	6.38	2.71	6.06	6.54	3.19	5.58	7.97	7.97	7.18
11 GE5	0.43	3.76	10.71	1.59	4.78	3.91	2.32	4.92	10.27	5.79	6.08	2.75	5.21	6.08	3.33	5.50	7.67	8.25	6.66
12 R87	1.02	1.28	12.29	3.97	6.40	1.54	1.15	3.97	6.66	4.74	6.27	2.30	4.87	5.63	3.33	7.17	9.09	9.99	8.32
13 R192	0.29	1.46	13.68	4.08	6.84	1.60	1.02	4.08	6.55	4.80	5.68	2.62	4.66	5.82	3.20	6.99	9.02	9.46	8.15
14 R63	1.05	1.64	14.05	5.53	6.88	1.49	1.05	3.89	5.68	4.63	5.98	2.09	4.78	5.68	3.29	6.58	8.82	9.27	7.62
15 R151	0.97	1.39	13.47	4.86	7.08	1.94	1.25	3.89	6.39	4.58	6.39	2.36	4.58	5.83	2.78	6.81	8.33	9.72	7.36
16 R197	2.72	1.29	8.80	1.94	3.62	1.81	1.16	4.53	8.80	5.56	6.08	3.10	5.82	7.12	4.53	6.99	9.18	9.18	7.76
17 R84	0.32	0.97	8.44	2.16	4.11	1.30	0.87	4.55	7.79	5.74	6.49	2.92	6.06	6.60	4.55	7.58	10.06	10.06	9.42
18 R93	0.51	0.89	12.47	2.67	4.33	1.15	0.76	4.07	7.38	5.47	6.23	2.54	5.34	6.36	4.07	7.51	9.92	9.92	8.40
19 BR47	0.22	1.23	11.22	3.25	6.62	2.69	1.80	4.15	6.62	5.27	5.72	2.24	4.83	5.72	2.81	7.52	9.43	10.21	8.42
20 BR56	0.72	0.57	8.45	2.15	3.58	1.29	1.00	4.44	7.88	6.30	6.59	3.01	5.16	6.59	3.44	8.31	10.46	11.17	8.88
21 BR84	0.71	0.71	10.09	2.56	4.26	0.85	0.57	4.55	7.24	5.54	6.39	2.98	5.11	6.39	3.55	8.38	10.09	10.23	9.80
22 BR43	0.40	1.40	9.62	3.01	4.01	1.20	1.20	5.21	8.22	5.41	6.21	3.41	6.21	6.21	4.01	7.01	9.62	9.62	8.02
23 BR211	0.46	1.74	10.88	2.66	1.74	3.70	2.43	4.63	7.52	5.67	5.56	2.66	5.67	6.37	3.47	7.18	9.26	9.84	8.56
24 BR189	0.12	1.10	9.67	2.45	4.04	1.22	0.73	4.16	7.47	6.24	6.49	2.45	5.39	7.10	3.43	8.57	11.26	12.48	5.63
25 BR167	0.13	0.50	7.57	2.02	3.78	0.76	0.50	4.16	7.94	6.31	6.81	2.90	5.30	7.19	3.66	9.08	11.60	13.11	6.68
26 BR176	1.02	1.02	11.17	3.61	7.56	1.24	0.90	4.40	6.43	5.19	6.43	2.60	4.40	5.42	3.39	7.11	9.71	9.93	8.47
27 CR22	0.77	1.16	9.02	2.19	3.48	0.64	0.52	4.77	7.35	6.44	7.35	3.22	5.28	6.70	3.61	8.38	10.57	10.70	7.86
28 KR12	1.30	1.30	10.60	2.83	4.48	1.18	0.82	5.06	7.66	5.89	6.95	3.18	5.30	6.48	3.42	7.30	9.19	9.89	7.18
29 GD3	1.11	1.43	13.95	3.96	5.55	0.79	0.63	4.60	6.97	6.02	6.97	2.69	4.91	6.50	3.01	6.66	9.03	9.19	6.02
30 GS21	0.50	3.63	6.44	0.66	3.47	6.60	3.96	4.95	11.55	5.28	5.61	3.47	3.30	5.28	2.64	6.77	10.73	8.25	6.93
31 A3	3.50	2.32	13.43	2.65	6.30	1.99	0.83	5.47	8.79	7.46	7.30	3.48	7.63	7.79	4.81	3.81	5.31	5.80	4.31
32 CR16	2.75	1.85	10.07	1.68	3.69	2.35	1.51	5.37	7.38	6.38	6.71	2.52	6.21	7.05	3.69	4.19	5.87	6.88	3.86

*Corresponds to the peaks labelled in Figure 3.4 and described in Table 3.5.



APPENDIX-F

COMPILATION OF M/Z 217 (STERANE) MASS FRAGMENTOGRAMS OF
BRANCH/CYCLIC FRACTION OF THE TURKISH OILS

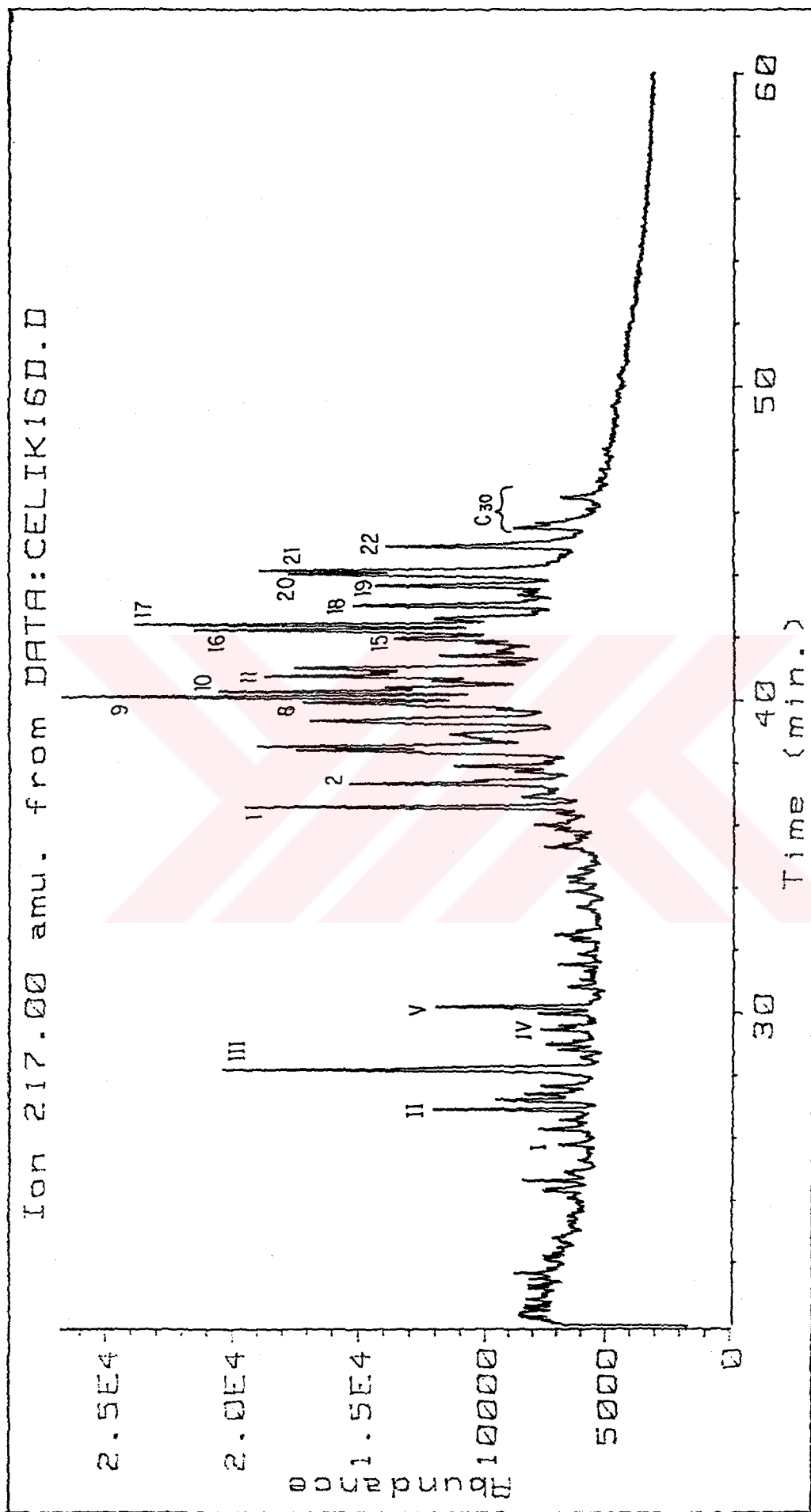


Figure-F.1 M/Z 217 mass fragmentogram of the Çelikli_16 (ÇE16) oil.

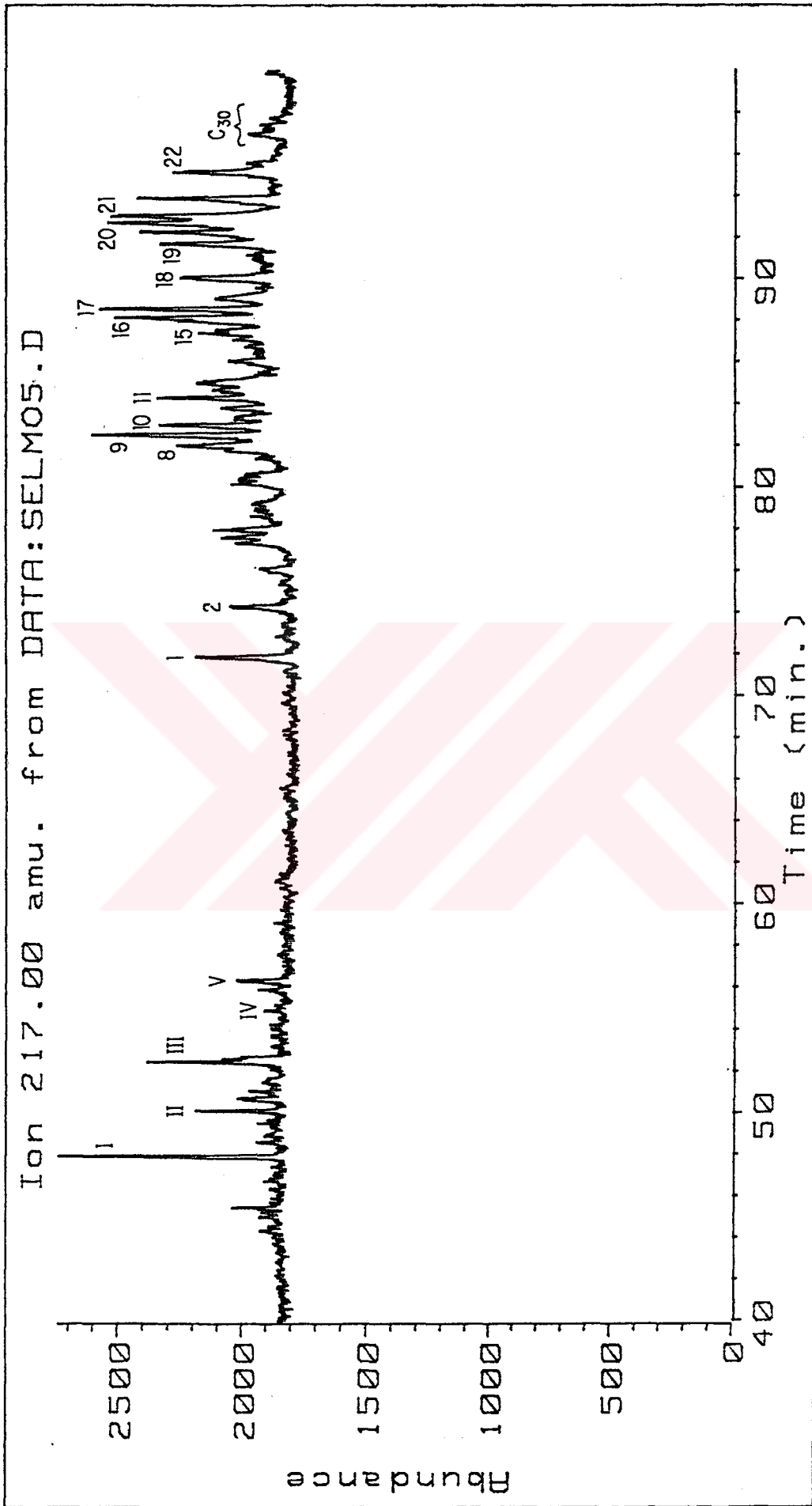


Figure-F.2 M/Z 217 mass fragmetogram of the Selmo_5 (S5) oil.

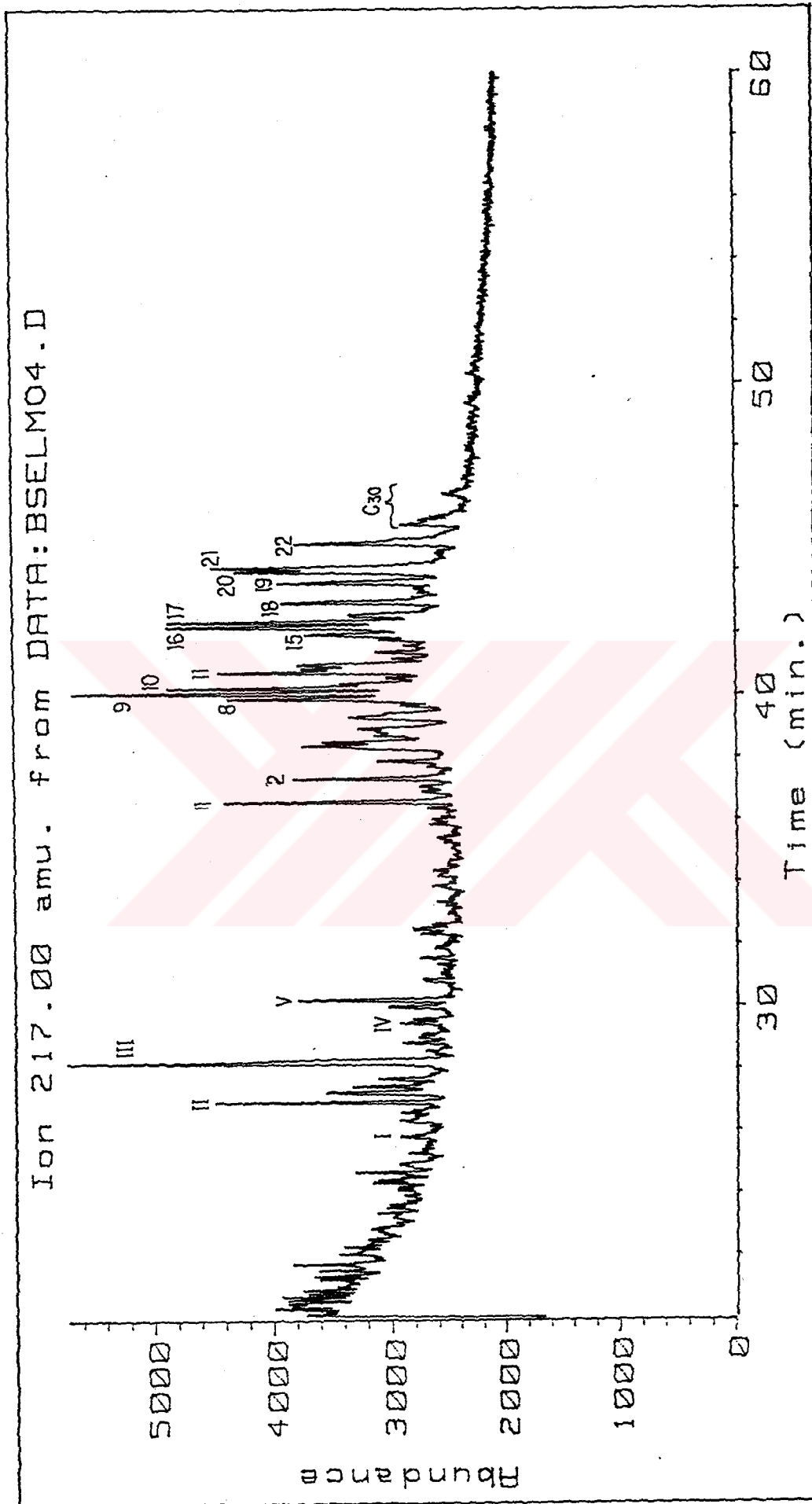


Figure - F.3 M/Z 217 mass fragmentogram of the Batı Şelmo_4 (BS4) oil.

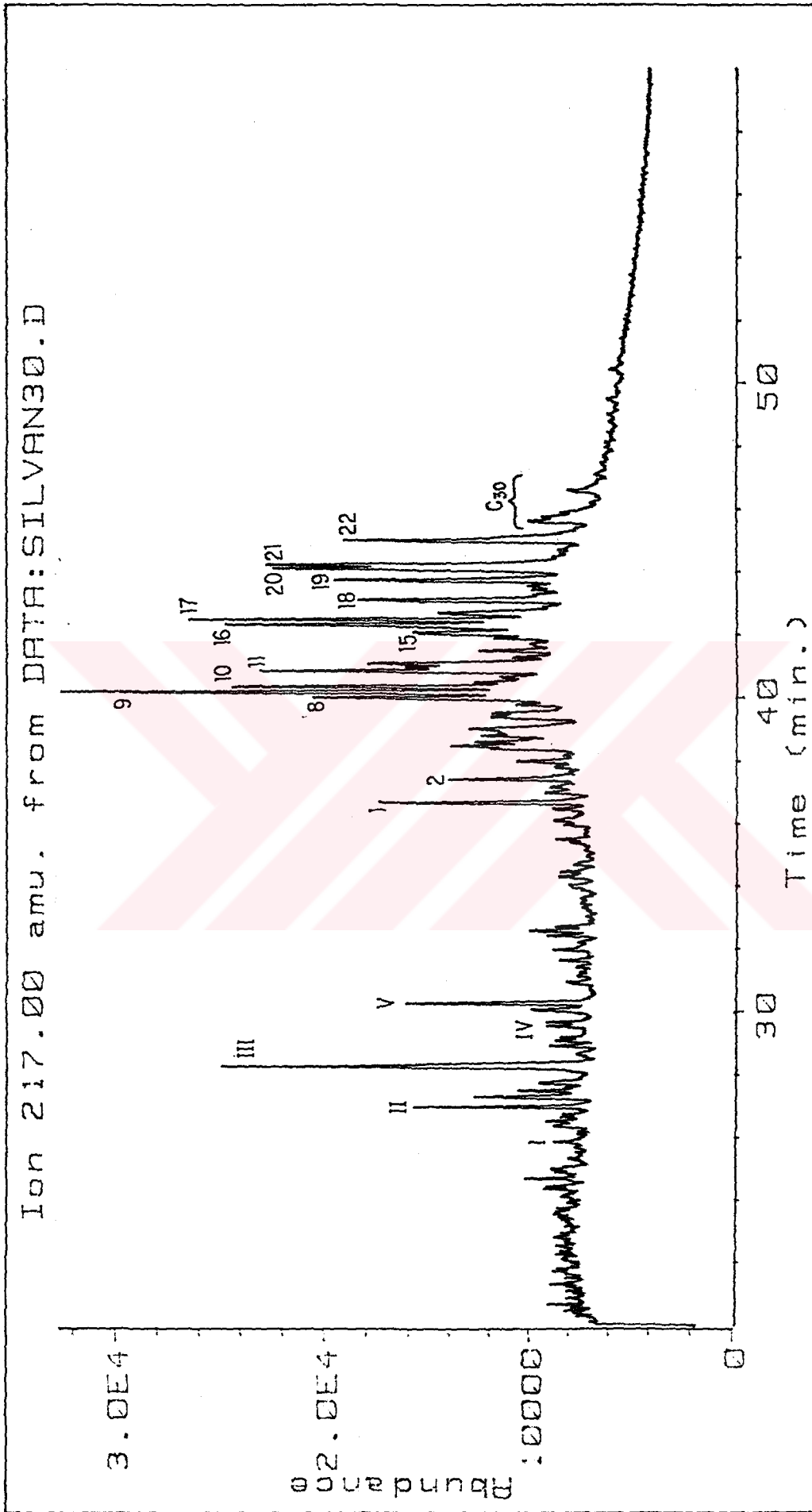
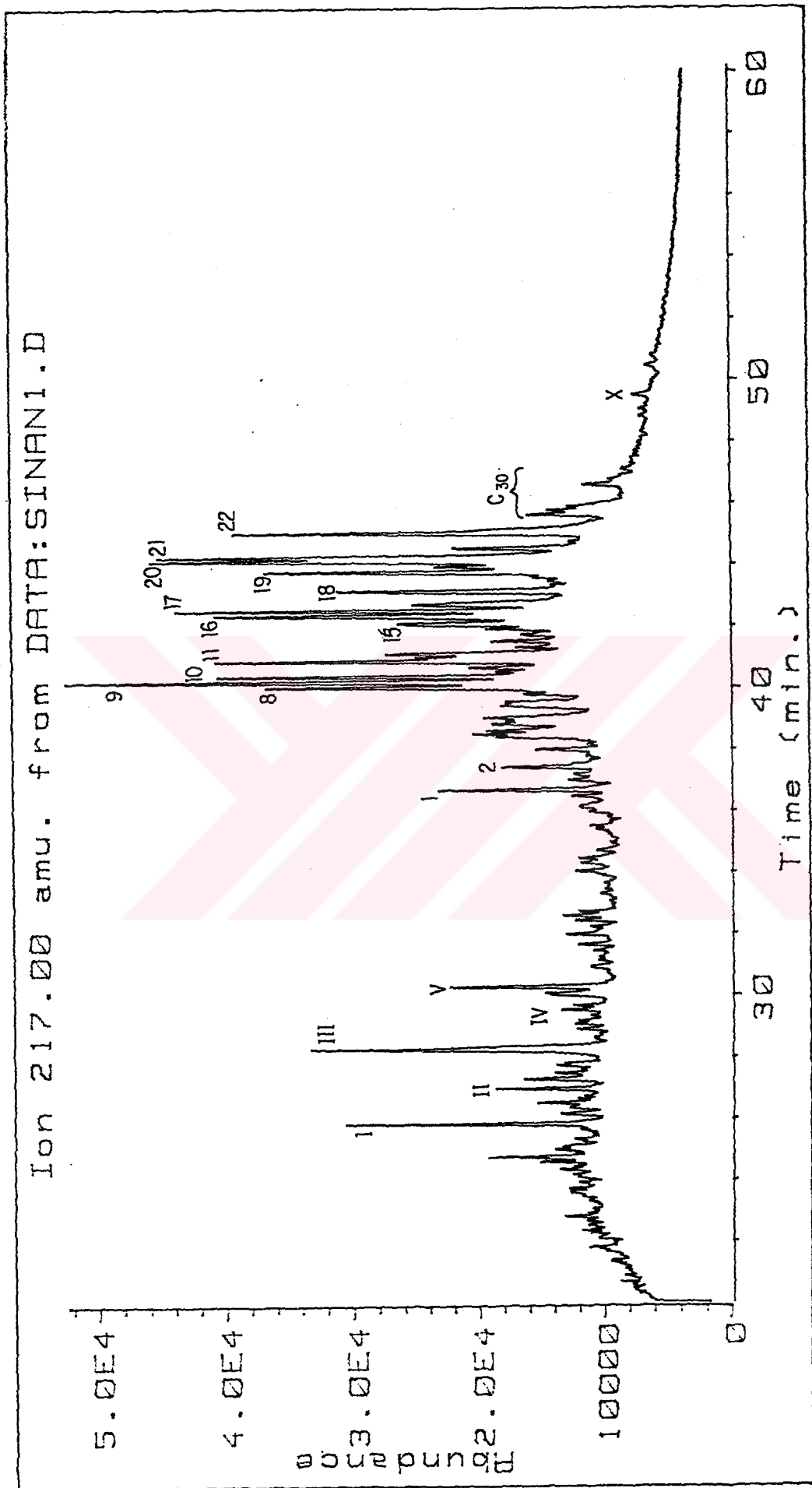


Figure.F.4 M/Z 217 mass chromatogram of the Silivanka_30 (S30) oil.



Figure_F.5 M/Z 217 mass fragmentogram of the Sinan_1 (SI1) oil.

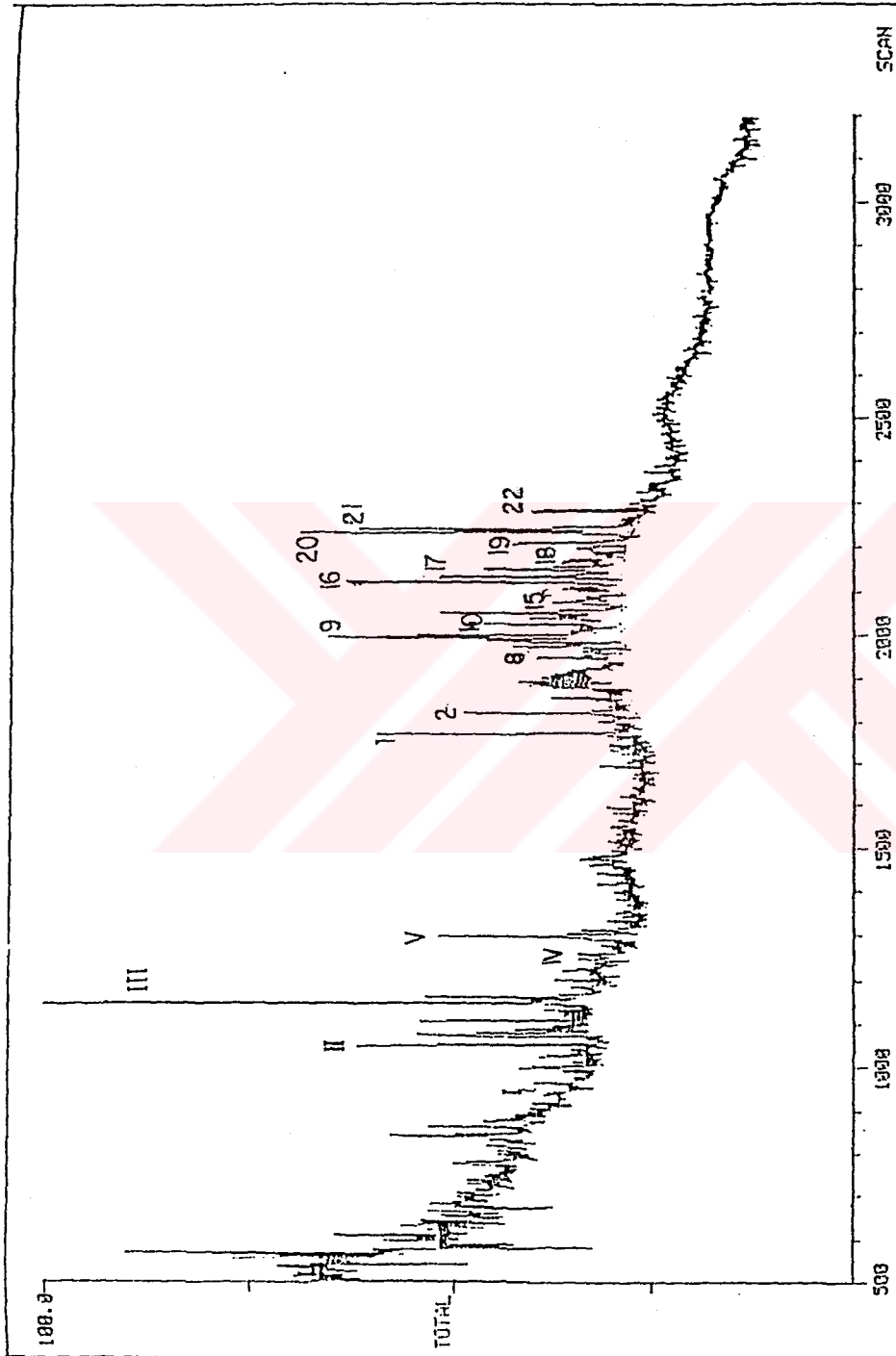


Figure - F.6 M/Z 217 mass fragmentogram of the Kastel - 2 (KA2) oil.

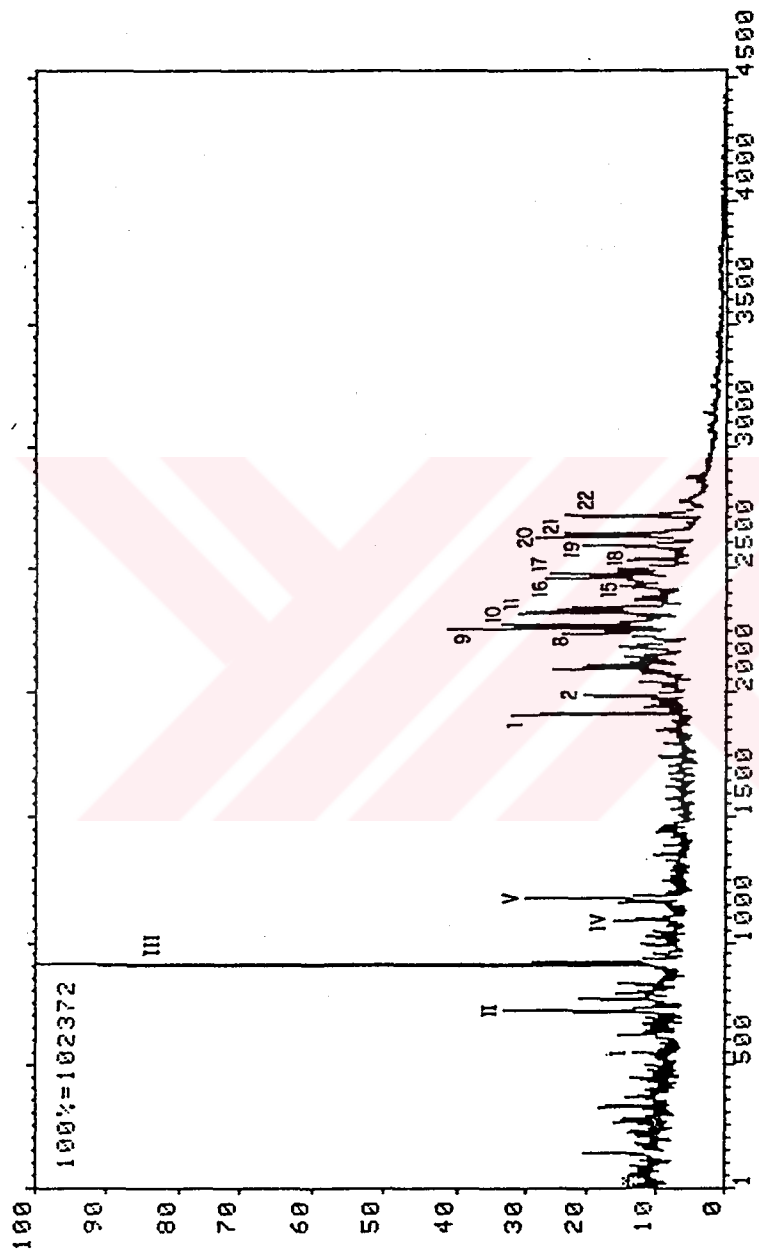


Figure. F.7 M/Z mass fragmetogram of the Kurtalan-1 (KU1) oil.

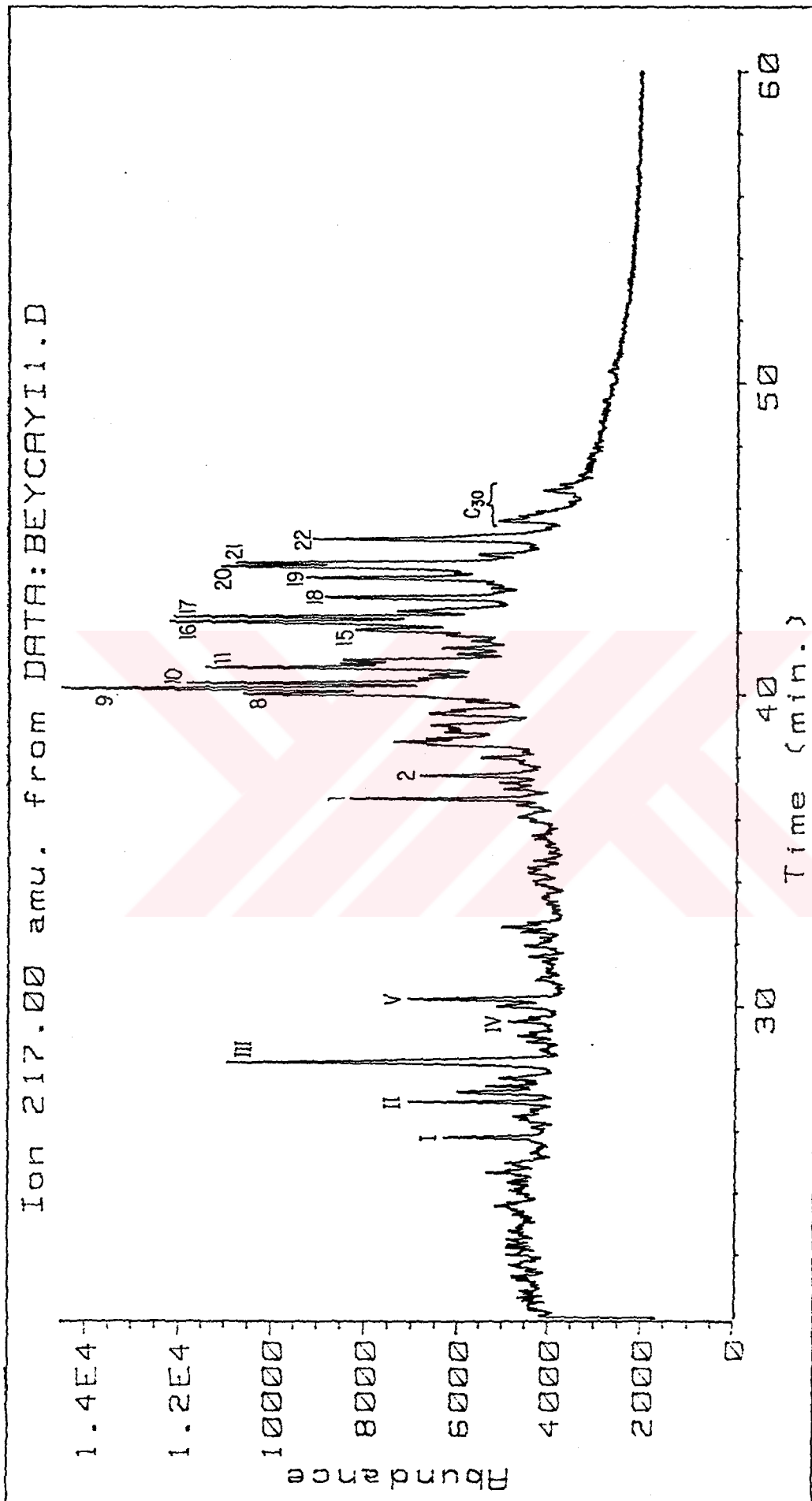


Figure. F.8 M/Z 217 mass fragmentogram of the Beyçayırı.1 (BE1) oil.

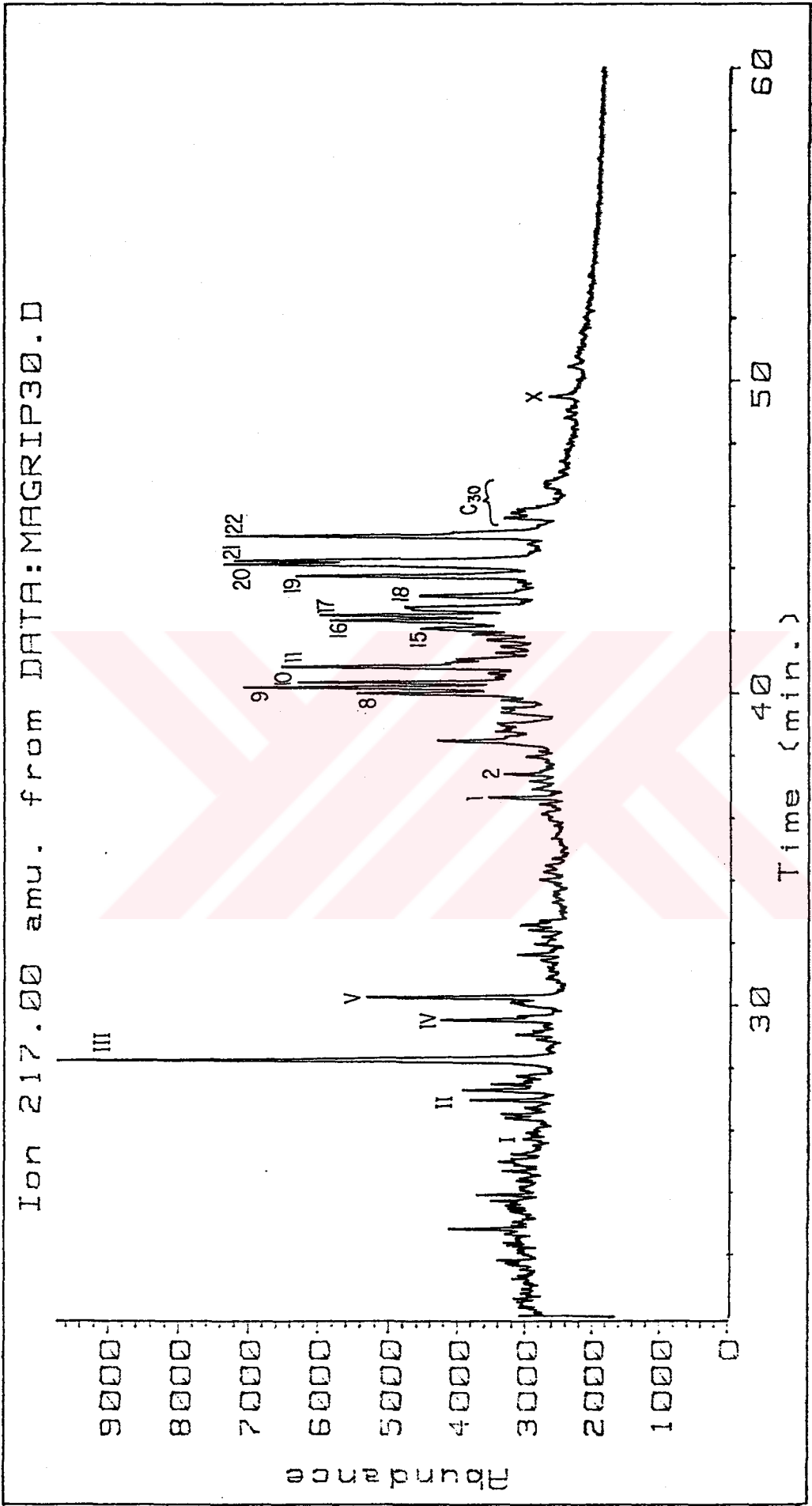


Figure - F.9 M/Z 217 mass fragmentogram of the Magrip-30 (M30) oil.

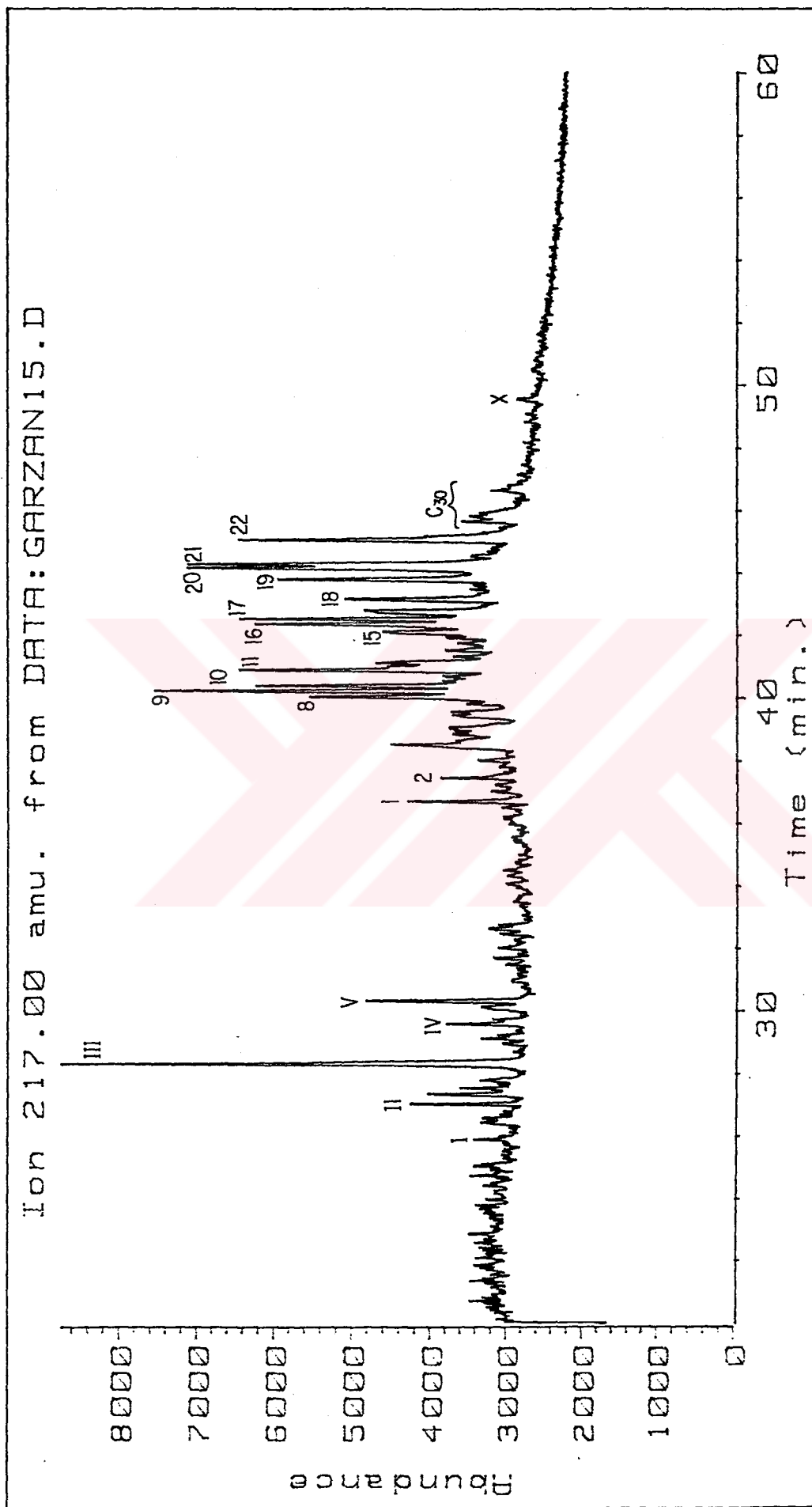


Figure - F.10 M/Z 217 mass fragmentogram of the Garzan_15 (GA15) oil.

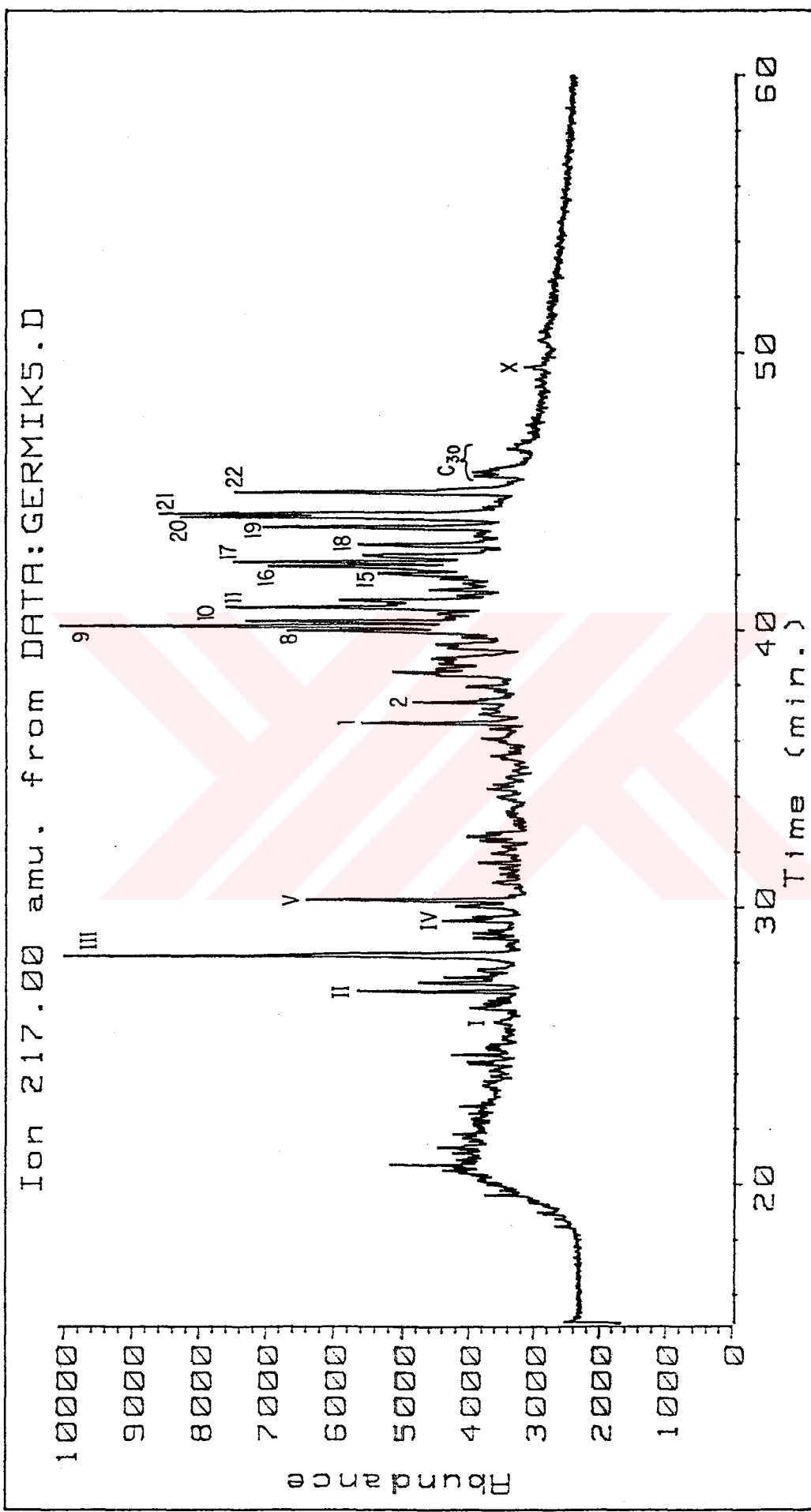


Figure-F.11 M/Z 217 mass fragmentogram of the Germik_5 (GE5) oil.

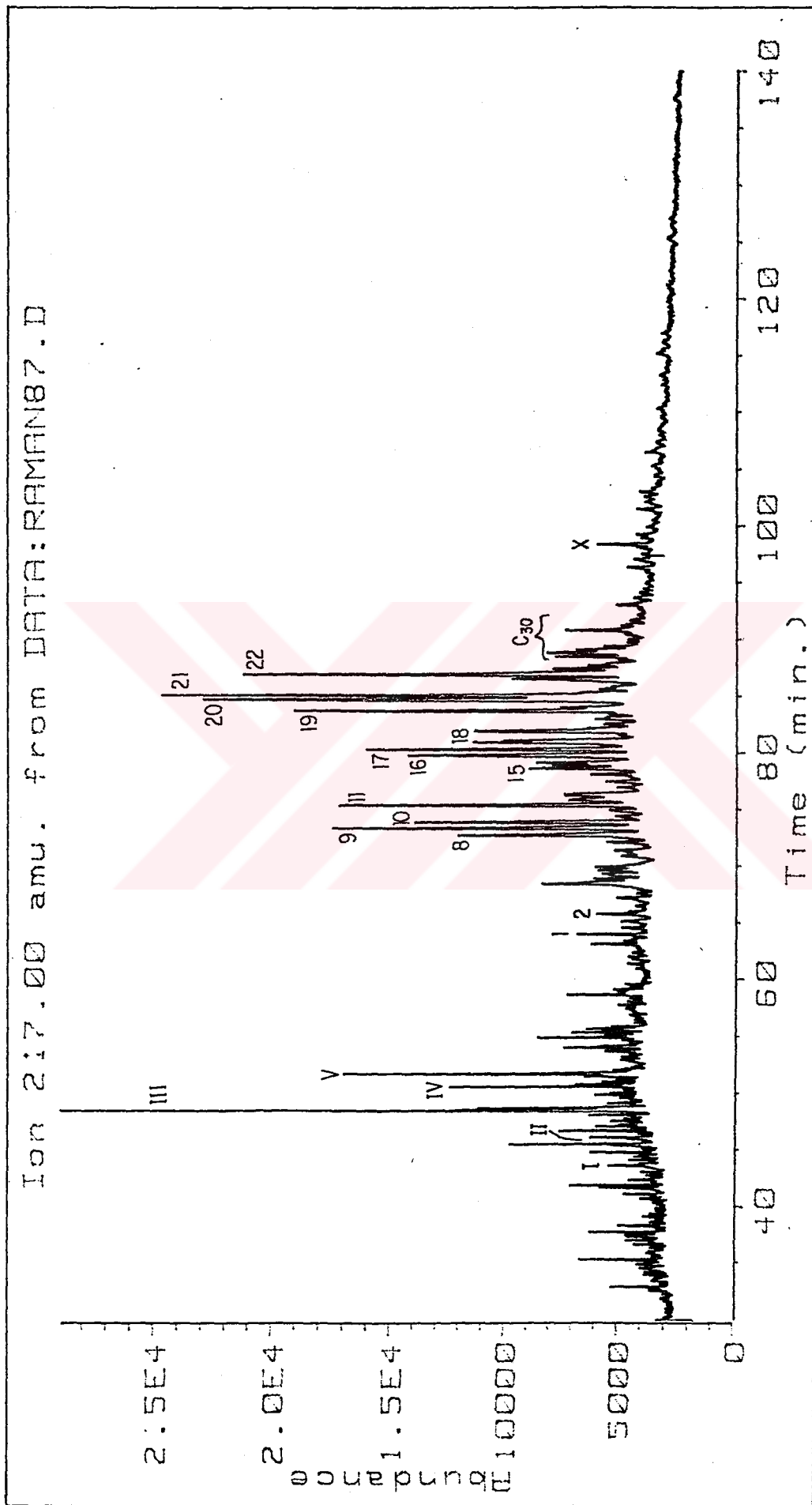


Figure - F.12 M/Z 217 mass fragmentogram of the Raman_87 (R87) oil.

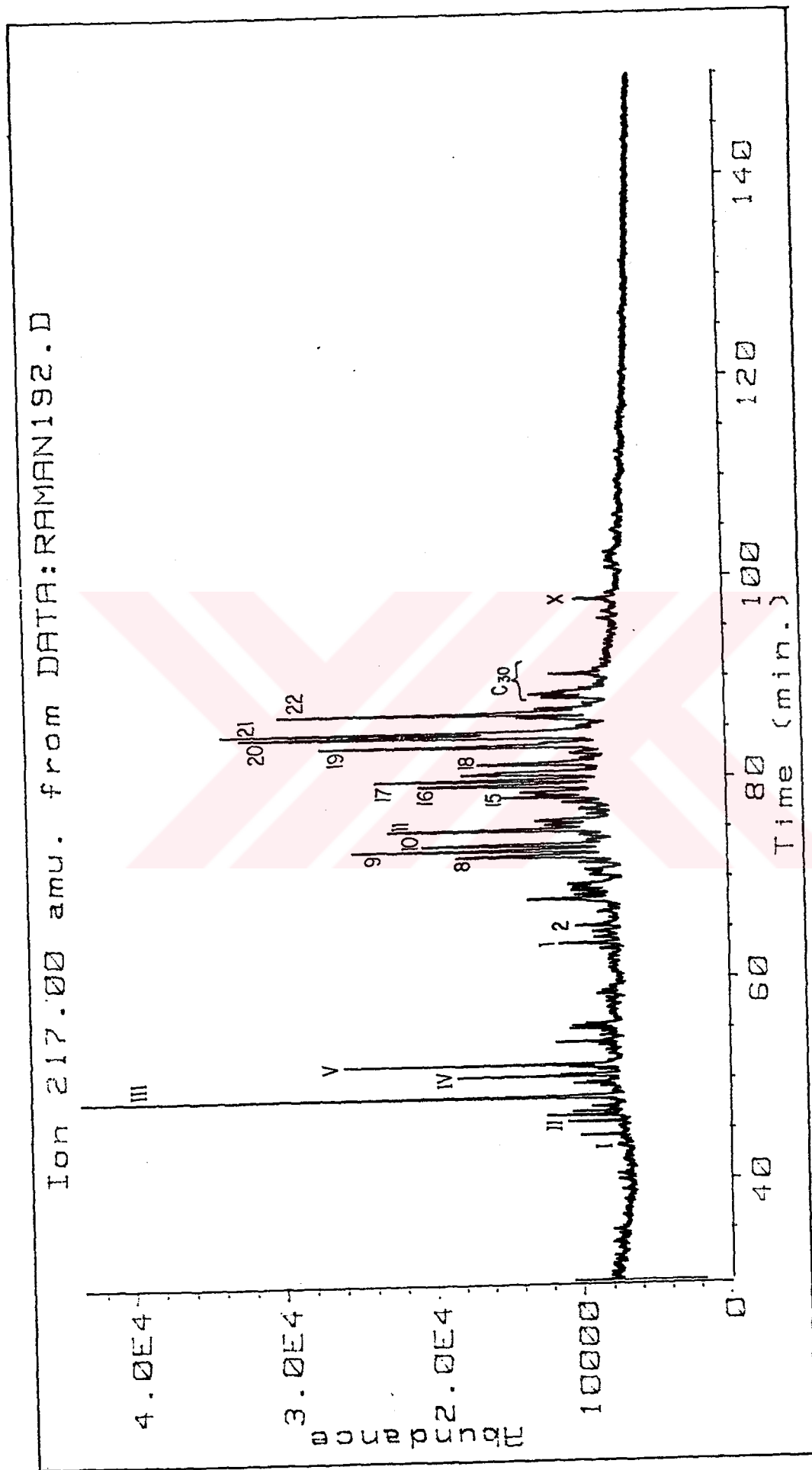


Figure-F.13 M/Z 217 mass fragmentogram of the Raman-192 (R192) oil.

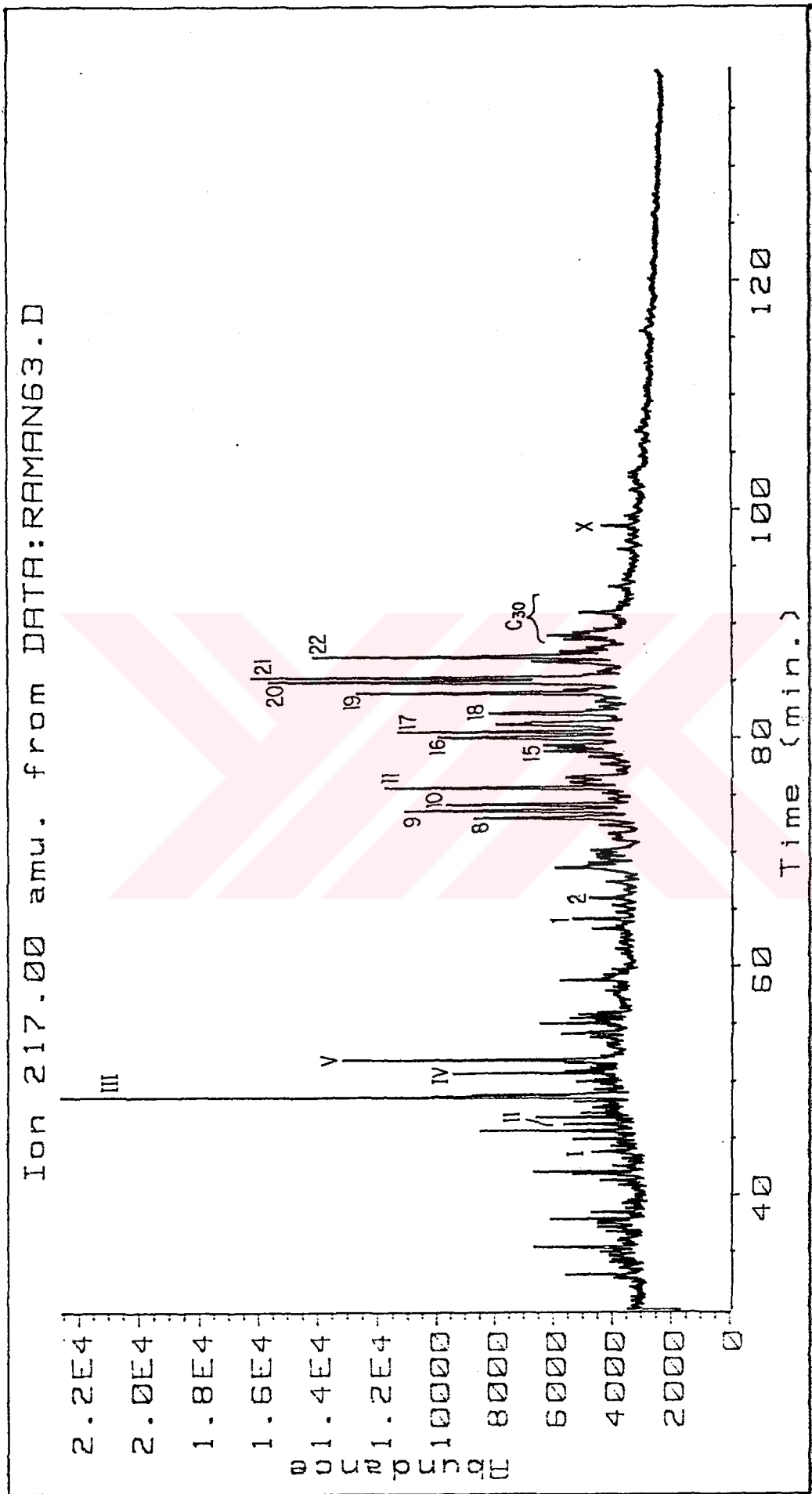
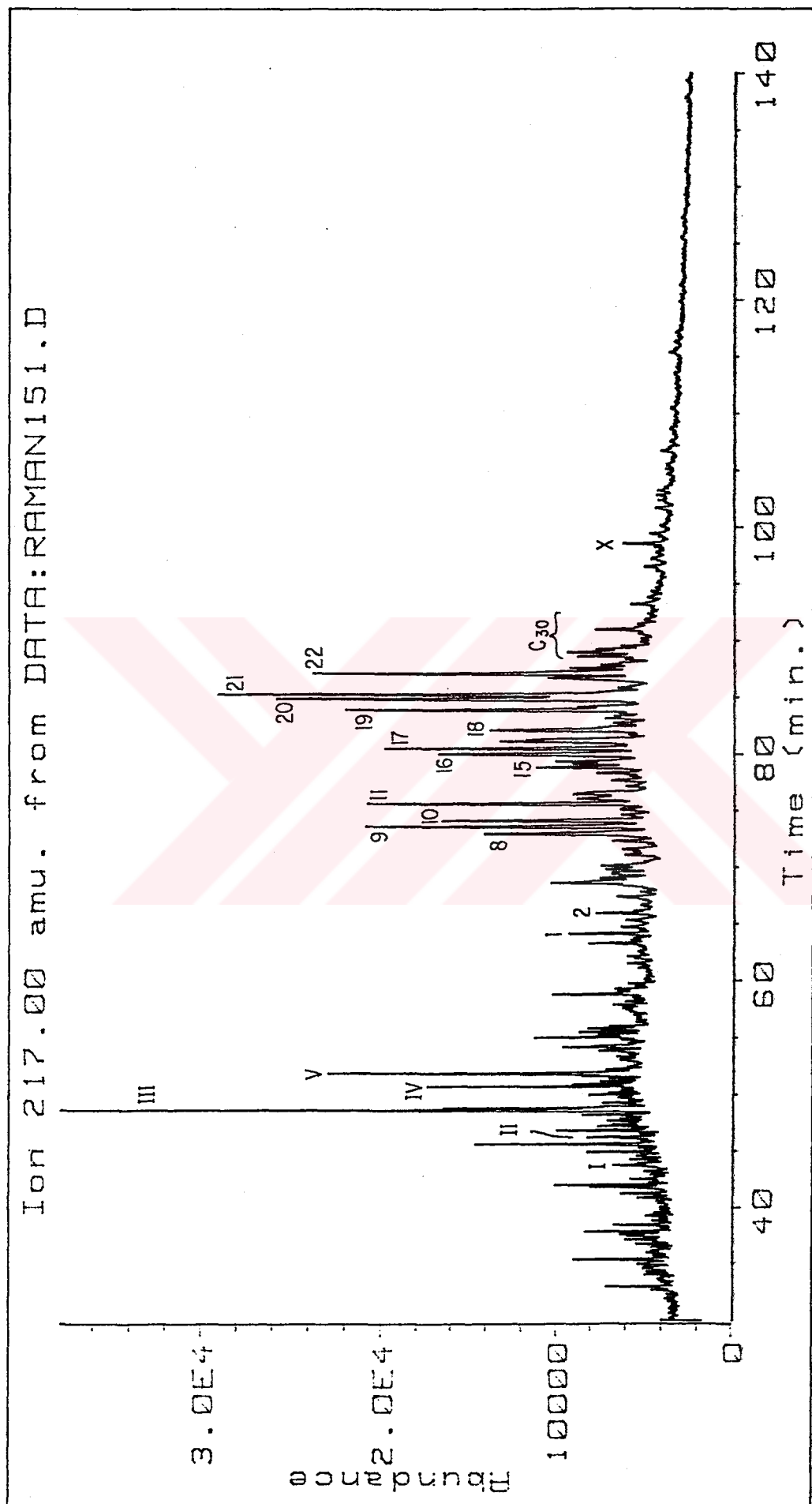


Figure-F.14 M/Z 217 mass fragmentogram of the Raman-63 (R63) oil.



Figure_F.15 M/Z 217 mass fragmentogram of the Raman_151 (R151) oil.

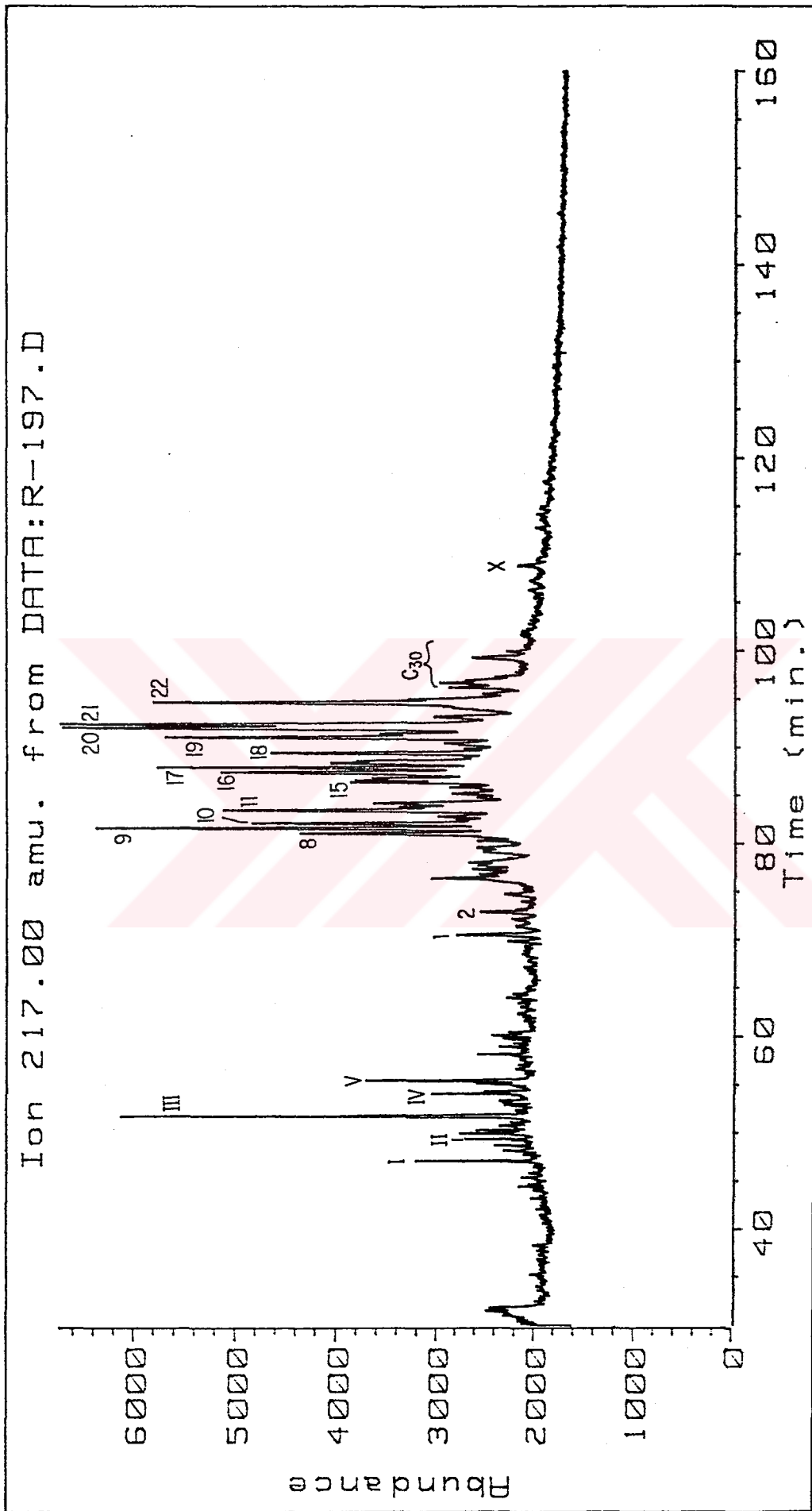


Figure-F.16 M/Z 217 mass fragmentogram of the Raman-197 (R197) oil.

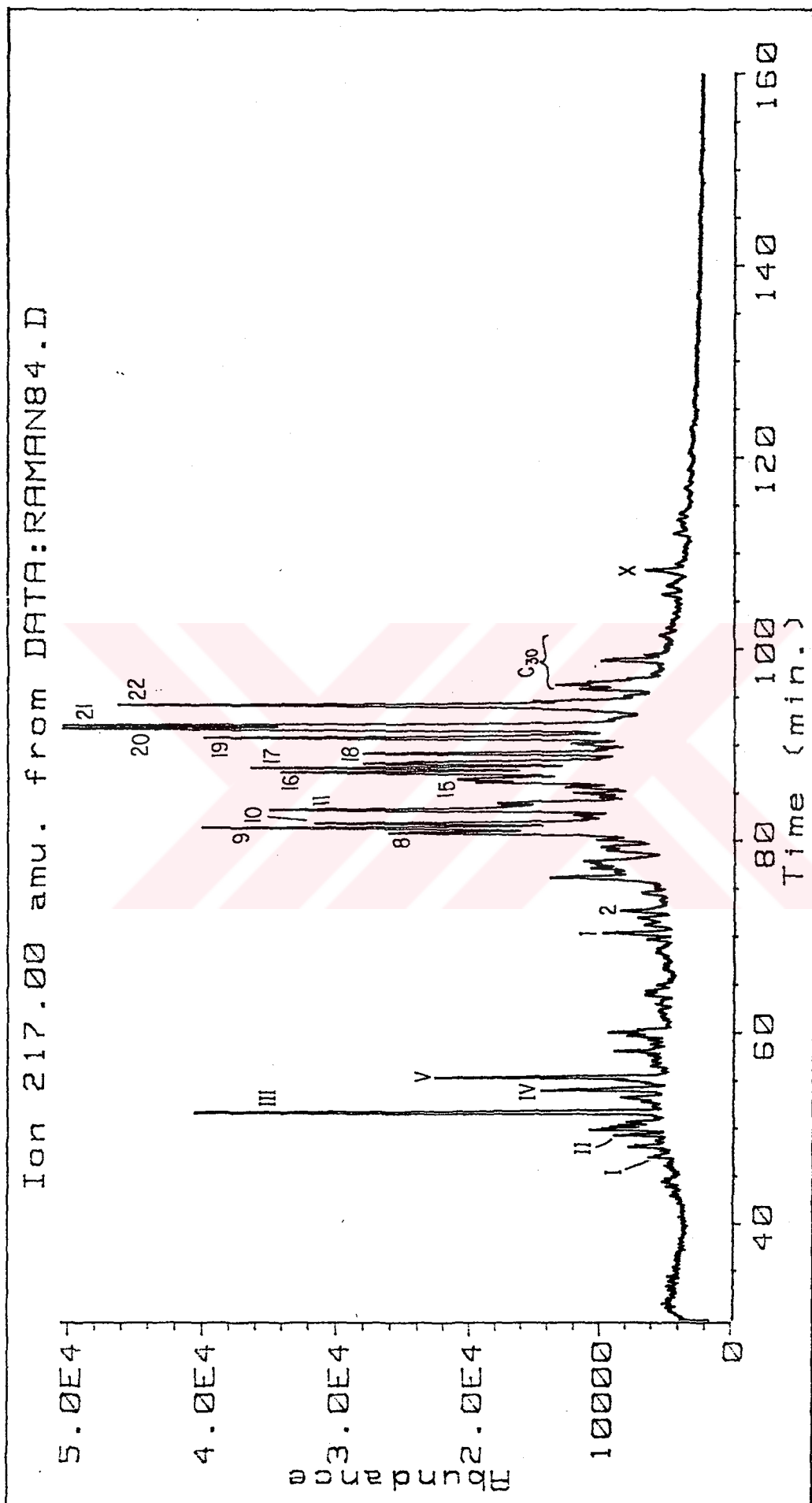


Figure-F.17 M/Z 217 mass fragmentogram of the Raman_84 (R84) oil.

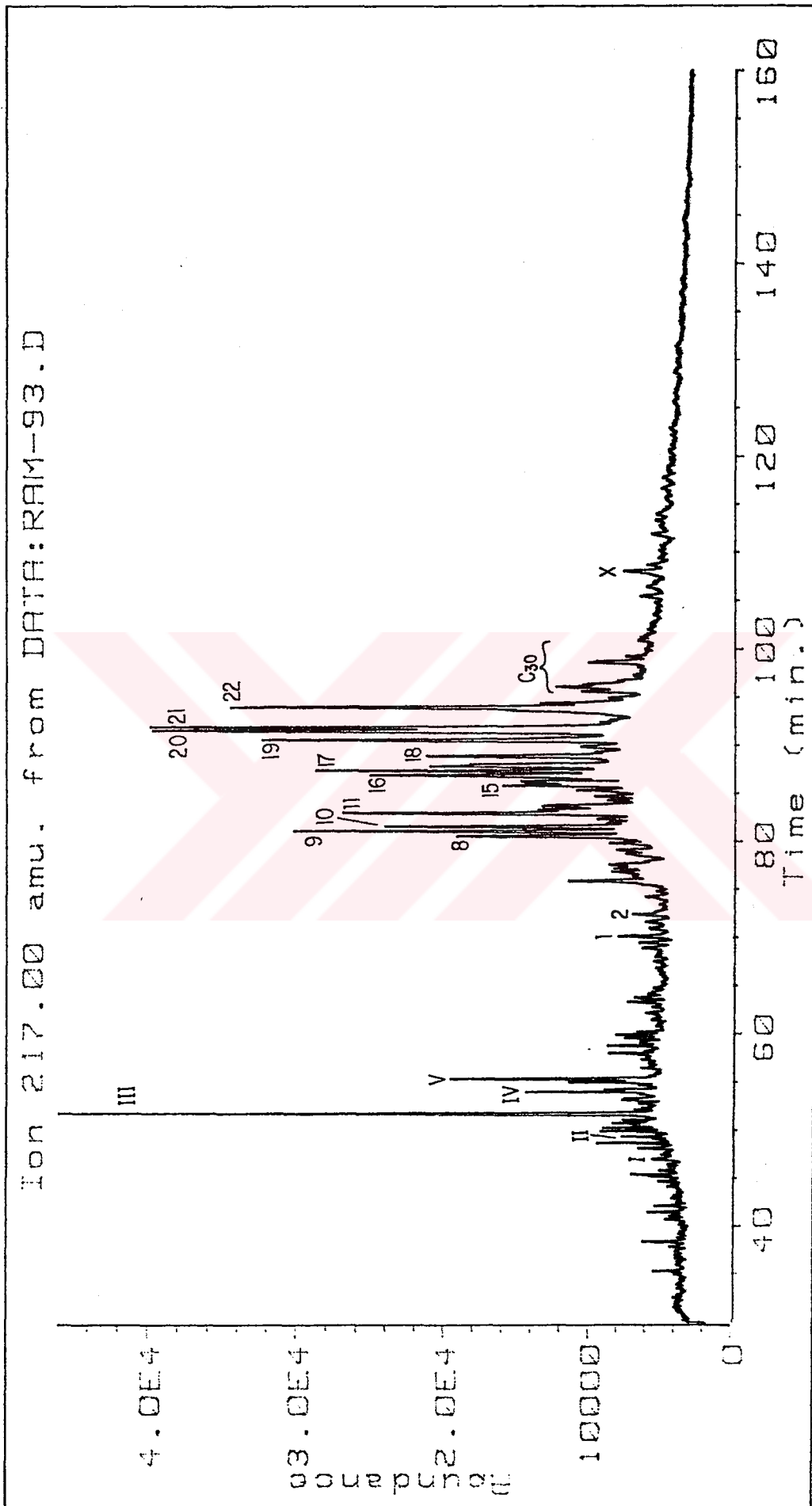


Figure-F.18 M/Z 217 mass fragmentogram of the Raman-93 (R93).oil.

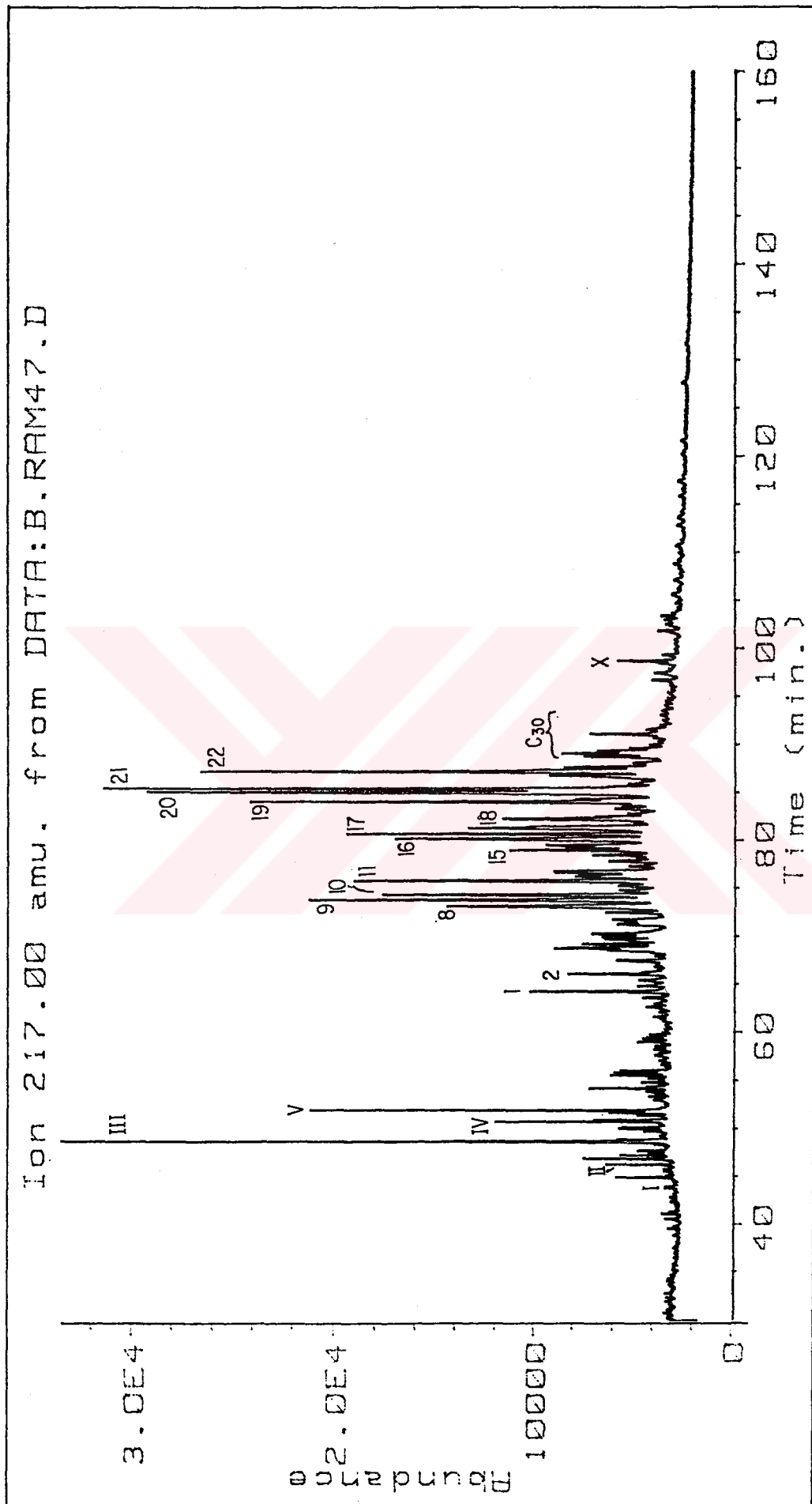


Figure - F.19 M/Z 217 mass fragmentogram of the Bati Raman_47 (BR47) oil.

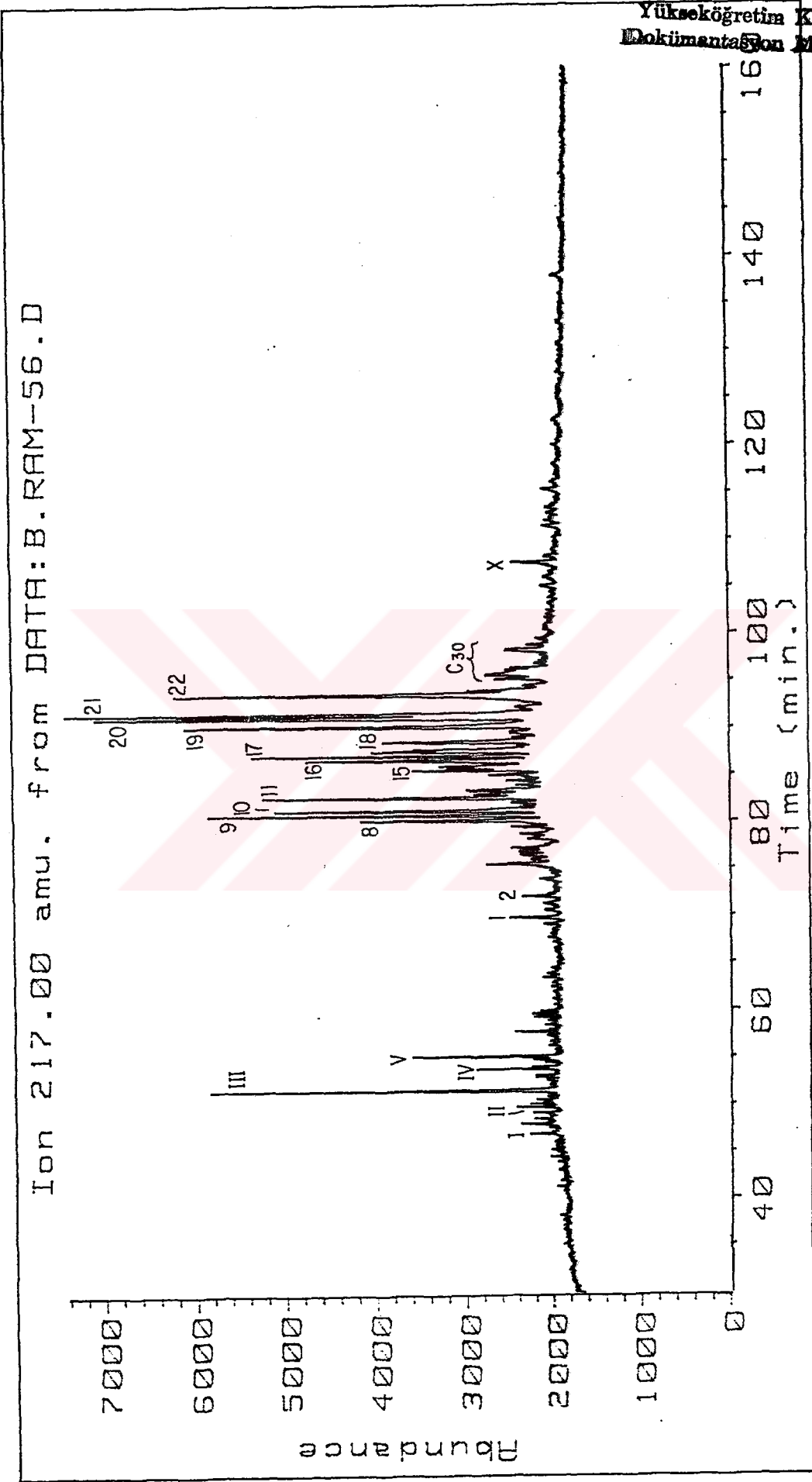


Figure. F.20 M/Z 217 mass fragmentogram of the Batı Raman -56 (BR56) oil.

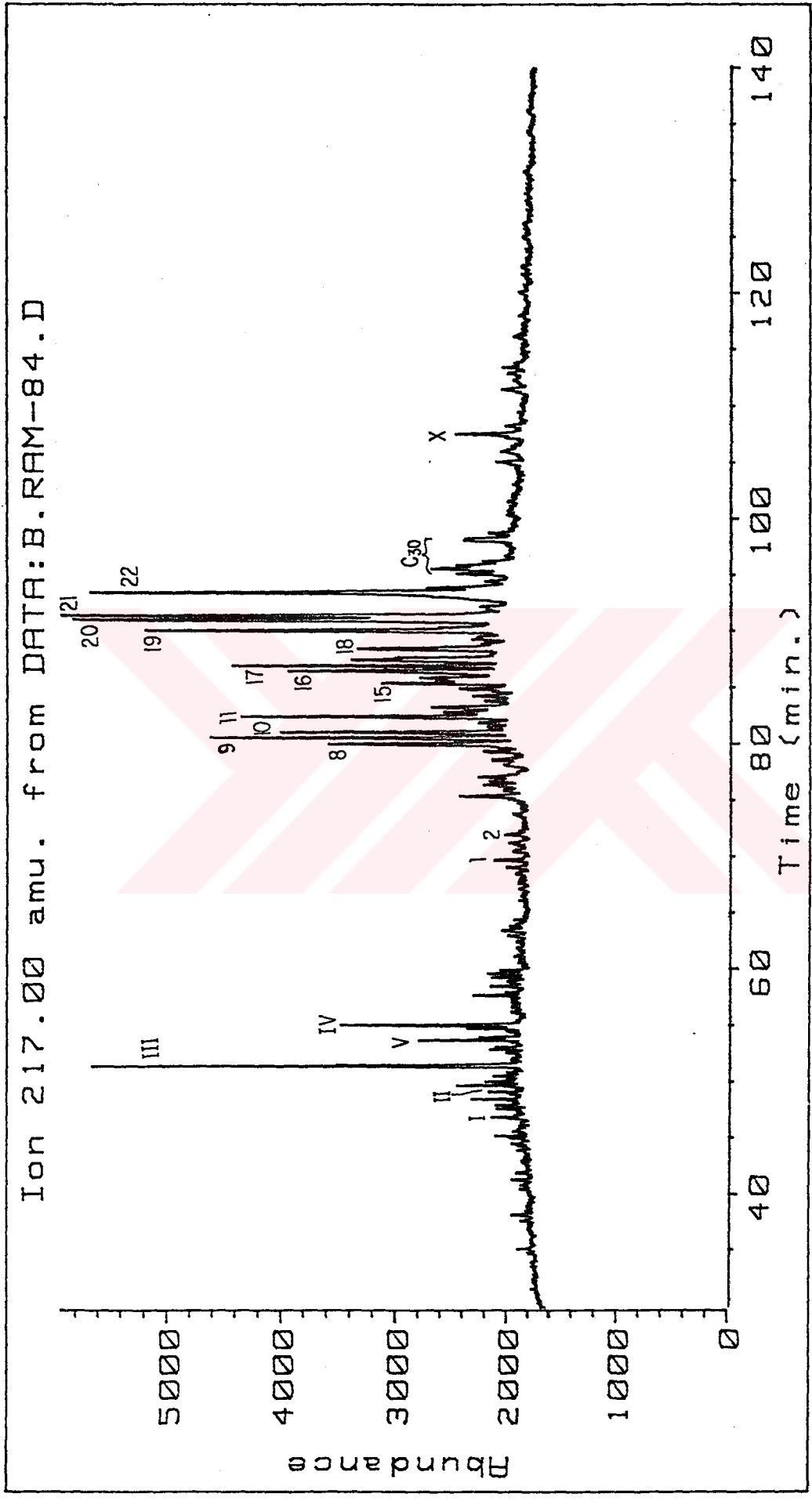


Figure - F.21 M/Z 217 mass fragmentogram of the Bati Raman_84 (BR84) oil.

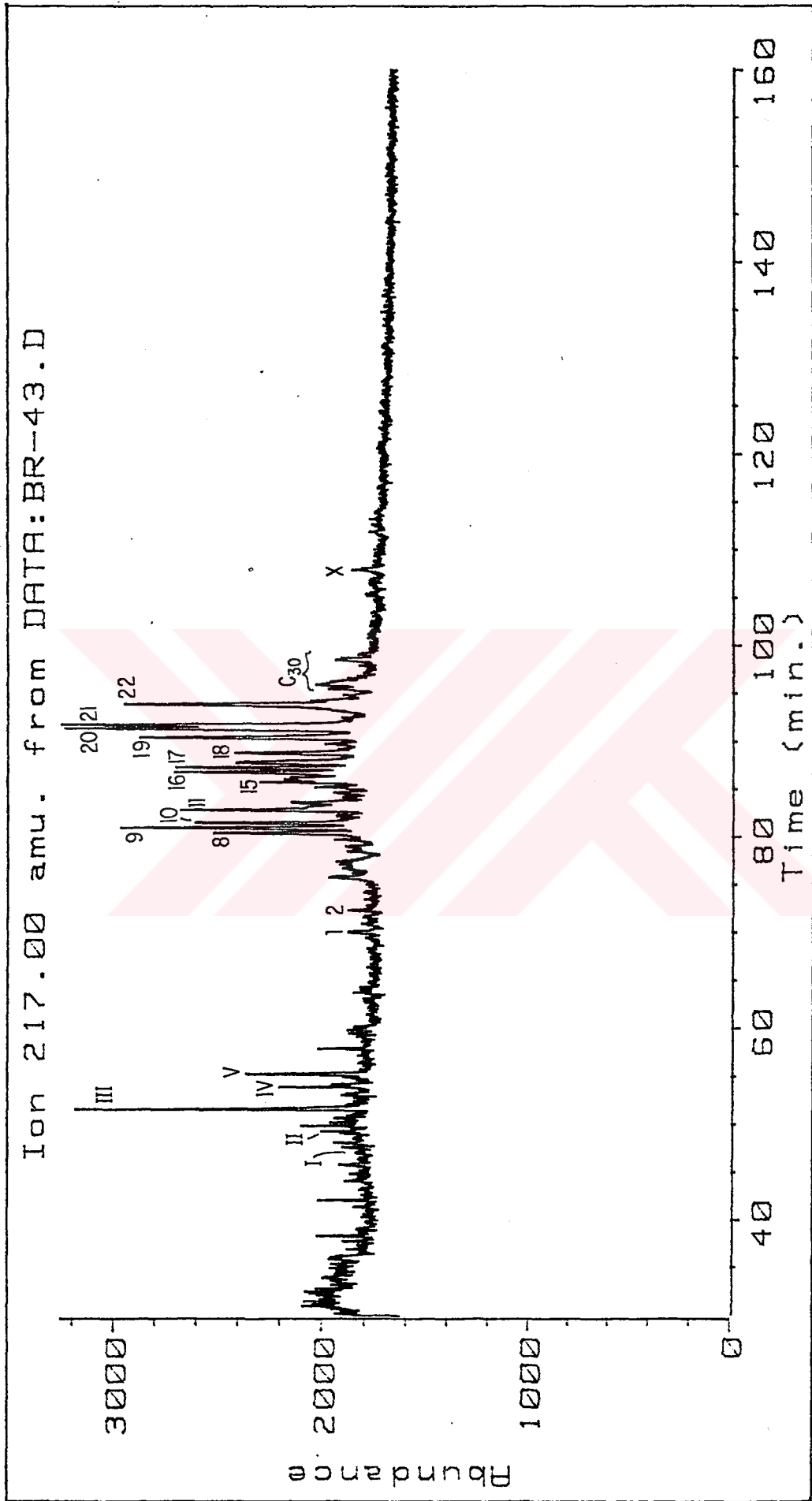


Figure - F.22 M/Z 217 mass fragmentogram of the Bati Raman_43 (BR43) oil.

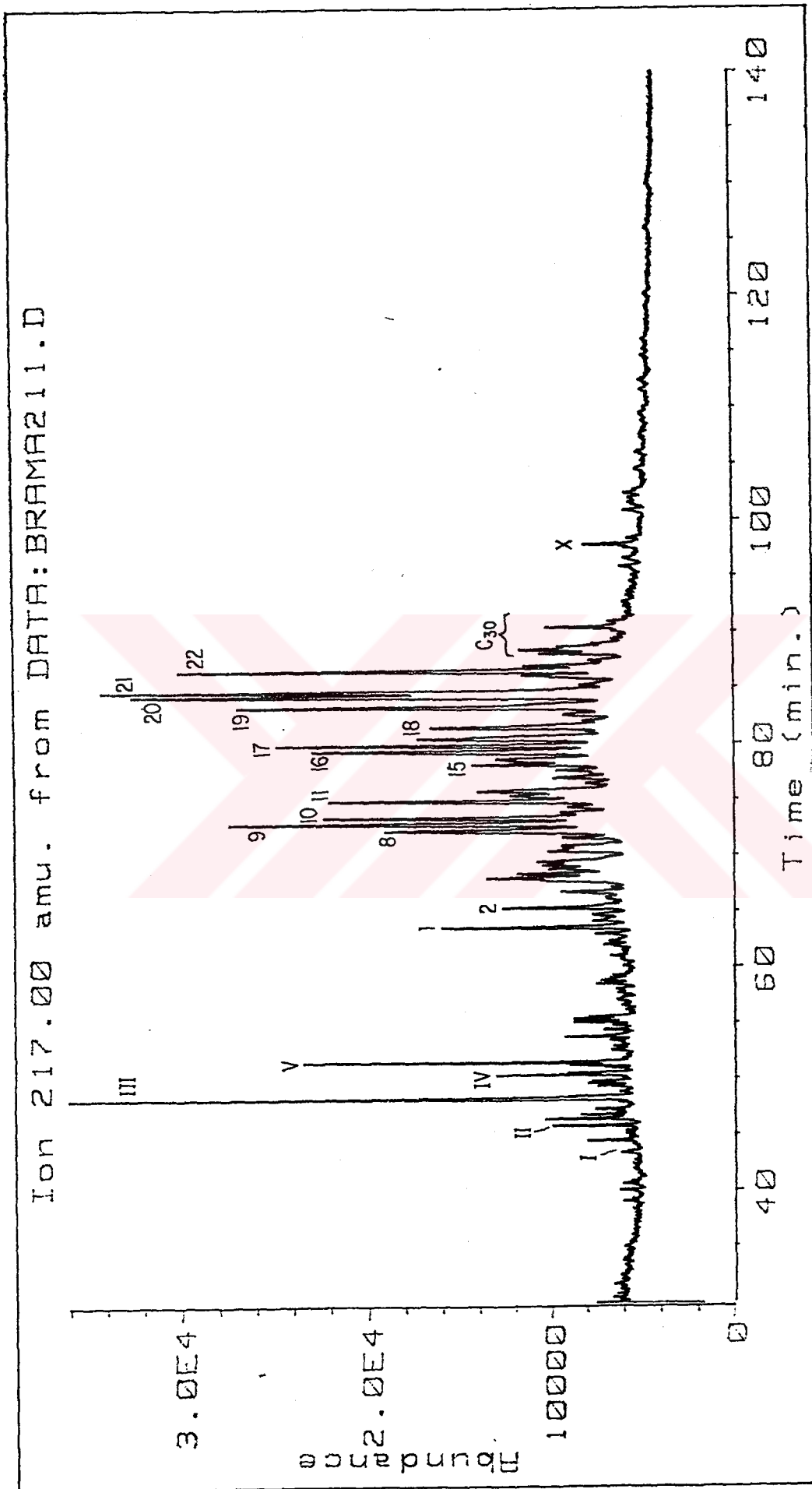


Figure - F.23 M/Z 217 mass fragmentogram of the Bath Raman -211 (BR211) oil.

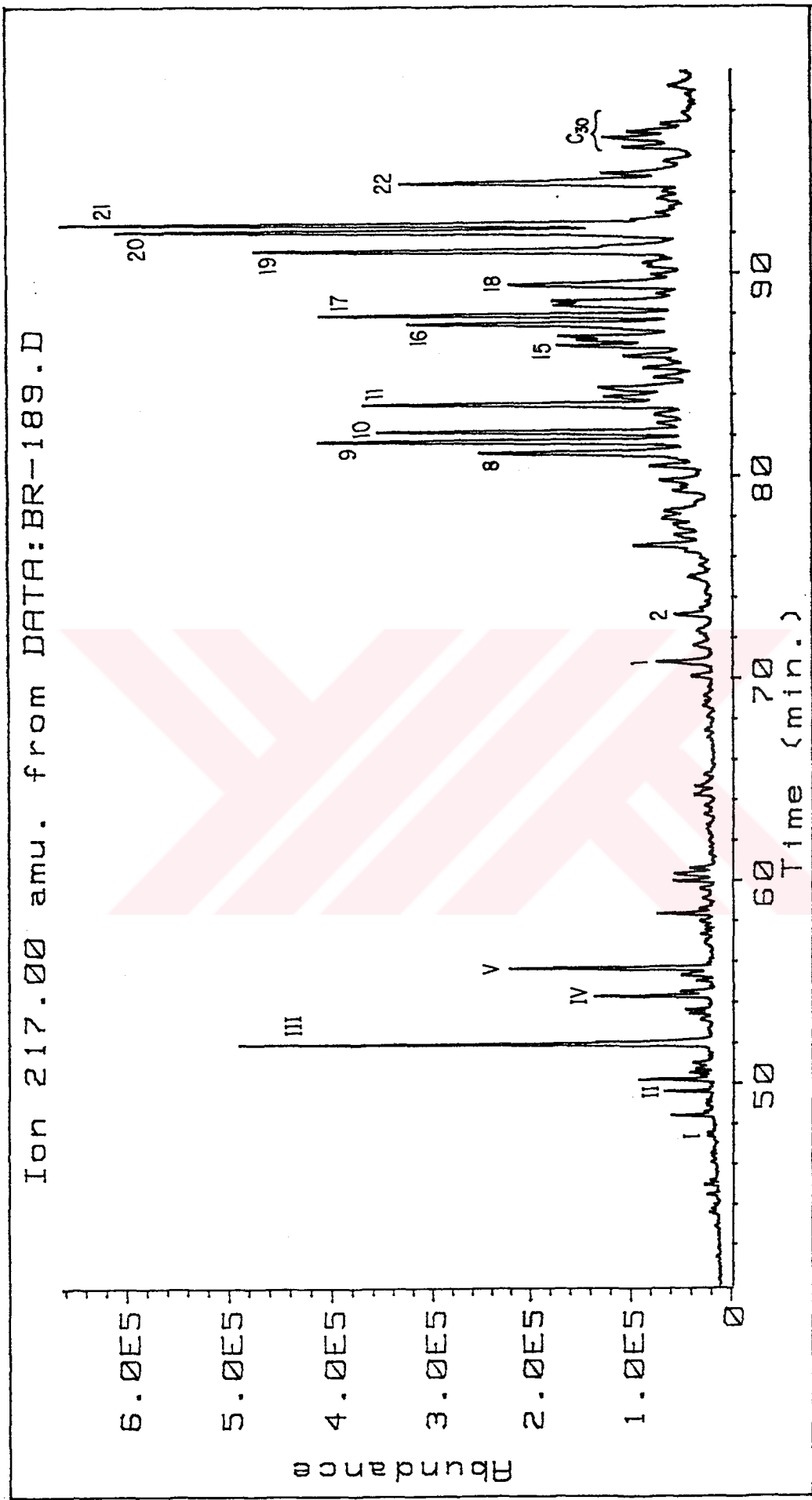


Figure - F.24 M/Z . 217 mass fragmentogram of the Bati Raman . 189 (BR189) oil.

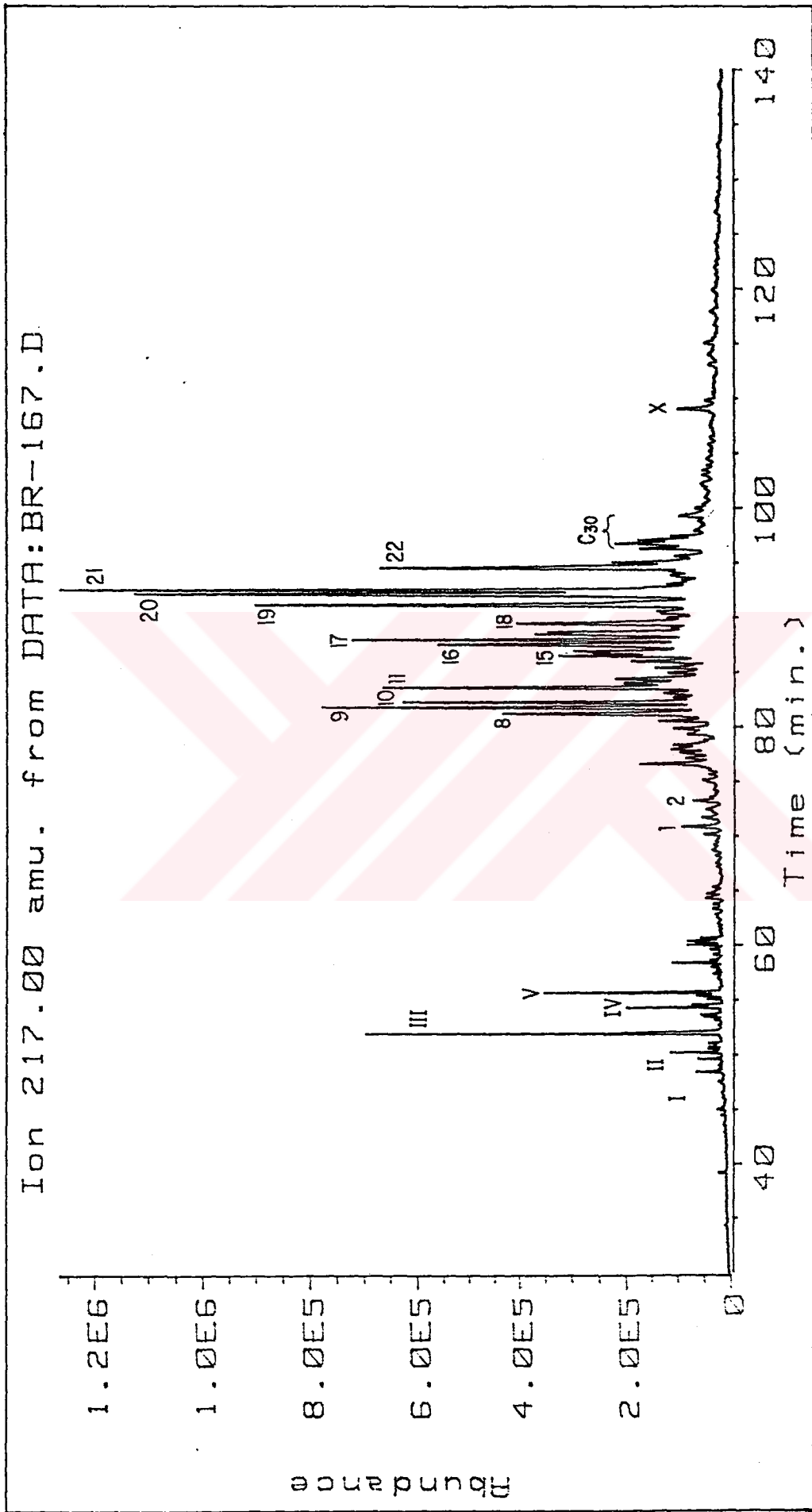


Figure F.25 M/Z 217 mass fragmentogram of the Bati Raman-167 (BR167) oil.

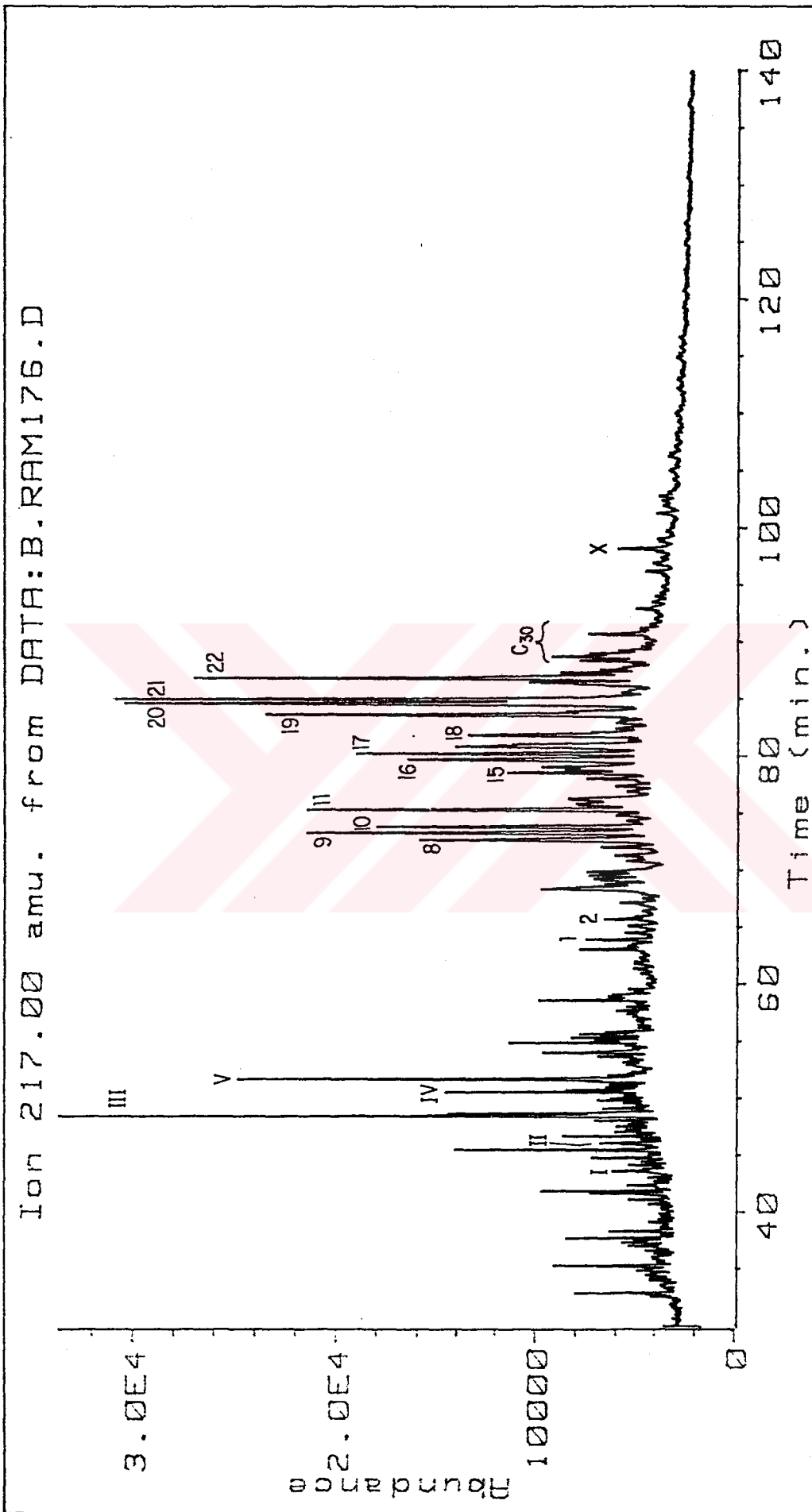


Figure-F.26 M/Z 217 mass chromatogram of the Bati Raman_176 (BR176) oil.

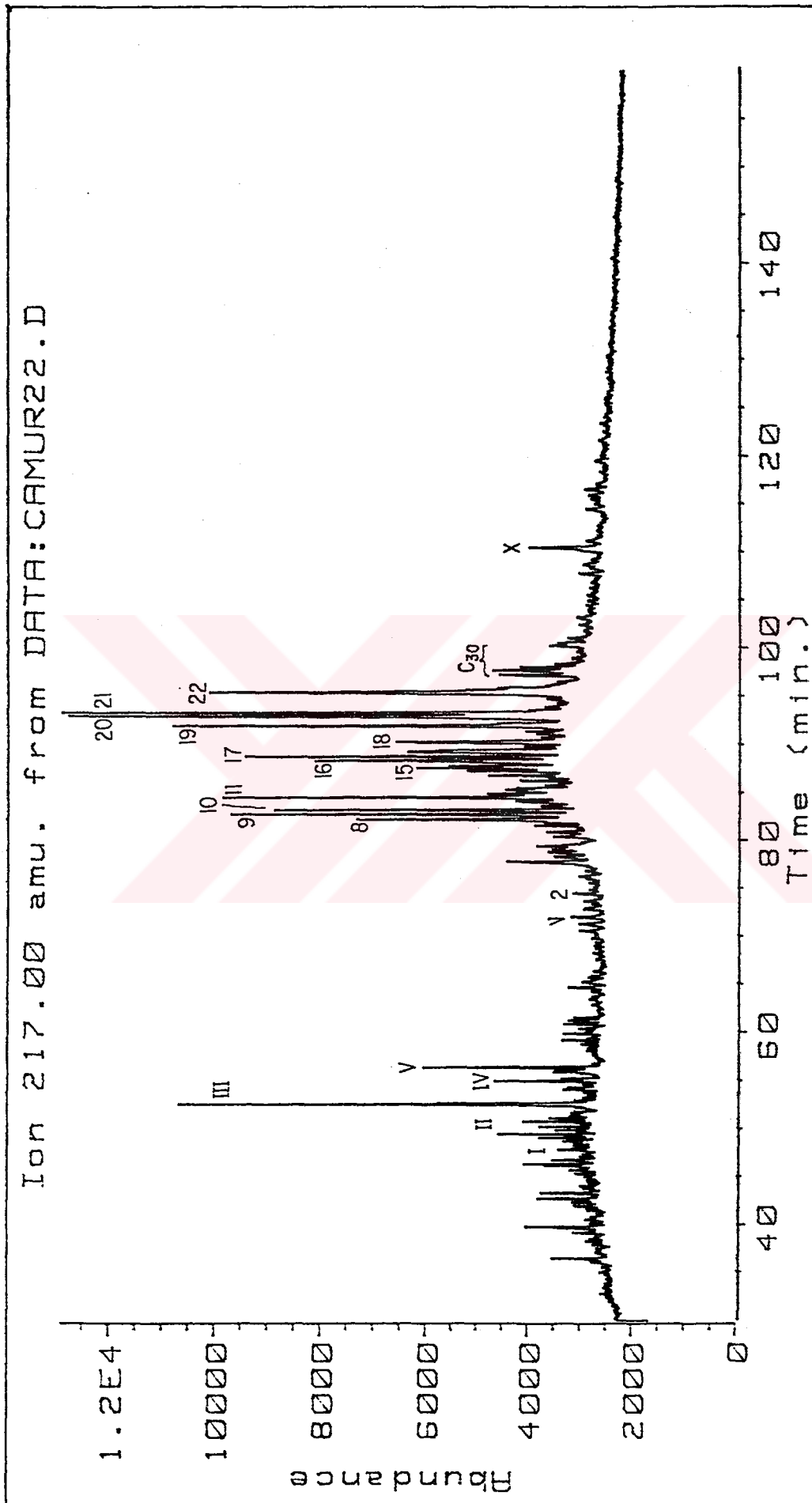


Figure-F.27 M/Z 217 mass fragmentogram of the Çamurlu-22 (CA22) oil.

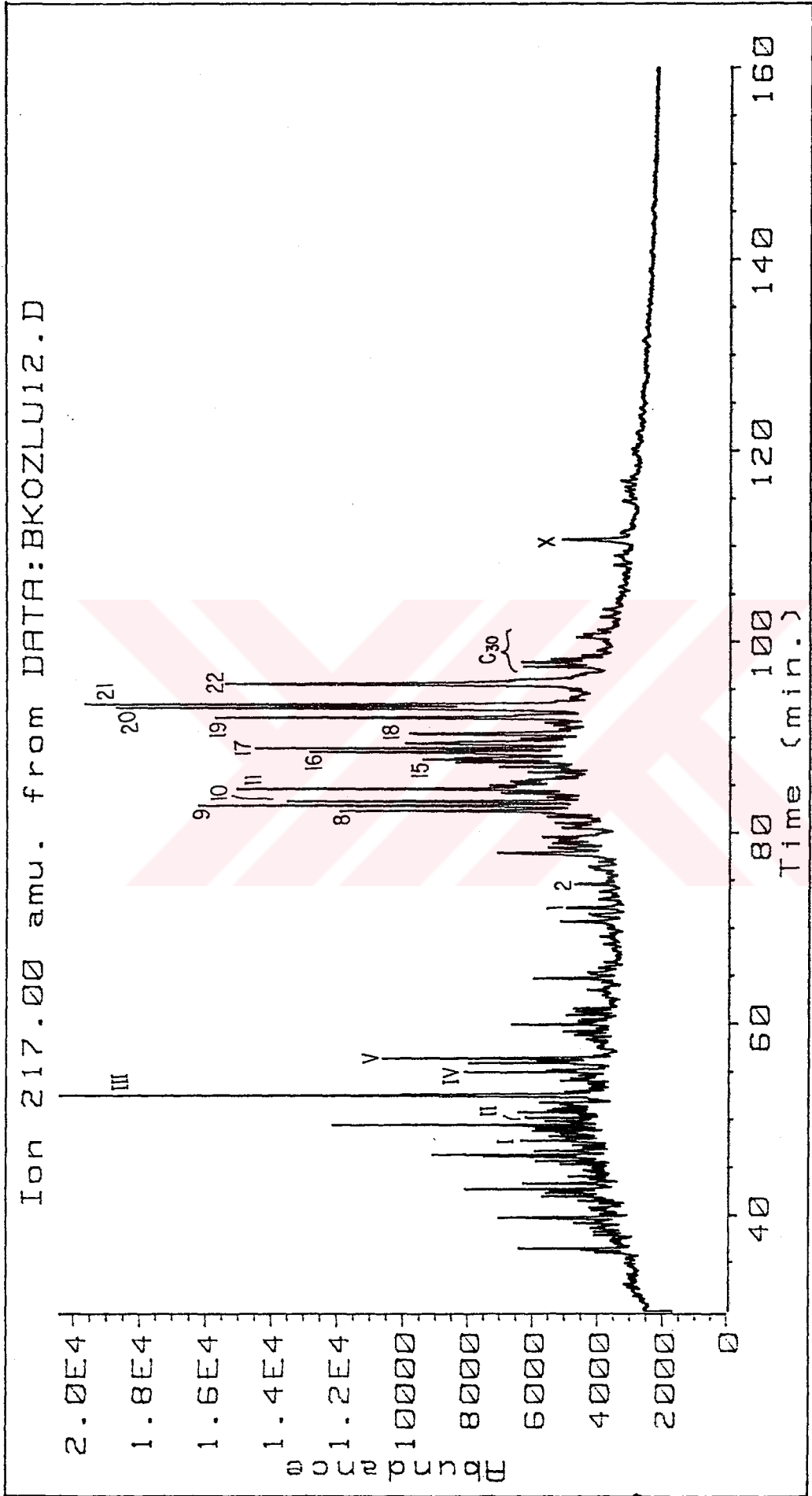


Figure-F.28 M/Z 217 mass fragmentogram of the Batı Kozluca_12 (BK12) oil.

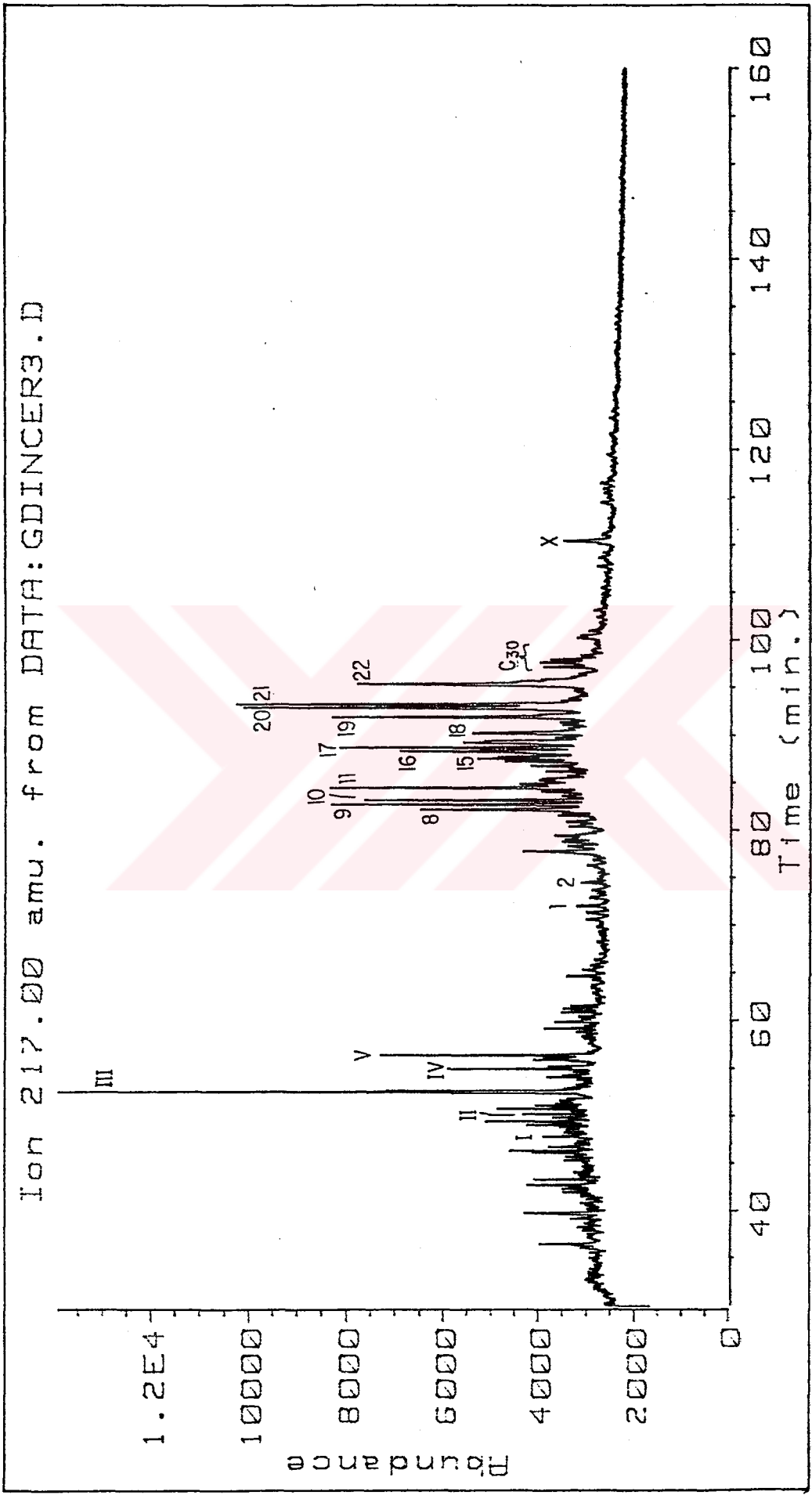


Figure .F.29 M/Z 217 mass fragmentogram of the Güney Dincer_3 (GD3) oil.

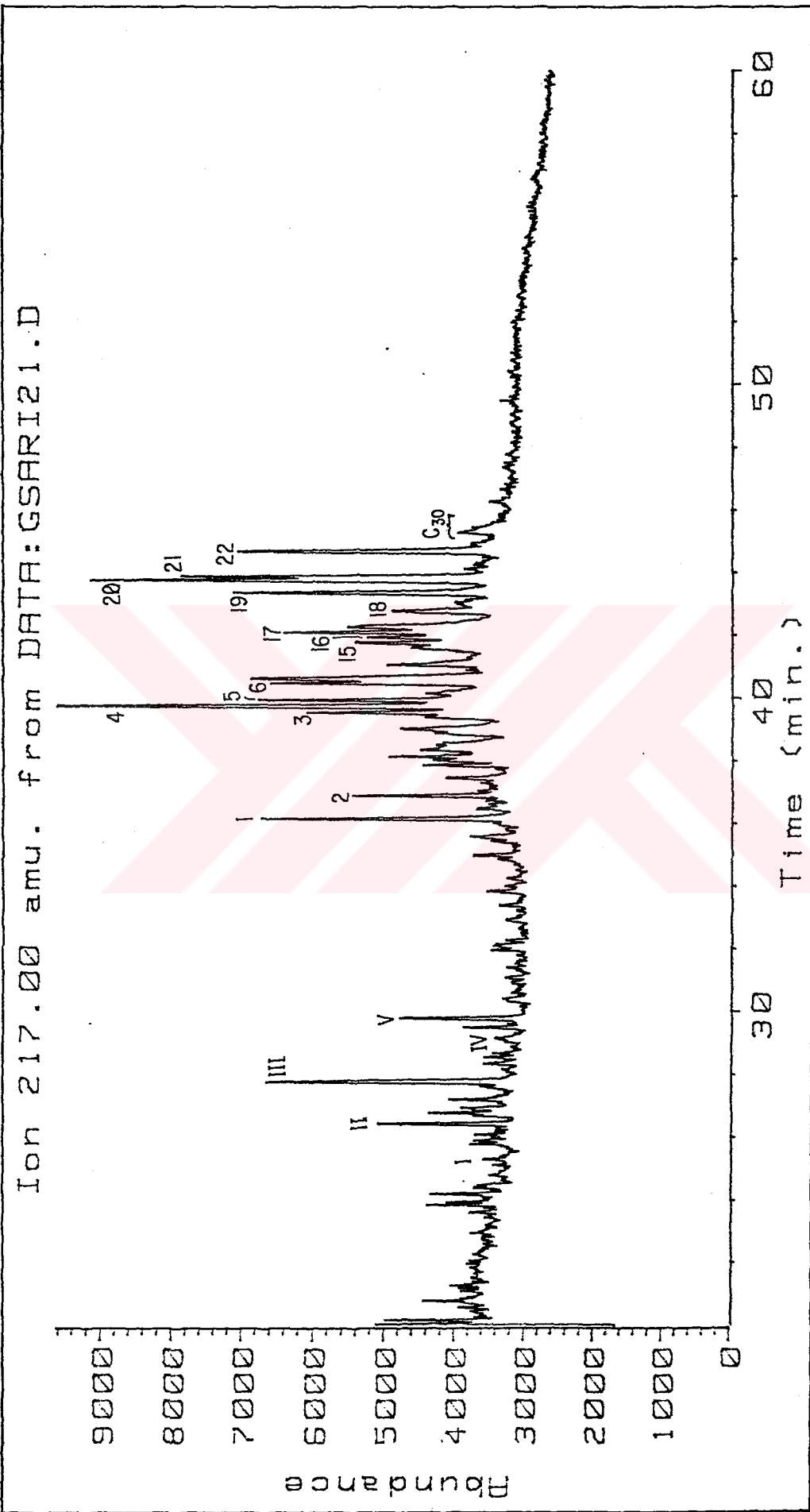


Figure.. F.30 M/Z 217 mass fragmentogram of the Güney Sarıcağ - 121 (GS121) oil.

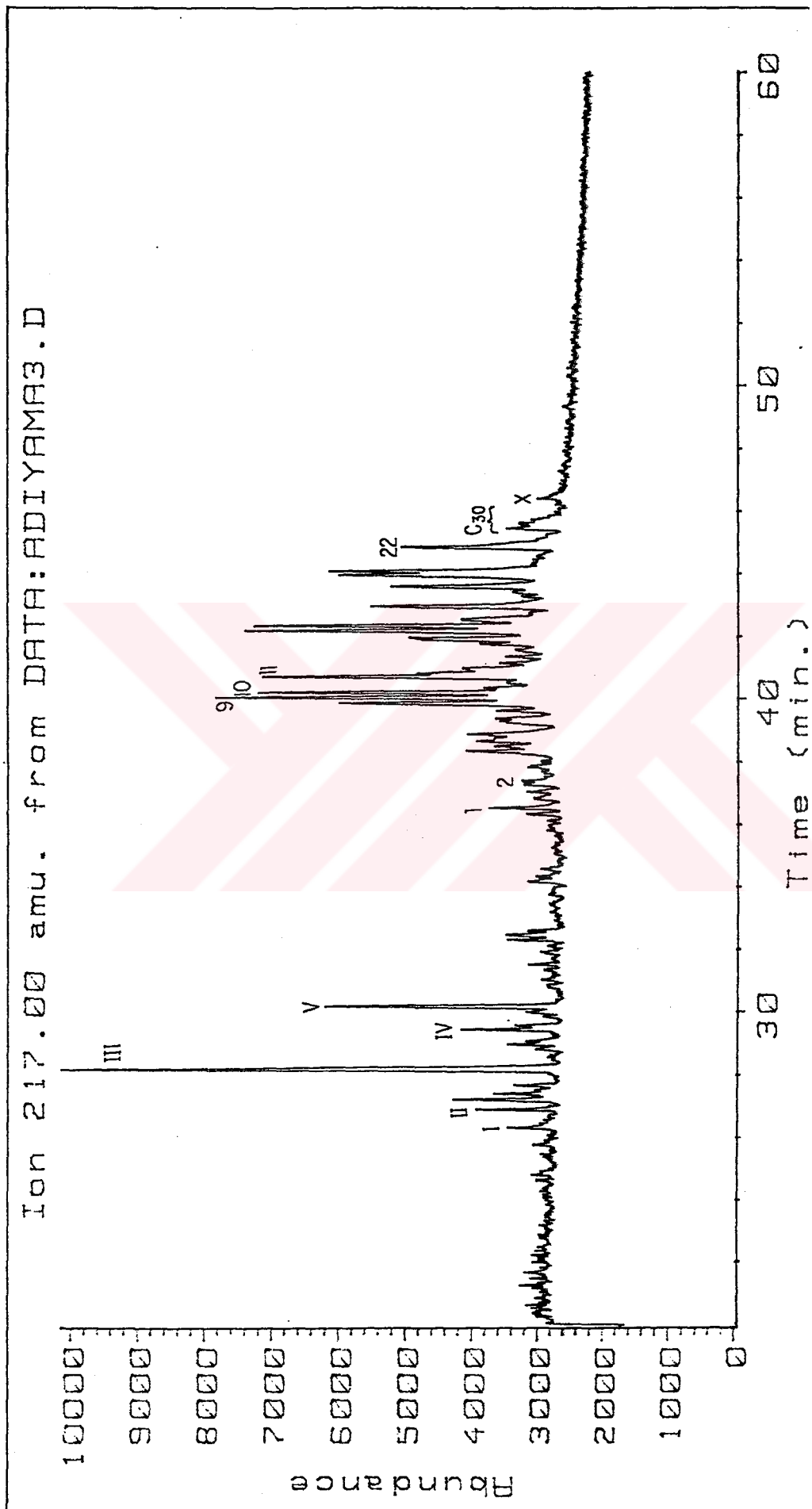


Figure. F.31 M/Z 217 mass fragmentogram of the Adiyaman_3 (A3) oil.

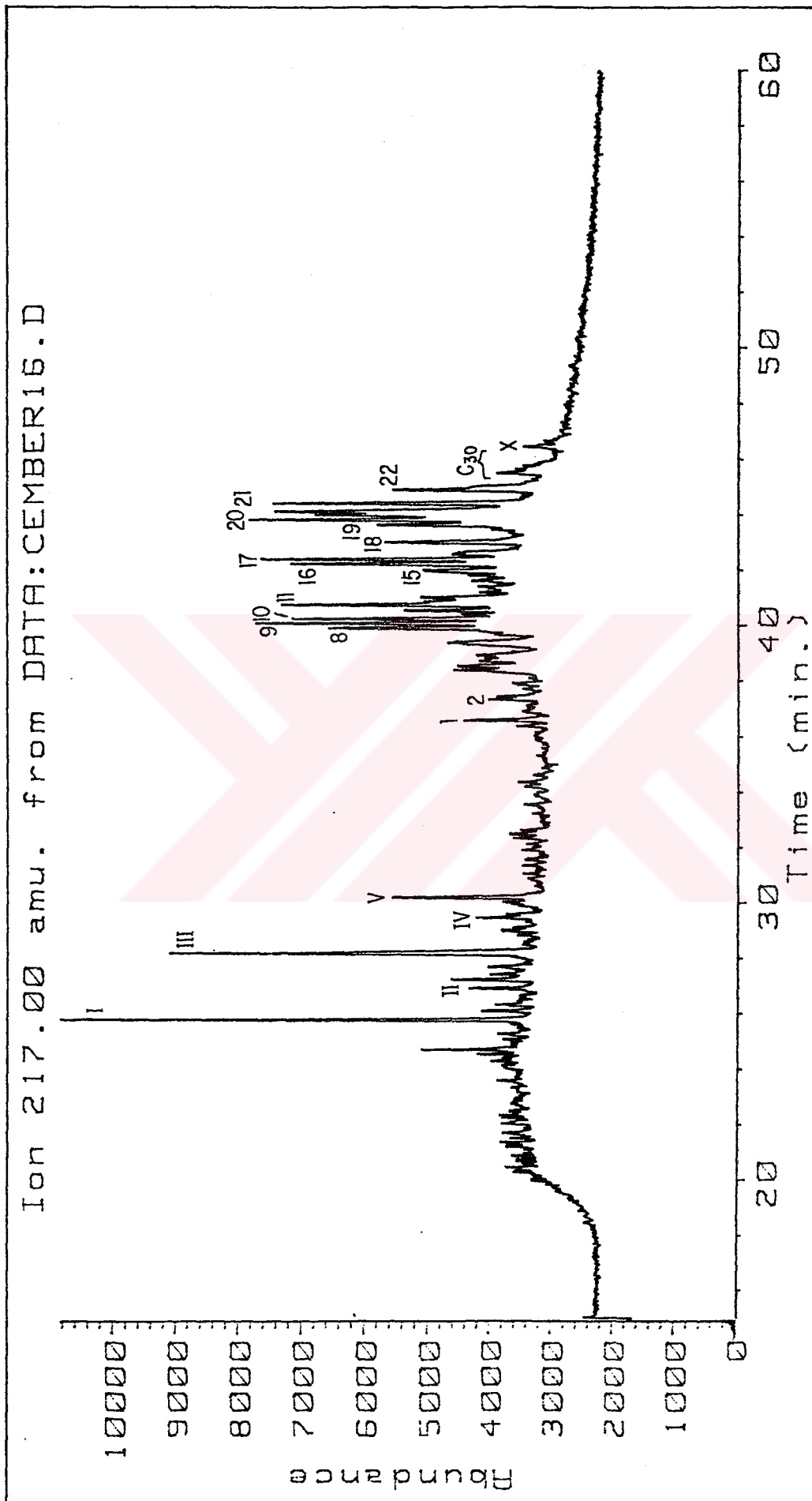


Figure.F.32 M/Z 217 mass fragmentogram of the Çemberlitaş.16 (CT16) oil.



APPENDIX-G

STABLE CARBON ISOTOPE RATIO DATA

Appendix-G. Stable carbon isotope data for the SE Turkey oils.

OIL SAMPLE	SATURATES	AROMATICS	DATA GENERATED BY
	$\delta^{13}C$	$\delta^{13}C$	
1 Çelikli-2	-27.60	-26.10	Robertson Research
2 Batı Şelmo-2	-28.00	-26.60	Robertson Research
3 Şelmo	-28.05	-26.77	Geochem Lab.
4 Batı Şelmo	-28.00	-26.80	Geochem Lab.
5 Silivanka-28	-28.10	-27.10	Robertson Research
6 Kastel-2	-29.10	-27.60	KSEPL
7 Kurtalan	-26.89	-25.56	Geochem Lab.
8 Mağrip-39	-27.40	-26.80	Robertson Research
9 Mağrip	-27.47	-27.12	Geochem Lab.
10 Garzan	-28.04	-27.34	Geochem Lab.
11 Raman-111	-27.60	-27.10	Robertson Research
12 Raman	-27.60	-28.10	KSEPL
13 Batı Raman-1	-28.30	-27.50	Robertson Research
14 Batı Raman	-28.15	-27.61	Geochem Lab.
15 Çamurlu	-28.07	-27.79	Geochem Lab.
16 Çamurlu-7	-27.90	-27.60	Robertson Research
17 Batı Kozluca	-27.74	-27.70	Geochem Lab.
18 Güney Diñer	-27.33	-27.63	Geochem Lab.
19 Güney Diñer-2	-27.30	-27.40	Robertson Research
20 Sarıcak-2	-29.70	-28.50	Robertson Research
21 Adıyaman-42	-27.90	-27.30	Robertson Research
22 Çamberlitaş-5	-27.90	-27.30	Robertson Research



APPENDIX-H

LINEAR REGRESSION CORRELATION COEFFICIENTS

Table_H.1 Linear regression correlation coefficient matrix of the tri_tetracyclic terpanes.

	a*	b	c1	c2	c3	d1	d2	e	f	g	TC*	h1	h2
a	1												
b	0.85	1											
c1	0.51	0.71	1										
c2	0.19	0.14	0.28	1									
c3	0.21	0.13	0.41	0.11	1								
d1	0.32	0.51	0.32	0.03	0.06	1							
d2	0.06	0.08	0.21	0.09	0.12	0.72	1						
e	-0.14	0.17	0.21	-0.32	-0.03	0.63	0.48	1					
f	-0.11	0.16	0.65	0.02	0.21	-0.14	-0.09	0.21	1				
g	-0.09	0.16	0.66	0.29	0.27	-0.11	-0.01	0.15	0.85	1			
TC*	-0.44	-0.71	-0.95	-0.24	-0.31	-0.46	-0.32	-0.42	-0.68	-0.69	1		
h1	0.02	0.22	0.72	0.07	0.18	-0.19	-0.15	0.04	0.86	0.79	-0.68	1	
h2	0.08	0.18	0.69	0.24	0.08	-0.25	-0.09	-0.09	0.75	0.71	-0.62	0.89	1

* Corresponds to the peaks labelled in Figure 3.3 and described in Table 3.4

Table-H.2 Linear regression correlation coefficient matrix of the pentacyclic terpanes.

A*	B	B1	C	D	E	E1	F	G	H	K	L	N	O	Q	R	S	T	
A	1																	
B	-0.23	1																
B1	-0.57	0.51	1															
C	-0.32	0.02	0.51	1														
D	-0.43	0.74	0.69	0.17	1													
E	-0.21	-0.79	-0.47	0.03	-0.52	1												
E1	-0.61	0.21	0.75	0.51	-0.38	0.07	1											
F	-0.19	0.14	-0.41	0.44	0.07	-0.04	0.31	1										
G	0.55	-0.72	-0.39	-0.81	0.57	-0.61	-0.31	0.73	1									
H	0.13	-0.82	-0.53	-0.68	0.62	-0.37	0.03	0.27	0.21	1								
K	0.11	0.19	-0.81	-0.14	-0.22	-0.55	0.24	0.27	0.21	0.42	1							
L	0.41	-0.62	-0.55	-0.78	0.38	-0.49	-0.21	0.83	0.69	0.42	0.31	1						
N	0.17	0.33	-0.77	0.03	-0.47	-0.41	0.21	0.09	-0.03	0.88	0.31	0.34	1					
O	0.04	-0.65	-0.57	-0.65	0.35	-0.31	0.12	0.61	0.76	0.47	0.74	0.34	0.76	1				
Q	-0.36	0.45	-0.57	0.32	-0.54	-0.01	0.41	-0.33	-0.21	0.71	-0.05	0.31	0.31	0.31	1			
R	-0.28	-0.47	-0.42	-0.33	0.21	-0.02	0.31	0.19	0.49	0.33	0.36	0.27	0.87	0.87	0.51	1		
S	-0.44	0.48	-0.47	0.41	-0.57	0.08	0.37	-0.39	-0.26	0.63	-0.16	0.68	0.21	0.97	0.44	0.44	1	
T	-0.43	-0.36	-0.07	-0.09	0.02	0.22	0.24	0.05	0.37	0.21	0.22	0.22	0.71	0.53	0.88	0.88	0.56	1

*Corresponds to the peaks labelled in Figure 3.3 and described in Table 3.4

Table-H.3 Linear regression correlation coefficient of the tri_tetra_pentacyclic terpanes.

	a*	b	c	d	e	f	g	TC*	h1+h2	11+12+k1	A	B	C	E	C31-C35	
a	1															
b	0.95	1														
c	0.81	0.92	1													
d	0.82	0.93	0.89	1												
e	0.82	0.94	0.92	0.97	1											
f	0.75	0.89	0.98	0.89	0.92	1										
g	0.69	0.81	0.93	0.79	0.85	0.95	1									
TC*	0.29	0.24	0.05	0.22	0.31	0.21	0.06	1								
h1+h2	0.74	0.86	0.97	0.83	0.89	0.98	0.98	0.11	1							
11+12+k1+	0.72	0.81	0.87	0.78	0.83	0.91	0.92	0.18	0.93	1						
A	0.76	0.79	0.72	0.72	0.74	0.77	0.76	0.37	0.77	0.91	1					
B	-0.45	-0.51	-0.51	-0.49	-0.39	-0.36	-0.41	0.55	-0.43	-0.38	-0.26	1				
C	-0.52	-0.65	-0.71	-0.57	-0.65	-0.73	-0.79	0.01	-0.76	-0.71	-0.51	0.31	1			
E	-0.17	-0.23	-0.12	-0.17	-0.25	-0.19	-0.09	-0.38	-0.13	-0.13	-0.11	-0.21	0.49	1		
C31-C35	-0.47	-0.42	-0.18	-0.31	-0.31	-0.16	-0.07	-0.18	-0.12	-0.23	-0.35	0.25	0.28	0.65	1	

* Corresponds to the peaks labelled in Figure 3.3 and described in Table 3.4.

Table - H.4 Linear regression correlation coefficients of the steranes.

	I*	II	III	IV	V	1	2	8	9	10	11	15	16	17	18	19	20	21	22
I	1																		
II	0.11	1																	
III	-0.25	0.21	1																
IV	-0.31	-0.51	0.59	1															
V	-0.33	-0.13	0.62	0.74	1														
1	0.11	0.89	-0.04	-0.62	-0.26	1													
2	0.07	0.88	-0.03	-0.59	-0.25	0.99	1												
8	0.27	0.09	-0.51	-0.53	-0.44	0.19	0.15	1											
9	0.01	0.49	-0.51	-0.82	-0.52	0.64	0.61	0.66	1										
10	0.05	0.41	-0.19	-0.66	-0.38	0.36	0.34	0.49	0.53	1									
11	-0.03	-0.66	-0.21	0.19	0.03	-0.67	-0.71	0.45	-0.07	0.12	1								
15	-0.06	-0.08	-0.52	-0.39	-0.42	-0.02	-0.03	0.68	0.55	0.25	0.43	1							
16	0.27	0.41	-0.26	-0.54	-0.36	0.36	0.35	0.46	0.41	0.74	-0.08	0.21	1						
17	0.27	-0.11	-0.64	-0.41	-0.48	0.02	-0.01	0.63	0.43	0.51	0.41	0.51	0.66	1					
18	0.21	-0.25	-0.61	-0.31	-0.37	-0.19	-0.22	0.62	0.31	0.24	0.44	0.59	0.53	0.82	1				
19	-0.32	-0.83	-0.26	0.38	-0.02	-0.75	-0.73	-0.28	-0.41	-0.48	0.41	0.06	-0.61	-0.11	0.04	1			
20	-0.33	-0.64	-0.25	0.26	-0.04	-0.57	-0.54	-0.46	-0.35	-0.43	0.14	-0.06	-0.56	-0.727	-0.17	0.91	1		
21	-0.29	-0.79	-0.24	0.39	0.03	-0.71	-0.68	-0.43	-0.48	-0.42	0.31	-0.09	-0.51	-0.29	-0.04	0.94	0.92	1	
22	-0.39	-0.73	-0.07	0.47	0.13	-0.64	-0.62	-0.26	-0.41	-0.62	0.26	0.03	-0.59	-0.31	0.01	0.81	0.68	0.67	1

* Corresponds to the peaks labelled in Figure 3.4 and described in Table 3.5.

Table_H.5 Linear regression correlation coefficients of the selected biomarker ratios.

	R1	R2	R3	R4	R5	R6	R7	R8	R9	R10	R11	R12	R13	R14	R15	R16	R17	R18	R19	R20	R21	R22	
R1	1																						
R2	-0.29	1																					
R3	-0.23	0.54	1																				
R4	0.15	-0.43	-0.51	1																			
R5	0.11	-0.54	-0.59	0.35	1																		
R6	0.15	-0.18	-0.19	0.26	0.52	1																	
R7	0.21	-0.21	-0.17	0.21	0.39	0.96	1																
R8	-0.03	-0.59	-0.49	0.35	0.65	-0.21	-0.26	1															
R9	-0.21	-0.09	0.09	-0.16	-0.21	-0.08	0.03	0.14	1														
R10	0.14	-0.48	-0.62	0.52	0.88	0.31	0.23	0.72	-0.21	1													
R11	0.26	-0.51	-0.48	0.27	0.31	0.25	0.32	0.26	0.08	0.33	1												
R12	0.11	-0.55	-0.38	0.51	0.78	0.53	0.47	0.45	-0.01	0.55	0.24	1											
R13	0.19	-0.41	-0.66	0.46	0.79	0.31	0.19	0.58	-0.17	0.81	0.37	0.45	1										
R14	0.01	-0.16	0.32	-0.01	0.16	0.71	0.75	-0.23	0.15	-0.05	0.01	0.47	-0.25	1									
R15	-0.17	0.23	0.76	-0.42	-0.51	-0.06	0.05	-0.32	0.51	-0.55	-0.34	-0.23	-0.59	0.52	1								
R16	0.08	0.01	-0.45	0.36	0.53	0.48	0.44	0.11	-0.08	0.55	0.21	0.32	0.59	-0.02	-0.39	1							
R17	-0.12	-0.02	0.03	0.11	-0.14	-0.09	-0.06	-0.06	-0.06	-0.13	0.18	-0.02	-0.06	-0.03	-0.04	0.05	1						
R18	-0.02	0.31	0.64	-0.45	-0.62	-0.24	-0.21	-0.49	-0.07	-0.63	-0.58	-0.57	-0.65	0.16	0.62	-0.53	-0.07	1					
R19	0.14	-0.05	-0.03	0.06	0.01	-0.03	-0.09	0.02	-0.03	-0.08	0.01	0.11	-0.04	-0.01	-0.09	-0.03	0.07	-0.09	1				
R20	-0.38	0.14	0.49	-0.37	-0.48	0.04	0.11	-0.44	0.46	-0.61	-0.32	-0.25	-0.63	0.44	0.75	-0.44	-0.04	0.61	-0.09	1			
R21	-0.07	0.02	0.47	-0.36	-0.52	-0.02	0.12	-0.42	0.48	-0.56	-0.23	-0.33	-0.61	0.37	0.78	-0.39	-0.11	0.65	-0.14	0.87	1		
R22	-0.05	-0.49	-0.55	0.58	0.87	0.42	0.32	0.61	0.03	0.76	0.19	0.65	0.62	0.13	-0.35	0.51	-0.17	-0.47	-0.04	-0.19	-0.25	1	

* Corresponds to the ratios explained in Table 3.7.

CURRICULUM VITAE

Kadir Gürgey was born in Denizli in 1950. He has a turkish citizenship. He graduated in 1974 from the istanbul Technical University, of istanbul, with a BS degree in geological engineering, and went on to take a MS degree from the University of Tulsa, of Tulsa, USA in 1983. He joined Turkish Petroleum Corporation (TPAO) in 1986 and currently, he is a research associate in the Organic Geochemistry Group of TPAO Research Center, Ankara, Turkey.

T. C.
Yükseköğretim Kurulu
Dokümantasyon Merkezi